Chapter 1

SUMO, a heavyweight player in plant abiotic stress responses

This chapter was adapted from Castro PH, Tavares RM, Bejarano ER, Azevedo H (2012) SUMO, a heavyweight player in plant abiotic stress responses. Cell Mol Life Sci 69: 3269-3283

CONTENTS

1.1. INTRODUCTION

Modulation of protein activity is essential for the functioning of a living organism, particularly during rapid environmental changes, when physiological responses must often occur quickly and reversibly. This modulation can take place by the addition of small molecules to target proteins, a process known as post-translation modification (PTM). Important modifiers of proteins include not only phosphate, methyl, acetyl, lipids and sugars, but also small peptides (Kerscher et al., 2006; Vertegaal, 2011). Ubiquitin is the foremost example, but a series of similar ubiquitin-like modifiers (UBLs) have also been described as sharing analogous structural conformation and conjugation machinery (Downes and Vierstra, 2005; Kerscher et al., 2006; Miura and Hasegawa, 2010). One such UBL, the Small Ubiquitin-like Modifier (SUMO), is an essential factor in development processes in eukaryotic organisms, being implicated in several cellular mechanisms such as maintenance of genome integrity, subcellular trafficking, transcription modulation, and regulation of the cell cycle (Hay, 2005; Lomeli and Vazquez, 2011). Unlike ubiquitin, SUMO is not traditionally associated to protein degradation, rather to the control of the target's conformation, which interferes with protein activity and creates or blocks interacting interfaces depending on the target at hand (Meulmeester and Melchior, 2008; Wilkinson and Henley, 2010). Since sumoylation and ubiquitination target the same type of amino acid, they were initially suggested to be antagonistic processes. This notion is currently evolving, as recruitment of ubiquitin by SUMO chains was shown to occur in humans and yeast via SUMO-Targeted Ubiquitin Ligases (STUbLs; Geoffroy and Hay, 2009). SUMO may therefore act as a positive regulator of the Ubiquitin Proteasome System (UPS), though STUbL plant homologs have yet to be established. In support of this mechanism, heat shock has been found to induce the formation of mixed SUMO/Ubiquitin chains in Arabidopsis (Miller et al., 2010).

One unique characteristic of SUMO is environmental stress challenges induce a drastic increase in SUMO-conjugates; this increase seems to be preserved among eukaryotic organisms (Kurepa et al., 2003; Manza et al., 2004; Zhou et al., 2004; Lallemand-Breitenbach et al., 2008; Golebiowski et al., 2009). In the model plant Arabidopsis, SUMO is specifically involved in a plethora of abiotic stress responses, including those to extreme temperatures, water-availability, salinity, oxidative stress and nutrient imbalance (Kurepa et al., 2003; Miura et al., 2005; Yoo et al., 2006; Catala et al., 2007; Miura et al., 2007b; Saracco et al., 2007; Conti et al., 2008; Cheong et al., 2009; Miura et al., 2009; Chen et al., 2011; Miura et al., 2011a; Miura et al., 2011b; Park et al., 2011a). In addition, it is involved in plant development and the response to pathogens (Lee et

al., 2007; Miura et al., 2010; van den Burg et al., 2010). Many of the known SUMO targets are related to RNA- and DNA-associated processes, namely transcription factors (TFs) and chromatin-remodeling components (Golebiowski et al., 2009; Miller et al., 2010; Park et al., 2011b). SUMO can be removed from conjugates by SUMO proteases, with the protein then returning to its non-modified state. Thus, the balance between conjugated/deconjugated forms is a major determinant in the modulation of SUMO-target function (Kurepa et al., 2003; Golebiowski et al., 2009). These highly reversible and transient modifications place SUMO as a rapid transcriptional regulator in response to stress.

The present review focuses on recent advances regarding the ever-growing link between PTM by SUMO and plant responses to environmental challenges. We also demonstrate how new information on the full range of SUMO targets may bring new insights into the modulation of the plant stress response.

1.2. A PRIMER OF THE SUMOYLATION PATHWAY

SUMO is a small protein of approximately 100-115 amino acids. Despite its relatively reduced homology to other UBLs, it shares a similar ubiquitin-like structural conformation characterized by a β-grasp fold that seems to act as a multi-functional scaffold (Fig. 1.1A; Downes and Vierstra, 2005; Burroughs et al., 2007). Unlike ubiquitin, SUMO possesses a flexible amino acidic extension in its N-terminal end, and its topology is differently charged (Bayer et al., 1998; Downes and Vierstra, 2005). The Arabidopsis genome contains eight putative SUMO copies, but only four paralogs have confirmed gene expression (SUM1 ~ SUM2 > SUM3 ~ SUM5; Saracco et al., 2007). At least three SUMOs can be found in *Oryza sativa* and four in *Populus trichocarpa* (Miura et al., 2007a; Reed et al., 2010). Arabidopsis SUM1 and -2 (SUM1/2) are functionally equivalent (Saracco et al., 2007) and in planta, SUM1, -3 and -5 isoforms have been shown to conjugate with high molecular weight target proteins (Budhiraja et al., 2009). SUMO isoforms display different conjugation profiles, and not all isoforms are capable of forming poly-SUMO chains (SUM1/2, but not SUM3; Kurepa et al., 2003; Colby et al., 2006; Saracco et al., 2007; van den Burg et al., 2010; Castano-Miquel et al., 2011). SUMO profiles show that SUM1/2 and SUM3 have different specificities and possibly different targets. In vitro, conjugation rates are highest for SUM1 and SUM2 >> SUM3 > SUM5, possibly because of differences on the residues are

important for the interaction with the E1 activating enzyme (van den Burg et al., 2010; Castano-Miquel et al., 2011).

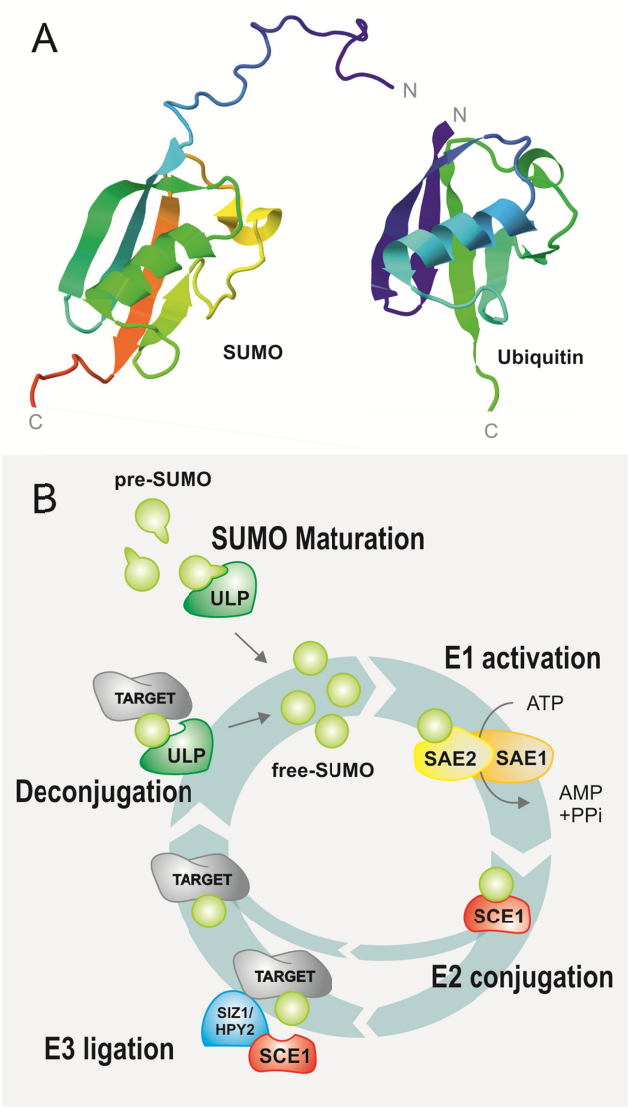

Figure 1.1. The sumoylation pathway. **A**, Three-dimensional (3D) structure of human small ubiquitin-like modifier (SUMO) 1 (acc. no. 1A5R) and ubiquitin (acc. no. 1UBQ), obtained from the Protein Data Bank (www.rcsb.org/pdb/home/home.do/) and visualized using Jmol, an open-source Java viewer for chemical structures in 3D (www.jmol.org/). **B**, The sumoylation cycle is a conserved five-step pathway (involving maturation, E1-activation, E2-conjugation, E3-ligation, deconjugation) and mediates the balance between the conjugated/deconjugated forms of a target protein. SUMO isoforms encode a pre-SUMO peptide that undergoes maturation by ubiquitin-like proteases (ULP). These SUMO-specific cysteine endopeptidases cleave the C-terminal end, exposing a di-glycine (GG) motif. In the presence of ATP, heterodimeric E1 SUMO-activating enzymes 1 and 2 (SAE1, SAE2) promote the C-terminal binding of SUMO to AMP (SUMO-AMP). A SUMO glycine (G) residue is also coupled to a cysteine (C) of the SAE2, through a high-energy thioester bond. The peptide is then conjugated to an E2 SUMO-conjugating enzyme (SCE1), through transesterification of a C residue in the E2. E2s are subsequently capable of transferring SUMO to a target protein. This step is mostly mediated by SUMO E3 ligases, even though E3-independent transfer is possible. An isopeptide bond is generated between the SUMO G residue and the ε-amino group of a lysine (K) side chain in the target protein's sumoylation consensus motif ψKXE (ψ, large hydrophobic residue; K, lysine; X, any amino acid; E, glutamic acid), although alternative sumoylation sites also exist. ULPs display isopeptidase in addition to endopeptidase activity, deconjugating SUMO from the target. This final step recycles SUMO and, most significantly, mediates the balance between the target's conjugated/deconjugated forms.

SUMO ubiquitin-like proteases (ULP), also designated sentrin/SUMO-specific proteases (SENP), process pre-SUMOs by removing C-terminal amino acids, exposing a di-glycine motif. Sumoylation by which the maturated SUMO is covalently attached to a target protein occurs through a three-step cascade (E1, E2, E3) similar to the ubiquitin pathway (Fig. 1.1B). The E1 (SUMO Activating Enzyme: SAE1-SAE2 heterodimer) promotes the ATP-dependent activation of SUMO, while the E2 (SUMO Conjugating Enzyme: SCE) mediates conjugation of SUMO to a target

protein. SUMO E3 ligases enhance the conjugation step. SUMO can be removed by the action of SUMO proteases, thereby recycling free SUMO into the pathway (Fig. 1.1B). Conjugation traditionally occurs in a lysine residue of the target protein, within a sumoylation consensus motif ψKXE (ψ, large hydrophobic residue; K, lysine; X, any amino acid; E, glutamic acid). Several alternative SUMO-conjugation sites have also been described, namely the inverted consensus motif, hydrophobic cluster motif, phosphorylation dependent SUMO motif (PDSM), and the negatively charged amino acid-dependent SUMO motif (NDSM; Gareau and Lima, 2010; Vertegaal, 2011). Positioning of the motif within the target is extremely important. Most validated SUMO consensus sites tend to be placed in extended loops or intrinsically disordered regions of the substrate outside of its globular fold, since the motif adopts an extended conformation to interact effectively with the E2. In addition, SUMO interacting motifs (SIMs) mediate non-covalent interactions between SUMO and various different SIM-containing proteins, adding complexity to the network of SUMO-dependent protein interactions. SIMs are traditionally composed of a short stretch of hydrophobic amino acids, (V/I)X(V/I)(V/I), flanked by acidic residues (Gareau and Lima, 2010).

Orthologs for the full scope of SUMO pathway components can be found in plant genomes. Genomic studies in *Arabidopsis thaliana* have validated the existence of a functional SUMO pathway in plants, revealing the important role of this pathway in developmental processes and the plant's response to external stimuli (Table 1.1). Mutations that disrupt the main conjugation machinery, i.e. SUMO peptides (SUM1/2), the SAE2 subunit of the E1 heterodimer, or the SUMO E2 conjugation enzyme SCE1, result in development arrest at the early stages of embryogenesis (Saracco et al., 2007); a similar finding has been observed in other models (Bossis and Melchior, 2006b). However, over-expression of SUMOs results in growth-defective plants (Budhiraja et al., 2009; van den Burg et al., 2010). To date, two E3 ligases have been characterized in Arabidopsis, the SIZ/PIAS-type SAP and Miz 1 (SIZ1) and the NSE2/MMS21-type High Ploidy 2 (HPY2), both with pleiotropic phenotypes in loss-of-function mutants, evidencing the importance of E3s within the pathway (Miura et al., 2005; Catala et al., 2007; Jin et al., 2008; Huang et al., 2009; Ishida et al., 2009; Miura et al., 2010). SUMO proteases are more abundant in the genome than any other SUMO pathway component, resulting in a high degree of redundancy (Chosed et al., 2006; Colby et al., 2006; Lois, 2010). Mutants also display developmental phenotypes: Early in Short Days 4 (ESD4) mutants are severely dwarfed and their developmental defects are incremented by the over-expression of SUM1 (Murtas et al., 2003); ULP1c and ULP1d, also designated Overly Tolerant to

Salt 2 and -1 (OTS2 and -1), respectively, act redundantly to regulate flowering and rosette growth (Chapter 4; Conti et al., 2008). More information can be found in a series of excellent reviews that recently addressed the diversity of the plant SUMO machinery and its impact on plant development (Lois, 2010; Miura and Hasegawa, 2010; Park et al., 2011c).

Table 1.1. Expressed Arabidopsis small ubiquitin-like modifier pathway components.

Component (AGI code)	Loss- or gain-of-function allele	Developmental phenotype	Abiotic stress-related phenotype	Reference
SUMO peptide				
SUM1 (At4g26840)	*sum1-1*	Wild-type		Saracco et al. (2007)
	35S::SUM1	Early flowering, short petioles	Lower ABA root growth inhibition; decreased acquired thermotolerance	Lois et al. (2003); Saracco et al. (2007); Cohen-Peer et al. (2010); van den Burg et al. (2010)
SUM2 (At5g55160)	*sum2-1*	Wild-type		Saracco et al. (2007)
	35S::SUM2	Early flowering, short petioles	Lower ABA root growth inhibition	Lois et al. (2003); van den Burg et al. (2010)
	sum1-1 sum2-1	Embryo lethal		Saracco et al. (2007)
	sum1-1 amiR-SUM2	Pleiotropic		van den Burg et al. (2010)
SUM3 (At5g55170)	*sum3-1*	Late flowering		van den Burg et al. (2010)
	35S::SUM3	Early flowering		van den Burg et al. (2010)
SUM5 (At2g32765)	n.d.	n.d.		
E1 (Activation)				
SAE1a (At4g24940)	*sae1a-1*	Wild-type		Saracco et al. (2007)
SAE1b (At5g50580)	n.d.	n.d.		
SAE2 (At2g21470)	*sae2-1*	Embryo lethal		Saracco et al. (2007)
E2 (Conjugation)				
SCE1 (At3g57870)	*sce1-5*, *sce1-6*	Embryo lethal		Saracco et al. (2007)
	co-SCE1a	n.d.	Higher ABA root growth inhibition	Lois et al. (2003)

Table 1.1. (Continued)

E3 (Ligation)				
HPY2/MMS21 (At3g15150)	*hpy2-1, hpy2-2 mms21-1*	Pleiotropic		Huang et al. (2009); Ishida et al. (2009)
SIZ1 (At5g60410)	*siz1-1, siz1-2, siz1-3*	Pleiotropic	Sensitivity to extreme temperatures, drought and copper; abnormal Pi-starvation responses; higher ABA-induced inhibition of germination and root growth; impaired in N-metabolism; tolerance to salt	Miura et al. (2005); Yoo et al. (2006); Catala et al. (2007); Miura et al. (2007b); Cheong et al. (2009); Miura et al. (2009); Chen et al. (2011); Miura et al. (2011a); Miura et al. (2011b); Park et al. (2011a)
Protease				
ESD4 (At4g15880)	*esd4-1, esd4-2*	Pleiotropic		Reeves et al. (2002); Murtas et al. (2003)
	35S::ESD4	Wild-type		Murtas et al. (2003)
	esd4-1	Pleiotropic		Murtas et al. (2003)
	35S::SUM1,2,3			
	esd4-1	Pleiotropic		Murtas et al. (2003)
	35S::preSUM1, 2,3			
ULP1a/ELS1 (At3g06910)	*els1-1*, *els1-2*	Slightly smaller		Hermkes et al. (2011)
	esd4-2 els1-1	Pleiotropic		Hermkes et al. (2011)
ULP1b (At4g00690)	n.d.	n.d.		
ULP1c/OTS2 (At1g10570)	*ots2-1*	Wild-type		Conti et al. (2008)
ULP1d/OTS1 (At1g60220)	*ots1-1*	Wild-type		Conti et al. (2008)
	35S::OTS1		Salt tolerance	Conti et al. (2008)
	ots1-1 ots2-1	Early flowering	Salt sensitivity	Conti et al. (2008)
	ots1-1 ots2-1 35S::HA:SUM1	Smaller rosette		Conti et al. (2009)
ULP2a (At4g33620)	n.d.	n.d.		
ULP2b (At1g09730)	n.d.	n.d.		

*ABA - abscisic acid; Pi - inorganic phosphate; n.d. - not determined; * – co-supression line*

1.3. THE SUMO-ABIOTIC STRESS ASSOCIATION

The accumulation of SUMO-conjugates during stress is ubiquitous in eukaryotes (Kurepa et al., 2003; Zhou et al., 2004; Golebiowski et al., 2009). In plants it has been observed in rice,

poplar and, more frequently, Arabidopsis following heat shock (Kurepa et al., 2003; Miura et al., 2005; Yoo et al., 2006; Saracco et al., 2007; Cheong et al., 2009; van den Burg et al., 2010), cold shock (Miura et al., 2007b; Miura and Ohta, 2010), drought (Catala et al., 2007), salt stress (Conti et al., 2008), exposure to excessive copper (Chen et al., 2011), and incubation with hydrogen peroxide, ethanol, and canavanine (Kurepa et al., 2003). Conjugation is accompanied by a decrease in the pool of free SUMOs and correlates with the duration and intensity of the stress (Kurepa et al., 2003; Miller and Vierstra, 2011). In the absence of the stimulus, SUMO-conjugate levels decrease within hours or even minutes, suggesting that sumoylation acts transiently (Kurepa et al., 2003; Golebiowski et al., 2009).

Functional approaches using *Arabidopsis thaliana* knockout mutants have implicated various SUMO pathway components in abiotic stress responses (Table 1.1). The lethality of SUM1/2, E1 and E2 knockouts has meant that most evidence has been obtained in E3 and ULP mutants. Null *SIZ1* alleles (*siz1-1*, *siz1-2* and *siz1-3*) display a series of abiotic stress-related phenotypes, including sensitivity to extreme temperatures, drought stress, and excess copper, altered phosphate-starvation responses, reduced nitrogen (N) assimilation, and salt tolerance (Table 1.1; Miura et al., 2005; Yoo et al., 2006; Catala et al., 2007; Miura et al., 2007b; Cheong et al., 2009; Miura et al., 2009; Chen et al., 2011; Miura et al., 2011a; Miura et al., 2011b; Park et al., 2011a). SIZ/PIAS family members are composed of different regulatory domains (Rytinki et al., 2009), and directed mutation studies have implicated the SIZ1 SP-RING domain (essential for SUMO conjugation and nuclear localization) in heat shock sensitivity during germination (Cheong et al., 2009). In rice, the two SIZ1 orthologs (OsSIZ1/2) are involved in heat stress-induced sumoylation, but can only partially complement the Arabidopsis *siz1* mutant (Park et al., 2010), suggesting that OsSIZ1/2 have slightly different functions. The accumulation of SUMO-conjugate levels during heat, cold, and drought stress and following exposure to excess copper has been shown to be essentially SIZ1 dependent, although the slight but visible presence of stress-responsive SUMO-conjugates in *siz1* suggests either alternative E3s or E3-independent conjugation (Miura et al., 2005; Catala et al., 2007; Miura et al., 2007b; Saracco et al., 2007; Chen et al., 2011). HPY2, an E3 ligase that also displays an SP-RING domain, has been mainly associated with the regulation of cell cycle division (Huang et al., 2009; Ishida et al., 2009). There are a number of other genes in the Arabidopsis genome, other genes possessing an SP-RING domain which are potential SUMO E3 ligases, including the PIAS-like 1 (At1g08910) and PIAS-like 2 (At5g41580) proposed by Novatchkova and co-workers (2004). Interestingly, PIAS-like 2 has been found to be

modified by SUM1 (Miller et al., 2010), though its involvement in stress-responses has yet to be reported.

Relative to other SUMO pathway components, there are a larger number of plant SUMO proteases and these have different SUMO isoform discrimination and enzymatic activities (Chosed et al., 2006; Colby et al., 2006). Plant SUMO proteases display some degree of functional redundancy which has delayed their characterization. The fact that SUMO targets seem to be conjugated transiently following stress imposition implicates ULP-dependent deconjugation in the abiotic stress response. The identification of abiotic stress-related phenotypes has been limited to the redundant gene pair ULP1c/OTS2 and ULP1d/OTS1. Conti and co-workers (2008) reported that this ULP1 pair is a determinant of salt tolerance, and subsequent evidence suggests they also act as negative regulators of drought tolerance (Chapter 4).

1.4. IDENTIFICATION OF SUMO TARGETS

Identification of the full set of sumoylated proteins is a major objective of current SUMO research, as it provides a molecular link between SUMO function and the numerous phenotypes displayed by SUMO pathway components. In non-plant models, various strategies have been employed to screen for SUMO targets, namely, purification of epitope-tagged SUMO, use of anti-SUMO antibodies or isolation through SIMs (Makhnevych et al., 2009; Vertegaal, 2011). In plants, initial approaches relied on hypothesis generation to identify candidate genes, based on phenotypic evidence and literature mining, and resulted in the identification of nine proteins that are sumoylated (Fig. 1.2A, subset 1; Miura et al., 2005; Miura et al., 2007b; Jin et al., 2008; Miura et al., 2009; Okada et al., 2009; Cohen-Peer et al., 2010; Castano-Miquel et al., 2011; Park et al., 2011a). Candidate genes were validated through a series of in bacteria, in planta, or in vitro studies. The majority of proteins play a regulatory role in gene expression, which is consistent with traditional SUMO function (Gill, 2005; Lyst and Stancheva, 2007; Garcia-Dominguez and Reyes, 2009). Importantly, most proteins are involved in abiotic stress responses, thereby validating the physiological and functional data in support of a major role for sumoylation in abiotic stress resistance. However, the discovery rate using candidate gene approaches is slow when the large number of hypothesized sumoylation targets within the plant proteome is taken into account. This limitation has led to a recent series of systematic functional genomics approaches being used to identify SUMO targets (Fig. 1.2A). These approaches can be categorized into the *in planta*

screening of Tag-SUMO conjugates coupled with peptide sequencing (herein designated SUMO-conjugates; Budhiraja et al., 2009; Miller et al., 2010; Park et al., 2011b) or the identification of protein-protein interaction (PPI) partners of the sumoylation machinery (herein designated Sumoylation-interacting; Matarasso et al., 2005; Xu et al., 2007; Garcia-Dominguez et al., 2008; Nigam et al., 2008; Elrouby and Coupland, 2010).

In plants, mass identification of SUMO-conjugates (Fig. 1.2A, subset 2) was first performed by Budhiraja and co-workers (2009), through in vivo expression of His-tagged SUM1, -3 and -5. Single step enrichment by affinity column chromatography was used before mass spectrometric protein identification, revealing 14 putative SUMO targets. Five of the candidates were subsequently shown to be sumoylated in vitro. Most targets are involved in DNA-related or RNA-dependent processes, namely regulation of chromatin structure, splicing, translation, and assembly and dis-assembly processes (Budhiraja et al., 2009). The highest rending SUMO-conjugate assay was performed by Miller and co-workers (2010), who developed a stringent method to isolate a total of 357 His-SUM1-conjugating proteins from Arabidopsis. Given the known involvement of SUMO in abiotic stress, Arabidopsis plants were subjected to heat and oxidative stresses in addition to the control treatment. Once more, the majority of targets consisted of nuclear proteins involved in chromatin remodeling/repair, transcription, RNA metabolism, and protein trafficking. Interestingly, many were condition specific, which supports a stress-specific modulation of the pool of SUMO-conjugates. Park and co-workers (2011b) used two-dimensional (2D) gel electrophoresis to screen for SUMO targets following heat stress imposition and identified a total of 27 proteins involved in DNA or RNA-related metabolism, signaling pathways, and general metabolism. The seemingly deficient coverage of SUMO targets evidenced by Budhiraja et al. (2009) and Park et al. (2011b) may be due to the use of overextended tags, which were shown to compromise SUMO function in Arabidopsis (Miller et al., 2010). For instance, 6xHis-FLAG3-SUM1 proteins failed to identify SUMO conjugates under conditions of no stress, when SUMO conjugation is lowest (Park et al., 2011b). Tagged SUMOs may also compete deficiently with the native peptide, a problem that was overcome by Miller and co-workers' (2010) use of a *sum1-1 sum2-1* background. As a result there is no significant overlap between the three sets of SUMO-conjugates, as evidenced by Venn diagram analysis (Fig. 1.2B).

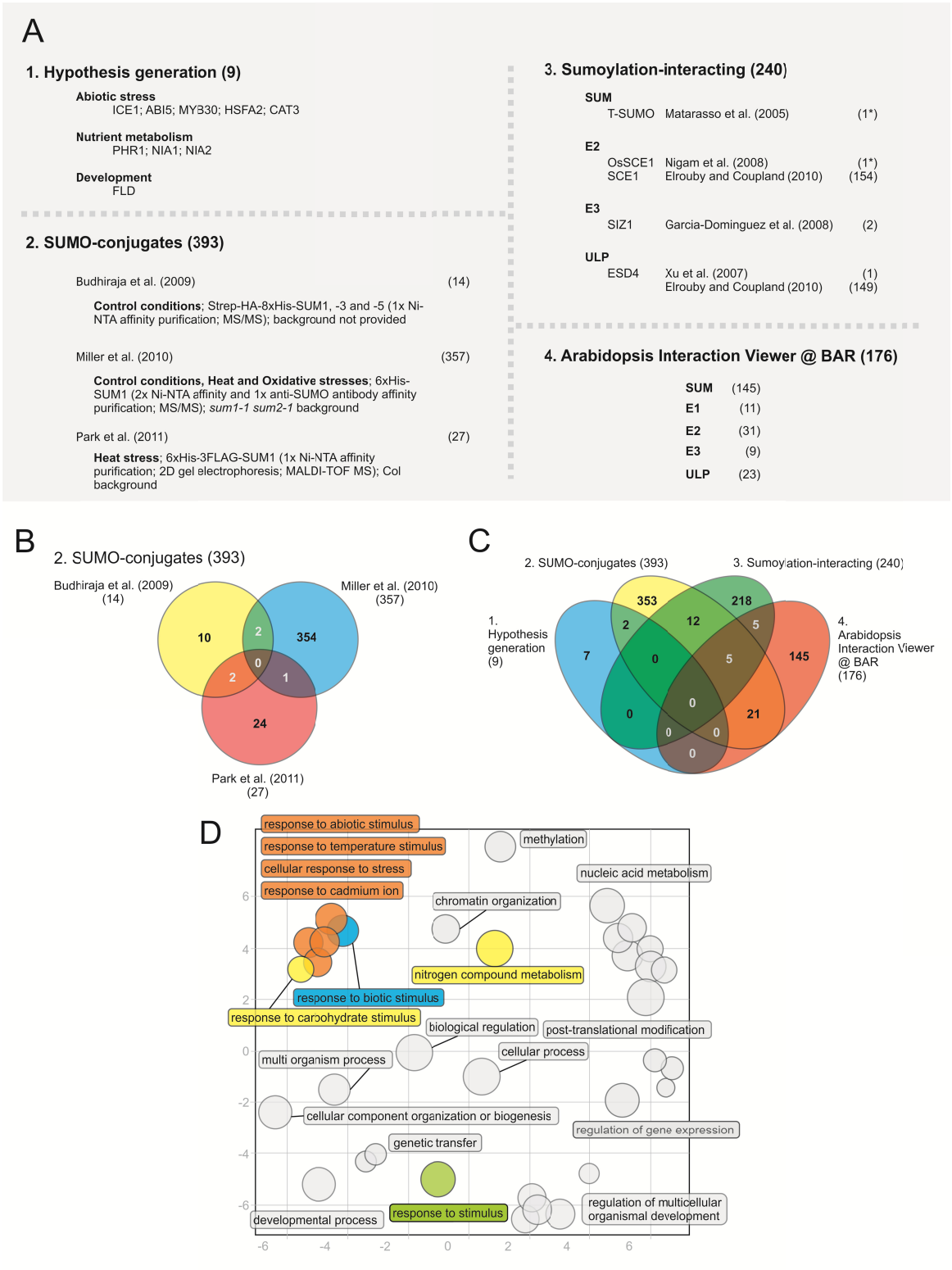

Figure 1.2. Annotation and characterization of the predicted plant SUMO targets. **A**, The four major strategies adopted for identifying plant SUMO targets have render a total of 768 proteins. **B**, Venn diagram analysis of the three existing SUMO-conjugate studies. **C**, Venn diagram analysis of the four subsets of strategies used to identify SUMO targets. **D**, Scatterplot of enriched gene ontology (GO) terms (biological process) for the subset of SUMO-conjugates. GO functional categorization was performed in VirtualPlant 1.2 software (virtualplant.bio.nyu.edu/cgi-bin/vpweb/), using the BioMaps function with a 0.01 *p*-value cutoff (Katari et al., 2010). Exclusion of GO term redundancy and subsequent scatterplot analysis were performed using the REVIGO tool (revigo.irb.hr/), with a 0.5 C-value

(Supek et al., 2011). *Bubble size* indicates the frequency of the GO term, *colored circles* indicate GO terms related to stress or nutritional stimuli. The scatterplot represents the cluster representatives in a 2D space (*x*- and *y*-axis) derived by applying multidimensional scaling to a matrix of the GO terms' semantic similarities (Supek et al., 2011). # Number of genes within the subset, *asterisk* non-Arabidopsis genes, *MALDI-TOF MS* matrix-assisted laser desorption/ionization-time of flight mass spectrometry.

In a sumoylation-interacting approach (Fig. 1.2A, subset 3), a high-throughput strategy aimed at identifying SUMO targets was carried out by Elrouby and Coupland (2010), who used yeast two-hybrid (Y2H) to identify 238 interactors of SUMO pathway components SCE1 and/or ESD4. An *Escherichia coli*-based sumoylation system was used to test a substantial number of targets, indicating that approximately half are bona fide SUMO substrates. Proteins involved in stress responses, namely temperature stress, were shown to be over-represented within Y2H interactors. A similar screening using SIZ1 as bait resulted in the identification of GTE3 and GTE5, members of global transcription factor group E that contain a bromodomain that is possibly involved in binding to acetylated histones (Garcia-Dominguez et al., 2008). Other Y2H interactions have been reported, including the interaction of Nuclear-pore Anchor (NUA) protein with ESD4. In other models, tomato Cys protease LeCp interacted with the SUM1/2 ortholog T-SUMO, and rice OsFKB20, a stress-inducible FK506-binding protein, interacted with OsSCE1 (Matarasso et al., 2005; Xu et al., 2007; Nigam et al., 2008). As an additional source of potential SUMO targets, we used the Arabidopsis Interactions Viewer function from BAR (Geisler-Lee et al., 2007), a database of almost 10^5 predicted and confirmed Arabidopsis interacting proteins, to identify estimated interactors for all components of the sumoylation machinery (Fig. 1.2A, subset 4). Our analysis rendered a total of 176 predicted interactors, mostly associated with SUMO peptides.

We cross-referenced all predicted plant SUMO targets in order to obtain an overview of all four subsets of proteins (Fig. 1.2C). Not surprisingly, four out of the five most over-represented proteins included SUM1, SAE2, SCE1, and SUMO E3 ligase candidate PIAS-like 2, which validates the current analysis. However, there was still no significant overlap between subsets, similar to an analogous study of yeast SUMO targets (Makhnevych et al., 2009). This limited overlap suggests that saturation is far from being achieved; however, it may also reflect the different methodologies employed, particularly considering that PPI-based approaches (subsets 3 and 4) may detect non-covalent interactions mediated by SIMs rather than bona fide sumoylation of substrates. Since SUMO-conjugate genes provide the highest confidence candidates, we analyzed gene ontology (GO) term enrichment for this subset (Fig. 1.2D). The REVIGO tool was used to exclude redundant GO terms, as redundancy tends to confound interpretation and inflate the perceived number of

biologically relevant results (Supek et al., 2011). As expected, functional categorization of biological processes revealed standard roles in SUMO function. However, over-represented GO terms also included stimuli that have been physiologically and functionally associated with the sumoylation pathway, namely, abiotic stress and nutrient-related stimuli. Using a detailed GO term categorization of the subset of 393 SUMO-conjugates, we identified 52 abiotic stress-related proteins (Appendix I - Table S1.1). These form a core of highly likely SUMO targets that link SUMO function to a wide range of abiotic stress responses. In non-plant models, many known targets are regulators of expression (acting as transcription factors, co-activators, or repressors; Bossis and Melchior, 2006b). A detailed analysis of these 52 genes we identified reveals a strong involvement in transcriptional regulation and nucleic acid binding activities, concomitant with the role for SUMO in the control of transcription during environmental challenges already envisaged by known plant SUMO targets (Miura et al., 2005; Miura et al., 2007b; Cohen-Peer et al., 2010).

1.5. MOLECULAR BASIS OF SUMO REGULATION OF ABIOTIC STRESS TOLERANCE

Extreme temperatures

During heat stress, protein stability is compromised, which affects cellular structures and organelles, including the nucleus (Richter et al., 2010). The best documented resistance proteins comprise transiently expressed Heat Shock Proteins (HSPs) which act as molecular chaperones of the native protein structure (Kotak et al., 2007; Richter et al., 2010), as well as Heat Shock Factors (HSFs) that function as key signaling effectors, modulating the transcription of heat-responsive genes (Kotak et al., 2007). Both types of proteins can be abundantly found in confirmed or predicted SUMO conjugates, including HSFA1D, HSFA2, HSFB2B, HSP70-1/HSC70-1, HSP17.4, HSC70-3/HSP70-3, HSP17.6C-CI and HSP70. HSP70 proteins are particularly over-represented in the different subsets of sumoylated proteins, which is consistent with their central role in protein folding processes, namely, during external stress (Mayer and Bukau, 2005). Interestingly, over-expression of HSC70 results in less accumulation of SUM1/2 conjugates following heat shock (Kurepa et al., 2003). The impact of sumoylation on these targets is unresolved, with the exception of the Arabidopsis transcription factor HSFA2 (Fig. 1.3A; Cohen-Peer et al., 2010). HSFA2 is a key element in acquired thermotolerance (Charng et al., 2007), and its activity in the nucleus seems to be repressed by SUM1 at position K315 (Cohen-Peer et al., 2010). Over-expression of SUM1 in

seedlings results in a reduced tolerance to repeated heat, implying that sumoylation acts negatively upon acquired thermotolerance (Cohen-Peer et al., 2010). Conversely, SIZ1 seems to be a positive regulator of basal responses (acting independently of salicylic acid), but not of acquired thermotolerance (Yoo et al., 2006; Saracco et al., 2007), which suggests the involvement of a SIZ1-independent pathway in the control of acquired thermotolerance. The seemingly antagonistic effect of SUMO pathway components on the different heat stress responses reflects the complex nature of these mechanisms. It also supports the idea that modulation of SUMO-conjugate steady-state levels during heat stress represents a dynamic and precisely fine-tuned process (Anckar et al., 2006). A microarray analysis study revealed that in the *siz1* mutant, eight HSPs and HSFs (e.g. *HSFA7A* and *HSF4/HSFB1*) were up-regulated under standard growth conditions, while no down-regulated HSP and HSF were observed (Catala et al., 2007). Similarly, *sHSP-CI* is consistently down-regulated following SUM1 over-expression (Cohen-Peer et al., 2010). Experimental evidence corroborates the notion that sumoylation acts mainly as an inhibitor of transcription (Gill, 2005). Apart from HSFs, other heat-related TFs are predicted to be sumoylated in association to heat stress, namely WRKY3 and WRKY4, two Group 1 members of the large WRKY TF family associated with numerous stress stimuli (Eulgem et al., 2000; Miller et al., 2010).

In addition to heat shock, SIZ1 is also important for cold acclimation and tolerance to freezing and chilling. More specifically, Miura and co-workers (2007b) found that upon cold imposition, SIZ1 positively affects the expression of the *C-repeat Binding Factor 3/Dehydration Responsive Element Binding factor 1a* (*CBF3/DREB1a*) TF and, consequently, its regulon. The *CBF3/DREB1a* regulator Inducer of CBF Expression 1 (ICE1) was shown to be sumoylated by SIZ1 at position K393, which does not seems to impact on ICE1 TF activity, rather it counteracts polyubiquitination by the E3 Ubiquitin ligase HOS1, decreasing ICE1-degradation and allowing *CBF3/DREB1a*-regulon expression (Fig. 1.3B). ICE1 sumoylation can also negatively regulate MYB15, a repressor of the *CBF3/DREB1a*-regulon that binds to MYB elements in the promoter of several cold-inducible genes (Fig. 1.3B; Miura et al., 2007b). It is likely that other SUMO substrates are involved in the response to cold, since the transgenic line *ICE1(K393R)* displays less sensitivity to freezing than the *siz1* mutant. Also, SUMO-conjugates increase drastically after cold imposition, indicating that numerous proteins are SUMO modified upon challenge. We identified various cold-related proteins within the subset of abiotic stress-related SUMO-conjugates (Appendix I - Table S1.1), namely, Stabilized 1 (STA1) and the components of transcriptional coactivator complexes ADA2a, ADA2b and GCN5.

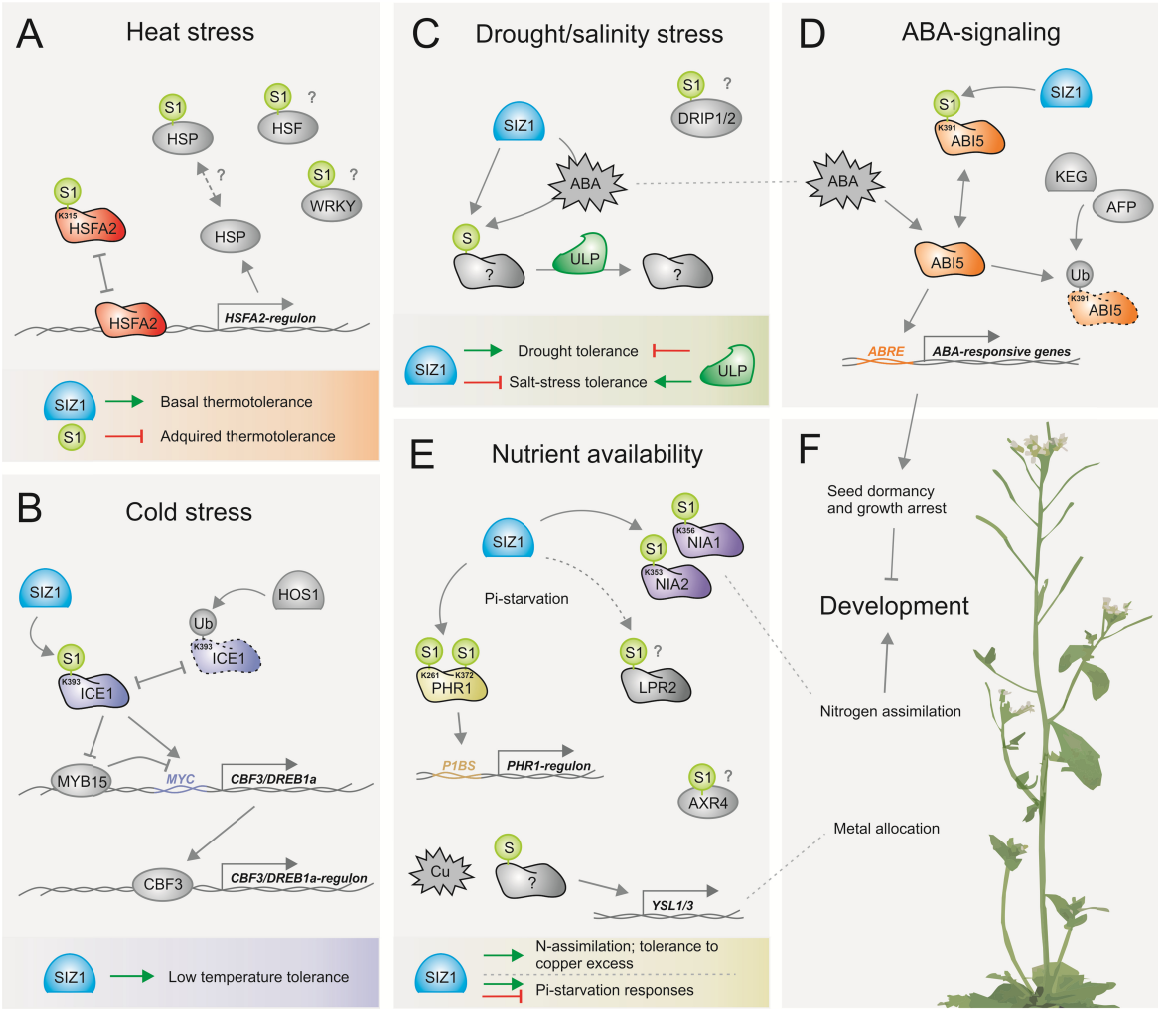

Figure 1.3. Molecular aspects of the SUMO-abiotic stress association in *Arabidopsis thaliana*. **A**, SIZ1 is a positive regulator of basal thermotolerance. Heat shock likely induces sumoylation of several heat shock factors (HSFs), heat shock proteins (HSPs), and WRKYs. Sumoylation of HSFA2 blocks its activity and consequently down-regulates acquired thermotolerance. **B**, Cold stress regulates the transcription factor (TF) ICE1 through SIZ1-dependent sumoylation, antagonizing HOS1-dependent ubiquitination (Ub) and the degradation of ICE1. Sumoylation activates ICE1 inhibiting *MYB15* expression and activating the *CBF3/DREB1a*-regulon. **C**, Salt and drought stress responses seem to be antagonistically regulated by SIZ1 and ULP1c/d. SIZ1 sumoylates and exerts a positive effect on key regulators of the drought response, while ULP1c/d may counteract this effect by removing SUMO from the target. **D**, ABI5, a key TF in the abscisic acid (ABA) signaling pathway, is sumoylated by SIZ1, which antagonizes ABI5-ubiquitination but also inactivates ABI5 TF activity. **E**, Nutrient availability can be controlled by SUMO. SIZ1 sumoylates nitrate reductases NIA1 and NIA2 contributing positively to nitrogen (N) assimilation. In response to inorganic phosphate (Pi) starvation, SIZ1 bi-sumoylates PHR1 and possibly LPR2, activating the expression of the PHR1-regulon and blocking LPR2 function in the remodeling of root architecture under conditions of Pi starvation. In response to excess copper (Cu), SIZ1 sumoylates an unknown target that directly or indirectly regulates expression of *YSL1/3*, important for metal re-allocation. **F**, Sumoylation impacts on development at various levels, including ABI5-mediated seed dormancy and growth arrest, nutrient homeostasis, and allocation of metal ions.

Drought and salt stresses

Drought and salt stresses have tremendous impact on plant growth and development, significantly affecting crop yield. Plants cope with water limitation using complex physiological and molecular strategies that can be generally grouped within the categories of escaping, avoiding or tolerating the stress (Verslues and Juenger, 2011). Drought induces SUMO-conjugate accumulation in Arabidopsis, a process partially dependent on the activity of the E3 ligase SIZ1 (Catala et al., 2007). SIZ1 seems to act positively on drought tolerance since the *siz1* mutant shows drought sensitivity to short- and long-term dehydration. In addition, microarray data indicates that an extensive number of drought-responsive genes are significantly deregulated in *siz1* mutant (Catala et al., 2007). In terms of the stress hormone abscisic acid (ABA), there is sufficient evidence to suggest that both ABA-dependent and -independent mechanisms are involved in the SUMO-drought association (Fig. 1.3C). In support of ABA-independent mechanisms, no significant difference in the sumoylation pattern following drought imposition was observed between wild-type and *aba2* (a mutant impaired in ABA biosynthesis; Catala et al., 2007). The authors suggest that SIZ1 participates in ABA-independent pathways mediated by TFs other than ERD1 and DREB2A, since their regulons are not transcriptionally affected in *siz1* mutant. On the other hand, sumoylation may control the activity of DREB2A by regulating DREB2A-Interacting Protein1 and -2 (DRIP1/2), predicted to be a SUM1 target by Miller and co-workers (2010). These two proteins contain C3HC4 RING domains functioning as E3 ubiquitin ligases that target DREB2A for proteolysis (Qin et al., 2008), therefore acting as negative regulators of drought responses.

In contrast, rice seedlings treated with ABA were shown to accumulate SUMO-conjugates (Chaikam and Karlson, 2010; Park et al., 2010). Most significantly, deregulated genes in *siz1-3* during drought have been found to have a 41% overlap with ABA-responsive genes, and under normal growth conditions, genes of the ABA biosynthetic pathway (namely *ABA1* and *NCED3*) are also deregulated (Nemhauser et al., 2006; Catala et al., 2007). Developmentally, the *siz1* mutant displays ABA hypersensitivity in cotyledon greening after germination, functionally associated to the SP-RING domain responsible for the ligase activity of SIZ1 (Cheong et al., 2009). Over-expression of SUM1/2 attenuated ABA-mediated growth inhibition while SCE1a-co-suppressed lines displayed the opposite phenotype (Lois et al., 2003). It is likely that ABA-signaling changes the sumoylation pattern of at least a small number of targets, enough to exert a phenotypical effect on the plant. A suitable target is the homeobox leucine zipper TF ATHB6, a SUMO-conjugate candidate that negatively regulates ABA-responses (Himmelbach et al., 2002). Strong evidence towards the

SUMO-ABA relationship, albeit distinct from the drought response, is the demonstrated sumoylation of ABA Insensitive 5 (ABI5), a bZIP TF that positively regulates ABA-dependent seed germination and desiccation via binding of the ABA-Responsive Element (ABRE, ACGTGG/TC) *cis*-element (Fig. 1.3D; Miura et al., 2009). SIZ1 knockout does not affect *ABI5* expression but enhances its regulon. The K391 residue of ABI5 is sumoylated in vivo and in vitro in a SIZ1-dependent fashion, rendering ABI5 inactive. In addition, sumoylation may also stabilize ABI5, by counteracting ubiquitin-dependent degradation mediated by the ubiquitin E3 ligase Keep On Going (KEG; Miura et al., 2009).

In contrast to the positive regulation of drought-stress responses, SIZ1 acts as a negative regulator of high salinity responses (Fig. 1.3C). In fact, *siz1* was first isolated from a second mutation screening that suppressed the *sos3* salt-sensitivity phenotype (Miura et al., 2005), and *siz1* seedlings are tolerant to salt. In parallel, the double knockout mutant for SUMO proteases *ULP1c/OTS2* and *ULP1d/OTS1* displays sensitivity to salt stress, while over-expression of *ULP1d/OTS1* increases salt tolerance (Conti et al., 2008). The mutant *ots1 ots2* disrupts SUMO deconjugation constitutively, increasing the accumulation of SUM1/2-conjugated proteins (but not SUM3), particularly in response to salt stress (Conti et al., 2008). Miura and co-workers (2011b) recently found that *siz1* accumulates less sodium (Na) and more potassium (K) in shoots comparatively to the wild-type, suggesting the involvement of ionic adjustments. Salt stress has also been shown to negatively modulate ULP1d/OTS1 (and probably ULP1c/OTS2) abundance via the ubiquitin-proteasome system rather than through transcription (Conti et al., 2008). Thus, it is possible that, at least partially, the increment of SUM1/2-conjugates during stress is due to the turnover of SUMO proteases, implying a new level of regulation in the sumoylation pathway.

Nutrient imbalance

Nutrient deficiency is a type of stress that severely conditions plant growth and development. To circumvent nutritional scarcity plants possess a wide range of strategies, involving morphological, biochemical and transcriptional remodeling. Sumoylation, by controlling the homeostasis of essential nutrients such as N, inorganic phosphate (Pi), and cooper (Cu), is emerging as a hub in nutritional sensing and response in plants (Fig. 1.3E). Under low Pi conditions, *siz1* mutant shows exacerbated Pi-starvation responses, such as inhibition of primary root growth, extensive lateral root and root hair development, increased root-to-shoot ratio, and anthocyanin accumulation, suggesting that this E3 acts as a negative regulator (Miura et al., 2005;

Miura et al., 2011a; Miura et al., 2011b). Remodeling of the root architecture during Pi-deficiency involves an altered auxin pattern, with SIZ1 acting as a negative regulator in the transcription of a series of auxin-responsive genes (Miura et al., 2011a). This regulation may involve the sumoylation of Auxin-Resistant 4 (AXR4, present in the list of abiotic stress-related SUMO-conjugates). AXR4 is involved in auxin redistribution and re-modulates root architecture in response to Pi starvation (Nacry et al., 2005). Miura and co-workers (2005) found that Phosphate Starvation Response 1 (PHR1), a key transcription factor in several Pi-starvation responses, is positively regulated by SIZ1-dependent sumoylation at positions K261 and K372 (Fig. 1.3E). In support of this finding, SIZ1 appears to positively regulate Pi-starvation genes such as *IPS1* and *RNS1*, which are part of the PHR1-regulon (Miura et al., 2005). Also, PHR1 expression is not significantly induced nor its subcellular localization affected by Pi-starvation (Rubio et al., 2001), suggesting modulation at PTM level.

Unlike *siz1*, no differences in root hair length and number have been observed in the *phr1* mutant (Rubio et al., 2001; Miura et al., 2005; Nilsson et al., 2007), suggesting the existence of additional pathways regulated by SIZ1/SUMO in response to Pi-starvation. One plausible candidate found in the SUMO conjugate list by Miller et al. (2010) is Low Phosphate Root-2 (LPR2). LPR2 and its paralog LPR1 are multicopper oxidases that positively control the decrease in primary root length and increase in thenumber of lateral roots upon Pi-starvation (Svistoonoff et al., 2007). Since the *lpr2* seems to be insensitive (while *siz1* is hypersensitive) to Pi-starvation, sumoylation may have a negative effect on LPR2 function. This antagonistic role is supported by the intermediate phenotype displayed by the *lpr1 siz1* double mutant in terms of root architecture, anthocyanin content, and regulation of Pi-starvation-responsive genes *PAP2*, *IPS1* and *PT2* (Wang et al., 2010).

SIZ1-dependent sumoylation also controls N homeostasis in Arabidopsis, positively regulating the catalytic activity of nitrate reductases NIA1 and NIA2 (Park et al., 2011a). These two enzymes are important for N-assimilation, explaining why *siz1* displays low N content. Moreover, the *siz1* pleiotropic phenotype is reverted by exogenous ammonium but not nitrate, reinforcing the notion that deficient N reduction is one of the main determinants of the *siz1* pleiotropic phenotype (Fig. 1.3E,F; Park et al., 2011a).

Nutrient availability is essential for normal growth, yet an excess on nutrients may lead to detrimental effects. For example, Cu is crucial factor in multiple biological processes, but overabundance induces reactive oxygen species (ROS) production and results in toxicity due to its

high redox activity (Cuypers et al., 2011). The involvement of SIZ1 in the control of Cu level and distribution was suggested by Chen and co-workers (2011), who showed that under conditions of excess Cu, the mutant *siz1* accumulated this nutrient in the aerial organs and showed Cu hypersensitivity. These phenotypes could be partially explained by the observed induction of the metal transporters *Yellow Stripe-Like1* and *3* (*YSL1/3*). Since sumoylated proteins increase in a Cu dose-dependent fashion, SUMO is likely to block transcription of *YSL1/3* (Fig. 1.3E; Chen et al., 2011). YSL transporters have been associated to iron and zinc remobilization (Curie et al., 2009), and in fact Chen and co-workers (2011) observed that manganese, zinc, and Pi also accumulate in the *siz1* mutant while the accumulation of potassium decreases, suggesting that sumoylation is closely involved in the allocation and homeostasis of metal ions as well as other nutrients.

1.6. ADDITIONAL INSIGHTS INTO SUMO FUNCTION AND REGULATION BY STRESS

In plants, SUMO seems to take part in the interplay between normal development and abiotic-stress coping modes. Hormones are important factors in many tolerance responses (Hirayama and Shinozaki, 2010; Qin et al., 2011), and should play a key role in the SUMO-abiotic stress association since mutants for SUMO pathway components have been shown to deregulate the metabolism/homeostasis of salicylic acid (SA), ABA, auxins, ethylene, brassinosteroids, jasmonic acid, and cytokinins (Lois et al., 2003; Matarasso et al., 2005; Catala et al., 2007; Lee et al., 2007; Jin et al., 2008; Huang et al., 2009; Ishida et al., 2009; Miura et al., 2009; Miller et al., 2010; Miura et al., 2010; Miura et al., 2011a). The foremost example is SA, which accumulates considerably in *sum1-1 amiR-SUM2*, and *siz1* mutants. Inhibiting SA levels in *siz1* by mutating PAD4 or ectopically expressing the bacterial salicylate hydrolase transgene *NahG* greatly reverts its pleiotropic phenotype (Lee et al., 2007). This includes the SIZ1-dependent response to cold but not that to basal thermotolerance, highlighting an underlying complexity (Yoo et al., 2006; Miura and Ohta, 2010).

SUMO modulation of abiotic stress responses occurs primarily at the nuclear level. Saracco and co-workers (2007) observed that sumoylated proteins concentrate in the nucleus, while part of the free SUMO is cytoplasmic, suggesting that SUMO exerts a function in the regulation and remodeling of the nuclear proteome. In agreement, isolated SUMO targets are mainly nuclear proteins (Budhiraja et al., 2009; Miller et al., 2010; Park et al., 2011b). In general, SUMO is assumed to be a repressor of transcription, namely by modification of chromatin-remodeling

complexes and more specifically by the promotion of histone deacetylation (van den Burg and Takken, 2009, 2010). Not surprisingly, chromatin remodeling is also a critical aspect of plant abiotic stress responses (Kim et al., 2010), and we have identified several chromatin-associated proteins such as GCN5, ADA2a, and ADA2b, within the subset of abiotic stress-related SUMO-conjugates (Appendix I - Table S1.1). A functional correlation is now emerging between sumoylation and mRNA fate in the nucleus (particularly in response to abiotic stress), since in non-plant models, sumoylation candidates are involved in all steps of mRNA processing and export from the nucleus (Meier, 2012). In support of this functional correlation, Arabidopsis ESD4, the first SUMO protease described in plants, is preferentially located in the nuclear periphery, associated to the nuclear pore complex component NUA (Xu et al., 2007), and possibly to the nucleoporin NUP160 (Muthuswamy and Meier, 2011). Mutants of these components accumulate SUMO-conjugates and Poly(A)+ RNA in the nucleus (Xu et al., 2007; Muthuswamy and Meier, 2011). The E3 ligase *siz1* mutant displays similar mRNA retention in the nucleus, while evidencing decreased SUMO levels, particularly in response to stress (Muthuswamy and Meier, 2011). It would appear that the disruption of SUMO homeostasis leads to mRNA accumulation in the nucleus, a phenomenon that can also be observed following abiotic stress (Muthuswamy and Meier, 2011).

Perhaps the most intriguing enigma lays in the regulation of the SUMO pathway. Part of the answer may reside in the fact that the sumoylation machinery itself is a target of SUMO modification. For example, upon being exposed to heat stress, the E1 subunit SAE1 and E2 SCE1 undergo reduced sumoylation while the sumoylation of SIZ1 increases substantially (Miller and Vierstra, 2011). Moreover, SUMO components may themselves be susceptible to temperature changes, as suggested by Castaño-Miquel and co-workers (2011) who showed that sumoylation is enhanced by high temperatures. Interestingly, SIZ1 is a target of multimeric sumoylation in lysines K100, K479 (a non-consensus site) and K488, the first also being modified by oxidative stress (Miller et al., 2010). In mammals, low physiological concentrations of H_2O_2 inhibit SUMO conjugation by inducing the formation of a disulfide bond between the catalytic cysteines of the E1 and E2 enzymes (Bossis and Melchior, 2006a), whereas higher ROS levels inhibit SUMO proteases, leading to increased conjugation (Xu et al., 2009). Modulation of sumoylation by the redox status of the cell is an interesting concept, given that most environmental stimuli trigger ROS signaling events in a wave-like manner (Mittler et al., 2011), consistent with the transient nature of the sumoylation/desumoylation cycle. Interestingly, *siz1* mutants display increased H_2O_2 levels (Kim, 2010). Ascorbate Peroxidase 1 (APX1) and Catalase 3 (CAT3), two important H_2O_2

scavengers and modulators of the cellular redox status (Miller et al., 2007; Mhamdi et al., 2010), are also likely to be sumoylated (Miller et al., 2010; Castano-Miquel et al., 2011). Future research efforts should not overlook the interplay between SUMO and ROS homeostasis.

An increasing focus of attention is the cross-talk between diverse PTMs (Gareau and Lima, 2010; Vertegaal, 2011). An attractive prospect is the identification in plants of human and yeast STUbL orthologs that would link sumoylation of a target to its ubiquitin-dependent protein degradation (Geoffroy and Hay, 2009). Acetylation can also target the same lysine residue as SUMO and ubiquitin (Bossis and Melchior, 2006b), and future focus on the three competing PTMs should be important. In non-plant models, sumoylation was also shown be both positively and negatively regulated by substrate phosphorylation (Bossis and Melchior, 2006b). In Arabidopsis, cross-talk between MAP Kinase 3/6/4 signaling and sumoylation has been suggested, with one example being the common targeting of WRKY TFs (van den Burg and Takken, 2010), opening up new possibilities for SUMO-abiotic stress interplay in plants.

1.7. FINAL CONSIDERATIONS AND FUTURE PERSPECTIVES

A strong correlation between sumoylation and abiotic stress tolerance seems to be conserved among eukaryotic organisms (Tempe et al., 2008), and SUMO has clearly emerged as a heavyweight PTM contender in the regulation of plant development, hormonal metabolism, resistance to pathogen challenge and, particularly, the response to environmental stimuli. Many SUMO targets act as key hubs in abiotic stress responses, yet in vivo, SUMO substrates are modified at very low steady states, a clear contradiction to the drastic phenotypes of mutants with altered SUMO pathways. One possible explanation for this paradox is that SUMO may be a PTM as common as phosphorylation. A first glimpse at the rapidly expanding number of SUMO targets suggests as much, with sumoylation candidates implicating this PTM in key abiotic stress responses. Future gene-centered approaches will be pivotal to confirm these hypotheses at a molecular level. Studies of SUMO pathway components should also be addressed. The E3 ligase SIZ1 is clearly a major abiotic stress determinant, but solving SUMO protease function and specificity will shed new light on the dynamics of SUMO conjugation/deconjugation cycles. Most significantly, future research should address the mechanistic influence of SUMO on target molecules, including chromatin remodeling and RNA-fate mechanisms. The use of high-throughput strategies, such as that of Miller et al. (2010), to accelerate the discovery of SUMO conjugates and

map them to different environmental challenges is now an attractive prospect, particularly when coupled with the use of null mutants of SUMO pathway components. It is clear that understanding the full impact of SUMO on the proteome during abiotic stress will be a demanding yet exciting challenge in forthcoming years.

1.8. OBJECTIVES AND OUTLINE OF THE THESIS

Unfavorable environmental conditions significantly disturb plant growth, and understanding the mechanisms and molecular basis behind the plant response to stress will help establish future strategies to optimize crop yield. Many fundamental advances in gene function discovery have been possible due to the genetic approaches that use *Arabidopsis thaliana* as model plant. Protein post-translational modification provides a molecular regulatory level that has been the focus of increasing attention, particularly in what concerns the plant response to environmental stimuli. SUMO, an ubiquitin-like modifying peptide, has been recently implicated in the regulation of various nuclear processes, including transcriptional control, that coordinate the response to numerous abiotic stresses.

The **main aim** of the current thesis was the functional characterization of SUMO pathway components as potential regulators of the plant abiotic stress response. Since most of these components lacked significant functional characterization, their implication on plant development and biotic stress was also addressed. Studies were carried out in the model plant *Arabidopsis thaliana*, which has been amply used in most plant sumoylation studies. Functional discovery combined a reverse genetics approach, based on loss-of-function T-DNA insertion mutants, and microarray-based transcriptomics. The SUMO E3 ligase SIZ1 is the most studied component of the pathway, and was one of the focus of the current thesis, namely to address the interplay between SUMO, mitogen-activated protein kinase (MAPK) cascades and ROS homeostasis. Another aim of the thesis was the functional study of previously uncharacterized SUMO pathway components, and for this purpose studies were carried out in two SUMO protease gene pairs: ULP1c/ULP1d and ULP2a/ULP2b. The present thesis is organized in seven chapters. The current chapter (**Chapter 1**) provides a general overview of the state of the art for SUMO function in plants, with a special focus on the regulatory role of SUMO on abiotic stress responses.

External stresses converge in the production of ROS, and sumoylation increases in response to oxidative stress. To our knowledge, no function has been previously singled out for

SUMO in the maintenance and/or regulation of ROS homeostasis in plants. Therefore, **Chapter 2** explores the SUMO-ROS relationship using as a model the Arabidopsis *siz1* mutant. We show that SIZ1 is involved in SUMO-conjugate increment in response to exogenous ROS (H_2O_2) and ROS inducers (methyl viologen, MV). In *siz1*, seedlings are sensitive to oxidative stress, and mutants accumulate different ROS throughout development. This deregulation in ROS homeostasis is partially due to SA accumulation in *siz1*. SUMO-related proteins converge with various ROS homeostatic genes. Simultaneously, oxidative stress-dependent SUMO-conjugates suggest a strong interplay between SUMO, ROS and SA at the nuclear level, namely with the involvement of chromatin remodeling proteins.

Albeit the biological importance of SUMO functioning, the mechanisms that indeed control SUMO cycle homeostasis are still unclear. It is likely that internal signaling cascades may control sumoylation. In **Chapter 3** we reported a match in expression patterns, targets and mutant phenotypes, between the MAPK and SUMO signaling cascades. Although no obvious sumoylation of MKK2 or MPK4 or even interaction of SUMOs with MPK4 was observed, mutants of these MAPK components phenocopy *siz1* defects and also control SUMO-conjugate accumulation.

In contrast to the low number of components involved in SUMO conjugation, there are several SUMO proteases coded in plant genomes. SUMO proteases are sources of selectivity, since they can discriminate different SUMO targets to be de-sumoylated, and display different expression patterns and subcellular localizations. Considering that most SUMO proteases are functionally unresolved, we produced homozygous T-DNA mutants for all Arabidopsis ULP family members, and focused on the novel functional characterization of several ULPs. In **Chapter 4** we characterize ULP1c and ULP1d involvement in plant development and the response to water deficit. We show that ULP1c and ULP1d proteases act redundantly to positively regulate growth and germination. GUS reporter assays indicate that both genes are expressed in various developmental stages, with focus on the vasculature. Microarray analysis show that genes involved in development, ABA-signalling and drought tolerance are deregulated in the *ulp1c/d* double mutant. The *ulp1c/d* mutant accumulates high levels of SUMO conjugates even under non-stress conditions, and displays tolerance to prolonged drought. We observe increased stomatal aperture and decreased stomatal density in *ulp1c/d*, with no impact on the response to rapid dehydration. Conversely, *ulp1c/d* displays diminished in vitro root growth under low water potential. Generation and analysis of the triple mutant *ulp1c/d siz1*, suggests that ULP1c/d and SIZ1 may display separate functions in the control of development and the response to low water potential.

In **Chapter 5** we report that ULP1c/d are negative regulators of defence responses against *Pseudomonas syringae* pv. *tomato* (*Pst*) DC3000. The *ulp1c/d* mutant seems to be more tolerant to *Pst* DC3000 infection, but no phenotypes were observed for *ULP1c* or *ULP1d* overexpression lines. Microarray analysis of *ulp1c/d* infiltrated with *Pst* DC3000 led us to conclude that upon infection, ULP1c/d contributes for gene expression regulation associated to various physiological traits. Examples include the up-regulation of *Xyloglucan endotransglucosylase/hydrolases* genes (*XTHs*) and the down-regulation of several auxin-induced genes. Since auxin-responsive genes were affected, we tested *ulp1c/d* for auxin phenotypes in normal growth conditions and upon *Pst* DC3000 challenging. Although no major changes in auxin pattern were observed in *ulp1c/d* using the transgenic line *proDR5::GUS*, *ulp1c/d* displayed sensitivity to exogenous supplementation of auxins.

In **Chapter 6**, we characterize the Arabidopsis SUMO protease pair ULP2a and ULP2b. These proteases are partially redundant and ULP2b seems to play a more dominant role. Phylogenetic and structural analyses place these two proteases in a ULP2-type subgroup that shares many features with SUMO chain editing proteases of non-plant species. The double mutant *ulp2a/b*, and less pronouncedly *ulp2b*, displays several morphological defects. An *ulp2a/b* microarray profile shows a clear deregulation in the expression of genes spatially mapped to the extremity of chromosomes. Some *ulp2a/b* phenotypes are antagonistic to *siz1*, including SUMO-conjugate accumulation, late flowering and higher pigment content. By introgressing *ulp2a/b* with the *siz1* background, we show that *ulp2a/b siz1* morphologically resembles *siz1* and displays a superimposing transcriptional profile with *siz1*, suggesting that ULP2a/b are epistatic to SIZ1.

In the last chapter, **Chapter 7**, we address the main conclusions of the thesis and provide an overview of future research lines.

The work presented in each chapter is arranged in a scientific paper-like manner. Contributions to the current work by collaborators are discriminated in each chapter cover, and the use of the first person plural is adopted as standard throughout the thesis.

1.9. REFERENCES

Anckar J, Hietakangas V, Denessiouk K, Thiele DJ, Johnson MS, Sistonen L (2006) Inhibition of DNA binding by differential sumoylation of heat shock factors. Mol Cell Biol **26:** 955-964

Bayer P, Arndt A, Metzger S, Mahajan R, Melchior F, Jaenicke R, Becker J (1998) Structure determination of the small ubiquitin-related modifier SUMO-1. J Mol Biol **280:** 275-286

Bossis G, Melchior F (2006a) Regulation of SUMOylation by reversible oxidation of SUMO conjugating enzymes. Mol Cell **21:** 349-357

Bossis G, Melchior F (2006b) SUMO: regulating the regulator. Cell Div **1:** 13

Budhiraja R, Hermkes R, Muller S, Schmidt J, Colby T, Panigrahi K, Coupland G, Bachmair A (2009) Substrates related to chromatin and to RNA-dependent processes are modified by Arabidopsis SUMO isoforms that differ in a conserved residue with influence on desumoylation. Plant Physiol **149:** 1529-1540

Burroughs AM, Balaji S, Iyer LM, Aravind L (2007) Small but versatile: the extraordinary functional and structural diversity of the beta-grasp fold. Biol Direct **2:** 18

Castano-Miquel L, Segui J, Lois LM (2011) Distinctive properties of Arabidopsis SUMO paralogues support the in vivo predominant role of AtSUMO1/2 isoforms. Biochem J **436:** 581-590

Catala R, Ouyang J, Abreu IA, Hu Y, Seo H, Zhang X, Chua NH (2007) The Arabidopsis E3 SUMO ligase SIZ1 regulates plant growth and drought responses. Plant Cell **19:** 2952-2966

Chaikam V, Karlson DT (2010) Response and transcriptional regulation of rice SUMOylation system during development and stress conditions. BMB Rep **43:** 103-109

Charng YY, Liu HC, Liu NY, Chi WT, Wang CN, Chang SH, Wang TT (2007) A heat-inducible transcription factor, HsfA2, is required for extension of acquired thermotolerance in Arabidopsis. Plant Physiol **143:** 251-262

Chen C, Chen Y, Tang I, Liang H, Lai C, Chiou J, Yeh K (2011) Arabidopsis SUMO E3 ligase SIZ1 is involved in excess copper tolerance. Plant Physiol **156:** 2225-2234

Cheong MS, Park HC, Hong MJ, Lee J, Choi W, Jin JB, Bohnert HJ, Lee SY, Bressan RA, Yun DJ (2009) Specific domain structures control abscisic acid-, salicylic acid-, and stress-mediated SIZ1 phenotypes. Plant Physiol **151:** 1930-1942

Chosed R, Mukherjee S, Lois LM, Orth K (2006) Evolution of a signalling system that incorporates both redundancy and diversity: Arabidopsis SUMOylation. Biochem J **398:** 521-529

Cohen-Peer R, Schuster S, Meiri D, Breiman A, Avni A (2010) Sumoylation of Arabidopsis heat shock factor A2 (HsfA2) modifies its activity during acquired thermotholerance. Plant Mol Biol **74:** 33-45

Colby T, Matthai A, Boeckelmann A, Stuible HP (2006) SUMO-conjugating and SUMO-deconjugating enzymes from Arabidopsis. Plant Physiol **142:** 318-332

Conti L, Kioumourtzoglou D, O'Donnell E, Dominy P, Sadanandom A (2009) OTS1 and OTS2 SUMO proteases link plant development and survival under salt stress. Plant Signal Behav **4:** 225-227

Conti L, Price G, O'Donnell E, Schwessinger B, Dominy P, Sadanandom A (2008) Small ubiquitin-like modifier proteases OVERLY TOLERANT TO SALT1 and -2 regulate salt stress responses in Arabidopsis. Plant Cell **20:** 2894-2908

Curie C, Cassin G, Couch D, Divol F, Higuchi K, Le Jean M, Misson J, Schikora A, Czernic P, Mari S (2009) Metal movement within the plant: contribution of nicotianamine and yellow stripe 1-like transporters. Ann Bot **103:** 1-11

Cuypers A, Smeets K, Ruytinx J, Opdenakker K, Keunen E, Remans T, Horemans N, Vanhoudt N, Van Sanden S, Van Belleghem F, Guisez Y, Colpaert J, Vangronsveld J (2011) The cellular redox state as a modulator in cadmium and copper responses in *Arabidopsis thaliana* seedlings. J Plant Physiol **168:** 309-316

Downes B, Vierstra RD (2005) Post-translational regulation in plants employing a diverse set of polypeptide tags. Biochem Soc Trans **33:** 393-399

Elrouby N, Coupland G (2010) Proteome-wide screens for small ubiquitin-like modifier (SUMO) substrates identify Arabidopsis proteins implicated in diverse biological processes. Proc Natl Acad Sci U S A **107:** 17415-17420

Eulgem T, Rushton PJ, Robatzek S, Somssich IE (2000) The WRKY superfamily of plant transcription factors. Trends Plant Sci **5:** 199-206

Garcia-Dominguez M, March-Diaz R, Reyes JC (2008) The PHD domain of plant PIAS proteins mediates sumoylation of bromodomain GTE proteins. J Biol Chem **283:** 21469-21477

Garcia-Dominguez M, Reyes JC (2009) SUMO association with repressor complexes, emerging routes for transcriptional control. Biochim Biophys Acta **1789:** 451-459

Gareau JR, Lima CD (2010) The SUMO pathway: emerging mechanisms that shape specificity, conjugation and recognition. Nat Rev Mol Cell Biol **11:** 861-871

Geisler-Lee J, O'Toole N, Ammar R, Provart NJ, Millar AH, Geisler M (2007) A predicted interactome for Arabidopsis. Plant Physiol **145:** 317-329

Geoffroy MC, Hay RT (2009) An additional role for SUMO in ubiquitin-mediated proteolysis. Nat Rev Mol Cell Biol **10:** 564-568

Gill G (2005) Something about SUMO inhibits transcription. Curr Opin Genet Dev **15:** 536-541

Golebiowski F, Matic I, Tatham MH, Cole C, Yin Y, Nakamura A, Cox J, Barton GJ, Mann M, Hay RT (2009) System-wide changes to SUMO modifications in response to heat shock. Sci Signal **2:** ra24

Hay RT (2005) SUMO: a history of modification. Mol Cell **18:** 1-12

Hermkes R, Fu YF, Nurrenberg K, Budhiraja R, Schmelzer E, Elrouby N, Dohmen RJ, Bachmair A, Coupland G (2011) Distinct roles for Arabidopsis SUMO protease ESD4 and its closest homolog ELS1. Planta **233:** 63-73

Himmelbach A, Hoffmann T, Leube M, Hohener B, Grill E (2002) Homeodomain protein ATHB6 is a target of the protein phosphatase ABI1 and regulates hormone responses in Arabidopsis. EMBO J **21:** 3029-3038

Hirayama T, Shinozaki K (2010) Research on plant abiotic stress responses in the post-genome era: past, present and future. Plant J **61:** 1041-1052

Huang L, Yang S, Zhang S, Liu M, Lai J, Qi Y, Shi S, Wang J, Wang Y, Xie Q, Yang C (2009) The Arabidopsis SUMO E3 ligase AtMMS21, a homologue of NSE2/MMS21, regulates cell proliferation in the root. Plant J **60:** 666-678

Ishida T, Fujiwara S, Miura K, Stacey N, Yoshimura M, Schneider K, Adachi S, Minamisawa K, Umeda M, Sugimoto K (2009) SUMO E3 ligase HIGH PLOIDY2 regulates endocycle onset and meristem maintenance in Arabidopsis. Plant Cell **21:** 2284-2297

Jin JB, Jin YH, Lee J, Miura K, Yoo CY, Kim WY, Van Oosten M, Hyun Y, Somers DE, Lee I, Yun DJ, Bressan RA, Hasegawa PM (2008) The SUMO E3 ligase, AtSIZ1, regulates flowering by controlling a salicylic acid-mediated floral promotion pathway and through affects on *FLC* chromatin structure. Plant J **53:** 530-540

Katari MS, Nowicki SD, Aceituno FF, Nero D, Kelfer J, Thompson LP, Cabello JM, Davidson RS, Goldberg AP, Shasha DE, Coruzzi GM, Gutierrez RA (2010) VirtualPlant: a software platform to support systems biology research. Plant Physiol **152:** 500-515

Kerscher O, Felberbaum R, Hochstrasser M (2006) Modification of proteins by ubiquitin and ubiquitin-like proteins. Annu Rev Cell Dev Biol **22:** 159-180

Kim JM, To TK, Nishioka T, Seki M (2010) Chromatin regulation functions in plant abiotic stress responses. Plant Cell Environ **33:** 604-611

Kim MG (2010) Alerted defense system attenuates hypersensitive response-associated cell death in Arabidopsis *siz1* mutant. J Plant Biol **53:** 70-78

Kotak S, Larkindale J, Lee U, von Koskull-Doring P, Vierling E, Scharf KD (2007) Complexity of the heat stress response in plants. Curr Opin Plant Biol **10:** 310-316

Kurepa J, Walker JM, Smalle J, Gosink MM, Davis SJ, Durham TL, Sung DY, Vierstra RD (2003) The small ubiquitin-like modifier (SUMO) protein modification system in Arabidopsis. Accumulation of SUMO1 and -2 conjugates is increased by stress. J Biol Chem **278:** 6862-6872

Lallemand-Breitenbach V, Jeanne M, Benhenda S, Nasr R, Lei M, Peres L, Zhou J, Zhu J, Raught B, de The H (2008) Arsenic degrades PML or PML-RARalpha through a SUMO-triggered RNF4/ubiquitin-mediated pathway. Nat Cell Biol **10:** 547-555

Lee J, Nam J, Park HC, Na G, Miura K, Jin JB, Yoo CY, Baek D, Kim DH, Jeong JC, Kim D, Lee SY, Salt DE, Mengiste T, Gong Q, Ma S, Bohnert HJ, Kwak SS, Bressan RA, Hasegawa PM, Yun DJ (2007) Salicylic acid-mediated innate immunity in Arabidopsis is regulated by SIZ1 SUMO E3 ligase. Plant J **49:** 79-90

Lois LM (2010) Diversity of the SUMOylation machinery in plants. Biochem Soc Trans **38:** 60-64

Lois LM, Lima CD, Chua NH (2003) Small ubiquitin-like modifier modulates abscisic acid signaling in Arabidopsis. Plant Cell **15:** 1347-1359

Lomeli H, Vazquez M (2011) Emerging roles of the SUMO pathway in development. Cell Mol Life Sci **68:** 4045-4064

Lyst MJ, Stancheva I (2007) A role for SUMO modification in transcriptional repression and activation. Biochem Soc Trans **35:** 1389-1392

Makhnevych T, Sydorskyy Y, Xin X, Srikumar T, Vizeacoumar FJ, Jeram SM, Li Z, Bahr S, Andrews BJ, Boone C, Raught B (2009) Global map of SUMO function revealed by protein-protein interaction and genetic networks. Mol Cell **33:** 124-135

Manza LL, Codreanu SG, Stamer SL, Smith DL, Wells KS, Roberts RL, Liebler DC (2004) Global shifts in protein sumoylation in response to electrophile and oxidative stress. Chem Res Toxicol **17:** 1706-1715

Matarasso N, Schuster S, Avni A (2005) A novel plant cysteine protease has a dual function as a regulator of 1-aminocyclopropane-1-carboxylic Acid synthase gene expression. Plant Cell **17:** 1205-1216

Mayer MP, Bukau B (2005) Hsp70 chaperones: cellular functions and molecular mechanism. Cell Mol Life Sci **62:** 670-684

Meier I (2012) mRNA export and sumoylation-Lessons from plants. Biochim Biophys Acta **1819:** 531-537

Meulmeester E, Melchior F (2008) Cell biology: SUMO. Nature **452:** 709-711

Mhamdi A, Queval G, Chaouch S, Vanderauwera S, Van Breusegem F, Noctor G (2010) Catalase function in plants: a focus on Arabidopsis mutants as stress-mimic models. J Exp Bot **61:** 4197-4220

Miller G, Suzuki N, Rizhsky L, Hegie A, Koussevitzky S, Mittler R (2007) Double mutants deficient in cytosolic and thylakoid ascorbate peroxidase reveal a complex mode of interaction between reactive oxygen species, plant development, and response to abiotic stresses. Plant Physiol **144:** 1777-1785

Miller MJ, Barrett-Wilt GA, Hua Z, Vierstra RD (2010) Proteomic analyses identify a diverse array of nuclear processes affected by small ubiquitin-like modifier conjugation in Arabidopsis. Proc Natl Acad Sci U S A **107:** 16512-16517

Miller MJ, Vierstra RD (2011) Mass spectrometric identification of SUMO substrates provides insights into heat stress-induced SUMOylation in plants. Plant Signal Behav **6:** 130-133

Mittler R, Vanderauwera S, Suzuki N, Miller G, Tognetti VB, Vandepoele K, Gollery M, Shulaev V, Van Breusegem F (2011) ROS signaling: the new wave? Trends Plant Sci **16:** 300-309

Miura K, Hasegawa PM (2010) Sumoylation and other ubiquitin-like post-translational modifications in plants. Trends Cell Biol **20:** 223-232

Miura K, Jin JB, Hasegawa PM (2007a) Sumoylation, a post-translational regulatory process in plants. Curr Opin Plant Biol **10:** 495-502

Miura K, Jin JB, Lee J, Yoo CY, Stirm V, Miura T, Ashworth EN, Bressan RA, Yun DJ, Hasegawa PM (2007b) SIZ1-mediated sumoylation of ICE1 controls *CBF3/DREB1A* expression and freezing tolerance in Arabidopsis. Plant Cell **19:** 1403-1414

Miura K, Lee J, Gong Q, Ma S, Jin JB, Yoo CY, Miura T, Sato A, Bohnert HJ, Hasegawa PM (2011a) SIZ1 regulation of phosphate starvation-induced root architecture remodeling involves the control of auxin accumulation. Plant Physiol **155:** 1000-1012

Miura K, Lee J, Jin JB, Yoo CY, Miura T, Hasegawa PM (2009) Sumoylation of ABI5 by the Arabidopsis SUMO E3 ligase SIZ1 negatively regulates abscisic acid signaling. Proc Natl Acad Sci U S A **106:** 5418-5423

Miura K, Lee J, Miura T, Hasegawa PM (2010) SIZ1 controls cell growth and plant development in Arabidopsis through salicylic acid. Plant Cell Physiol **51:** 103-113

Miura K, Ohta M (2010) SIZ1, a small ubiquitin-related modifier ligase, controls cold signaling through regulation of salicylic acid accumulation. J Plant Physiol **167:** 555-560

Miura K, Rus A, Sharkhuu A, Yokoi S, Karthikeyan AS, Raghothama KG, Baek D, Koo YD, Jin JB, Bressan RA, Yun DJ, Hasegawa PM (2005) The Arabidopsis SUMO E3 ligase SIZ1 controls phosphate deficiency responses. Proc Natl Acad Sci U S A **102:** 7760-7765

Miura K, Sato A, Ohta M, Furukawa J (2011b) Increased tolerance to salt stress in the phosphate-accumulating Arabidopsis mutants *siz1* and *pho2*. Planta **234:** 1191-1199

Murtas G, Reeves PH, Fu YF, Bancroft I, Dean C, Coupland G (2003) A nuclear protease required for flowering-time regulation in Arabidopsis reduces the abundance of SMALL UBIQUITIN-RELATED MODIFIER conjugates. Plant Cell **15:** 2308-2319

Muthuswamy S, Meier I (2011) Genetic and environmental changes in SUMO homeostasis lead to nuclear mRNA retention in plants. Planta **233:** 201-208

Nacry P, Canivenc G, Muller B, Azmi A, Van Onckelen H, Rossignol M, Doumas P (2005) A role for auxin redistribution in the responses of the root system architecture to phosphate starvation in Arabidopsis. Plant Physiol **138:** 2061-2074

Nemhauser JL, Hong F, Chory J (2006) Different plant hormones regulate similar processes through largely nonoverlapping transcriptional responses. Cell **126:** 467-475

Nigam N, Singh A, Sahi C, Chandramouli A, Grover A (2008) SUMO-conjugating enzyme (Sce) and FK506-binding protein (FKBP) encoding rice (*Oryza sativa* L.) genes: genome-wide analysis, expression studies and evidence for their involvement in abiotic stress response. Mol Genet Genomics **279:** 371-383

Nilsson L, Muller R, Nielsen TH (2007) Increased expression of the MYB-related transcription factor, PHR1, leads to enhanced phosphate uptake in *Arabidopsis thaliana*. Plant Cell Environ **30:** 1499-1512

Novatchkova M, Budhiraja R, Coupland G, Eisenhaber F, Bachmair A (2004) SUMO conjugation in plants. Planta **220:** 1-8

Okada S, Nagabuchi M, Takamura Y, Nakagawa T, Shinmyozu K, Nakayama J, Tanaka K (2009) Reconstitution of Arabidopsis thaliana SUMO pathways in *E. coli*: functional evaluation of SUMO machinery proteins and mapping of SUMOylation sites by mass spectrometry. Plant Cell Physiol **50:** 1049-1061

Park BS, Song JT, Seo HS (2011a) Arabidopsis nitrate reductase activity is stimulated by the E3 SUMO ligase AtSIZ1. Nat Commun **2:** 400

Park HC, Choi W, Park HJ, Cheong MS, Koo YD, Shin G, Chung WS, Kim WY, Kim MG, Bressan RA, Bohnert HJ, Lee SY, Yun DJ (2011b) Identification and molecular properties of SUMO-binding proteins in Arabidopsis. Mol Cells **32:** 143-151

Park HC, Kim H, Koo SC, Park HJ, Cheong MS, Hong H, Baek D, Chung WS, Kim DH, Bressan RA, Lee SY, Bohnert HJ, Yun DJ (2010) Functional characterization of the SIZ/PIAS-type SUMO E3 ligases, OsSIZ1 and OsSIZ2 in rice. Plant Cell Environ **33:** 1923-1934

Park HJ, Kim WY, Park HC, Lee SY, Bohnert HJ, Yun DJ (2011c) SUMO and SUMOylation in plants. Mol Cells **32:** 305-316

Qin F, Sakuma Y, Tran LS, Maruyama K, Kidokoro S, Fujita Y, Fujita M, Umezawa T, Sawano Y, Miyazono K, Tanokura M, Shinozaki K, Yamaguchi-Shinozaki K (2008) Arabidopsis DREB2A-interacting proteins function as RING E3 ligases and negatively regulate plant drought stress-responsive gene expression. Plant Cell **20:** 1693-1707

Qin F, Shinozaki K, Yamaguchi-Shinozaki K (2011) Achievements and challenges in understanding plant abiotic stress responses and tolerance. Plant Cell Physiol **52:** 1569-1582

Reed JM, Dervinis C, Morse AM, Davis JM (2010) The SUMO conjugation pathway in Populus: genomic analysis, tissue-specific and inducible SUMOylation and in vitro de-SUMOylation. Planta **232:** 51-59

Reeves PH, Murtas G, Dash S, Coupland G (2002) *early in short days 4*, a mutation in Arabidopsis that causes early flowering and reduces the mRNA abundance of the floral repressor *FLC*. Development **129:** 5349-5361

Richter K, Haslbeck M, Buchner J (2010) The heat shock response: life on the verge of death. Mol Cell **40:** 253-266

Rubio V, Linhares F, Solano R, Martin AC, Iglesias J, Leyva A, Paz-Ares J (2001) A conserved MYB transcription factor involved in phosphate starvation signaling both in vascular plants and in unicellular algae. Genes Dev **15:** 2122-2133

Rytinki MM, Kaikkonen S, Pehkonen P, Jaaskelainen T, Palvimo JJ (2009) PIAS proteins: pleiotropic interactors associated with SUMO. Cell Mol Life Sci **66:** 3029-3041

Saracco SA, Miller MJ, Kurepa J, Vierstra RD (2007) Genetic analysis of SUMOylation in Arabidopsis: conjugation of SUMO1 and SUMO2 to nuclear proteins is essential. Plant Physiol **145:** 119-134

Supek F, Bosnjak M, Skunca N, Smuc T (2011) REVIGO summarizes and visualizes long lists of gene ontology terms. PLoS One **6:** e21800

Svistoonoff S, Creff A, Reymond M, Sigoillot-Claude C, Ricaud L, Blanchet A, Nussaume L, Desnos T (2007) Root tip contact with low-phosphate media reprograms plant root architecture. Nat Genet **39:** 792-796

Tempe D, Piechaczyk M, Bossis G (2008) SUMO under stress. Biochem Soc Trans **36:** 874-878

van den Burg HA, Kini RK, Schuurink RC, Takken FL (2010) Arabidopsis small ubiquitin-like modifier paralogs have distinct functions in development and defense. Plant Cell **22:** 1998-2016

van den Burg HA, Takken FL (2009) Does chromatin remodeling mark systemic acquired resistance? Trends Plant Sci **14:** 286-294

van den Burg HA, Takken FL (2010) SUMO-, MAPK-, and resistance protein-signaling converge at transcription complexes that regulate plant innate immunity. Plant Signal Behav **5:** 1597-1601

Verslues PE, Juenger TE (2011) Drought, metabolites, and Arabidopsis natural variation: a promising combination for understanding adaptation to water-limited environments. Curr Opin Plant Biol **14:** 240-245

Vertegaal AC (2011) Uncovering ubiquitin and ubiquitin-like signaling networks. Chem Rev **111:** 7923-7940

Wang X, Du G, Meng Y, Li Y, Wu P, Yi K (2010) The function of LPR1 is controlled by an element in the promoter and is independent of SUMO E3 Ligase SIZ1 in response to low Pi stress in Arabidopsis thaliana. Plant Cell Physiol **51:** 380-394

Wilkinson KA, Henley JM (2010) Mechanisms, regulation and consequences of protein SUMOylation. Biochem J **428:** 133-145

Xu XM, Rose A, Muthuswamy S, Jeong SY, Venkatakrishnan S, Zhao Q, Meier I (2007) NUCLEAR PORE ANCHOR, the Arabidopsis homolog of Tpr/Mlp1/Mlp2/megator, is involved in mRNA export and SUMO homeostasis and affects diverse aspects of plant development. Plant Cell **19:** 1537-1548

Xu Z, Chan HY, Lam WL, Lam KH, Lam LS, Ng TB, Au SW (2009) SUMO proteases: redox regulation and biological consequences. Antioxid Redox Signal **11:** 1453-1484

Yoo CY, Miura K, Jin JB, Lee J, Park HC, Salt DE, Yun DJ, Bressan RA, Hasegawa PM (2006) SIZ1 small ubiquitin-like modifier E3 ligase facilitates basal thermotolerance in Arabidopsis independent of salicylic acid. Plant Physiol **142:** 1548-1558

Zhou W, Ryan JJ, Zhou H (2004) Global analyses of sumoylated proteins in *Saccharomyces cerevisiae*. Induction of protein sumoylation by cellular stresses. J Biol Chem **279:** 32262-32268

Chapter 2

Arabidopsis thaliana SUMO E3 ligase SIZ1 is a key modulator of reactive oxygen species homeostasis

Daniel Couto contributed to the ROS staining and enzymatic activities estimation. Sara Freitas and Miguel Ângelo contributed to the characterization of phenotypes.

CONTENTS

2.1. INTRODUCTION

Incorporation of molecular oxygen (O_2) into metabolic processes considerably expanded energetic efficiency but also led to the concomitant production of partially reduced or activated forms of oxygen, designated reactive oxygen species (ROS). Potentially dangerous ROS forms can occur by energy transfer (singlet oxygen, $^1O_2$) or by electron transfer reactions (superoxide, $O_2^{\bullet-}$; hydrogen peroxide, H_2O_2; hydroxyl radical, $HO^{\bullet}$; Apel and Hirt, 2004). ROS are predominantly produced as by-products of metabolism, namely in chloroplasts, mitochondria and peroxisomes, and a competent network of ROS scavenging mechanisms has evolved to ensure appropriate ROS homeostatic levels (Mittler et al., 2004). In recent years, ROS have been increasingly viewed as central and extremely effective signalling molecules, contributing for the integration of hormone signals and plant development (Gadjev et al., 2006; Mittler et al., 2011). In fact, ROS can induce transcriptional changes that are specific of their chemical nature and subcellular origin (Gadjev et al., 2006; Rosenwasser et al., 2011). Production of ROS is a common feature of plant stress responses, and it is believed to play a key role in the signal transduction pathways that lead to transcriptional reprogramming (Gadjev et al., 2006; Miller et al., 2010a).

Post-translational modifications (PTMs) are essential, rapid and reversible protein activity modulators. These modifications are particularly important for plants that, being sessile, require optimal and swift responses to a constantly changing environment. One PTM of pivotal importance employs modification by ubiquitin and small ubiquitin-like peptides (UBLs). Ubiquitin is the focus of intensive research, but the UBL class includes the increasingly important Small Ubiquitin-like Modifier (SUMO; Miura and Hasegawa, 2010). Modification by SUMO can exert different effects on a target protein, including conformational changes, and creation or blocking of interacting interfaces (Wilkinson and Henley, 2010). Most SUMO targets are associated to nuclear-related functions, involving histone regulation, formation of subnuclear bodies, remodeling of chromatin complexes, and ultimately contributing for transcription regulation (Lyst and Stancheva, 2007; Cubenas-Potts and Matunis, 2013). The mechanism by which SUMO is attached to a target is named sumoylation: SUMO peptides are first processed by SUMO proteases (ULP/SENP family) exposing an N-terminal di-glycine motif, and are then conjugated to a target protein via SUMO E1 activases (SAE1/SAE2 heterodimer) and SUMO E2 conjugases (SCE), with the aid of SUMO E3 ligases (e.g. SIZ/PIAS family); deconjugation of the SUMO peptide is carried out by SUMO proteases (Gareau and Lima, 2010). SUMO homeostasis has been proved to be fundamental for plant development because mutations in pathway components result in embryonic lethality or

pleiotropic phenotypes (Murtas et al., 2003; Catala et al., 2007; Saracco et al., 2007; Ishida et al., 2009; Miura et al., 2010). Most functional studies have been carried out in *siz1* mutants that are dwarf but not lethal (Catala et al., 2007; Miura et al., 2010). SIZ1 is involved in many abiotic stress tolerance mechanisms, including the response to extreme temperatures, drought, salinity, and altered levels of nutrient availability (Castro et al., 2012). One interesting feature of SUMO is that SUMO-conjugates rapidly accumulate upon stress conditions, placing SUMO in the first stages of the plant response to stress, most likely associated to transcriptional re-programming (Castro et al., 2012).

Sumoylation machinery components are themselves targets of SUMO modification, a process that may be modulated by stress. While E1 subunit SAE1 and E2 SCE1 seem to be less sumoylated in response to heat shock, SIZ1 is heavily and transiently sumoylated at multiple lysines (Miller et al., 2010b; Miller and Vierstra, 2011; Miller et al., 2013). In addition, other stress conditions such as H_2O_2 and ethanol induce SIZ1 sumoylation, being SIZ1 one of the most SUMO-modified targets reported by high-throughput analysis of the sumoylome (Miller et al., 2013). SUMO-conjugates accumulate in response to oxidative conditions, but the mechanism through which conjugates increase is still unresolved. Cellular redox fluxes in response to multiple environmental stimuli may ultimately regulate SUMO-conjugates levels. At low concentrations of H_2O_2, a disulfide bond within the catalytic cysteines of the mammal E1 and E2 is produced, inhibiting sumoylation (Bossis and Melchior, 2006). Meanwhile, higher concentrations of ROS lead to inhibition of SUMO protease activity (Xu et al., 2008), suggesting that in non-plant models, SUMO pathway components are highly responsive to the cellular redox status. Examples of possible plant SUMO conjugates that are part of the ROS scavenging network include APX1 and CAT3 (Miller et al., 2010b; Castano-Miquel et al., 2011). Recently, Miller et al. (2013) reported that APX1 is highly and specifically over-sumoylated in response to H_2O_2 treatment.

In the present study we provide evidence towards a reciprocal regulation between ROS levels and sumoylation. We demonstrated that SIZ1 is important for SUMO-conjugate induction in response to oxidative conditions. Moreover the *siz1* mutant displayed altered ROS homeostasis, constitutively accumulating H_2O_2, superoxide ion and singlet oxygen. In addition, *siz1* shoots are sensitive to both exogenous and endogenous ROS. These *siz1* phenotypes can be greatly recovery by the expression of the transgenic salicylate hydroxylase *NahG*, implicating salicylic acid (SA) in the de-regulation of ROS homeostatic levels.

2.2. RESULTS

Endogenous and exogenous ROS induce SIZ1-dependent sumoylation

There is strong evidence towards a correlation between sumoylation and ROS homeostatic levels, since in non-plant models, oxidative stress has been linked with an increase in high molecular weight SUMO-conjugate levels (Manza et al., 2004; Zhou et al., 2004; Bossis and Melchior, 2006). The existence of this phenomenon in plants was first identified in hydroponically-grown Arabidopsis seedlings subjected to exogenous H_2O_2 (Kurepa et al., 2003; Miller et al., 2013). To better resolve how ROS determine the plant sumoylation status, we infiltrated 10-day-old Arabidopsis seedlings with an exogenous ROS source (H_2O_2) and induced internal ROS using methyl viologen (MV), prior to analyzing the SUMO-conjugate profile. The total protein immunoblot was performed using antibodies raised against the main Arabidopsis SUMO peptides SUM1/2 and SUM3. The Arabidopsis SUMO E3 ligase SIZ1 is the major E3 associated to abiotic stress responses (Castro et al., 2012). SIZ1 null alleles are standard for functional studies on sumoylation in Arabidopsis, therefore experiments were carried out using the knockout *siz1-2* mutant.

As depicted in Figure 2.1A, an increase in SUM1/2-conjugates was observed following both H_2O_2 and MV challenges. Endogenous generation of ROS via MV generated higher SUMO-conjugate levels when compared to exogenous ROS generation by H_2O_2. Consistently, a clear dose-dependent response was observed for MV, whereas no obvious dose-dependency was observed at existing concentrations of exogenously applied H_2O_2. Results suggest that priming SUMO conjugation with MV was more efficient, and should be subsequently used as a methodology. As expected, accumulation of SUM1/2-conjugates was severely impaired in the loss-of-function mutant for the E3 ligase SIZ1 (Fig. 2.1A), placing SIZ1 as a modulator of ROS-dependent increase of SUM1/2-conjugation. In contrast to SUM1/2, SUM3-conjugates did not accumulate in response to oxidative stress (Fig. 2.1B). Overall results suggest that SUM1/2 are the main Arabidopsis SUMO isoforms that respond to ROS, and that their conjugation is greatly SIZ1-dependent.

The *siz1* mutant displays altered responses to oxidative stress

The correlation between SUMO-conjugates and increased ROS levels suggests a role for sumoylation in the response to oxidative stress. Thus we analyzed *siz1-2* behavior in the presence of MV, which generates oxidative stress mostly by promoting the formation of superoxide ion in

photosynthetically active tissues (Fujii et al., 1990; Scarpeci et al., 2008). We observed that shoots in *siz1-2* were sensitive to the presence of high concentrations of MV in the medium (Fig. 2.2A-C). Interestingly, low MV doses produced an increment in shoot growth, but this was only observed in wild-type plants (Fig. 2.2A,B). In vertically-grown *siz1-2*, inhibition of shoot growth was accompanied by increased root growth (Fig. 2.2C,D). The germination rate, which is constitutively delayed in *siz1-2*, was not differentially affected in relation to the wild-type in the presence of MV (data not shown). We also exposed *siz1-2* to H_2O_2-dependent oxidative stress. For that purpose, 10-day-old seedlings were incubated overnight with different concentrations of H_2O_2 and oxidative damage was assessed by analyzing chlorophyll pigmentation (Fig. 2.2E; data not shown). Similar to MV treatments, results suggest that *siz1-2* is more sensitive to exogenously-applied H_2O_2.

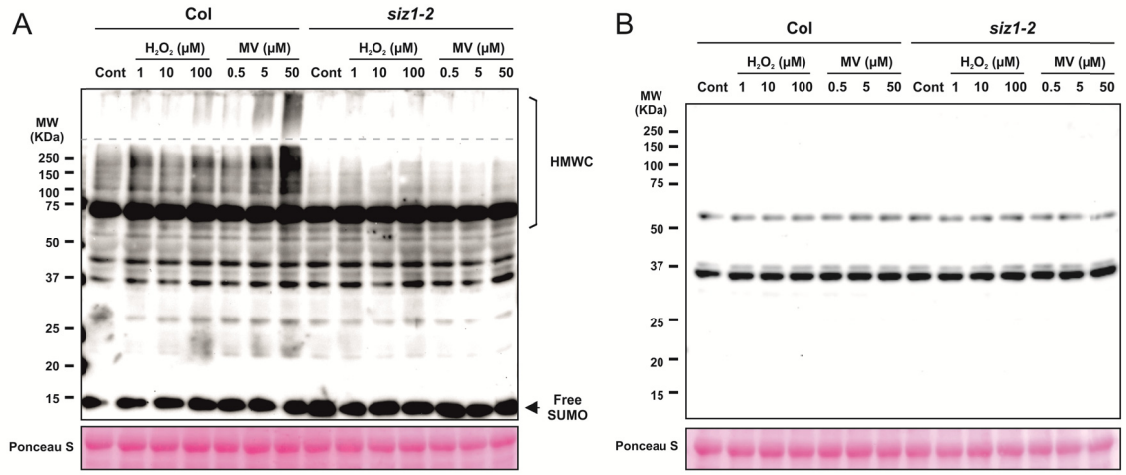

Figure 2.1. Western blot analysis of high molecular weight SUMO-conjugates (HMWC) following infiltration of 10-day-old wild-type (Col) and *siz1-2* seedlings with increasing concentrations of H_2O_2 and methyl viologen (MV). Protein extracts (20 μg per lane) were analyzed by protein gel blots using anti-AtSUM1 (**A**) and anti-AtSUM3 (**B**) polyclonal antibodies. As a loading control, Ponceau S staining of the large subunit of Rubisco (55 kDa) is displayed.

The *siz1* mutant accumulates superoxide ion and hydrogen peroxide

Since ROS control various aspects of plant development (Mittler et al., 2004; Schippers et al., 2012) and several SUMO pathway mutants have developmental defects (Castro et al., 2012), we analyzed homeostatic levels of the major ROS hydrogen peroxide (H_2O_2) and superoxide ion ($O_2^{\cdot-}$) at various developmental stages of *siz1-2*. We used vacuum infiltration with specific 3,3'-diaminobenzidine (DAB) and nitroblue tetrazolium (NBT) probes to respectively stain H_2O_2 and $O_2^{\cdot-}$, a methodology that has been successfully employed in Arabidopsis (Ramel et al., 2009). In adult plants, when *siz1* developmental defects are most extreme, *siz1-2* accumulated more H_2O_2 (Fig. 2.3A). Dwarfism in soil-grown adult *siz1* has been coupled with increased cell density

(~2.3-fold) in *siz1* leaves (Catala et al., 2007). To test whether ROS accumulation correlated with increased cell density, we performed DAB staining in 21- and 10-day-old in vitro-grown seedlings, which are developmentally similar to the wild-type (Fig. 2.3B,C; Catala et al., 2007). Increased DAB staining in *siz1-2* was consistent in younger plants (Fig. 2.3A-C), suggesting that ROS accumulation does not correlate with cell density.

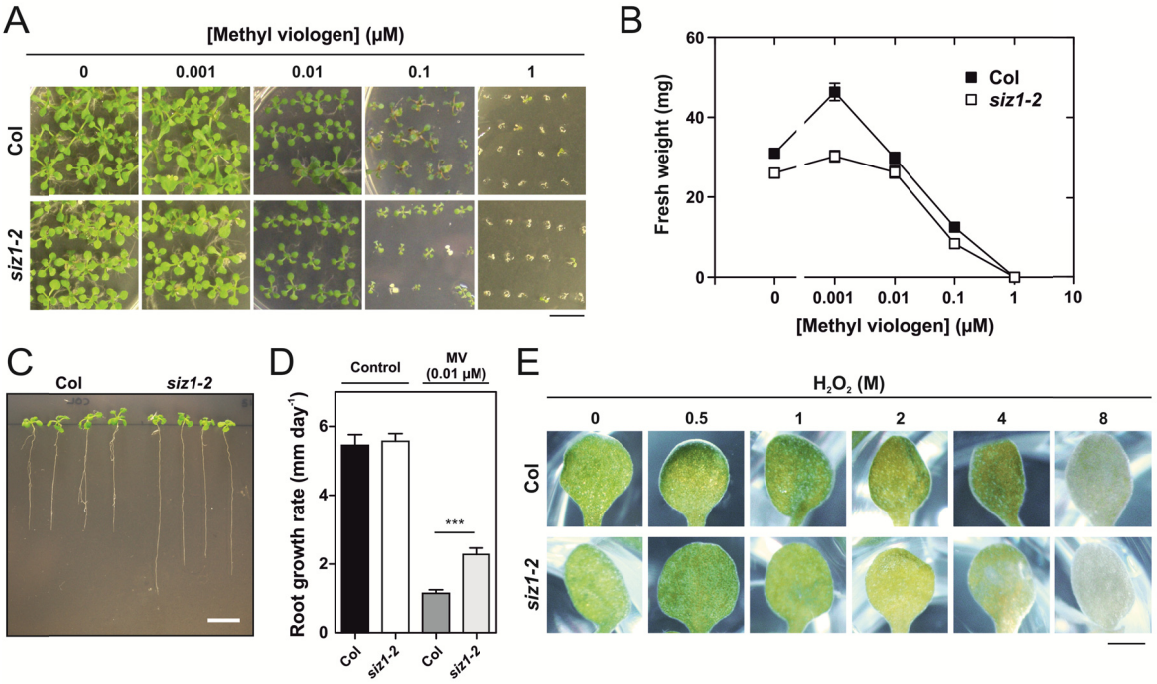

Figure 2.2. Characterization of the *siz1* response to oxidative stress imposition. **A**, Morphology of Col and *siz1-2* plants germinated and horizontally-grown for 3 weeks in MS media supplemented with different concentrations of MV. **B**, Plant fresh weight of Col and *siz1-2* germinated and horizontally-grown for 3 weeks in MS media supplemented with different concentrations of MV; error bars represent standard error of the means (SEM), n ≥ 4. **C**, 7-day-old Col and *siz1-2* seedlings were vertically grown for 10 days in MS media supplemented with 0.01 µM MV; bar represents 1 cm. **D**, Measurement of root growth during MV-induced oxidative stress; error bars represent SEM, n = 20. **F**, Pigment bleaching of 10-day-old seedlings induced by increasing concentrations of H_2O_2. Asterisks represent statistically significant differences between genotypes (unpaired t test; ***, P<0.001); bar represents 1 mm.

Meanwhile, adult plants displayed almost no NBT staining, and most importantly, *siz1-2* superoxide ion levels were seemingly identical to the wild-type (Fig. 2.3A). In younger plants however, superoxide ion accumulated in *siz1-2* plants, particularly in emerging leaves (Fig. 2.3B,C). In 10-day-old seedlings, both DAB and NBT staining were stronger in the leaf vasculature, which is consistent with the *SIZ1* expression pattern (Catala et al., 2007), while in roots, *siz1-2* displayed a marked increase in DAB staining (Fig. 2.3D) which was not apparent for NBT staining (Fig. 2.3E). Overall results suggest that *siz1-2* is compromised in its capacity to maintain ROS homeostasis, and that ROS accumulation precedes the development of the dwarf *siz1* phenotype.

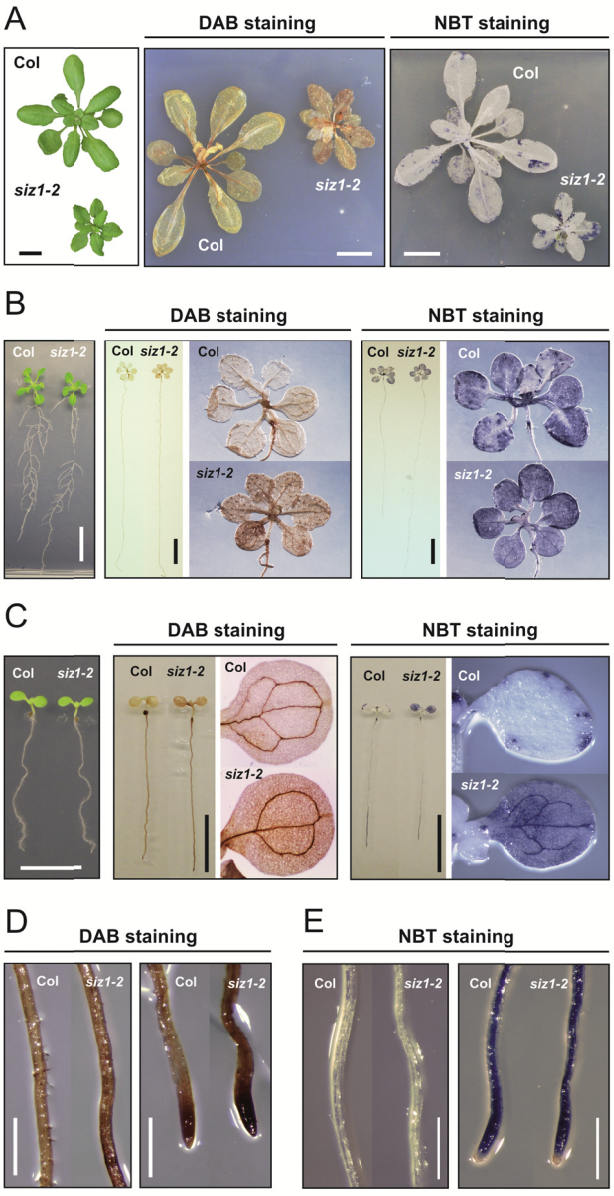

Figure 2.3. Histochemical staining of wild-type (Col) and *siz1-2* plants using 3,3-diaminobenzidine (DAB) to detect H_2O_2 and nitroblue tetrazolium (NBT) to detect O^{2-} levels. **A**, Morphology and staining with DAB or NBT of 4-week-old soil-grown plants. **B**, Morphology and staining with DAB or NBT of 21-day-old in vitro-grown plants. **C**, Morphology and staining with DAB or NBT of 10-day-old in vitro-grown plants. **D**, DAB staining of roots from 10-day-old in vitro-grown plants. **E**, NBT staining of roots from 10-day-old in vitro-grown plants. Bar indicates 1 cm (A-C) and 0.5 mm (D,E).

SA levels correlate with ROS homeostatic levels

Defects in *siz1* have been tightly linked with SA over-accumulation (Lee et al., 2007; Miura et al., 2010). High SA content has been shown to promote an increase in ROS levels (Mateo et al., 2006; Rivas-San Vicente and Plasencia, 2011), which could explain the ROS accumulation phenotype of *siz1* mutants. We therefore crossed *siz1-2* with *NahG*, a transgenic line expressing a bacterial SA hydroxylase that converts SA into catechol (Katagiri et al., 1965; Delaney et al., 1994). As previously reported, *NahG* partially reverts the dwarfed phenotype of *siz1-2* by removing excess SA (Appendix II – Fig. S2.1A; Lee et al., 2007; Miura et al., 2010). Subsequent analysis showed that in *siz1-2 NahG* seedlings, H_2O_2 accumulation decreased significantly in seedling leaves and

roots (Fig. 2.4A,B), while superoxide accumulation was abolished (Fig. 2.4C). This result was also observed in latter developmental stages (Appendix II – Fig. S2.1B,C).

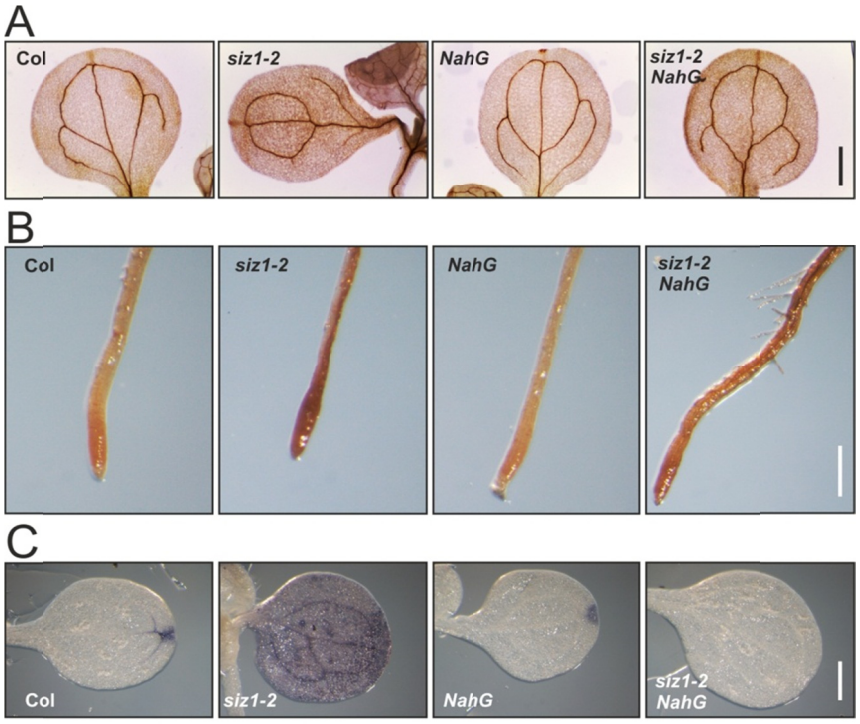

Figure 2.4. Analysis on the influence of salicylic acid (SA) in *siz1* ROS homeostasis, by introgression of *siz1-2* with the transgenic SA hydroxylase *NahG*. **A,B**, Histochemical DAB staining of 10-day-old seedling cotyledon leaves (A) and roots (B). **C**, Histochemical NBT staining of 10-day-old seedling cotyledon leaves. Bars indicate 0.5 mm.

SIZ1 mutant seedlings are not affected in major ROS scavenging enzyme activities

Overall oxidative damage in *siz1* seedlings was quantified by estimating lipid peroxidation levels (Fig. 2.5A). Surprisingly, no significant changes in lipid peroxide content were observed at this developmental stage. Taking into consideration that ROS homeostatic levels are maintained by various detoxification mechanisms, with a major role played by ROS-scavenging enzymes (Mittler et al., 2004), we subsequently analyzed whether altered ROS levels in *siz1-2* reflected changes in the total activity of the main scavenging enzyme classes. Surprisingly, the total activity of catalase (CAT), ascorbate peroxidase (APX), superoxide dismutase (SOD), and the total peroxidase activity (PPOD) were not significantly altered in 10-day-old *siz1-2* mutant plants (Fig. 2.5). Results suggest that at this development stage, *siz1* is not defective in its ROS scavenging activity, or is perhaps inhibited in its capacity to mount an effective response to oxidative stress leading to accumulation of ROS. Data is, however, preliminary and further confirmation as well as analysis in adult plants is required.

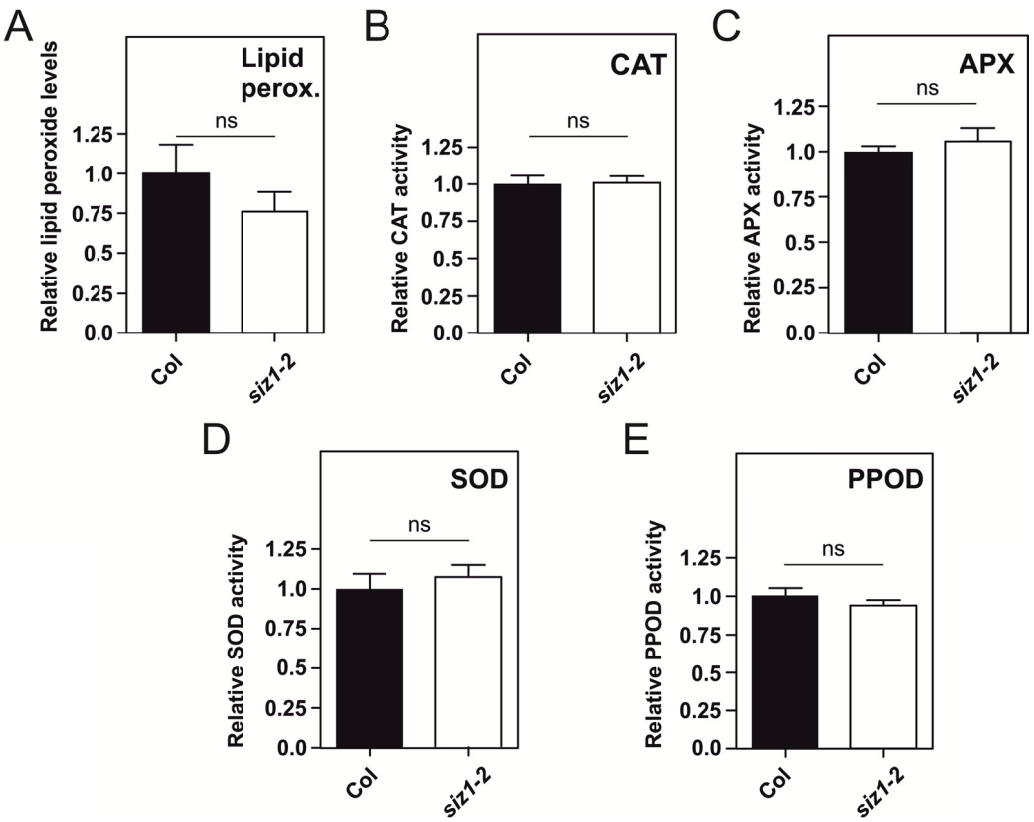

Figure 2.5. Lipid peroxidation levels and activity of ROS-scavenging enzymes in 10-day-old *siz1-2* seedlings, in relation to the wild-type (Col). **A**, Production of MDA-TBA complexes as a consequence of lipid peroxide presence; n = 4. **B**, Total catalase (CAT) activity; n = 9. **C**, Total ascorbate peroxidase (APX) activity; n = 4. **D**, Total superoxide dismutase (SOD) activity; n = 5. **E**, Total pyrogallol peroxidase (PPOD) activity; n = 8. Error bars represent SEM; *ns* represents non-significance ($P > 0.05$) following an unpaired t test.

Sumoylation interplays with key components of the ROS homeostatic network

Management of ROS levels requires a highly dynamic and redundant network of genes encoding both ROS-scavenging and ROS-producing proteins, designated the ROS Gene Network (RGN; Mittler et al., 2004). The complete *Arabidopsis thaliana* RGN has been annotated, as well as the full set of predicted peroxidases (PRX) existing in the Arabidopsis genome. Altogether, they comprise >200 genes that make out a framework to functionally address ROS homeostasis. This data was used to assess the potential interplay between sumoylation and ROS homeostasis, through a series of in silico studies.

A major objective of current SUMO research is the identification of the full set of SUMO targets, and a combination of protein-centered and high-throughput approaches has allowed for the compilation of hundreds of SUMO-related genes, namely (1) the compiled set of SUMO conjugates that have been experimentally validated or sequenced following tag-SUMO approaches

(Castro et al., 2012); (2) the compiled set of known protein-protein interactors with the SUMO conjugation/deconjugation machinery (Castro et al., 2012). Data included a subset of SUMO conjugates that differentially increase following oxidative stress (Miller et al., 2013). We first cross-referenced the RGN and PRX datasets with SUMO-related genes. Surprisingly only six overlapping genes were observed, all encoding RGN members (Fig. 2.6A,B; Table 2.1). Major ROS-scavenging enzymes APX1, CAT1, CAT3 and FSD1, as well as the thioredoxin-like TTL1, were identified as SUMO targets, and APX1 was within the subset of oxidative stress-induced SUMO conjugates (Table 2.1). The thioredoxin ATHX was identified as a predicted protein interactor of the SUMO pathway E2 enzyme (SCE1) and the SUMO protease ESD4 (Fig. 2.6B; Elrouby and Coupland, 2010).

Table 2.1. Involvement of ROS Gene Network components and peroxidases with SUMO. Arabidopsis genes of all described SUMO-conjugates (Castro et al., 2012; Lopez-Torrejon et al., 2013; Miller et al., 2013), as well as differentially expressed genes in adult *siz1-3* (Catala et al., 2007) and 10-day-old *siz1-2* (current work), were cross-referenced with ROS Gene Network and typical Arabidopsis peroxidases (biol.unt.edu/~rmittler/re4.htm).

AGI Code	Gene Name	Description	Functional association to SUMO
ROS Gene Network			
At1g07890	*APX1; CS1; MEE6*	Ascorbate peroxidase 1	SUMO conjugate (oxidative stress inducible)
At1g20630	*CAT1*	Catalase 1	SUMO conjugate; down-regulated in *siz1-2* seedlings
At1g20620	*CAT3; SEN2*	Catalase 3	SUMO conjugate
At4g25100	*FSD1*	Fe superoxide dismutase 1	SUMO conjugate; up-regulated in *siz1-2* seedlings
At1g06830		Glutaredoxin family protein	Up-regulated in *siz1-2* seedlings
At1g63940	*MDAR6*	Monodehydroascorbate reductase 6	Up-regulated in *siz1-2* seedlings
At3g24170	*GR1*	Glutathione-disulfide reductase	Up-regulated in *siz1-2* seedlings
At1g53300	*TTL1*	Tetratricopetide-repeat thioredoxin-like 1	SUMO conjugate
At1g50320	*ATHX; THX*	Thioredoxin X	Sumoylation interactor
At4g15680		Thioredoxin superfamily protein	Up-regulated in *siz1-2* seedlings
At5g07460	*ATMSRA2; PMSR2*	Peptidemethionine sulfoxide reductase 2	Up-regulated in *siz1-2* seedlings
At1g08830	*CSD1*	Copper/zinc superoxide dismutase 1	Down-regulated in *siz1-2* seedlings
At1g48130	*PER1*	1-cysteine peroxiredoxin 1	Down-regulated in *siz1-2* seedlings
At2g28190	*CSD2; CZSOD2*	Copper/zinc superoxide dismutase 2	Down-regulated in *siz1-2* seedlings
At1g03850	*GRXS13*	Glutaredoxin family protein	Up-regulated in adult *siz1-3*
At1g32350	*AOX1D*	Alternative oxidase 1D	Up-regulated in adult *siz1-3*
At1g45145	*ATH5; LIV1; TRX5*	Thioredoxin H-type 5	Up-regulated in adult *siz1-3*

Table 2.1. (Continued)

At3g62960		Thioredoxin superfamily protein	Up-regulated in adult *siz1-3*
At4g33040		Thioredoxin superfamily protein	Up-regulated in adult *siz1-3*
At5g20230	*BCB*; *SAG14*	Blue-copper-binding protein	Up-regulated in adult *siz1-3*
At5g47910	*RBOHD*	Respiratory burst oxidase homologue D	Up-regulated in adult *siz1-3*
Peroxidases			
At2g37130		Peroxidase superfamily protein	Up-regulated in *siz1-2* seedlings
At3g01190		Peroxidase superfamily protein	Up-regulated in *siz1-2* seedlings
At3g21770		Peroxidase superfamily protein	Up-regulated in *siz1-2* seedlings
At3g49120	*ATPCB; PERX34; PRX34; PRXCB*	Peroxidase CB	Up-regulated in *siz1-2* seedlings
At1g14540		Peroxidase superfamily protein	Up-regulated in adult *siz1-3*
At3g28200		Peroxidase superfamily protein	Down-regulated in adult *siz1-3*

Sumoylation operates mostly in the cell nucleus and is assumed to act largely as a transcriptional repressor (van den Burg and Takken, 2009, 2010), therefore we analyze how loss of sumoylation impacted on ROS homeostatic genes at the gene expression level. In order to generate transcriptional data at the early stages of development when a deregulation of both $O_2^{\cdot-}$ and H_2O_2 was shown to occur in the absence of clear developmental differences (Fig. 2.3), we performed microarray analysis of 10-day-old *siz1-2* seedlings. Analysis rendered 380 up-regulated and 232 down-regulated genes in the *siz1-2* mutant. Gene ontology (GO) term enrichment analysis showed the differentially expressed genes (DEGs) to be functionally related to nutrient and secondary metabolism, including cell wall modification, as well as the response to abiotic stimulus and regulation of hormone levels (Fig. 2.7A). DEGs did not significantly overlap with the previously estimated transcriptome of adult 4-week-old *siz1-3* mutants, which was over-represented with genes related to brassinosteroids, auxin, abscisic acid, jasmonic acid (JA) and light responses (Catala et al., 2007). Venn analysis revealed that only 20% of DEGs at the seedling stage co-expressed at the adult stage (Fig. 2.7B).

We subsequently cross-referenced differentially-expressed genes at both stages with RGN and PRX datasets (Fig. 2.7C,D; Table 2.1). In 10-day-old seedlings we noticed that several major ROS scavenging enzymes were differentially expressed (Fig. 2.7C). Analysis revealed that copper/zinc superoxide dismutases *CSD1* and *-2* were down-regulated, while *Fe superoxide dismutase 1* (*FSD1*) was up-regulated. In addition, *CAT1* was down-regulated and glutathione reductase *GR1* was up-regulated. In late stages of *siz1* development, no traditional ROS scavenging

enzymes were transcriptionally de-regulated (Fig. 2.7D). However, *RBOHD*, an important NADPH oxidase involved ROS systemic signaling (Miller et al., 2009) was over-expressed in *siz1* adult plants and may contribute to superoxide and subsequently higher H_2O_2 levels. Several thioredoxins were also up-regulated in both seedlings and adult plants (Fig. 2.7C,D; Table 2.1).

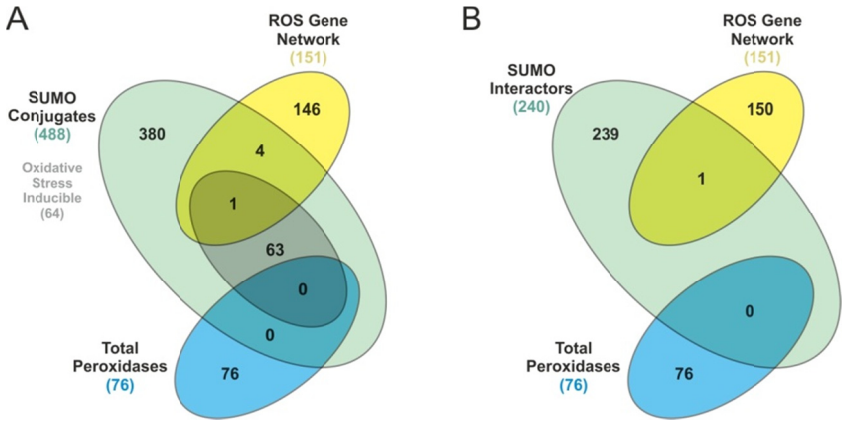

Figure 2.6. Comparison of SUMO-related against ROS-related genes in Arabidopsis. **A**, Venn diagram analysis of predicted ROS Gene Network (RGN) members and predicted peroxidases (PRX), versus the set of currently predicted SUMO conjugates, including the subset of SUMO conjugates induced following oxidative stress. **B**, Venn diagram analysis of RGN and PRX, versus the set of predicted protein-protein interactors of the SUMO conjugation/deconjugation machinery.

Additionally, we cross-referenced genes differentially expressed in 10-day-old *siz1-2* mutants with the differential transcriptional signature that has been associated with various forms of ROS generation. Surprisingly, no significant co- or anti-expression was observed, even though the most significant overlap was observed for high-light (HL) stress (Fig. 2.7E). In the presence of HL, production of ROS occurs in promoted in the chloroplast by over-reduction of the photosynthetic apparatus, generating singlet oxygen in PSII and superoxide ion in PSI.

SIZ1 controls singlet oxygen and chlorophyll levels independently of SA

Based on the previous indications, we decided to verify whether singlet oxygen levels were also de-regulated in *siz1*. Singlet oxygen ($^1O_2$) is a ROS produced in light-involving reactions, mainly via chlorophylls and metabolites such as phytoalexins, traditionally associated to plant defence against pathogens (Triantaphylides and Havaux, 2009). To detect and quantify singlet oxygen in light-adapted *siz1-2* seedlings, we performed vacuum infiltration with the green fluorescence-emitting probe Singlet Oxygen Sensor Green (SOSG). As depicted in Figure 2.8A, under standard conditions *siz1-2* displayed higher levels of singlet oxygen in comparison to the wild-type. Densitometric quantification proved fluorescence levels to be ~40% higher in the mutant

(Fig. 2.8B). To establish SA-dependence of the observed phenotype, levels were also analyzed in the *NahG* background. Results showed that *NahG* plants were phenotypically similar to the wild-type, whereas *siz1-2 NahG* plants displayed singlet oxygen levels that were comparable to those of *siz1-2* (Fig. 2.8A,B). This indicated that over-production of singlet oxygen in *siz1-2* was SA-independent. We also observed that red autofluorescence levels, which correlate with chlorophyll fluorescence, were also reduced in *siz1-2* and *siz1-2 NahG* mutants (Fig. 2.8A). Quantification indicated a ~25% reduction in autofluorescence in both these backgrounds (Fig. 2.8C), suggesting that chlorophyll levels are substantially reduced in *siz1-2*, in a SA-independent manner.

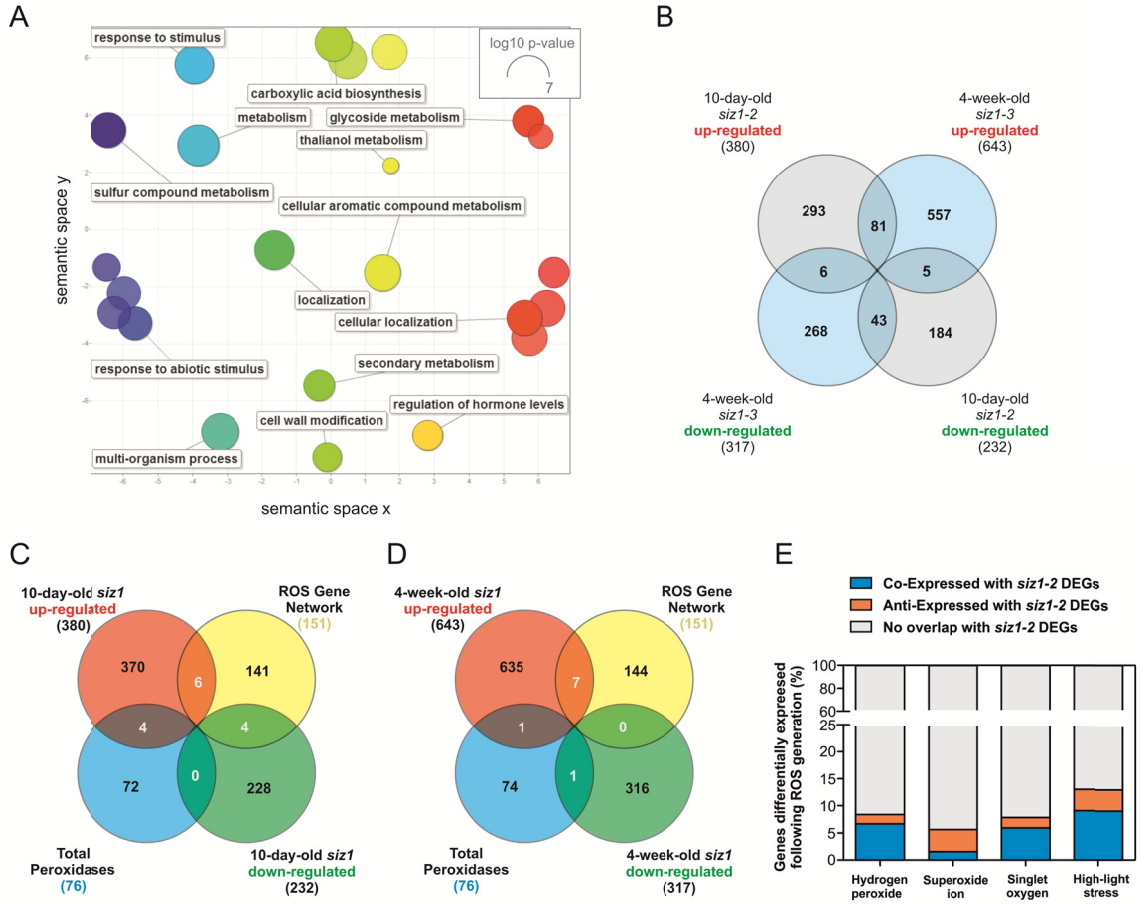

Figure 2.7. Microarray analysis of 10-day-old *siz1-2* seedlings. **A**, Scatterplot analysis of enriched gene ontology (GO) terms for *siz1-2* differentially expressed genes (DEGs), using VirtualPlant (Katari et al., 2010) and REVIGO (Supek et al., 2011); bubble size shows the frequency of the GO term. **B**, Venn diagram comparing 10-day-old *siz1-2* seedling DEGs with previously published 4-week-old *siz1-3* adult plants DEGs (Catala et al., 2007). **C**, Venn diagram representation of RGN and PRX comparison against genes differentially expressed in 10-day-old *siz1-2* seedlings. **D**, Venn diagram representation of RGN and PRX comparison against genes differentially expressed in 4-week-old *siz1-3* plants. **E**, Percentage of *siz1-2* DEGs co- or anti-expressing with the differential transcriptome that follows exposure to different oxidative stress-generating conditions.

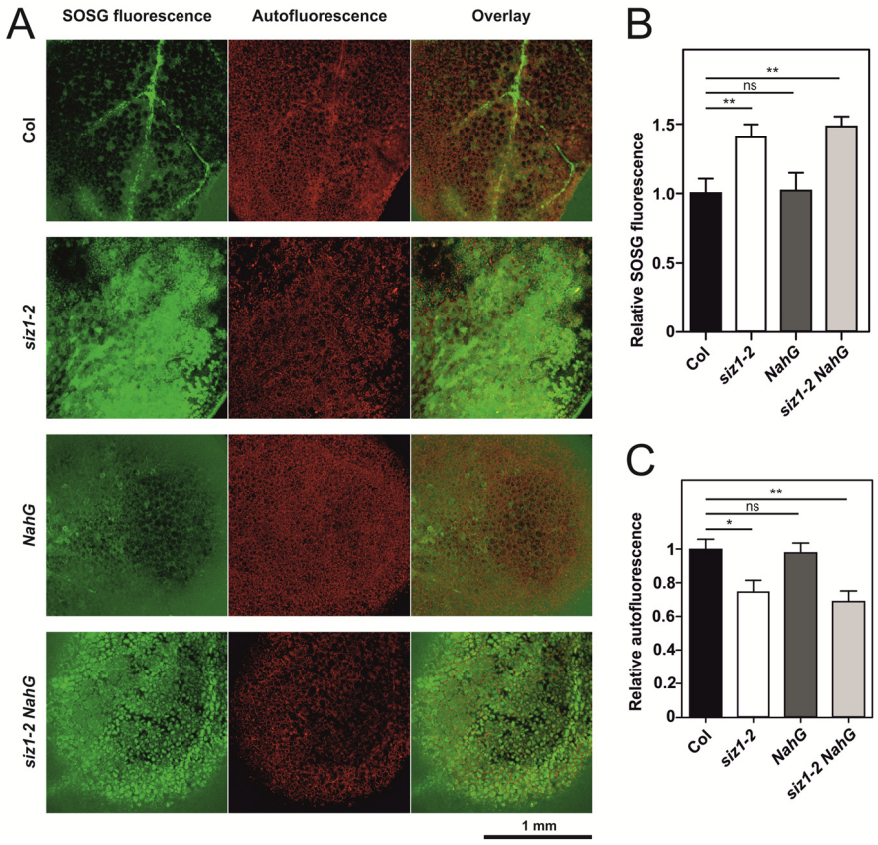

Figure 2.8. Analysis of singlet oxygen levels using SOSG fluorescence, in 10-day-old Wt (Col), *siz1-2*, *NahG* and *siz1-2 NahG* seedlings. **A**, Confocal microscopy observation of singlet oxygen levels (SOSG green fluorescence) and autofluorescence (red); bar indicates 1 mm. **B**, Quantification of SOSG fluorescence in relation to the control (Wt). **C**, Quantification of chlorophyll autofluorescence in relation to the Wt. Error bars represent SEM, n ≥ 8. Asterisks indicate statistically significant differences with respect to the wild-type (unpaired t test; ns, non-significant; *, $P < 0.05$; **, $P < 0.01$; ***, $P < 0.001$).

2.3. DISCUSSION

ROS positively control the SUMO-conjugate pool

Until recently, reactive oxygen species were considered mere toxic byproducts of aerobic metabolism. Presently, ROS are recognized as essential signaling molecules involved in many aspects of plant functioning (Mittler et al., 2011). SUMO-conjugates have been sown to increase rapidly in response to oxidative conditions, and this increment has been observed in various eukaryotic organisms, including yeast and human cells (Manza et al., 2004; Zhou et al., 2004; Bossis and Melchior, 2006). In plants, previous studies reported a similar increase in SUMO-conjugate levels following exogenous application of H_2O_2 to hydroponically-grown Arabidopsis seedlings (Kurepa et al., 2003; Miller et al., 2013). In the present study we challenged Arabidopsis

seedlings with methyl viologen, a contact herbicide commercially known as Paraquat and commonly used as an oxidative-stress generator (Scarpeci et al., 2008). MV acts as an alternative electron acceptor from photosystem I and transfers it to molecular oxygen promoting the endogenous formation of superoxide ion in the chloroplast (Fujii et al., 1990; Scarpeci et al., 2008). In the present study we showed how endogenous ROS generation by MV was more effective than exogenous application of H_2O_2 in the promotion of sumoylation, establishing a positive and dose-dependent correlation between intracellular ROS levels and the pool of high-molecular weight SUMO-target conjugates (Fig. 2.1). SUMO-conjugates produced in response to oxidative stress were specifically composed of SUM1/2 (Fig. 2.1), since we could not detect obvious pattern changes in the SUM3 profile. These findings are in agreement with previous reports stating that SUM3-conjugates do not change in response to salt (Conti et al., 2008), a stress condition that leads to ROS production (Miller et al., 2010a). Castaño-Miquel et al. (2011) have shown that SUM3 cannot efficiently establish non-covalent interactions with SUMO E2 conjugase, limiting conjugation efficiency. Nevertheless, many SUM3 targets were predicted by Elrouby and Coupland (2010) through a yeast two-hybrid screening and in vitro sumoylation assay, suggesting that in addition to covalent attachments, SUM3 may interact via non-covalent interactions. In sum, we show that intracellular increase in oxidative stress seems to control the generation of SUM1/2- but not SUM3-conjugates.

SUMO controls ROS homeostatic levels and oxidative stress responses via SIZ1

We observed that SIZ1, the major plant SUMO E3 ligase, was essential for the accumulation of SUMO-conjugates that took place in response to oxidative stress (Fig. 2.1). High-throughput strategies for the identification of SUMO-conjugates have shown that SIZ1 is one of the most heavily sumoylated targets in response to stress imposition, including exogenous application of H_2O_2 (Miller et al., 2013). Both indications point towards an involvement of SIZ1 in the response to oxidative stress. We subsequently showed that *siz1-2* leaves were more susceptible to oxidative stress by both H_2O_2 and MV (Fig. 2.2). Conversely, *siz1-2* roots grew better in MV comparatively to wild-type. These differences may relate to the fact that MV-dependent oxidative stress is mostly generated in photosynthetically-active tissues, when it receives electrons at the PSI and transfers them to molecular oxygen producing superoxide (Fujii et al., 1990; Scarpeci et al., 2008). Also, ROS have been shown to be important for various developmental root traits (Swanson and Gilroy, 2010). In root tips, superoxide ion was shown to accumulate in the meristem, while

H_2O_2 accumulated in the elongation zone (Tsukagoshi et al., 2010). The balance between both ROS was shown to be important for the transition from cell proliferation to differentiation, impacting on root growth.

Considering that *siz1* displayed altered responses to oxidative stress, we analyzed how impaired sumoylation impacted on the homeostatic levels of major ROS. Indeed, the SIZ1 knockout resulted in the accumulation of the major ROS hydrogen peroxide, superoxide, and singlet oxygen (Figs. 2.3 and 2.8). Particularly, hydrogen peroxide levels were increased in *siz1* from early to later stages of development. These results place SIZ1 as a homeostatic regulator of ROS levels in plants.

SUMO is likely to interplay with ROS-scavenging mechanisms

SIZ1 may inhibit the generation of ROS by acting as a positive regulator of ROS scavenging enzymes, controlling their detoxifying activities either at the transcriptional or PTM levels (Table 2.1). Recently, targets of sumoylation in response to oxidative stress were identified (Miller et al., 2013), revealing that levels of SUMO-conjugated APX1 increase significantly in H_2O_2-treated plants (Table 2.1). APX1 is a cytosolic and highly expressed ascorbate peroxidase that is essential for the control of ROS homeostatic levels and can exert a protective effect on various organelles (Davletova et al., 2005; Maruta et al., 2012). APX1 is part of the ascorbate-glutathione (Asc-Glu) cycle, responsible for the recycling of the pool of these major anti-oxidant molecules (Mittler et al., 2004). Other ROS-scavenging enzymes that have been identified as SUMO targets include CAT1, CAT3 and FSD1 (Table 2.1). Like APX, catalases are high specificity for H_2O_2 (Mhamdi et al., 2010) and therefore major components of the ROS detoxifying network. Unlike CAT1, CAT3 is highly expressed, and as a class II catalase, is associated with vascular tissues (Mhamdi et al., 2010). This is interesting since various SUMO pathway components including SIZ1 are preferably expressed in the vasculature (Chapter 4; Catala et al., 2007; Hermkes et al., 2011; Ishida et al., 2012).

Despite the fact that several peroxidases and RGN members are transcriptionally de-regulated in *siz1* and some even constitute potential SUMO targets (Table 2.1), we were unable to observe obvious differences in CAT, SOD, APX, or PPOD activities in *siz1-2* seedlings (Fig. 2.5). To better resolve this preliminary data, subsequent studies should focus on later developmental stages, and take into consideration tissue specificity as well as isoform analysis by in-gel activity assays. One interesting aspect is the issue of subcellular localization, since SIZ1 is nuclear (Miura et al., 2005) and these enzymes are cytosolic (APX1 and FSD1) or predicted to be peroxisomal

(CAT1 and -3), which might hint to SIZ1-independent sumoylation (Myouga et al., 2008; Mhamdi et al., 2010). Also, mutants for FSD1, CAT1 or CAT3 do not develop great phenotypic differences when compared to the wild-type (Myouga et al., 2008; Mhamdi et al., 2010). APX1 knockout is smaller and accumulates more H_2O_2 in response to high light (Davletova et al., 2005). Analysis of the genes associated to sumoylation (Table 2.1) indicates a prevalence of stress-responsive genes, which suggests a preponderant role for SUMO on the oxidative stress response.

ROS accumulation involves SA signaling

We have found that ROS production is partially a consequence of SA accumulation in the *siz1* background. The *siz1* mutant displays common features to an autoimmune mutant: SA accumulation, cell death lesions, up-regulation of *Pathogen-Related* genes, dwarfed phenotype, and increased tolerance to the hemibiotrophic pathogen *Pseudomonas syringae* pv. *tomato* DC3000 (Lee et al., 2007; Miura et al., 2010). The expression of *NahG* in *siz1* greatly reverts the dwarfism and many of these autoimmune responses (Appendix II – Fig. S2.1; Lee et al., 2007; Miura et al., 2010). In the case of ROS levels, *NahG* partially suppressed the accumulation of H_2O_2 and $O_2^{\cdot-}$ but not of $^1O_2$ (Fig. 2.4), suggesting that SA-dependent and independent mechanisms of ROS level maintenance are controlled by SIZ1.

One interesting gene de-regulated in *siz1* is the *NADPH oxidase/respiratory burst oxidase homologue protein D* (*RBOHD*), which is up-regulated in 4-week-old mutants (Table 2.1). RBOHD is considered a master regulator in Arabidopsis ROS-generated responses (Marino et al., 2012). Generally, RBOHs are transmembrane proteins that produce superoxide ion by transferring electrons to an extracellular O_2 electron acceptor (Marino et al., 2012). Unlike remaining RBOHs which seem to play specific roles, RBOHD is widely expressed and assumes a more housekeeping function in Arabidopsis (Marino et al., 2012). It is also essential for the propagation of ROS signals triggered by stress conditions, including the response to pathogens (Miller et al., 2009; Pogany et al., 2009). The mutant *rbohd* accumulates more SA in standard conditions (Miller et al., 2009). More significantly, *RBOHD* expression is controlled by SA (Devadas et al., 2002), therefore, overexpression of *RBOHD* in *siz1* may be one of the causes of SA-dependent ROS accumulation. Introgression of a *rbohd* mutation into the *siz1* background will be important to genetically establish a correlation between RBOHD and SIZ1 in the control of ROS homeostatic levels.

Oxidative stress-dependent SUMO-conjugates suggest interplay between SUMO, ROS and SA at the nuclear level

The most intriguing set of targets proteins that increase their SUMO-conjugate levels in response to oxidative stress are chromatin remodeling proteins, with special focus for repression complexes involved in histone deacetylase recruitment (Mazur and van den Burg, 2012; Miller et al., 2013). Many adaptors within these complexes are sumoylated, including LEUNIG (LUG), LEUNIG HOMOLOG (LUH), SEUSS (SEU), TOPLESS (TPL) and TPL-related proteins (TPRs). TPL and TPRs are associated with many transcription factors and repressors. For instance, Pauwels et al. (2010) revealed that TPL/TPR interact with the ethylene-responsive element binding factor-associated amphiphilic repression (EAR) motif of the protein Novel Interactor of JAZ (NINJA), creating a repressive complex associated with JAZs and the TF MYC2. This complex blocks early JA-genes in the absence of JA. The TOPLESS interactome includes many TFs and many are enriched in EAR motifs (Causier et al., 2012), highlighting the idea that TPL interacts with TFs to promote transcription repression. However, no direct interactions were observed between TPL and the histone deacetylase HDA19 (Causier et al., 2012). Zhu et al. (2010) observed the TPR1 and HDA19 interaction in pull-down experiments, suggesting that they are part of a complex where additional factors might mediate such associations. Interestingly, Groucho, the mammalian TPL homolog, is multisumoylated by SUMO1, a process that is fundamental for HDAC1 recruitment via SIM to establish the corepressor complex (Ahn et al., 2009). SUMO might be the link that establishes these co-repressor complexes, and oxidative stress may trigger these assemblies, as suggested by SUMO-conjugate increment in response to H_2O_2 (Miller et al., 2013).

Additionally, components of the SAGA complex are also highly sumoylated following oxidative stress, including the histone acetylase GCN5 and the adaptors ADA2a and ADA2b that enhance GCN5 activity and recruit GCN5 to TFs (Gamper et al., 2009; Miller et al., 2013). In yeast, GCN5 sumoylation inhibits the induction of gene expression (Sterner et al., 2006), placing SUMO as a negative regulator of acetylation. Altogether, it would seem that SUMO blocks histone acetylation and enhances deacetylation through GCN5 and HDA19, respectively. Long et al. (2006) reported that the *tpl-1* mutant's aberrant development was suppressed by *gcn5* and enhanced by *had19*, likely by sharing common targets for gene expression regulation. Accordingly, it was reported that GCN5-HDA19 forms an antagonist duet in the control of histone acetylation/deacetylation status to regulate light-responsive genes (Benhamed et al., 2006). In addition, HDA19 is involved in the repression of SA-induced expression (but not ET/JA) including

EDS1, *PAD4*, *EDS5*, *ICS1*, *GDG1*, *PR1*, and *PR2* (Choi et al., 2012). These genes are up-regulated in *siz1* mutants (Catala et al., 2007; Lee et al., 2007). SIZ1 may modulate transcriptional regulation, via sumoylation of corepressor components such as members of the TPL/Groucho/TUP1 family that recruits histone deacetylases to the promoters of key proteins of SA biosynthesis and signaling pathways.

The *siz1* mutant displays a conditional phenotype

In the present study we generated microarray data of 10-day-old in vitro-grown seedlings, which were compared to Catala et al. (2007) experiments in *siz1-3* adult plants, showing just 20% of overlapping DEGs (Fig. 2.7B). First, in addition to the different developmental stages, we should take into consideration that our plants were grown in in vitro conditions, which reproduce ideal growth conditions in what concerns nutrient availability and exposure to environmental fluctuations. Park et al. (2011) reported that N-assimilation is one determinant of *siz1* constitutive defence responses and that, in supplemented ammonium conditions, *siz1* partially recovers the wild-type phenotype. Second, in our experiment we used the *siz1-2* and Catala et al. (2007) used *siz1-3* allele. Nevertheless, in all reported works, both seem to function as null alleles that lead to identical morphological phenotypes (Miura et al., 2010). Results suggest that the *siz1* pleiotropic phenotype is conditional, depending on environmental conditions such as temperature (Chapter 2) and N-supplementation. These conditions ultimately influence the SA levels in *siz1* mutants, one of the major causes of the *siz1* phenotype. *NahG*, and to a little extent *sid2* mutations (data not shown), can revert the *siz1* dwarfism phenotype. This can be explained by a possible redundancy of ICS1/SID2 with ICS2 (At1g18870), the existence of alternative SA biosynthesis pathways, or the hypothesis that precursors of SA may exert a SA-like effect (Vlot et al., 2009). Alternatively, catechol, the byproduct of *NahG*, may lead to unpredictable effects, like the already suggested production of hydrogen peroxide (van Wees and Glazebrook, 2003). SIZ1 controls the expression of additional genes and in fact no key SA-associated genes were observed in in vitro-grown seedlings. Interestingly, these include the down-regulation of genes associated to the chlorophyll biosynthetic pathway, and in fact *siz1* mutants display a constitutive reduction in chlorophyll levels (data not shown). More specifically, microarray data indicates that *NADPH:protochlorophyllide oxidoreductase A* (*PORA*) is down-regulated in *siz1* (Catala et al., 2007). *PORA* is involved in the light-dependent conversion of protochlorophyllide (Pchlide) to chlorophyllide a, and *PORA* down-regulation can lead to the accumulation of Pchlide (Buhr et al., 2008). The observed

overproduction of singlet oxygen (Fig. 2.8) can thus be explained by the fact that, in the presence of light, Pchlide suffers photoreduction to generate singlet oxygen (Buhr et al., 2008).

Final considerations

In eukaryotes, sumoylation is an essential player in the molecular control of both development and the response to a constantly changing environment (Castro et al., 2012). Specifically in plants, sumoylation has developed increasing preeminence over the last decade, and discovering the molecular basis of SUMO function and regulation can have an extensive impact on crop development. Future studies should address how SIZ1 seems to contribute, at multiple levels, to the modulation of ROS homeostasis. Focus should also be put on the possible role of SIZ1 in the assembly of transcriptional repression complexes, likely to modulate ROS homeostasis and impact on the repression of defence genes that are deleterious for plant growth.

2.4. MATERIALS AND METHODS

Plant material and growth conditions

The *Arabidopsis thaliana* lines are in the ecotype Columbia-0 (Col) background. The T-DNA insertion mutant *siz1-2* (SALK_065397; Miura et al., 2005) was ordered from the NASC European Arabidopsis Stock Centre (arabidopsis.info). The transgenic line *NahG*, that expresses a bacterial SA hydroxylase, was kindly provided by Miguel Botella (University of Malaga, Spain). Homozygous lines for *siz1-2 NahG* were determined by *siz1-2* phenotype reversion of F3 seedlings as previously described (Lee et al., 2007). The primers used for genotyping are listed in Table S2.1 (Appendix II).

Synchronized seeds were stratified for 3 days at 4°C in the dark. Surface sterilization was performed in a horizontal laminar flow chamber by sequential immersion in 70% (v/v) ethanol for 5 min and 20% (v/v) commercial bleach for 10 min before washing five times with sterile ultra-pure water. Seeds were resuspended in sterile 0.25% (w/v) agarose, sown onto 1.2% agar-solidified MS medium (Murashige and Skoog, 1962) containing 1.5% sucrose, 0.5 g L^{-1} MES, pH 5.7, and grown vertically in culture rooms with a 16 h light/8 h dark cycle under cool white light (80 µE m^{-2} s^{-1} light intensity) at 23°C. For standard growth, 7-day-old in vitro-grown seedlings were transferred to a soil to vermiculite (4:1) mixture, and maintained under identical growth conditions, with regular watering. Oxidative stress was generated by supplementing MS media with methyl viologen

(MV, Sigma), or by vacuum infiltrating plant material with H_2O_2 or MV solutions for three cycles of 5 min, followed by incubation under standard light conditions for 3 h.

Detection by staining of ROS

In situ H_2O_2 levels were estimated using the 3,3'-diaminobenzidine (DAB; Sigma) staining method adapted from Thordal-Christensen et al. (1997). Plant tissue was vacuum-infiltrated (three cycles of 5 min) with 1 mg mL^{-1} DAB solution, and correct with NaOH to pH 3.8. Samples were incubated overnight in the dark at room temperature. To remove chlorophyll content, plant tissue was cleared in 96% ethanol at 70°C.

Plant infiltration with nitroblue tetrazolium (*NBT Color Development Substrate*, *Sigma*) allowed the in situ detection of superoxide ion. The NBT staining method was adapted from Jabs et al. (1996). Plants and seedlings were vacuum-infiltrated (three cycles of 5 min) with 0.5 mg mL^{-1} NBT in 10 mM sodium phosphate buffer, pH 7.8. Samples were incubated for 1 h in the dark at room temperature and then cleared in 96% ethanol at 70°C until complete removal of chlorophyll.

Singlet oxygen levels were detected using Singlet Oxygen Sensor Green (SOSG) fluorescence, as previously described (Flors et al., 2006; Ramel et al., 2009). Briefly, 10-day-old seedling were immersed and infiltrated in the dark under vacuum (three cycles of 5 min) with a solution of 100 µM SOSG (S36002, Invitrogen) in 50 mM phosphate potassium buffer (pH 7.5). Seedlings were then placed again on control or high light (200 µmol Photon m^{-2} s^{-2}) conditions for 30 min, before being photographed in a confocal fluorescence microscope for image acquisition or an optical fluorescence microscope for fluorescence quantification. Quantification of fluorescence levels was performed in ImageJ (rsb.info.nih.gov/ij/index.html).

RNA extraction and microarray analysis

The RNA from seedlings was extracted using an *RNeasy Plant Mini kit* (QIAGEN) and treated with *Recombinant DNase I* (Takara Biotechnology), followed by a new column cleaning step using an *RNeasy Plant Mini kit* (QIAGEN). RNA quantity and quality were assessed using both a Nanodrop ND-1000 spectrophotometer and standard agarose-gel electrophoretic analysis.

Genome-wide transcription studies were performed using the ATH1 microarray chip (Affymetrix) with three independent replicates per genotype, each replicate represented RNA from a pool of four different MS plates containing 10-day-old plants grown at standard conditions. Microarray execution and differential expression analysis were conducted at Unité de Recherche en

Génomique Végétale (Université d'Evry Val d'Essonne, France). The method to determine DEGs was based on variance modelisation by common variance of all genes (Gagnot et al., 2008).

Protein extraction and immunoblotting

Plant tissue was grinded in a microtube in liquid nitrogen with the help of polypropylene pestles. Protein extracts were obtained by adding extraction buffer [50 mM Tris; 150 mM NaCl; 0.2% (v/v) Triton X-100] supplemented with *Complete Protease Inhibitor Cocktail* (Roche) as per the manufacturer's instructions. Following incubation for 1 h at 4°C with agitation, microtubes were centrifuged two times for 30 min at 16000 *g*. The supernatant was subsequently recovered and stored at -80°C. Protein was spectrophotometrically quantified using *Bradford reagent* (Sigma; Bradford, 1976). Equal amounts of protein were resolved by standard SDS-PAGE in a 10% (w/v) acrylamide resolving gel, using a *Mini-PROTEAN Cell* (Bio-Rad) apparatus. For immunoblotting, proteins were transferred to a PVDF-membrane using a *Mini Trans-Blot Cell* (Bio-Rad). The membrane was blocked for 1 h at 23°C or overnight at 4°C in blocking solution (5% dry milk powder in PBST). The primary antibody Anti-AtSUMO1 (ABCAM) or Anti-SUMO3 (ABCAM) was added in a 1:2000 dilution and incubated for 2 to 3 h. The membrane was washed three times with 10 mL of PBST for 10 min, and incubated with the secondary antibody (anti-rabbit, *Santa Cruz*; 1:10,000 in blocking solution) for 1 h. The membrane was washed as previously detailed and developed by a chemiluminescence reaction using the *Immune-Star WesternC Kit* (Bio-Rad) and a *ChemiDoc XRS system* (Bio-Rad) for image acquisition. PVDF membranes were incubated for 15 min with Ponceau S solution [0.1% (w/v) Ponceau S; 5% (v/v) acetic acid] to stain total protein levels.

Enzymatic activity and lipid peroxidation detection

Lipid peroxidation was quantified spectrophotometrically by the MDA-TBA method, which quantifies the end product of lipid peroxidation malondialdehyde (MDA) by reaction at low pH and high temperature with 2-thiobarbituric acid (TBA; Loreto and Velikova, 2001). Quantification of the MDA-TBA complex was performed by determining the absorbance of the supernatant at 532 nm and deducting non-specific absorbance at 600 nm. The absorbances were measured in a microplate spectrophotometer (SpectraMax 340PC; Molecular Devices). The molar extinction coefficient of MDA-TBA complex, at 532 nm, is 155 mM^{-1} cm^{-1}.

Pyrogallol peroxidase activity (PPOD) was determined by measuring the increase in absorbance at 430 nm due to the formation of purpurogallin (Radic et al., 2006). Catalase (CAT) activity was determined by monitoring H_2O_2 removal as a decrease in absorbance at 240 nm (Dutilleul et al., 2003). Superoxide dismutase activity was determined by measuring the inhibition of the photochemical reduction of NBT at 560 nm (Campa-Cordova et al., 2009). Ascorbate peroxidase (APX) activity was measured by monitoring the rate of H_2O_2 -dependent oxidation of ascorbate at 290 nm (Ramel et al., 2009). For all essays except APX activity, total soluble protein was extracted as previously described. For APX activity, leaf tissue was ground in liquid nitrogen, mixed with 0.5 mL of extraction buffer containing 50 mm Na-phosphate (pH 7.0), 0.25 mM EDTA, 2% (w/v) polyvinylpyrrolidone-25, 10% (w/v) glycerol, and 1 mM ascorbic acid, and centrifuged at 14000 *g* for 10 min at 0°C (Panchuk et al., 2002). Proteins levels were quantified using *Bradford reagent* (Sigma) method (Bradford, 1976).

Bioinformatic analyses

Venn diagrams were obtained using Venn Diagram Generator (www.pangloss.com/seidel/Protocols/venn.cgi). Microarray execution and differential expression analysis were outsourced (Gagnot et al., 2008). GO term functional categorization was performed in VirtualPlant 1.3 (virtualplant.bio.nyu.edu/cgi-bin/vpweb/), using the BioMaps function with a 0.01 *p*-value cutoff (Katari et al., 2010). Redundancy exclusion and scatterplot analysis were performed using REVIGO (revigo.irb.hr/), with a 0.4 C-value. The scatterplot represents the cluster representatives in a two dimensional space (x- and y-axis) derived by applying multidimensional scaling to a matrix of the GO terms' semantic similarities (Supek et al., 2011).

2.5. REFERENCES

Ahn JW, Lee YA, Ahn JH, Choi CY (2009) Covalent conjugation of Groucho with SUMO-1 modulates its corepressor activity. Biochem Biophys Res Commun **379:** 160-165

Apel K, Hirt H (2004) Reactive oxygen species: metabolism, oxidative stress, and signal transduction. Annu Rev Plant Biol **55:** 373-399

Benhamed M, Bertrand C, Servet C, Zhou DX (2006) Arabidopsis GCN5, HD1, and TAF1/HAF2 interact to regulate histone acetylation required for light-responsive gene expression. Plant Cell **18:** 2893-2903

Bossis G, Melchior F (2006) Regulation of SUMOylation by reversible oxidation of SUMO conjugating enzymes. Mol Cell **21:** 349-357

Bradford MM (1976) A rapid and sensitive method for the quantitation of microgram quantities of protein utilizing the principle of protein-dye binding. Anal Biochem **72:** 248-254

Buhr F, El Bakkouri M, Valdez O, Pollmann S, Lebedev N, Reinbothe S, Reinbothe C (2008) Photoprotective role of NADPH:protochlorophyllide oxidoreductase A. Proc Natl Acad Sci U S A **105:** 12629-12634

Campa-Cordova AI, Nunez-Vazquez EJ, Luna-Gonzalez A, Romero-Geraldo MJ, Ascencio F (2009) Superoxide dismutase activity in juvenile *Litopenaeus vannamei* and *Nodipecten subnodosus* exposed to the toxic dinoflagellate *Prorocentrum lima*. Comp Biochem Physiol C Toxicol Pharmacol **149:** 317-322

Castano-Miquel L, Segui J, Lois LM (2011) Distinctive properties of Arabidopsis SUMO paralogues support the in vivo predominant role of AtSUMO1/2 isoforms. Biochem J **436:** 581-590

Castro PH, Tavares RM, Bejarano ER, Azevedo H (2012) SUMO, a heavyweight player in plant abiotic stress responses. Cell Mol Life Sci **69:** 3269-3283

Catala R, Ouyang J, Abreu IA, Hu Y, Seo H, Zhang X, Chua NH (2007) The Arabidopsis E3 SUMO ligase SIZ1 regulates plant growth and drought responses. Plant Cell **19:** 2952-2966

Causier B, Ashworth M, Guo W, Davies B (2012) The TOPLESS interactome: a framework for gene repression in Arabidopsis. Plant Physiol **158:** 423-438

Choi SM, Song HR, Han SK, Han M, Kim CY, Park J, Lee YH, Jeon JS, Noh YS, Noh B (2012) HDA19 is required for the repression of salicylic acid biosynthesis and salicylic acid-mediated defense responses in Arabidopsis. Plant J **71:** 135-146

Conti L, Price G, O'Donnell E, Schwessinger B, Dominy P, Sadanandom A (2008) Small ubiquitin-like modifier proteases OVERLY TOLERANT TO SALT1 and -2 regulate salt stress responses in Arabidopsis. Plant Cell **20:** 2894-2908

Cubenas-Potts C, Matunis MJ (2013) SUMO: A multifaceted modifier of chromatin structure and function. Dev Cell **24:** 1-12

Davletova S, Rizhsky L, Liang H, Shengqiang Z, Oliver DJ, Coutu J, Shulaev V, Schlauch K, Mittler R (2005) Cytosolic ascorbate peroxidase 1 is a central component of the reactive oxygen gene network of Arabidopsis. Plant Cell **17:** 268-281

Delaney TP, Uknes S, Vernooij B, Friedrich L, Weymann K, Negrotto D, Gaffney T, Gut-Rella M, Kessmann H, Ward E, Ryals J (1994) A central role of salicylic acid in plant disease resistance. Science **266:** 1247-1250

Devadas SK, Enyedi A, Raina R (2002) The Arabidopsis *hrl1* mutation reveals novel overlapping roles for salicylic acid, jasmonic acid and ethylene signalling in cell death and defence against pathogens. Plant J **30:** 467-480

Dutilleul C, Garmier M, Noctor G, Mathieu C, Chetrit P, Foyer CH, de Paepe R (2003) Leaf mitochondria modulate whole cell redox homeostasis, set antioxidant capacity, and determine stress resistance through altered signaling and diurnal regulation. Plant Cell **15:** 1212-1226

Elrouby N, Coupland G (2010) Proteome-wide screens for small ubiquitin-like modifier (SUMO) substrates identify Arabidopsis proteins implicated in diverse biological processes. Proc Natl Acad Sci U S A **107:** 17415-17420

Flors C, Fryer MJ, Waring J, Reeder B, Bechtold U, Mullineaux PM, Nonell S, Wilson MT, Baker NR (2006) Imaging the production of singlet oxygen in vivo using a new fluorescent sensor, Singlet Oxygen Sensor Green. J Exp Bot **57:** 1725-1734

Fujii T, Yokoyama E-i, Inoue K, Sakurai H (1990) The sites of electron donation of Photosystem I to methyl viologen. Biochim Biophys Acta **1015:** 41-48

Gadjev I, Vanderauwera S, Gechev TS, Laloi C, Minkov IN, Shulaev V, Apel K, Inze D, Mittler R, Van Breusegem F (2006) Transcriptomic footprints disclose specificity of reactive oxygen species signaling in Arabidopsis. Plant Physiol **141:** 436-445

Gagnot S, Tamby JP, Martin-Magniette ML, Bitton F, Taconnat L, Balzergue S, Aubourg S, Renou JP, Lecharny A, Brunaud V (2008) CATdb: a public access to Arabidopsis transcriptome data from the URGV-CATMA platform. Nucleic Acids Res **36:** D986-990

Gamper AM, Kim J, Roeder RG (2009) The STAGA subunit ADA2b is an important regulator of human GCN5 catalysis. Mol Cell Biol **29:** 266-280

Gareau JR, Lima CD (2010) The SUMO pathway: emerging mechanisms that shape specificity, conjugation and recognition. Nat Rev Mol Cell Biol **11:** 861-871

Hermkes R, Fu YF, Nurrenberg K, Budhiraja R, Schmelzer E, Elrouby N, Dohmen RJ, Bachmair A, Coupland G (2011) Distinct roles for Arabidopsis SUMO protease ESD4 and its closest homolog ELS1. Planta **233:** 63-73

Ishida T, Fujiwara S, Miura K, Stacey N, Yoshimura M, Schneider K, Adachi S, Minamisawa K, Umeda M, Sugimoto K (2009) SUMO E3 ligase HIGH PLOIDY2 regulates endocycle onset and meristem maintenance in Arabidopsis. Plant Cell **21:** 2284-2297

Ishida T, Yoshimura M, Miura K, Sugimoto K (2012) MMS21/HPY2 and SIZ1, two Arabidopsis SUMO E3 ligases, have distinct functions in development. PLoS One **7:** e46897

Jabs T, Dietrich RA, Dangl JL (1996) Initiation of runaway cell death in an Arabidopsis mutant by extracellular superoxide. Science **273:** 1853-1856

Katagiri M, Maeno H, Yamamoto S, Hayaishi O, Kitao T, Oae S (1965) Salicylate Hydroxylase, a Monooxygenase Requiring Flavin Adenine Dinucleotide. II. The Mechanism of Salicylate Hydroxylation to Catechol. J Biol Chem **240:** 3414-3417

Katari MS, Nowicki SD, Aceituno FF, Nero D, Kelfer J, Thompson LP, Cabello JM, Davidson RS, Goldberg AP, Shasha DE, Coruzzi GM, Gutierrez RA (2010) VirtualPlant: a software platform to support systems biology research. Plant Physiol **152:** 500-515

Kurepa J, Walker JM, Smalle J, Gosink MM, Davis SJ, Durham TL, Sung DY, Vierstra RD (2003) The small ubiquitin-like modifier (SUMO) protein modification system in Arabidopsis. Accumulation of SUMO1 and -2 conjugates is increased by stress. J Biol Chem **278:** 6862-6872

Lee J, Nam J, Park HC, Na G, Miura K, Jin JB, Yoo CY, Baek D, Kim DH, Jeong JC, Kim D, Lee SY, Salt DE, Mengiste T, Gong Q, Ma S, Bohnert HJ, Kwak SS, Bressan RA, Hasegawa PM, Yun DJ (2007) Salicylic acid-mediated innate immunity in Arabidopsis is regulated by SIZ1 SUMO E3 ligase. Plant J **49:** 79-90

Long JA, Ohno C, Smith ZR, Meyerowitz EM (2006) TOPLESS regulates apical embryonic fate in Arabidopsis. Science **312:** 1520-1523

Lopez-Torrejon G, Guerra D, Catala R, Salinas J, del Pozo JC (2013) Identification of SUMO targets by a novel proteomic approach in plants. J Integr Plant Biol **55:** 96-107

Loreto F, Velikova V (2001) Isoprene produced by leaves protects the photosynthetic apparatus against ozone damage, quenches ozone products, and reduces lipid peroxidation of cellular membranes. Plant Physiol **127:** 1781-1787

Lyst MJ, Stancheva I (2007) A role for SUMO modification in transcriptional repression and activation. Biochem Soc Trans **35:** 1389-1392

Manza LL, Codreanu SG, Stamer SL, Smith DL, Wells KS, Roberts RL, Liebler DC (2004) Global shifts in protein sumoylation in response to electrophile and oxidative stress. Chem Res Toxicol **17:** 1706-1715

Marino D, Dunand C, Puppo A, Pauly N (2012) A burst of plant NADPH oxidases. Trends Plant Sci **17:** 9-15

Maruta T, Inoue T, Noshi M, Tamoi M, Yabuta Y, Yoshimura K, Ishikawa T, Shigeoka S (2012) Cytosolic ascorbate peroxidase 1 protects organelles against oxidative stress by wounding- and jasmonate-induced H_2O_2 in Arabidopsis plants. Biochim Biophys Acta **1820:** 1901-1907

Mateo A, Funck D, Muhlenbock P, Kular B, Mullineaux PM, Karpinski S (2006) Controlled levels of salicylic acid are required for optimal photosynthesis and redox homeostasis. J Exp Bot **57:** 1795-1807

Mazur MJ, van den Burg HA (2012) Global SUMO proteome responses guide gene regulation, mRNA biogenesis, and plant stress responses. Front Plant Sci **3:** 215

Mhamdi A, Queval G, Chaouch S, Vanderauwera S, Van Breusegem F, Noctor G (2010) Catalase function in plants: a focus on Arabidopsis mutants as stress-mimic models. J Exp Bot **61:** 4197-4220

Miller G, Schlauch K, Tam R, Cortes D, Torres MA, Shulaev V, Dangl JL, Mittler R (2009) The plant NADPH oxidase RBOHD mediates rapid systemic signaling in response to diverse stimuli. Sci Signal **2:** ra45

Miller G, Suzuki N, Ciftci-Yilmaz S, Mittler R (2010a) Reactive oxygen species homeostasis and signalling during drought and salinity stresses. Plant Cell Environ **33:** 453-467

Miller MJ, Barrett-Wilt GA, Hua Z, Vierstra RD (2010b) Proteomic analyses identify a diverse array of nuclear processes affected by small ubiquitin-like modifier conjugation in Arabidopsis. Proc Natl Acad Sci U S A **107:** 16512-16517

Miller MJ, Scalf M, Rytz TC, Hubler SL, Smith LM, Vierstra RD (2013) Quantitative proteomics reveals factors regulating RNA biology as dynamic targets of stress-induced SUMOylation in Arabidopsis. Mol Cell Proteomics **12:** 449-463

Miller MJ, Vierstra RD (2011) Mass spectrometric identification of SUMO substrates provides insights into heat stress-induced SUMOylation in plants. Plant Signal Behav **6:** 130-133

Mittler R, Vanderauwera S, Gollery M, Van Breusegem F (2004) Reactive oxygen gene network of plants. Trends Plant Sci **9:** 490-498

Mittler R, Vanderauwera S, Suzuki N, Miller G, Tognetti VB, Vandepoele K, Gollery M, Shulaev V, Van Breusegem F (2011) ROS signaling: the new wave? Trends Plant Sci **16:** 300-309

Miura K, Hasegawa PM (2010) Sumoylation and other ubiquitin-like post-translational modifications in plants. Trends Cell Biol **20:** 223-232

Miura K, Lee J, Miura T, Hasegawa PM (2010) SIZ1 controls cell growth and plant development in Arabidopsis through salicylic acid. Plant Cell Physiol **51:** 103-113

Miura K, Rus A, Sharkhuu A, Yokoi S, Karthikeyan AS, Raghothama KG, Baek D, Koo YD, Jin JB, Bressan RA, Yun DJ, Hasegawa PM (2005) The Arabidopsis SUMO E3 ligase SIZ1 controls phosphate deficiency responses. Proc Natl Acad Sci U S A **102:** 7760-7765

Murashige T, Skoog F (1962) A revised medium for rapid growth and bio assays with tobacco tissue cultures. Physiol Plant **15:** 473-475

Murtas G, Reeves PH, Fu YF, Bancroft I, Dean C, Coupland G (2003) A nuclear protease required for flowering-time regulation in Arabidopsis reduces the abundance of SMALL UBIQUITIN-RELATED MODIFIER conjugates. Plant Cell **15:** 2308-2319

Myouga F, Hosoda C, Umezawa T, Iizumi H, Kuromori T, Motohashi R, Shono Y, Nagata N, Ikeuchi M, Shinozaki K (2008) A heterocomplex of iron superoxide dismutases defends chloroplast nucleoids against oxidative stress and is essential for chloroplast development in Arabidopsis. Plant Cell **20:** 3148-3162

Panchuk, II, Volkov RA, Schoffl F (2002) Heat stress- and heat shock transcription factor-dependent expression and activity of ascorbate peroxidase in Arabidopsis. Plant Physiol **129:** 838-853

Park BS, Song JT, Seo HS (2011) Arabidopsis nitrate reductase activity is stimulated by the E3 SUMO ligase AtSIZ1. Nat Commun **2:** 400

Pauwels L, Barbero GF, Geerinck J, Tilleman S, Grunewald W, Perez AC, Chico JM, Bossche RV, Sewell J, Gil E, Garcia-Casado G, Witters E, Inze D, Long JA, De Jaeger G, Solano R, Goossens A (2010) NINJA connects the co-repressor TOPLESS to jasmonate signalling. Nature **464:** 788-791

Pogany M, von Rad U, Grun S, Dongo A, Pintye A, Simoneau P, Bahnweg G, Kiss L, Barna B, Durner J (2009) Dual roles of reactive oxygen species and NADPH oxidase RBOHD in an Arabidopsis-*Alternaria* pathosystem. Plant Physiol **151:** 1459-1475

Radic S, Radic-Stojkovic M, Pevalek-Kozlina B (2006) Influence of NaCl and mannitol on peroxidase activity and lipid peroxidation in *Centaurea ragusina* L. roots and shoots. J Plant Physiol **163:** 1284-1292

Ramel F, Sulmon C, Bogard M, Couee I, Gouesbet G (2009) Differential patterns of reactive oxygen species and antioxidative mechanisms during atrazine injury and sucrose-induced tolerance in *Arabidopsis thaliana* plantlets. BMC Plant Biol **9:** 28

Rivas-San Vicente M, Plasencia J (2011) Salicylic acid beyond defence: its role in plant growth and development. J Exp Bot **62:** 3321-3338

Rosenwasser S, Rot I, Sollner E, Meyer AJ, Smith Y, Leviatan N, Fluhr R, Friedman H (2011) Organelles contribute differentially to reactive oxygen species-related events during extended darkness. Plant Physiol **156:** 185-201

Saracco SA, Miller MJ, Kurepa J, Vierstra RD (2007) Genetic analysis of SUMOylation in Arabidopsis: conjugation of SUMO1 and SUMO2 to nuclear proteins is essential. Plant Physiol **145:** 119-134

Scarpeci TE, Zanor MI, Carrillo N, Mueller-Roeber B, Valle EM (2008) Generation of superoxide anion in chloroplasts of *Arabidopsis thaliana* during active photosynthesis: a focus on rapidly induced genes. Plant Mol Biol **66:** 361-378

Schippers JH, Nguyen HM, Lu D, Schmidt R, Mueller-Roeber B (2012) ROS homeostasis during development: an evolutionary conserved strategy. Cell Mol Life Sci **69:** 3245-3257

Sterner DE, Nathan D, Reindle A, Johnson ES, Berger SL (2006) Sumoylation of the yeast Gcn5 protein. Biochemistry **45:** 1035-1042

Supek F, Bosnjak M, Skunca N, Smuc T (2011) REVIGO summarizes and visualizes long lists of gene ontology terms. PLoS One **6:** e21800

Swanson S, Gilroy S (2010) ROS in plant development. Physiol Plant **138:** 384-392

Thordal-Christensen H, Zhang Z, Wei Y, Collinge DB (1997) Subcellular localization of H_2O_2 in plants. H_2O_2 accumulation in papillae and hypersensitive response during the barley—powdery mildew interaction. Plant J **11:** 1187-1194

Triantaphylides C, Havaux M (2009) Singlet oxygen in plants: production, detoxification and signaling. Trends Plant Sci **14:** 219-228

Tsukagoshi H, Busch W, Benfey PN (2010) Transcriptional regulation of ROS controls transition from proliferation to differentiation in the root. Cell **143:** 606-616

van den Burg HA, Takken FL (2009) Does chromatin remodeling mark systemic acquired resistance? Trends Plant Sci **14:** 286-294

van den Burg HA, Takken FL (2010) SUMO-, MAPK-, and resistance protein-signaling converge at transcription complexes that regulate plant innate immunity. Plant Signal Behav **5:** 1597-1601

van Wees SC, Glazebrook J (2003) Loss of non-host resistance of Arabidopsis *NahG* to *Pseudomonas syringae* pv. *phaseolicola* is due to degradation products of salicylic acid. Plant J **33:** 733-742

Vlot AC, Dempsey DA, Klessig DF (2009) Salicylic Acid, a multifaceted hormone to combat disease. Annu Rev Phytopathol **47:** 177-206

Wilkinson KA, Henley JM (2010) Mechanisms, regulation and consequences of protein SUMOylation. Biochem J **428:** 133-145

Xu Z, Lam LS, Lam LH, Chau SF, Ng TB, Au SW (2008) Molecular basis of the redox regulation of SUMO proteases: a protective mechanism of intermolecular disulfide linkage against irreversible sulfhydryl oxidation. FASEB J **22:** 127-137

Zhou W, Ryan JJ, Zhou H (2004) Global analyses of sumoylated proteins in *Saccharomyces cerevisiae*. Induction of protein sumoylation by cellular stresses. J Biol Chem **279:** 32262-32268

Zhu Z, Xu F, Zhang Y, Cheng YT, Wiermer M, Li X (2010) Arabidopsis resistance protein SNC1 activates immune responses through association with a transcriptional corepressor. Proc Natl Acad Sci U S A **107:** 13960-13965

Chapter 3

Crosstalk between SUMO and MAPK signalling cascades

Y2H assays were performed together with Araceli Castillo.

CONTENTS

3.1. INTRODUCTION

The post-translational modifier (PTM) SUMO has clearly emerged as a heavyweight contender in the regulation of the plant response to environmental stimuli. Many SUMO targets act as key hubs in these responses, and sumoylation may be a PTM as important as phosphorylation, making it a high profile topic in current biology in general, and plant science in particular (Castro et al., 2012). The mechanism by which SUMO is attached to a target is designated as sumoylation: SUMO peptides are first processed by SUMO proteases (ULP/SENP family) exposing an N-terminal di-glycine motif, and then conjugated to a target's lysine via SUMO E1 activases (SAE1/SAE2 heterodimer), SUMO E2 conjugases (SCE) and aided by SUMO E3 ligases (e.g. SIZ/PIAS family). Deconjugation of the SUMO peptide can be carried out by the same SUMO proteases. Additionally, SUMO may establish non-covalent interactions with proteins that contain SUMO interacting motifs (SIMs). SIMs are composed of a short stretch of hydrophobic amino acids, (V/I)X(V/I)(V/I) or (V/I)(V/I)X(V/I), and flanked by acidic residues (Gareau and Lima, 2010).

The SIZ1 SUMO E3 ligase was previously associated with abiotic stress-responses, mainly by remodeling the activity of transcription factors (TFs; Castro et al., 2012). In addition, SIZ1 has been singled out as an important regulator of flowering time, plant growth and development (Catala et al., 2007; Jin et al., 2008; Miura et al., 2010). The *siz1* mutant displays a dwarf phenotype typical of constitutive autoimmune responses, characterized by salicylic acid (SA) over-accumulation (Lee et al., 2007; Miura et al., 2010). SIZ1 belongs to the PIAS/SIZ1 family, which is known for encompassing multifunctional proteins that possess several domains involved in functions other than sumoylation (Reindle et al., 2006; Sharrocks, 2006; Rytinki et al., 2009). None withstanding, *siz1* defects have been specifically related to dysfunctional capacity of SIZ1 to aid sumoylation, since the point mutation C379A in the catalytic SP-RING domain is sufficient to promote the *siz1* dwarfism phenotype (Cheong et al., 2009). In agreement, mutants that seriously compromise sumoylation upstream of SIZ1, such as *sum1 amiRSUM2* and dominant negative SCE1(C94S), display dwarfed phenotypes that are similar to *siz1* (van den Burg et al., 2010; Tomanov et al., 2013). SIZ1 is considered the main SUMO E3 ligase. A second functionally characterized E3 ligase, HPY2/MMS21, also displays a dwarfed phenotype but it is not SA-related (Ishida et al., 2012). SIZ1 and HPY2 expression patterns do not overlap, and reciprocal expression does not complement the single mutants (Ishida et al., 2012). Thus SIZ1 and HPY2 are likely to play different roles in the control of plant growth and development (Ishida et al., 2012).

MAPK cascades are common signal transducers in eukaryotes, acting as sequential phosphorylation cascades that link external stimulus to a rapid and adequate cellular response (MAPK-Group, 2002). In the pathway, MAP kinases (MPKs) are activated by upstream MAPK kinases (MKKs) that phosphorylate conserved threonine and tyrosine residues. In turn, MKKs are activated by MAPK kinase kinases (MEKKs) in serine and/or threonine residues (MAPK-Group, 2002). MAPKs act upon gene transcription regulation, and many described MPK targets are TFs (Fiil et al., 2009; Popescu et al., 2009; Yang et al., 2013). MAPK cascades have been associated with abiotic and biotic stress responses, as well as plant growth and development (Rodriguez et al., 2010). A good example of these pathways' mode-of-action is the MEKK1-MKK1/2-MPK4 cascade, whose loss-of-function mutants exhibit a gradient of phenotypic severity (Qiu et al., 2008b). Part of their phenotype results from constitutive autoimmune responses, including over-accumulation of SA, constitutive *Pathogen Releated* (*PR*) genes expression, and resistance to pathogens (Petersen et al., 2000; Gao et al., 2008; Qiu et al., 2008b; Zhang et al., 2012b). Moreover, the MEKK1-MKK1/2-MPK4 cascade has been implicated in the regulation of ROS levels (Pitzschke et al., 2009). Mutants within this cascade are ROS-accumulators, lacking the capacity to maintain homeostatic levels of ROS (Petersen et al., 2000; Nakagami et al., 2006; Gao et al., 2008).

Recently, van den Burg and Takken (2010) proposed that in plants, SUMO and MAPK-dependent phosphorylation of key proteins may collaborate in the regulation of the biotic stress-response. This cross-talk has been reported in other biological models, assuming the form of (1) sumoylation of MAPK components (Sobko et al., 2002; Woo et al., 2008; Kubota et al., 2011), (2) modification-by-phosphorylation of sumoylation machinery components (Yang and Sharrocks, 2006), (3) sharing of common targets. The later seems the most common situation, and common targets often include transcription factors such as HSFs, Bcl11b, Elk-1, PEA3, and STAT1 (Yang et al., 2003; Hietakangas et al., 2006; Vanhatupa et al., 2008; Guo and Sharrocks, 2009; Zhang et al., 2012a). Hietakangas et al. (2006) reported that some SUMO consensus sites contain an adjacent proline residue susceptible for phosphorylation (ΨKxExxSP), designed as phosphorylation-dependent sumoylation motif (PDSM). In this case, phosphorylation of the PDSM contributes for the sumoylation of the target (Hietakangas et al., 2006).

In the current work we proposed to explore MAPK and SUMO cross-talk in Arabidopsis. We found that the transcription profiles of *mkk1/2* and *mpk4* greatly overlapped with previously the published microarray profile of *siz1* (Catala et al., 2007). In agreement, we found that many transcription factors were commonly regulated by SUMO and MAPK. In our experiments we failed

to detect in vitro sumoylation of MKK2 or MPK4 or protein-protein interaction between MPK4 and SUMO in a yeast-two-hybrid (Y2H) assay. However, MAPK cascade components were found to regulate sumoylation levels in vivo in a SIZ1-dependent fashion. The present work is the first report on MAPK and SUMO interplay in plants.

3.2. RESULTS

When comparing the transcriptomic profile of *siz1* mutants at different developmental stages (10-day-old seedlings *vs* 4-week-old adult plants), roughly 20% of the differentially expressed genes (DEGs) overlap (Fig. 2.7B). One notorious difference between the two arrays is that SA-associated genes are mainly deregulated in adult plants (Fig. 2.7B). This is evident by the up-regulation in adult plants of central genes in plant defence such as *EDS1*, *PAD4*, *ICS1/SID2*, *NPR1* and many *PRs*. The autoimmune phenotype of the adult *siz1* mutants results in constitutive innate defence responses and several morphological defects (Lee et al., 2007; Miura et al., 2010). In contrast, *siz1* seedlings, growing in vitro, do not display such drastic development defects (Fig. 2.3; Catala et al., 2007).

To determine the molecular basis behind the adult *siz1* phenotype, we performed exploratory analysis for transcriptomic profiles that mimic the differential expression pattern of adult *siz1*. The *siz1* most significant up- and down-regulated genes (Catala et al., 2007) were matched against the differential transcriptome of publicly available Arabidopsis genotypes using the *Signature* feature of Genevestigator (Hruz et al., 2008). Strong matches were observed between *siz1* and MAPK cascade components *mkk1/2* (which scored highest) and *mpk4*, as well as mutants involved in biotic stress and SA-signaling such as *cpr5*, *bio4*, *csn5*, *cs26*, *lht1*, and *nudt7* (Fig. 3.1A). MEKK1-MKK1/2-MPK4 cascade mutants share several phenotypical features with *siz1*, including SA accumulation, constitutive *PR* genes expression, resistance to *Pst* DC3000, and ROS accumulation (Petersen et al., 2000; Nakagami et al., 2006; Gao et al., 2008; Qiu et al., 2008b; Zhang et al., 2012b), suggesting convergence between both signaling pathways. Therefore, when we cross-referenced predicted SUMO targets with putative MPK interactors, 63 matches were observed, a higher frequency than randomly expected (Fig. 3.1B). MPKs with the highest number of common targets were MPK4 and MPK6 (Fig. 3.1C). Although MPK4 is the usual target for MKK1/2, MKK2 can also phosphorylate MPK6 in vivo (Teige et al., 2004). In in vitro conditions, MKK1 can also modify MPK1, -2, -4, -5 and -6, and MKK2 can also modify MPK2, -4 and -6

(Popescu et al., 2009). To summarize, MKK1/2 may act towards MPK2, 4 and 6 which are the highest consensus modifiers of SUMO targets (Fig. 3.1C; Appendix III – Table S3.1). These observations reinforce the potential for cross-talk between the sumoylation pathway and MAPKs, with emphasis on MKK1/MKK2.

In non-plant organisms, some MKKs and MPKs were found to be SUMO targets (Sobko et al., 2002; Woo et al., 2008; Kubota et al., 2011). Curiously, *MKK1* and *MKK2* are up-regulated in *siz1* under normal conditions (Catala et al., 2007), yet the *siz1* phenotype suggests loss of MKK1/2 function, leading to the possibility of SIZ1-dependent post-translational regulation of MKK1/2. Taking in consideration that MKK1 and MKK2 are redundant (Gao et al., 2008; Qiu et al., 2008b), we checked MKK2 for in vitro sumoylation. Since MPK4 shares a similar transcriptomic profile and many SUMO targets, we explored if MPK4 was also a target of sumoylation. The sumoylation system consisted in the overexpression of mammalian SUMO, E1s and E2 (the system does not include an E3 ligase) in *E. coli* along with the target (Mencia and de Lorenzo, 2004). Constructs 6xHis-MKK2 and 6xHis-MPK4 were created to subsequently facilitate detection by immunoblotting. Results showed no obvious MKK2 shift corresponding to a putative MKK2-SUMO conjugate (Fig. 3.2A), while our positive control PCNA (Strzalka et al., 2012) showed a clear upper shift for the PCNA-SUMO isoform. Also, MPK4 did not show an obvious shift (Fig. 3.2B). We observed that the MPK4 sumoylation residues predicted using SUMOplot (www.abgent.com) were not canonical (Fig. 3.2C), and in these cases, sumoylation normally requires the activity of E3 ligases, which were absent in the *E. coli* expression essay. We performed a 3D topological model of MPK4, based on PDB ID 4IC7 structure, and observed that potential sumoylation sites were not openly exposed in the protein surface, which might indicate that MPK4 is not sumoylated. However, we observed within the catalytic domain several hydrophobic regions that matched the consensus site for SIMs (Fig. 3.2D). This raised the hypothesis that MPK4 may indeed interact with the SUMO peptide. Therefore, we tested if MPK4 interacted with Arabidopsis SUM1 and SUM3 in an Y2H assay. Results indicated that no interactions occur between Binding Domain (BD)-MPK4 and Activation Domain (AD)-SUM1, AD-SUM3 or the SUMO E2 AD-SCE1 (Fig. 3.2E). Nevertheless, MPK4 was capable of interacting weakly with itself (BD-MPK4 with AD-MPK4), BD-SCE1 with AD-SUM1 (as expected) and also the internal positive controls BD-p53/AD-AgT and BD-SNF4/AD-SNF1 were consistent, validating the Y2H experiment (Fig. 3.2E).

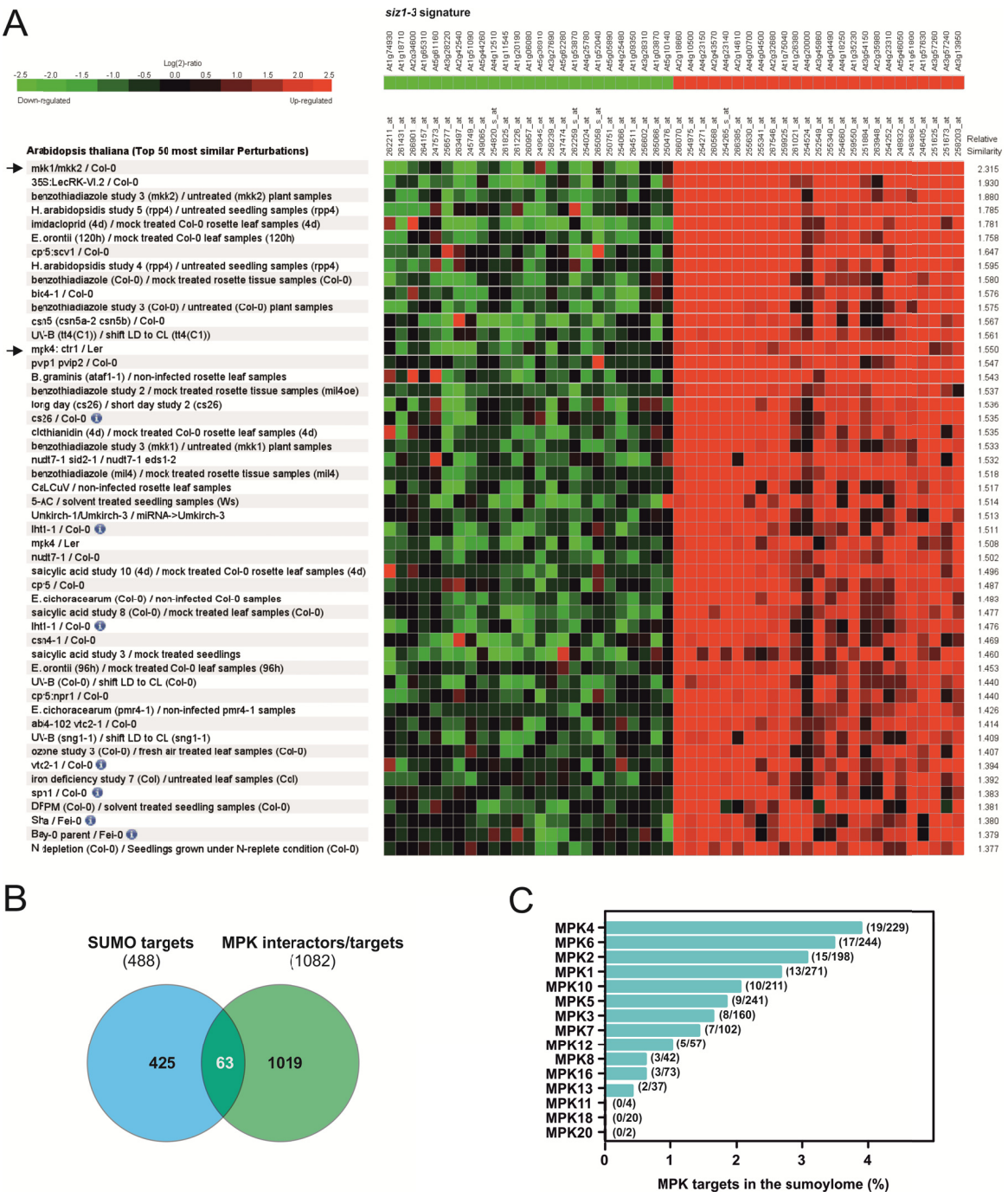

Figure 3.1. In silico analysis of SUMO and MAPK pathway crosstalk. **A**, Identification of the 50-most similar transcriptomic profiles that match the top 25 up- and down-regulated genes in *siz1-3* (Catala et al., 2007), using the Signature tool in Genevestigator (Hruz et al., 2008); arrows indicate MAPK pathway components. **B**, Venn diagram comparison of published SUMO targets against mitogen activated protein kinases (MPKs) interactors and targets obtained in the Arabidopsis Interactions Viewer (Geisler-Lee et al., 2007). **C**, Percentage of specific MPK targets within SUMO conjugates (sumoylome); parenthesis refer to the number of SUMO-conjugates per number of predicted MPK interactors.

To explore the genetic basis behind a potential SIZ1 and MAPK cascade convergence, we introgressed into the *siz1* background the mutants *mkk1*, *mkk2*, *mkk1/2* (Qiu et al., 2008b) and *mpk4* from SALK (Fig. 3.3A). The MPK4 mutant (*mpk4*, SALK_056245) was genotyped and expression of *MPK4* was assessed by quantitative Real-Time PCR (qPCR) and western blot, since it was uncharacterized at the beginning of the present study (Fig. 3.3B-E). The *MPK4* transcript was almost undetectable and no protein was detected by immunoblot in the mutant. Already in the early stages of development, *mpk4* showed abnormal root growth (Fig. 3.3F) and seedling lethality (data not shown). In fact, all the MEKK1-MKK1/2-MPK4 cascade components mutants are lethal in the seedling stage (reviewed by Rodriguez et al., 2010). Unlike *mkk1/2*, the *mkk1* and *mkk2* single mutants do not show development defects due to functional redundancy (Gao et al., 2008; Qiu et al., 2008b). This lethality was circumvented by permanently growing plants in a higher though moderate temperature (28°C; Fig. 3.4A), as previously described (Gao et al., 2008; Qiu et al., 2008b). While *mkk1/2* greatly recovered to a wild-type phenotype (Fig. 3.4A), *mpk4* still showed some development defects (Fig. 3.3G, 3.4A), including aberrant flowering development (Fig. 3.3F). Interestingly, *siz1* developmental defects were also greatly recovered by temperature (Fig. 3.4A), a previously unreported result. We subsequently analyzed the SUMO profile of the mutants, and as expected *siz1* displayed a reduction in high molecular weight SUMO conjugates (Fig. 3.4B). We observed that *mpk4* accumulated more SUM1/2-conjugates, while *mkk1/2* and to some extent *mkk2* accumulated less SUM1/2-conjugates (Fig. 3.4B). We also noticed that sometimes *mkk1/2* did not recover to a wild-type phenotype (herein designated *dwarf*); in those situations the SUM1/2-conjugates levels were increased. Results suggest that developmental fitness of the mutants correlate with their overall SUMO-conjugate level. SUM3-conjugates unexpectedly increased in the *siz1* mutant but not in any of the other mutants (Fig. 3.4C).

We also performed an anti-MPK4 immunoblot, and results suggested that more than one band might be present. Given the observed molecular weight, the band is likely to reflect the phosphorylated MPK4 form (Fig. 3.4D). In agreement, the *mkk1/2* mutant showed a thinner band. No differences were observed in *siz1* comparing to the wild-type, suggesting that SIZ1 may not interfere significantly with MPK4 phosphorylation. At normal temperature, MPK4 levels seemed higher in comparison to plants growing at 28°C (Fig. 3.4D).

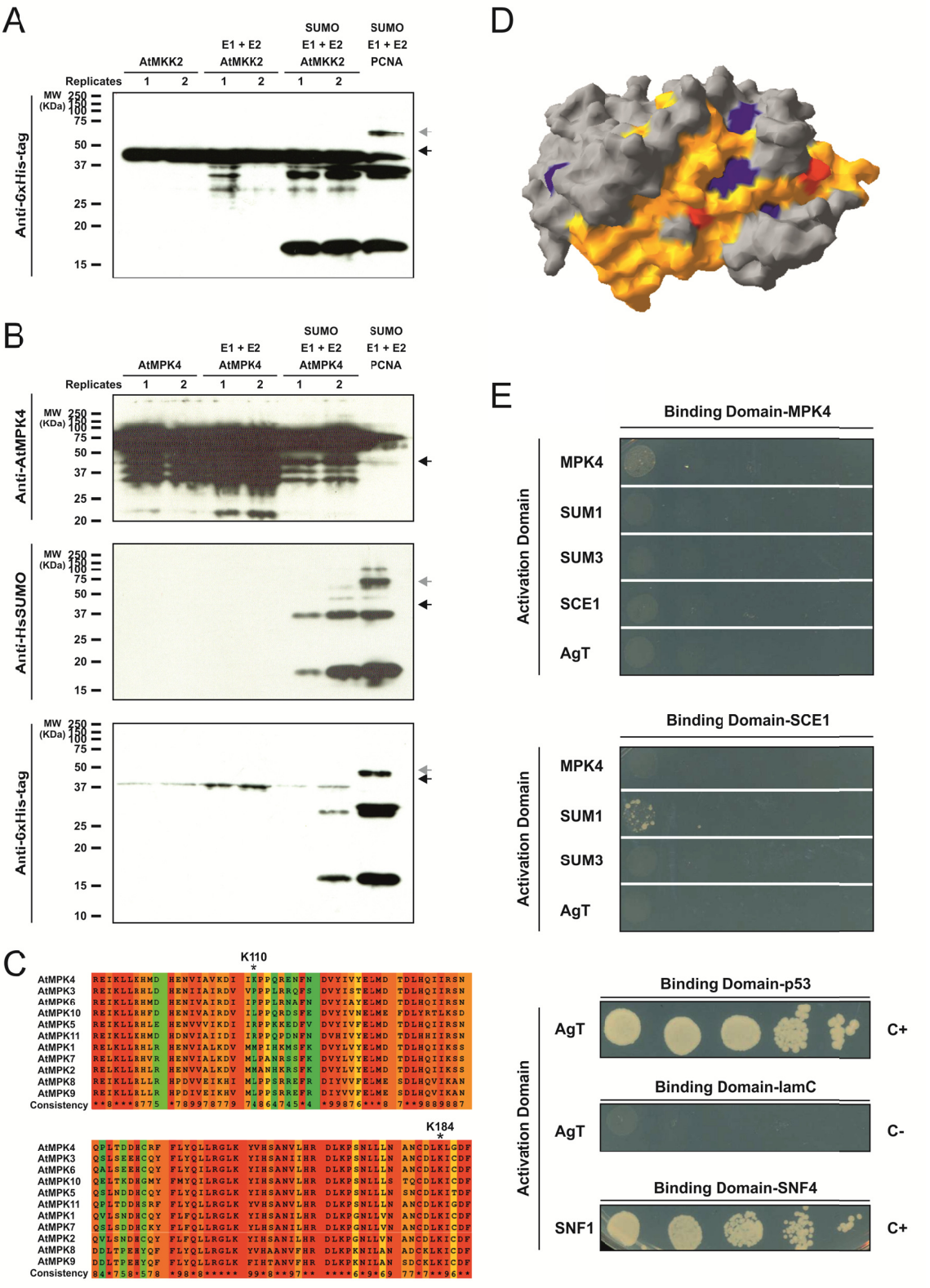

Figure 3.2. Analysis of the potential interaction between MAPK and SUMO components. **A,B**, Sumoylation in bacteria system (Mencia and de Lorenzo, 2004) of Arabidopsis MKK2 (A) and MPK4 (B) both with an N-terminus 6xHis tag. Predicted protein weight of the sumoylated form is indicated with a black arrow (MKK2 or MPK4) or a grey arrow (PCNA). **C**, Protein partial sequence alignment of Arabidopsis MPKs. Arrows indicate the predicted sumoylable lysine (K) in MPK4. Consistency between sequences indicates the levels of conservation of each residue. **D**, Predicted tridimensional structure of MPK4, highlighting the catalytic domain (yellow), predicted SUMO site residues (red), and

SUMO-interacting motifs (blue). Structural extrapolation based on PDB ID 4IC7. **E**, Yeast two-hybrid assay between MPK4 and SUMO components such SUM1, SUM3, and SUMO E2 conjugase SCE1. Yeast were grown for 7 days on plates lacking histidine and supplemented with 2 mM 3-AT. The interactions AD-AgT with BD-p53 and AD-SNF1 with BD-SNF4 are positive controls, while AD-AgT with BD-lamC are negative controls.

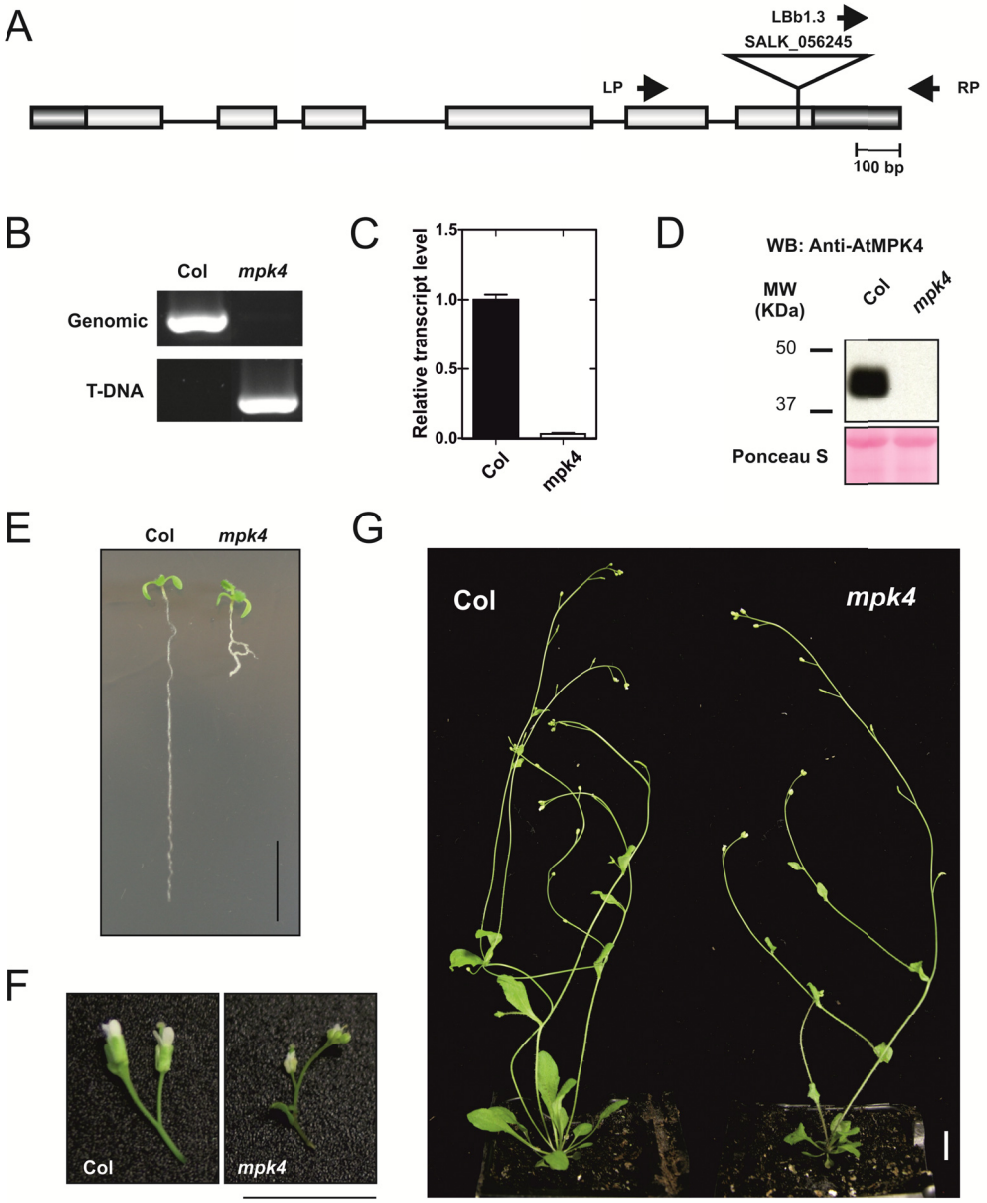

Figure 3.3. Characterization of the MPK4 T-DNA insertion mutant. **A**, Schematic representation of *MPK4* (At4g01370) with indication of T-DNA insertion site (inverted triangle) and primer locations for diagnostic PCR genotyping (arrows); exons and UTRs are represented by grey and black boxes, respectively. **B**, Diagnostic PCR confirmation of *mpk4* T-DNA homozygous line. **C**, Quantitative RT-PCR analysis of *MPK4* relative expression levels in the wild-type (Col) and *mpk4* backgrounds. **D**, Western blot analysis of protein extracts from 1-month-old Col and *mpk4* plants, grown at 28°C. Protein extracts (50 µg per lane) were analyzed by protein gel blots using anti-AtMPK4 polyclonal antibodies. As a loading control, Ponceau S staining of the large subunit of Rubisco (55 kDa) is displayed. **E**, Morphology of 10-day-old *mpk4* and wild-type (Col) seedlings. **F**, Flower morphological defects of *mpk4*. Plants were grown for 1 month at 28°C and then transferred to 23°C to produce flowers. **G**, Morphology of Col and *mpk4* soil-grown 4-week-old plants at 28°C. Scale bars indicate 1 cm.

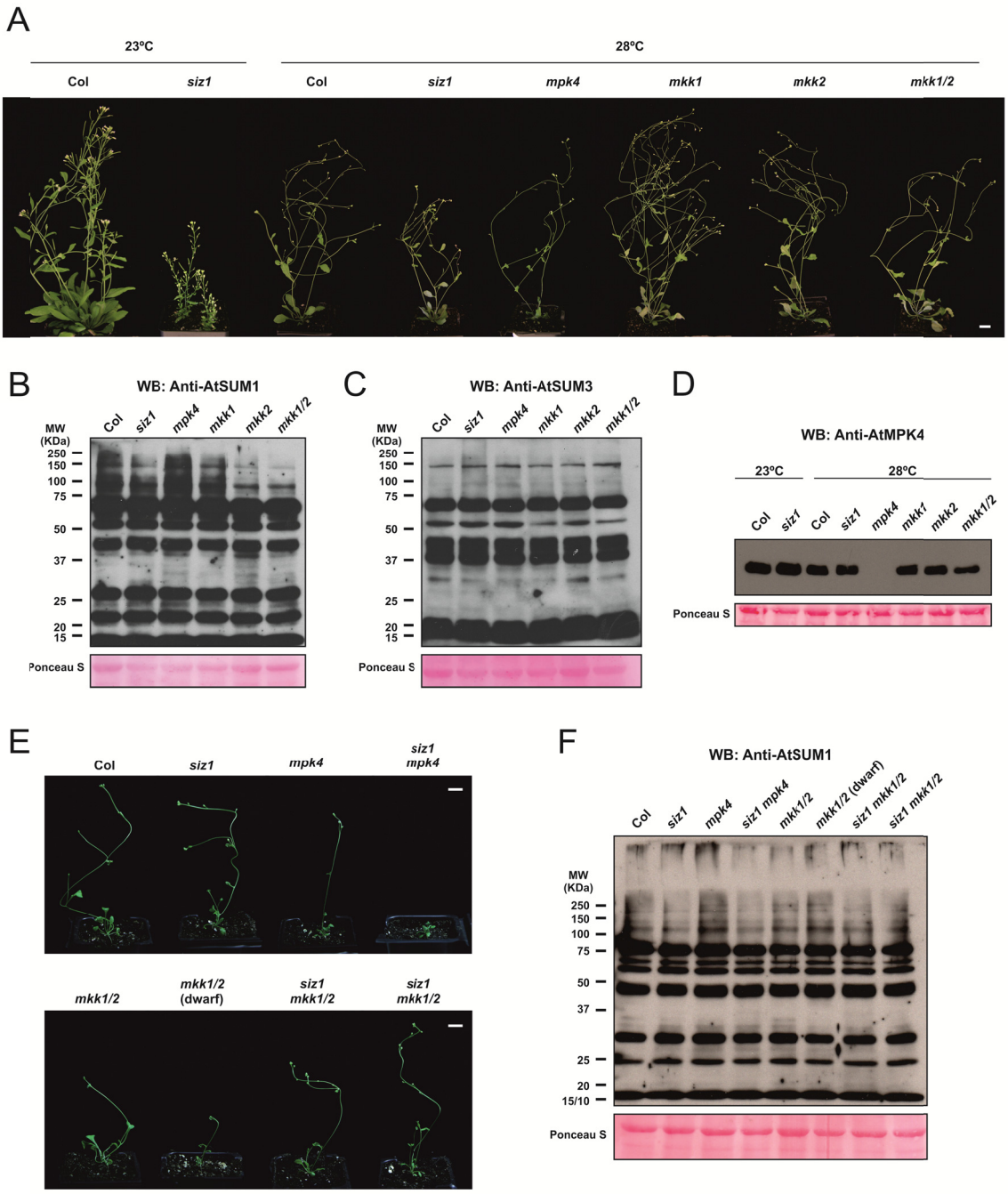

Figure 3.4. Characterization of loss-of-function mutants for SIZ1 and MAPK cascade components MKK1/2 and MPK4 in terms of morphology and sumoylation profile. **A**, Morphology of plants grown for 10 days in vitro and for 4 weeks in soil at 23°C or 28°C. Scale bar indicates 1 cm. **B-D**, Western blot analysis of protein extracts from 1-month-old Col, *siz1*, *mpk4*, *mkk1*, *mkk2* and *mkk1/2* growing at 28°C, using anti-AtSUMO1 (B), anti-AtSUMO3 (C), and anti-AtMPK4 (D). Ponceau S staining of the large subunit of Rubisco (55 kDa) was used as loading control. **E**, Morphology of *mpk4* and *mkk1*/2 mutants in *siz1* background, grown for10 days in vitro and for 3 weeks in soil at 28°C. Scale bar indicates 1 cm. **F**, Western blot analysis of 1 month-old *mpk4* and *mkk1*/2 mutants in *siz1* background, using anti-SUMO1.

Concerning introgressed SIZ1 and MAPK mutants, *siz1 mkk1/2* showed a *siz1*-like phenotype, while *siz1 mpk4* was much more dwarfed (Fig. 3.4E). The SUM1/2-conjugate accumulation in *mpk4* decreased in *siz1 mpk4*, placing SIZ1 as partially responsible for SUM1/2-conjugate increment in *mpk4* (Fig. 3.4F). The triple mutant *siz1 mkk1/2* did not show great differences in relation to *siz1* or *mkk1/2* (Fig. 3.4F). Overall results suggest a clear convergence between SUMO and MAPK signaling pathways, though MAPK components display a differential role in the interplay with sumoylation.

3.3. DISCUSSION

In this report we describe the first experimental evidence of SUMO and MAPK cross-talk in plants. The similarity of the transcriptomic profile of *siz1* adult plants with that of *mkk1/2* and *mpk4* mutants suggests that both pathways may cooperate in the coordination of the activity of common targets (Fig. 3.1A). In fact, most of the targets for both pathways are transcription regulators and a significant number are common to SUMO and MPKs (Fig. 3.1B-C; Popescu et al., 2009; Castro et al., 2012; Mazur and van den Burg, 2012). It is therefore feasible that SUMO machinery components and MPK-signaling elements such as the MEKK1-MKK1/2-MPK4 cascade converge at some point to regulate transcription. Similarly, it was previously reported that SIZ1 is located in the nucleus and MKK1/2 and MPK4 interact in the plasma membrane and nucleus (Miura et al., 2005; Gao et al., 2008), allowing direct modulation of common targets.

A potential direct interaction between both PTMs may occur, as was previously described for non-plant models. This crosstalk may occur by the sumoylation of MAPK cascade components (Sobko et al., 2002; Woo et al., 2008; Kubota et al., 2011), phosphorylation of sumoylation machinery elements (Yang and Sharrocks, 2006), or the modulation of activity in common targets (Yang et al., 2003; Hietakangas et al., 2006; Vanhatupa et al., 2008; Guo and Sharrocks, 2009; Zhang et al., 2012a). For instance, the *Dictyostelium* MEK1 is sumoylated in the nucleus in response to chemoattractant stimulation, then it is released into the cytoplasm where it activates the MAPK ERK1 (Sobko et al., 2002). To check if components of the MEKK1-MKK1/2-MPK4 cascade were sumoylated, we employed an in bacteria sumoylation system described by Mencia and de Lorenzo (2004). In our experiment we could not detect an obvious SUMO-conjugated version of MKK2 or MPK4, although good levels of unconjugated proteins were obtained (Fig. 3.2A,B). Given that *Dictyostelium* MEK1 activity and phosphorylation are critical for its sumoylation

(Sobko et al., 2002), perhaps MKK1/2 and MPK4 might also need to be activated first prior to be sumoylated. Another possible explanation for the absence of sumoylation of these MAPKs, is that it occurs in a SUMO E3 ligase-dependent fashion, a component that is missing in our sumoylation system. Kubota et al. (2011) reported that MEK1/2 is sumoylated by a specific SUMO E3 ligase that is, in fact, the upstream kinase MEKK1. At the plasma membrane, MEKK1 interacts with SUMO E2 conjugase UBC9 and with MEK1/2, sumoylating the latter (Kubota et al., 2011). MPK4 potential sumoylation sites, predicted by SUMOplot, are not canonical (Fig. 3.2C) and in these cases the sumoylation requires the activity of an E3 ligase (Yunus and Lima, 2009). In favor of this idea, MPK4 was incapable of interacting with the SUMO E2 conjugase SCE1 in an Y2H assay (Fig. 3.2E). Meanwhile, positional analysis of predicted MPK4 sumoylation sites within the topological model suggests that MPK4 sumoylation is unlikely to occur due to lysine seems inaccessible (Fig. 3.2D).The 3D location of SIMs inside the MPK4 catalytic pocket (Fig. 3.2D) suggested that this MAPK would interact directly with SUMOs by non-covalent bounding. However no interaction with SUM1 or SUM3 was observed in the context of our experiments (Fig. 3.2E).

As described for other biological systems, phosphorylation of some targets may enhance its sumoylation (Hietakangas et al., 2006). It is likely that phosphorylation-dependent sumoylation also occurs in plants since MKK1/2-MPK4 and SUMO share some common targets (Fig. 3.1C). Examples include WRKY transcription factors such as WRKY33. WRKY33 is a target for MPK4 phosphorylation and was pointed as a SUMO-conjugate in a high-throughput identification of SUM1-conjugates (Qiu et al., 2008a; Miller et al., 2010). WRKY33 is an important regulator of *PAD3* expression, contributing for camalexin synthesis after pathogen attack. The *wrky33* mutant partially suppresses the *mpk4* phenotype (Qiu et al., 2008a). Interestingly, *PAD3* is also up-regulated in *siz1-3* (Catala et al., 2007). The phosphorylation of the mouse PEA3 TF contributes for its sumoylation (Guo and Sharrocks, 2009) and it would be important to determine if this also occurs to WRKY33. Other transcription factors involved in plant defence mechanisms have been predicted to be modified by both pathways (van den Burg and Takken, 2010). Thus SUMO-MAPK crosstalk would be particularly important in the response to pathogen attack, as both pathways were singled out as negative regulators of innate immunity (Lee et al., 2007; Gao et al., 2008; Qiu et al., 2008b; van den Burg et al., 2010).

Mutants for the MEKK1-MKK1/2-MPK4 components and SUMO machinery mutants such as those for SUM1/2 and SIZ1 are dwarfed, partially due to SA-accumulation (Petersen et al., 2000; Brodersen et al., 2006; Lee et al., 2007; Qiu et al., 2008b; van den Burg et al., 2010),

sharing common developmental phenotypes. We previously reported that *siz1* constitutively accumulates ROS, partially due to SA-accumulation (Chapter 2). Also *mekk1*, *mkk1/2* and *mpk4* mutants accumulate ROS and their differentially expression gene patterns show a great overlap with ROS and SA-regulated gene expression (Pitzschke et al., 2009). It is well described that SUMO-conjugation levels increase in response to oxidative stress (Chapter 2; Kurepa et al., 2003). This induction is partially dependent on SIZ1-activity since the mutant still shows some increase in SUMO-conjugates after H_2O_2 treatment (Chapter 2). Considering that SIZ1 is highly sumoylated in response to oxidative stress (Miller et al., 2013), it is likely that SIZ1 plays a role in the regulation of sumoylation in response to ROS oscillation, especially in response to stress conditions. MAPKs have been singled out as ROS sensors, and the MEKK1-MKK1/2-MPK4 cascade, also involved in ROS homeostasis regulation, may be activated to regulate SUMO-conjugate levels.

The *mkk1/2* and *mpk4* mutants are seedling lethal when grown at standard conditions, but at moderately increase temperatures (28-32°C) mutants are able to grow (Su et al., 2007; Gao et al., 2008; Qiu et al., 2008b). The *mkk1/2* mutant showed in some occasions a dwarf phenotype, probably because 28°C is the threshold for recovery from the dwarf phenotype (Fig. 3.4E). Nevertheless, when *mkk1/2* is similar to the wild-type, the sumoylation levels are relatively low (Fig. 3.4F). In contrast, when *mkk1/2* is dwarfed, the sumoylation levels increase (Fig. 3.4F). In the case of *mpk4*, the development defects are moderately attenuated by a mild increase in temperature (Fig. 3.4A). MPK4 also functions in other processes apart of MAPK cascades, including a role in microtubule organization (reviewed by Komis et al., 2011), and that accounts for the great root defects in early stages, not observed in *mkk1/2*. The *mpk4* root phenotype is independent of *siz1* (data not shown). The increment of sumoylation in *mpk4* is, at least partially, due to SIZ1 since the double *siz1 mpk4* mutant shows a decrease in SUMO-conjugate pattern (Fig. 3.4F). The double mutant *siz1 mpk4* enhanced the dwarfism of the single *mpk4*, while *siz1-2* is similar to wild-type (Fig. 3.4F). One important aspect to take in consideration is that the MEKK1-MKK1/2-MPK4 is indirectly guarded by the resistance (R) protein SUMM2 (Kong et al., 2012; Zhang et al., 2012b). The constitutively autoimmune responses are practically lost in MAPK mutants in the *summ2* background (Zhang et al., 2012b). Interestingly, expression of *SUMM2* increases in the *siz1-3* mutant (Catala et al., 2007). It is possible that, to some extent, *SUMM2* up-regulation in *siz1* may contribute for the enhanced dwarfism of *mpk4* even when grown at higher temperatures. In addition, *SUMM2* up-regulation may also contribute for *siz1* dwarfism. Moderately higher temperature inhibit defence responses triggered by R genes (Alcazar and Parker, 2011).

This inhibition is due to the inability of SNC1 and RPS4 to localize in the nucleus, a mechanism dependent on the ABA increment at high temperature (Mang et al., 2012). SUMO is a regulator of both ABA signaling and nuclear-cytoplasm trafficking (Palancade and Doye, 2008; Miura et al., 2009; Zheng et al., 2012) therefore, sumoylation may be an important mechanims in R-mediated immunity at the transcription and post-transcriptional levels.

3.4. MATERIALS AND METHODS

Plant material and growth conditions

The *Arabidopsis thaliana* wild-type ecotype Columbia-0 (Col) and T-DNA insertion mutants SALK_065397 (*siz1-2*; Miura et al., 2005) and SALK_056245 (*mpk4-2*) were ordered through the NASC European Arabidopsis Stock Centre (arabidopsis.info) or the Arabidopsis Biological Resource Stock Center (www.biosci.ohio-state). The mutants SALK_027645 (*mkk1-3*), SAIL_551_H_01 (*mkk2-1*) and double mutant *mkk1 mkk2* (*mkk1/2*) seeds were kindly provided by Peter C. Morris (Heriot-Watt University, UK; Qiu et al., 2008b). Homozygous insertion mutants were genotyped based on SIGnAL T-DNA Primer Design (signal.salk.edu/tdnaprimers.2.html), using primers in Table S3.2 (Appendix III) and previously described by Qiu et al. (2008b).

Seeds were stratified for 3 days at 4°C in the dark. Seeds were surface sterilized in a horizontal laminar flow chamber by immersing sequentially in 70% (v/v) ethanol for 5 min and 20% (v/v) commercial bleach for 10 min before washing five times with sterile ultra-pure water. Seeds were resuspended in sterile 0.25% (w/v) agarose, sown onto 1.2% (w/v) agar-solidified MS medium (Murashige and Skoog, 1962) containing 1.5% (w/v) sucrose, 0.5 g L^{-1} MES, pH 5.7, and grown vertically in culture rooms with a 16 h light/8 h dark cycle under cool white light (80 µE m^{-2} s^{-1} light intensity) at 22-23°C. In vitro-grown 7-day-old seedlings were transferred to a soil to vermiculite (4:1) mixture. Plants were watered regularly and maintained at 23°C or 28°C with 80% humidity. Plants were genotyped by PCR before the experimental assays.

Quantitative Real-Time PCR

RNA was extracted from plant tissue using an *RNeasy Plant Mini kit* (QIAGEN). Estimation of RNA quantity and quality was performed using both a Nanodrop ND-1000 spectrophotometer and standard agarose-gel electrophoretic analysis. Afterwards, RNA samples were treated with

Recombinant DNase I (Takara Biotechnology) and cDNA was generated using a *SuperScript II Reverse Transcriptase kit* (Invitrogen). For the qPCR reaction mixture *SsoFast EvaGreen Supermix* (BioRad) was used according to the manufacturer's indications. The reaction was performed in a *MyiQ Single-Color Real-Time PCR Detection system* (Bio-Rad).

Primers for qPCR (Appendix III - Table S3.3) were designed using NCBI Primer-BLAST (www.ncbi.nlm.nih.gov/tools/primer-blast/; Ye et al., 2012) to ensure specific amplification within the Arabidopsis transcriptome, 100-250 bp PCR amplification product size, 50-60% GC content and ~60°C T_m. *ACT2* (At3g18780) was used as a reference gene (Lozano-Duran et al., 2011).

Plasmid construction, bacteria transformation and yeast two-hybrid assay

The Arabidopsis *MPK4* and *MKK2* open reading frames were amplified from cDNA using the *Expand High Fidelity PCR System* (Roche) that contains Taq DNA polymerase and Tgo DNA polymerase with proofreading activity. The primers were designed to incorporate the appropriate restriction sites (Appendix III – Table S3.4): *NheI* and *XhoI* to clone into pET28b (Novagen), and *NotI* and *AscI* to clone into pENTR (Invitrogen). The amplification product was sub-cloned into the pGEM-T Easy vector (Promega) and sequenced. The pENTR-MPK4 vector was used to transfer the MPK4 ORF by recombination into yeast two-hybrid vectors pGADT7 and pGBT9 (Clontech) using the *Gateway LR Clonase II* enzyme mix (Invitrogen).

Escherichia coli strain NCM631 competent cells (Govantes et al., 1996) were transformed with pET28-MPK4 or pET28-MKK2. Sequential transformations and gene overexpression were performed according to Mencia and de Lorenzo (2004). Y2H assays were performed as described in Castillo et al. (2004).

Protein extraction and Immunoblotting

Plant tissue was frozen in liquid nitrogen and grinded in a microtube with polypropylene pestles. Protein extracts were prepared by adding extraction buffer [50 mM Tris; 150 mM NaCl; 0.2% (v/v) Triton X-100] supplemented with *Complete Protease Inhibitor Cocktail* (Roche) as per the manufacturer's instructions. Samples were incubated for 1 h at 4°C with agitation and then centrifuged for 30 min at 16000 *g*. The supernatant was recovered and stored at -80°C. Protein was spectrophotometrically quantified using *Bradford reagent* (Bio-Rad; Bradford, 1976). In the case of in bacteria sumoylation, cell culture suspensions were directly re-suspended in sample buffer and boiled at 95°C.

Equal amounts of protein were resolved by standard SDS-PAGE in a 10% (w/v) acrylamide resolving gel, using a *Mini-PROTEAN Cell* (Bio-Rad) apparatus. For immunoblotting, proteins were transferred to a PVDF-membrane using a *Semi-dry Transfer Unit TE 77* (Hoefer) or *Trans-Blot Turbo Transfer System* (Bio-Rad). The membrane was blocked for 1 h at RT in blocking solution [5% (w/v) dry milk powder in PBST]. The primary antibody was added in a dilution 1:2000 of anti-AtSUMO1 (ABCAM), 1:2000 of anti-AtSUMO3 (ABCAM), 1:500 of anti-HsSUMO (Abgent), 1:3000 of anti-6xHis-tag (Biomedal), or 1:1000 of anti-AtMPK4 (Sigma) and incubated for 3 to 5 h. The membrane was washed three times with 10 mL of PBST for 10 min, and incubated with the secondary antibody (anti-rabbit IgG-HRP or anti-mouse IgG-HRP, Sigma and GE Healthcare, respectively; 1:10,000 in blocking solution) for 1 h. The membrane was washed as previously detailed and developed by a chemiluminescence reaction using the *Immune-Star WesternC Kit* (Bio-Rad) and detected by photographic film. As a protein loading control, PVDF membranes were stained with Ponceau S solution [0.1% (w/v) Ponceau S; 5% (v/v) acetic acid].

Bioinformatics analysis

Protein sequence alignment of the Arabidopsis MAPK family was performed using PRALINE (Simossis and Heringa, 2005). The SUMO plot Analysis Program was used to predict the highest probable SUMO attachment lysine (www.abgent.com/tools/). The structural extrapolation of AtMPK4 protein was performed using the SWISS-MODEL workspace (Arnold et al., 2006), as previously detailed (Bordoli et al., 2009). The program DeepView/Swiss-PdbViewer was used to display and manipulate the extrapolated protein structure (Johansson et al., 2012).

The comparison of the most deregulated genes in the microarray data with available transcriptomic profiles was done using the Signature tool in Genevestigator (Hruz et al., 2008). MPKs interactors and targets were obtained from the Arabidopsis Interactions Viewer (Geisler-Lee et al., 2007). Venn diagrams were calculated using Venn Diagram Generator (www.pangloss.com/seidel/Protocols/venn.cgi).

3.5. REFERENCES

Alcazar R, Parker JE (2011) The impact of temperature on balancing immune responsiveness and growth in Arabidopsis. Trends Plant Sci **16:** 666-675

Arnold K, Bordoli L, Kopp J, Schwede T (2006) The SWISS-MODEL workspace: a web-based environment for protein structure homology modelling. Bioinformatics **22:** 195-201

Bordoli L, Kiefer F, Arnold K, Benkert P, Battey J, Schwede T (2009) Protein structure homology modeling using SWISS-MODEL workspace. Nat Protoc **4:** 1-13

Bradford MM (1976) A rapid and sensitive method for the quantitation of microgram quantities of protein utilizing the principle of protein-dye binding. Anal Biochem **72:** 248-254

Brodersen P, Petersen M, Bjorn Nielsen H, Zhu S, Newman MA, Shokat KM, Rietz S, Parker J, Mundy J (2006) Arabidopsis MAP kinase 4 regulates salicylic acid- and jasmonic acid/ethylene-dependent responses via EDS1 and PAD4. Plant Journal **47:** 532-546

Castillo AG, Kong LJ, Hanley-Bowdoin L, Bejarano ER (2004) Interaction between a geminivirus replication protein and the plant sumoylation system. J Virol **78:** 2758-2769

Castro PH, Tavares RM, Bejarano ER, Azevedo H (2012) SUMO, a heavyweight player in plant abiotic stress responses. Cell Mol Life Sci **69:** 3269-3283

Catala R, Ouyang J, Abreu IA, Hu Y, Seo H, Zhang X, Chua NH (2007) The Arabidopsis E3 SUMO ligase SIZ1 regulates plant growth and drought responses. Plant Cell **19:** 2952-2966

Cheong MS, Park HC, Hong MJ, Lee J, Choi W, Jin JB, Bohnert HJ, Lee SY, Bressan RA, Yun DJ (2009) Specific domain structures control abscisic acid-, salicylic acid-, and stress-mediated SIZ1 phenotypes. Plant Physiol **151:** 1930-1942

Fiil BK, Petersen K, Petersen M, Mundy J (2009) Gene regulation by MAP kinase cascades. Curr Opin Plant Biol **12:** 615-621

Gao M, Liu J, Bi D, Zhang Z, Cheng F, Chen S, Zhang Y (2008) MEKK1, MKK1/MKK2 and MPK4 function together in a mitogen-activated protein kinase cascade to regulate innate immunity in plants. Cell Res **18:** 1190-1198

Gareau JR, Lima CD (2010) The SUMO pathway: emerging mechanisms that shape specificity, conjugation and recognition. Nat Rev Mol Cell Biol **11:** 861-871

Geisler-Lee J, O'Toole N, Ammar R, Provart NJ, Millar AH, Geisler M (2007) A predicted interactome for Arabidopsis. Plant Physiol **145:** 317-329

Govantes F, Molina-Lopez JA, Santero E (1996) Mechanism of coordinated synthesis of the antagonistic regulatory proteins NifL and NifA of *Klebsiella pneumoniae*. J Bacteriol **178:** 6817-6823

Guo B, Sharrocks AD (2009) Extracellular signal-regulated kinase mitogen-activated protein kinase signaling initiates a dynamic interplay between sumoylation and ubiquitination to regulate the activity of the transcriptional activator PEA3. Mol Cell Biol **29:** 3204-3218

Hietakangas V, Anckar J, Blomster HA, Fujimoto M, Palvimo JJ, Nakai A, Sistonen L (2006) PDSM, a motif for phosphorylation-dependent SUMO modification. Proc Natl Acad Sci U S A **103:** 45-50

Hruz T, Laule O, Szabo G, Wessendorp F, Bleuler S, Oertle L, Widmayer P, Gruissem W, Zimmermann P (2008) Genevestigator v3: a reference expression database for the meta-analysis of transcriptomes. Adv Bioinformatics **2008:** 420747

Ishida T, Yoshimura M, Miura K, Sugimoto K (2012) MMS21/HPY2 and SIZ1, two Arabidopsis SUMO E3 ligases, have distinct functions in development. PLoS One **7:** e46897

Jin JB, Jin YH, Lee J, Miura K, Yoo CY, Kim WY, Van Oosten M, Hyun Y, Somers DE, Lee I, Yun DJ, Bressan RA, Hasegawa PM (2008) The SUMO E3 ligase, AtSIZ1, regulates flowering by controlling a salicylic acid-mediated floral promotion pathway and through affects on *FLC* chromatin structure. Plant J **53:** 530-540

Johansson MU, Zoete V, Michielin O, Guex N (2012) Defining and searching for structural motifs using DeepView/Swiss-PdbViewer. BMC Bioinformatics **13:** 173

Komis G, Illes P, Beck M, Samaj J (2011) Microtubules and mitogen-activated protein kinase signalling. Curr Opin Plant Biol **14:** 650-657

Kong Q, Qu N, Gao M, Zhang Z, Ding X, Yang F, Li Y, Dong OX, Chen S, Li X, Zhang Y (2012) The MEKK1-MKK1/MKK2-MPK4 kinase cascade negatively regulates immunity mediated by a mitogen-activated protein kinase kinase kinase in Arabidopsis. Plant Cell **24:** 2225-2236

Kubota Y, O'Grady P, Saito H, Takekawa M (2011) Oncogenic Ras abrogates MEK SUMOylation that suppresses the ERK pathway and cell transformation. Nat Cell Biol **13:** 282-291

Kurepa J, Walker JM, Smalle J, Gosink MM, Davis SJ, Durham TL, Sung DY, Vierstra RD (2003) The small ubiquitin-like modifier (SUMO) protein modification system in Arabidopsis. Accumulation of SUMO1 and -2 conjugates is increased by stress. J Biol Chem **278:** 6862-6872

Lee J, Nam J, Park HC, Na G, Miura K, Jin JB, Yoo CY, Baek D, Kim DH, Jeong JC, Kim D, Lee SY, Salt DE, Mengiste T, Gong Q, Ma S, Bohnert HJ, Kwak SS, Bressan RA, Hasegawa PM, Yun DJ (2007) Salicylic acid-mediated innate immunity in Arabidopsis is regulated by SIZ1 SUMO E3 ligase. Plant J **49:** 79-90

Lozano-Duran R, Rosas-Diaz T, Gusmaroli G, Luna AP, Taconnat L, Deng XW, Bejarano ER (2011) Geminiviruses subvert ubiquitination by altering CSN-mediated derubylation of SCF E3 ligase complexes and inhibit jasmonate signaling in *Arabidopsis thaliana*. Plant Cell **23:** 1014-1032

Mang HG, Qian W, Zhu Y, Qian J, Kang HG, Klessig DF, Hua J (2012) Abscisic acid deficiency antagonizes high-temperature inhibition of disease resistance through enhancing nuclear accumulation of resistance proteins SNC1 and RPS4 in Arabidopsis. Plant Cell **24:** 1271-1284

MAPK-Group (2002) Mitogen-activated protein kinase cascades in plants: a new nomenclature. Trends Plant Sci **7:** 301-308

Mazur MJ, van den Burg HA (2012) Global SUMO proteome responses guide gene regulation, mRNA biogenesis, and plant stress responses. Front Plant Sci **3:** 215

Mencia M, de Lorenzo V (2004) Functional transplantation of the sumoylation machinery into *Escherichia coli*. Protein Expression and Purification **37:** 409-418

Miller MJ, Barrett-Wilt GA, Hua Z, Vierstra RD (2010) Proteomic analyses identify a diverse array of nuclear processes affected by small ubiquitin-like modifier conjugation in Arabidopsis. Proc Natl Acad Sci U S A **107:** 16512-16517

Miller MJ, Scalf M, Rytz TC, Hubler SL, Smith LM, Vierstra RD (2013) Quantitative proteomics reveals factors regulating RNA biology as dynamic targets of stress-induced SUMOylation in Arabidopsis. Mol Cell Proteomics **12:** 449-463

Miura K, Lee J, Jin JB, Yoo CY, Miura T, Hasegawa PM (2009) Sumoylation of ABI5 by the Arabidopsis SUMO E3 ligase SIZ1 negatively regulates abscisic acid signaling. Proc Natl Acad Sci U S A **106:** 5418-5423

Miura K, Lee J, Miura T, Hasegawa PM (2010) SIZ1 controls cell growth and plant development in Arabidopsis through salicylic acid. Plant Cell Physiol **51:** 103-113

Miura K, Rus A, Sharkhuu A, Yokoi S, Karthikeyan AS, Raghothama KG, Baek D, Koo YD, Jin JB, Bressan RA, Yun DJ, Hasegawa PM (2005) The Arabidopsis SUMO E3 ligase SIZ1 controls phosphate deficiency responses. Proc Natl Acad Sci U S A **102:** 7760-7765

Murashige T, Skoog F (1962) A revised medium for rapid growth and bio assays with tobacco tissue cultures. Physiol Plant **15:** 473-475

Nakagami H, Soukupova H, Schikora A, Zarsky V, Hirt H (2006) A Mitogen-activated protein kinase kinase kinase mediates reactive oxygen species homeostasis in Arabidopsis. J Biol Chem **281:** 38697-38704

Palancade B, Doye V (2008) Sumoylating and desumoylating enzymes at nuclear pores: underpinning their unexpected duties? Trends Cell Biol **18:** 174-183

Petersen M, Brodersen P, Naested H, Andreasson E, Lindhart U, Johansen B, Nielsen HB, Lacy M, Austin MJ, Parker JE, Sharma SB, Klessig DF, Martienssen R, Mattsson O, Jensen AB, Mundy J (2000) Arabidopsis MAP kinase 4 negatively regulates systemic acquired resistance. Cell **103:** 1111-1120

Pitzschke A, Djamei A, Bitton F, Hirt H (2009) A major role of the MEKK1-MKK1/2-MPK4 pathway in ROS signalling. Mol Plant **2:** 120-137

Popescu SC, Popescu GV, Bachan S, Zhang Z, Gerstein M, Snyder M, Dinesh-Kumar SP (2009) MAPK target networks in *Arabidopsis thaliana* revealed using functional protein microarrays. Genes Dev **23:** 80-92

Qiu JL, Fiil BK, Petersen K, Nielsen HB, Botanga CJ, Thorgrimsen S, Palma K, Suarez-Rodriguez MC, Sandbech-Clausen S, Lichota J, Brodersen P, Grasser KD, Mattsson O, Glazebrook J, Mundy J, Petersen M (2008a) Arabidopsis MAP kinase 4 regulates gene expression through transcription factor release in the nucleus. EMBO J **27:** 2214-2221

Qiu JL, Zhou L, Yun BW, Nielsen HB, Fiil BK, Petersen K, Mackinlay J, Loake GJ, Mundy J, Morris PC (2008b) Arabidopsis mitogen-activated protein kinase kinases MKK1 and MKK2 have overlapping functions in defense signaling mediated by MEKK1, MPK4, and MKS1. Plant Physiol **148:** 212-222

Reindle A, Belichenko I, Bylebyl GR, Chen XL, Gandhi N, Johnson ES (2006) Multiple domains in Siz SUMO ligases contribute to substrate selectivity. J Cell Sci **119:** 4749-4757

Rodriguez MC, Petersen M, Mundy J (2010) Mitogen-activated protein kinase signaling in plants. Annu Rev Plant Biol **61:** 621-649

Rytinki MM, Kaikkonen S, Pehkonen P, Jaaskelainen T, Palvimo JJ (2009) PIAS proteins: pleiotropic interactors associated with SUMO. Cell Mol Life Sci **66:** 3029-3041

Sharrocks AD (2006) PIAS proteins and transcriptional regulation–more than just SUMO E3 ligases? Genes Dev **20:** 754-758

Simossis VA, Heringa J (2005) PRALINE: a multiple sequence alignment toolbox that integrates homology-extended and secondary structure information. Nucleic Acids Res **33:** W289-294

Sobko A, Ma H, Firtel RA (2002) Regulated SUMOylation and ubiquitination of DdMEK1 is required for proper chemotaxis. Dev Cell **2:** 745-756

Strzalka W, Labecki P, Bartnicki F, Aggarwal C, Rapala-Kozik M, Tani C, Tanaka K, Gabrys H (2012) *Arabidopsis thaliana* proliferating cell nuclear antigen has several potential sumoylation sites. J Exp Bot **63:** 2971-2983

Su SH, Suarez-Rodriguez MC, Krysan P (2007) Genetic interaction and phenotypic analysis of the Arabidopsis MAP kinase pathway mutations *mekk1* and *mpk4* suggests signaling pathway complexity. FEBS Lett **581:** 3171-3177

Teige M, Scheikl E, Eulgem T, Doczi R, Ichimura K, Shinozaki K, Dangl JL, Hirt H (2004) The MKK2 pathway mediates cold and salt stress signaling in Arabidopsis. Mol Cell **15:** 141-152

Tomanov K, Hardtke C, Budhiraja R, Hermkes R, Coupland G, Bachmair A (2013) Small Ubiquitin-Like Modifier Conjugating Enzyme with Active Site Mutation Acts as Dominant Negative Inhibitor of SUMO Conjugation in Arabidopsis(F). J Integr Plant Biol **55:** 75-82

van den Burg HA, Kini RK, Schuurink RC, Takken FL (2010) Arabidopsis small ubiquitin-like modifier paralogs have distinct functions in development and defense. Plant Cell **22:** 1998-2016

van den Burg HA, Takken FL (2010) SUMO-, MAPK-, and resistance protein-signaling converge at transcription complexes that regulate plant innate immunity. Plant Signal Behav **5:** 1597-1601

Vanhatupa S, Ungureanu D, Paakkunainen M, Silvennoinen O (2008) MAPK-induced Ser727 phosphorylation promotes SUMOylation of STAT1. Biochem J **409:** 179-185

Woo CH, Shishido T, McClain C, Lim JH, Li JD, Yang J, Yan C, Abe J (2008) Extracellular signal-regulated kinase 5 SUMOylation antagonizes shear stress-induced antiinflammatory response and endothelial nitric oxide synthase expression in endothelial cells. Circ Res **102:** 538-545

Yang SH, Jaffray E, Hay RT, Sharrocks AD (2003) Dynamic interplay of the SUMO and ERK pathways in regulating Elk-1 transcriptional activity. Mol Cell **12:** 63-74

Yang SH, Sharrocks AD (2006) PIASxalpha differentially regulates the amplitudes of transcriptional responses following activation of the ERK and p38 MAPK pathways. Mol Cell **22:** 477-487

Yang SH, Sharrocks AD, Whitmarsh AJ (2013) MAP kinase signalling cascades and transcriptional regulation. Gene **513:** 1-13

Ye J, Coulouris G, Zaretskaya I, Cutcutache I, Rozen S, Madden TL (2012) Primer-BLAST: A tool to design target-specific primers for polymerase chain reaction. BMC Bioinformatics **13:** 134

Yunus AA, Lima CD (2009) Structure of the Siz/PIAS SUMO E3 ligase Siz1 and determinants required for SUMO modification of PCNA. Mol Cell **35:** 669-682

Zhang LJ, Vogel WK, Liu X, Topark-Ngarm A, Arbogast BL, Maier CS, Filtz TM, Leid M (2012a) Coordinated regulation of transcription factor Bcl11b activity in thymocytes by the mitogen-activated protein kinase (MAPK) pathways and protein sumoylation. J Biol Chem **287:** 26971-26988

Zhang Z, Wu Y, Gao M, Zhang J, Kong Q, Liu Y, Ba H, Zhou J, Zhang Y (2012b) Disruption of PAMP-induced MAP kinase cascade by a *Pseudomonas syringae* effector activates plant immunity mediated by the NB-LRR protein SUMM2. Cell Host Microbe **11:** 253-263

Zheng Y, Schumaker KS, Guo Y (2012) Sumoylation of transcription factor MYB30 by the small ubiquitin-like modifier E3 ligase SIZ1 mediates abscisic acid response in *Arabidopsis thaliana*. Proc Natl Acad Sci U S A **109:** 12822-12827

Chapter 4

SUMO proteases ULP1c and ULP1d are required for development and drought stress responses in *Arabidopsis thaliana*

Daniel Couto contributed to the phenotype characterization of ULP1c and ULP1d mutants, generation of *proULP1::GUS* lines and GUS staining assays. Alberto Macho performed the RNA extractions for the microarray. Sara Freitas contributed to phenotype characterization.

CONTENTS

4.1. INTRODUCTION

To cope with a constantly changing environment, plants have developed a number of molecular, biochemical and morphological strategies to withstand stress. One major problem faced by plants is the reduced water availability that results from stresses such as dehydration, salinity and extreme temperatures. Tactics to overcome low water availability include the control of stomata opening, root morphology and hydraulic properties, modulation of photosynthesis, cell wall modification and the accumulation of osmotically compatible metabolites (Aroca et al., 2012; Setter, 2012). To implement these strategies, plants carry out physiological adjustments and gene expression reprogramming, partially through phytohormone signaling circuits (Kilian et al., 2012). The most preponderant hormone is abscisic acid (ABA), a key regulator of many stress responses and particularly important for dehydration avoidance and drought tolerance, including the biosynthesis of protective components, the control of stomata movement, seed maturation and germination (Cutler et al., 2010; Raghavendra et al., 2010; Sreenivasulu et al., 2012).

Post-translational modifications (PTMs) are essential regulators of plant stress responses, rapidly modulating protein function. Among PTMs, modification by ubiquitin and ubiquitin-like small peptides (UBLs) has been deemed essential to the control of key components in abiotic stress responses (Miura and Hasegawa, 2010; Lyzenga and Stone, 2012). Small Ubiquitin-like Modifier (SUMO) is a UBL that has gained preponderance in the past decade, since several functional studies have implicated this peptide in the fast and reversible modulation of protein activity without the necessity for degradation or *de novo* synthesis. SUMO may exert different effects depending on the target protein, controlling its conformation, or even creating or blocking interacting interfaces (Wilkinson and Henley, 2010). Since ubiquitination and sumoylation target the same type of amino acid, the latter often blocks lysine modification by ubiquitin, creating an antagonism between these two PTMs (Hay, 2005). More recently, SUMO chains were found to be recognized by SUMO-Targeted Ubiquitin Ligases (STUbLs), positively contributing for protein degradation via the Ubiquitin Proteasome System (Geoffroy and Hay, 2009). Even though the existence of plant STUbLs is yet to be established, mixed SUMO/ubiquitin chains were observed in Arabidopsis following heat shock (Miller et al., 2010).

Generally, SUMO conjugates accumulate drastically during stress, a feature that seems characteristic of all eukaryotes (Kurepa et al., 2003; Zhou et al., 2004; Lallemand-Breitenbach et al., 2008). In plants, SUMO conjugation has been associated to extreme temperatures, drought and salinity tolerance, oxidative stress modulation and control of nutritional homeostasis (Castro et

al., 2012). Many of these stress responses involve the coordinated regulation of hormones, such as salicylic acid (SA), ABA and auxins (Miura et al., 2009; Miura et al., 2010; Miura et al., 2011). SUMO modulation of cellular processes occurs primarily at the nuclear level, as SUMO pathway components and most known SUMO targets are located in the nucleus (Budhiraja et al., 2009; Miller et al., 2010; Miura and Hasegawa, 2010; Park et al., 2011). Sumoylation is normally considered to have a repressor effect on transcription, targeting key regulators of nuclear mechanisms such as transcription factors (TFs) and chromatin remodeling components (Garcia-Dominguez and Reyes, 2009; van den Burg and Takken, 2009).

A cyclic pathway mediates the conjugation and deconjugation of SUMO to target proteins. Pre-SUMO peptides are initially maturated by SUMO proteases, designated Ubiquitin-Like Proteases (ULPs). Through their endopeptidase activity, ULPs cleave the C-terminal end of the pre-SUMO, exposing a di-glycine motif. Sumoylation, the covalent attachment of SUMO to a target, is similar to ubiquitination in that it requires the sequential activity of three enzymes, E1, E2, and E3 (Gareau and Lima, 2010). Through the heterodimer SUMO E1-activating enzyme (SAE), and E2-conjugating enzyme (SCE), an isopeptide bond is established between SUMO and the target's ε-amino group of lysines, in an ATP-dependent reaction. This lysine is normally within the consensus ΨKXE sequence (Ψ, large hydrophobic residue; K, lysine; X, any amino acid; E, glutamic acid). In vivo this process is greatly enhanced by SUMO E3 ligases that aid in the reaction and promote specificity (Gareau and Lima, 2010). SUMO itself can be sumoylated, and for instance the major Arabidopsis SUMO isoforms SUM1 and -2 (but not SUM3) contain sumoylation sites enabling the formation of SUMO chains (Colby et al., 2006; van den Burg et al., 2010; Castano-Miquel et al., 2011). Both the SUMO peptide and SUMO-chains can be removed from the target by ULPs presenting isopeptidase activity, allowing the SUMO peptide to re-enter the conjugation pathway.

SUMO seems to be essential for plant development. Disruption of SUMO conjugation components, namely SAE2, SCE1 and the SUM1/SUM2 peptides, results in developmental arrest in the early stages of embryogenesis, while mutants for the SUMO E3 ligases SIZ1 and HPY2/MMS21 display pleiotropic phenotypes (Catala et al., 2007; Saracco et al., 2007; Jin et al., 2008; Huang et al., 2009; Ishida et al., 2009; Miura et al., 2010). In contrast to the low number of SUMO-conjugating components, ULPs comprise a family of at least seven elements in the model plant *Arabidopsis thaliana* (ESD4, ULP1a/ELS1, ULP1b, ULP1c/OTS2, ULP1d/OTS1, ULP2a and ULP2b), which may confer both specificity and redundancy to the SUMO pathway (Chosed et al., 2006; Colby et al., 2006; Lois, 2010). ESD4 and ULP1a were previously associated to the control

of flowering time and plant development (Murtas et al., 2003; Hermkes et al., 2011). Although ESD4 and ULP1a are phylogenetically close they do not seem to be redundant since the single mutants display dissimilar phenotypes (the *ulp1a* mutant is nearly wild-type while *esd4* is severely dwarfed) and they have different subcellular localizations (Xu et al., 2007; Hermkes et al., 2011).

Functional characterization of SUMO proteases remains largely incomplete. To the best of our knowledge, the only known association between plant ULPs and abiotic stress was reported for ULP1c/OTS2 and ULP1d/OTS1, with both proteins acting redundantly in the tolerance to salt stress. A *ots1 ots2* double mutant was shown to be sensitive to salt and accumulate SUMO conjugates, while *ULP1d* overexpression lines were salt tolerant and displayed reduced SUMO-conjugate levels after stress imposition (Conti et al., 2008). In this work we showed that *ULP1c/d* are highly expressed and display unequal redundancy in the control of developmental traits, particularly rosette growth. Genome-wide transcriptome analysis of *ulp1c/d* indicates that a surprisingly large set of differentially expressed genes are associated with drought and ABA responses. These results led us to investigate the role of ULP1c and ULP1d in the response to ABA and water stress indicating that ULP1c and ULP1d are essential modulators of water deficit responses.

4.2. RESULTS

ULP1c and *ULP1d* show a similar expression pattern

The fairly large number of Arabidopsis ULPs and the high phylogenetic proximity of several family members suggests the existence of various redundant gene pairs, one of which comprising Arabidopsis SUMO protease genes *ULP1c/OTS2* (At1g10570) and *ULP1d/OTS1* (At1g60220; Chosed et al., 2006; Colby et al., 2006; Lois, 2010). ULP1c/d have been implicated in salt stress responses (Conti et al., 2008), yet little is known on their involvement on other abiotic stress responses or their importance to plant development.

To gain insight on ULP1c and ULP1d function, we first determined the spatial and developmental expression pattern, by generating *promoter::GUS* constructs that were subsequently transformed into Arabidopsis (Fig. 4.1). The genomic sequence of the promoters comprised the intergenic region for *ULP1c* and the 2 kbp region upstream of the start codon for *ULP1d* (Fig. 4.1A,B).

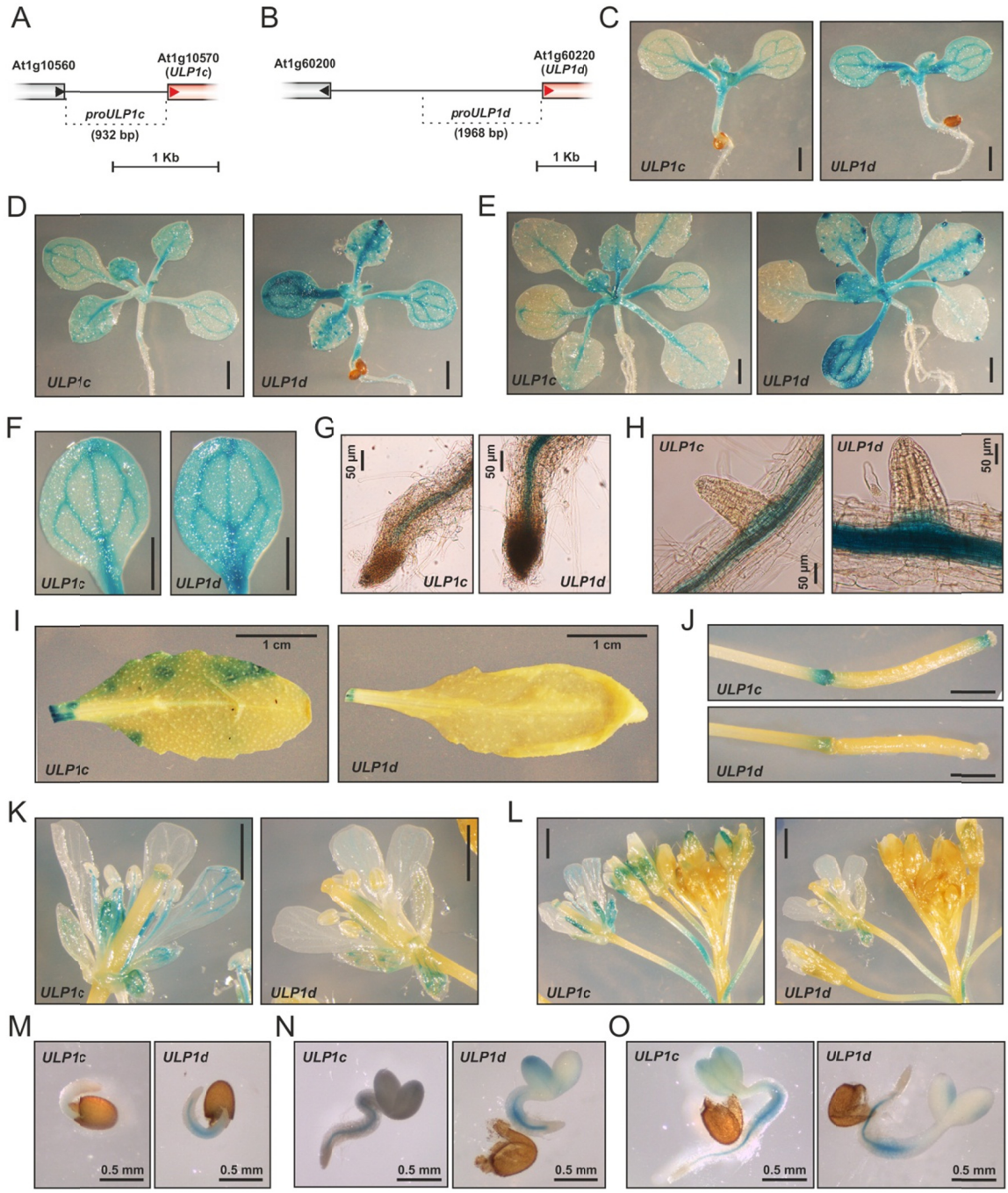

Figure 4.1. Expression profile of *proULP1c*::*GUS* and *proULP1d*::*GUS* by histochemical β-glucoronidase (GUS) staining. **A,B**, Schematic representation of the *ULP1c* (A) and *ULP1d* (B) promoter regions used for promoter::GUS fusions. **C**, 10-day-old shoots. **D**, 15-day-old shoots. **E**, 21-day-old shoots. **F**, Cotyledons in 10-day-old seedlings. **G**, Root tip in 10-day-old seedlings. **H**, Emerging lateral root in 10-day-old seedlings. **I**, 5-week-old leaves. **J**, Developing silique. **K,L**, Flower structures. **M-O**, Seed germination. Scale bar indicates 1 mm unless stated.

Analysis of several independent lines showed a similar expression pattern between *ULP1c* and *ULP1d* in plate-grown 10-, 15- and 21-day-old seedlings (Fig. 4.1C-E). Expression could be detected in the entire leaves and cotyledons, with special prevalence in vascular tissues and petioles (Fig. 4.1F), but no specific staining of stomata was observed. In roots, *proULP1c::GUS* and

proULP1d::GUS expression was restricted to the vascular tissue (Fig. 4.1G,H). A slight increase in GUS signal was observed in emerging lateral root regions. In leaves of adult soil-grown plants, expression of both genes was reduced (Fig. 4.1I). For most tissues, *ULP1d* expression was stronger than that of *ULP1c*. In flowers and siliques, *proULP1c::GUS* lines showed stronger staining than *proULP1d::GUS* although the pattern remained similar (Fig. 4.1J-L). Staining was observed at the top and at the base of developing siliques, in the vascular tissues of petals and sepals, in the stamen filament and at the base of the stigma. Both genes seemed to be expressed in early germination stages (Fig. 4.1M-O).

Expression patterns were consistent with publicly available gene expression maps of Arabidopsis development based on systematic microarray data (Appendix IV - Fig. S4.1A), including the prevalently higher expression of *ULP1d* over *ULP1c* (Appendix IV - Fig. S4.1B). Additional data supports the existence of functional redundancy between both genes: (1) co-expression analysis using GeneMANIA (genemania.org/) showed that *ULP1c* and *ULP1d* are highly co-expressed and share various genes in their co-expression networks (Appendix IV – Fig. S4.2A); (2) *ULP1c/d* are the highest co-expressing members of annotated Arabidopsis ULPs (Appendix IV – Fig. S4.2B); (3) phylogenetic reconstruction and syntenic relationship analysis places them as highly similar genes originated by a recent duplication event (Appendix IV - Fig. S4.2C,D).

ULP1c and ULP1d have a role in plant growth and seed germination

The importance of SUMO in development is supported by the pleiotropic phenotype of non-lethal loss-of-function mutants of the pathway, including the SUMO protease ESD4 and the E3 ligases SIZ1 and HPY2/MMS21 (Murtas et al., 2003; Catala et al., 2007; Huang et al., 2009; Ishida et al., 2009; Miura et al., 2010). Therefore, to investigate the role of SUMO proteases *ULP1c and ULP1d* in Arabidopsis, we isolated previously uncharacterized T-DNA lines for *ULP1c* (*ulp1c-2*; SALK_050441) and *ULP1d* (*ulp1d-2*; SALK_029340), with insertion sites located upstream from SALK lines *ots1-1* and *ots2-1* (Fig. 4.2A,B). Homozygous lines were selected using diagnostic PCR, and quantitative RT-PCR (qPCR) was used to confirm disruption in gene expression (Fig. 4.2C). In order to avoid the possible redundancy between *ULP1c* and *ULP1d*, the *ulp1c-2 ulp1d-2* double mutant (herein designated *ulp1c/d*) was generated.

The ubiquitous expression of *ULP1c* and *ULP1d* (Fig. 4.1, Appendix IV – Fig. S4.1) suggested their involvement in various aspects of development; therefore we performed a morphological characterization of the single and double mutants. As previously reported (Conti et

al., 2008), in vitro-grown seedlings were not significantly altered in morphology or root growth rate (Appendix IV - Fig. S4.3A,B). Four-week-old plants for wild-type (Col-0), single *ulp1c-2* and *ulp1d-2* and double *ulp1c/d* mutant genotypes are depicted in Figure 4.2D. Quantification of shoot fresh weight (Fig. 4.2E), rosette radius (Fig. 4.2F) and number of leaves (Fig. 4.2G) indicated that *ulp1c/d* plants have reduced growth. Interestingly, *ulp1d-2* also showed apparent differences in shoot growth (Fig. 4.2D), although only for rosette radius were these differences statistically significant. Overall results indicate a role for ULP1c/d in plant development during the adult stage and the existence of unequal redundancy in the control of plant growth, with a more significant role played by ULP1d.

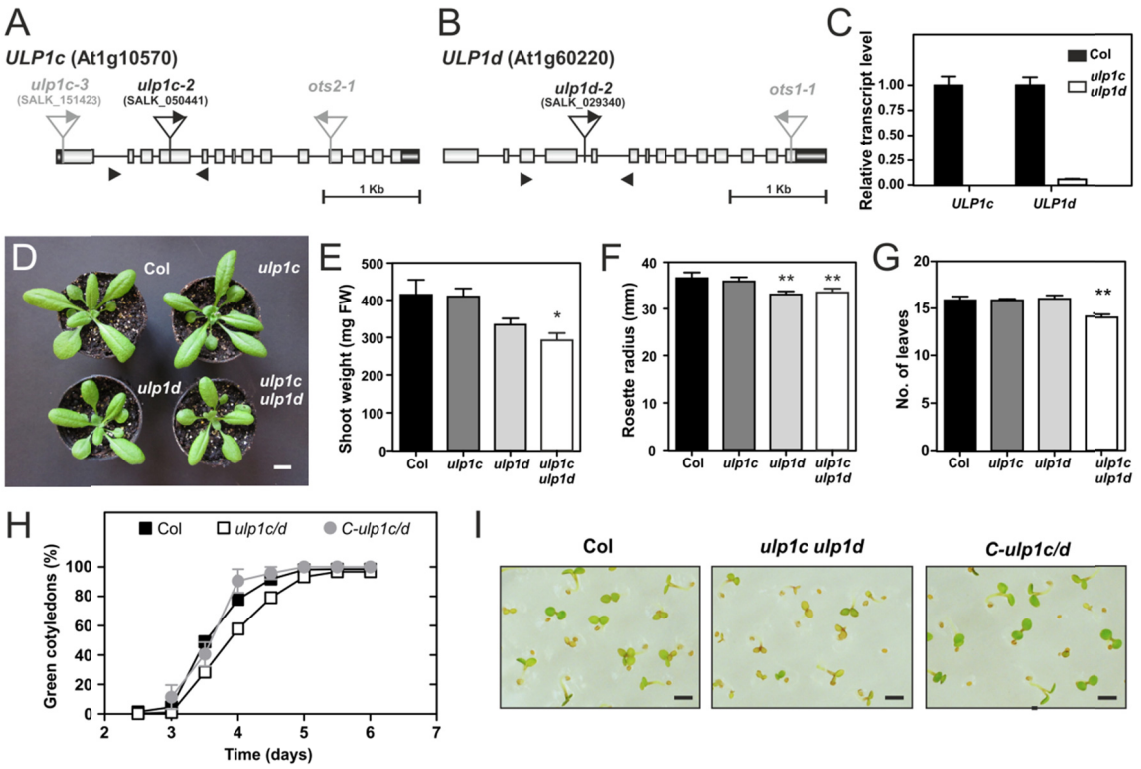

Figure 4.2. Developmental characterization of *ulp1c*, *ulp1d* and *ulp1c ulp1d* mutants. **A,B**, Schematic representation of *ULP1c* (At1g10570) (A) and *ULP1d* (At1g60220) (B), with indication of T-DNA insertion sites (inverted triangles) and primer locations for diagnostic PCR genotyping (arrows); selected T-DNA lines are highlighted; exons and UTRs are represented by grey and black boxes, respectively. **C**, Quantitative RT-PCR analysis of *ULP1c* and *ULP1d* relative expression levels in the wild-type (Col) and *ulp1c/d* backgrounds. **D**, Morphology of soil-grown 4-week-old plants; scale bar indicates 1 cm. **E**, Fresh weight of the shoot of 4-week-old plants ($n = 9$). **F**, Maximum radius of the rosette of 4-week-old plants ($n \geq 12$). **G**, Leaf number in 4-week-old plants ($n = 9$). **H**, Seed germination rate (formation of green cotyledons; $n \geq 4$). **I**, Seedling morphology four days after germination; scale bar indicates 1 mm. Error bars represent standard error of the means (SEM). Asterisks represent statistically significant differences of mutants in relation to the wild-type (unpaired t test; *, $P<0.05$; **, $P<0.01$).

Lethality of SUM1/2, E1 and E2 knockouts in Arabidopsis imply a fundamental role for sumoylation in embryo formation (Saracco et al., 2007), therefore we investigated whether seed development or germination were also compromised in *ulp1c/d*. While siliques did not show differences in morphology or seed number (Appendix IV - Fig. S4.3C,D), seeds displayed a delay of approximately one day in the formation of green cotyledons (Fig. 4.2H,I). Complementation of *ulp1c/d* by ectopic expression of a *pro35S::ULP1d* construct in the mutant background (*C-ulp1c/d*) reverted the delayed germination phenotype, indicating a role for ULP1c and ULP1d in seed germination.

Microarray transcript profiling of *ulp1c/d*

In order to further investigate ULP1c and ULP1d function, microarray analysis using the Affymetrix ATH1 chip was performed in 5-week-old wild-type and *ulp1c/d* plants. A total of 59 genes were up-regulated and 53 were down-regulated by at least two-fold in the *ulp1c/d* double mutant relative to the wild-type. Indicative of the success of the microarray, *ULP1c* and *ULP1d* ranked highest amongst down-regulated genes and were excluded from the analysis. The most significant differentially expressed genes (DEGs) are summarized in Table 4.1. Gene Ontology (GO) analysis showed an overrepresentation of genes functionally related to shoot development, including organ morphogenesis, which is consistent with *ulp1c/d* developmental defects (Fig. 4.3A). Genes involved in the plant response to pathogens (fungi in particular) were also differentially expressed. Meanwhile, a substantial number of genes (particularly up-regulated genes) correlated with the plant response to abiotic stress, including responses to temperature and ABA stimuli (Fig. 4.3A; Table 4.1). Thus, ~38% and ~23% of *ulp1c/d* DEGs co-expressed with genes differentially expressed after drought and ABA treatment, respectively (Fig. 4.3B,C; Nemhauser et al., 2006; Catala et al., 2007). The microarray data was validated by analyzing by qPCR the expression of four up-regulated and two down-regulated genes including drought-related genes *RD20* and *GOLS1* (Fig. 4.3D).

Genes with identical expression patterns are normally controlled by the same transcription factor, thus sharing common *cis*-elements in their promoters. Since sumoylation is a known modulator of transcriptional regulators, we used the online database and bioinformatics tool Athena (O'Connor et al., 2005) to identify statistically over-represented *cis*-elements in the promoters of *ulp1c/d* DEGs (Table 4.2). Interestingly, all the identified TF-binding site motifs (DREB1A/CBF3, ABRE-like, G-box and ATHB6) have been previously associated to ABA/drought-dependent

transcription regulation. Overall results strongly support a role for ULP1c/d in abiotic stress responses, particularly those regarding drought and ABA.

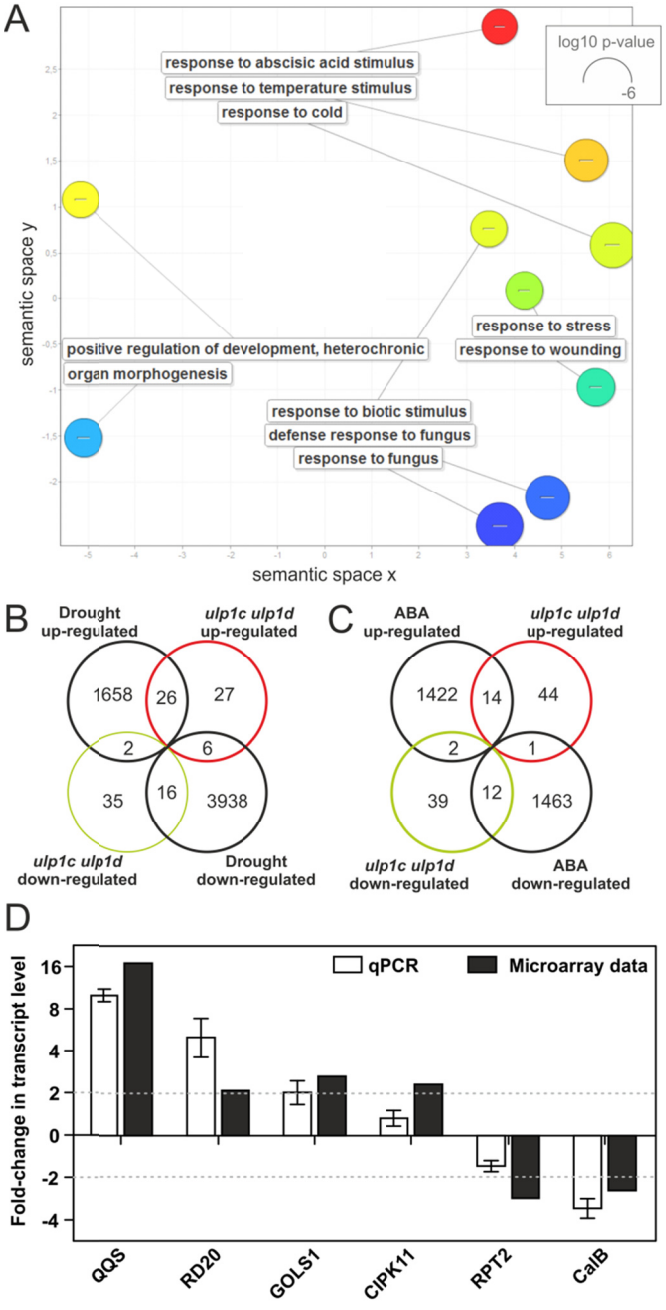

Figure 4.3. Microarray analysis of *ulp1c/d* in standard growth conditions. **A**, Redundancy exclusion and scatterplot analysis of enriched Gene Ontology (GO) terms for *ulp1c/d* differentially expressed genes. GO term functional categorization (for *Biological Process*) was performed in VirtualPlant 1.2 (virtualplant.bio.nyu.edu/cgi-bin/vpweb/), redundancy exclusion and scatterplot analysis were performed in REVIGO (revigo.irb.hr/). The scatterplot represents the cluster representatives in a two dimensional space (x- and y-axis) derived by applying multidimensional scaling to a matrix of the GO terms' semantic similarities (Supek et al., 2011); bubble size indicates the frequency of the GO term. **B,C**, Venn diagram comparison of differentially expressed genes in *ulp1c/d* against differential expression following drought stress (B) and abscisic acid (ABA) (C) treatment (Nemhauser et al., 2006; Catala et al., 2007). **D**, Quantitative RT-PCR (qPCR) analysis of *ULP1c/d* regulation of gene expression. Relative expression levels (fold difference) in *ulp1c/d vs* wild-type (Col) plants were compared to microarray data for the following genes: *QQS* (At3g30720); *RD20* (At2g33380); *GOLS1* (At2g47180); *CIPK11* (At2g30360); *RPT2* (At2g30520); *CalB* (for *Calcineurin B subunit-related*; At2g45670). As a loading control, *ACT2* (At3g18780) mRNA was amplified within each sample. Error bars represent three independent biological replicates.

ULP1c/d are negative regulators of drought tolerance

Previous studies have shown a role for the E3 ligases SIZ1 and MMS21 in drought responses (Catala et al., 2007; Miura et al., 2012; Zhang et al., 2012), and the present microarray analysis of *ulp1c/d* suggests a role for ULP1c and ULP1d in drought tolerance. Therefore we analyzed single *ulp1c* and *ulp1d* mutants and the *ulp1c/d* double mutant for drought- and

ABA-related phenotypes. Long-term drought stress was imposed to three-week-old wild-type (Col), *ulp1c*, *ulp1d* and *ulp1c/d* plants by withholding water for two weeks.

Table 4.1. Genes constitutively deregulated in *ulp1c/d* in comparison to the wild-type. Categories were considered based on gene ontology (GO) term enrichment, *BAR Classification SuperViewer* (bar.utoronto.ca/ntools/cgi-bin/ntools_classification_superviewer.cgi) and TAIR (www.arabidopsis.org/).

AGI ID	Gene name	Log2 ratio	*p*-value	Description
Development				
At5g10140	*FLC, FLF, AGL25*	-1,72	0,00E+0	Transcriptional repressor of floral transition
At5g63420	*EMB2746*	-1,31	4,70E-6	Embryo defective at globular stage
At1g53230	*TCP3*	-1,28	1,22E-5	TF involved in leaf differentiation
At3g15030	*TCP4, MEE35*	-1,17	3,67E-4	TF involved in leaf differentiation
At4g03190	*AFB1, GRH1*	-1,11	1,85E-3	Auxin binding and ubiquitin-protein ligase
At2g37630	*MYB91, PHAN, AS1*	-1,05	8,90E-3	TF involved in leaf development
At4g23750	*CRF2, TMO3*	-0,98	4,57E-2	Cytokinin response TF
At5g65870	*PSK5*	1,01	2,06E-2	Growth factor
At1g53160	*SPL4*	1,16	4,42E-4	TF involved in flowering transition
At1g69490	*ANAC029, NAP*	1,34	2,14E-6	TF regulator of leaf senescence
At4g20140	*GSO1*	1,39	4,18E-7	Embryonic epidermal surface development
At1g52920	*GCR2, GPCR*	2,45	0,00E+0	G-protein coupled receptor involved in ABA signalling
Stress responses				
At2g30520	*RPT2*	-1,50	8,60E-9	Root phototropism
At4g16990	*RLM3*	-1,13	9,90E-4	Resistance to *L. maculans*
At2g21050	*LAX2*	-1,02	1,65E-2	Auxin influx carrier
At1g09350	*GOLS3*	-1,02	1,74E-2	Galactinol synthase
At2g33380	*RD20, CLO-3*	1,07	4,57E-3	Response to desiccation
At2g30020	*AP2C1*	1,18	2,65E-4	Protein phosphatase 2C modulator of innate immunity
At5g50720	*HVA22E*	1,18	2,35E-4	ABA- and stress inducible
At2g30360	*CIPK11, PKS5, SNRK3.22, SIP4*	1,22	8,06E-5	Kinase inhibitor of plasma membrane H·ATPase; response to salt
At3g16470	*JR1, JAL35*	1,40	2,89E-7	Jasmonate responsive gene
At2g47180	*GOLS1*	1,41	2,18E-7	Galactinol synthase
At3g16460	*JAL34*	1,58	5,19E-10	Jacalin lectin family protein
At1g45145	*ATH5, LIV1*	1,65	3,96E-11	Cytosolic thioredoxin
At2g34930		1,65	3,96E-11	LRR family protein
At3g47340	*ASN1, DIN6*	2,15	0,00E+0	Glutamine-dependent asparagine synthetase; N-assimilation
Cell Wall				
At4g28250	*EXPB3*	-1,05	9,10E-3	Putative beta-expansin / allergen protein
At1g32170	*XTH30, XTR4*	1,55	1,36E-9	Xyloglucan endotransglucosylase / hydrolase
At1g10550	*XTH33*	1,71	4,95E-12	Xyloglucan endotransglucosylase / hydrolase

TF - Transcription factor

Table 4.2. *Cis*-elements over-represented in the promoter region of genes differentially expressed in *ulp1c/d*. The subset of genes was submitted to Athena scanning analysis (O'Connor et al., 2005) for binding site enrichment. Only up-regulated genes showed significant differences.

***Cis*-element name** (conserved sequence*)	**No. of genes**	**Frequency prediction in the genome vs observed in the genes** (*p*-value)	**Corresponding TFs**	**Description**	**References**
DREB1A/CBF3 binding site motif (RCCGACNT)	12	7% *vs* 21% (<10e-4)	DREB1A/CBF3	Drought, salinity and freezing response	Maruyama et al. (2004)
ABRE-like binding site motif (BACGTGKM)	21	20% *vs* 37% (< 10e-3)	bZIPs (AREB/ABF)	ABA responsive element	Fujita et al. (2013)
CACGTG motif, G-box (CACGTG)	20	15% *vs* 35% (< 10e-3)	bHLHs, bZIPs (AREB/ABF)	ABA-inducible element	Shen and Ho (1995); Toledo-Ortiz et al. (2003); Fujita et al. (2013)
ATHB6 binding site motif (CAATTATTA)	9	3% *vs* 16% (< 10e-3)	ATHB6	ABA signalling	Himmelbach et al. (2002)

** R (A/G), M (A/C), K (G/T), B (C/G/T), N (A/C/G/T)*

As shown in Fig. 4.4A, wild-type and *ulp1c* plants started to wilt and to accumulate anthocyanins, while *ulp1d* and *ulp1c/d* plants remained equivalent to that of plants that were watered. Early flowering was also observed in *ulp1c/d* as previously reported (Conti et al., 2008). The involvement of *ULP1c/d* in drought tolerance was confirmed by a second long-term drought stress assay using perlite as the growth matrix; perlite retains more water than the normal soil mixture, enabling water loss to occur more gradually. Once again, after three weeks of water deprival, the fitness of Col plants was reduced when compared to *ulp1c/d* plants (Fig. 4.4B).

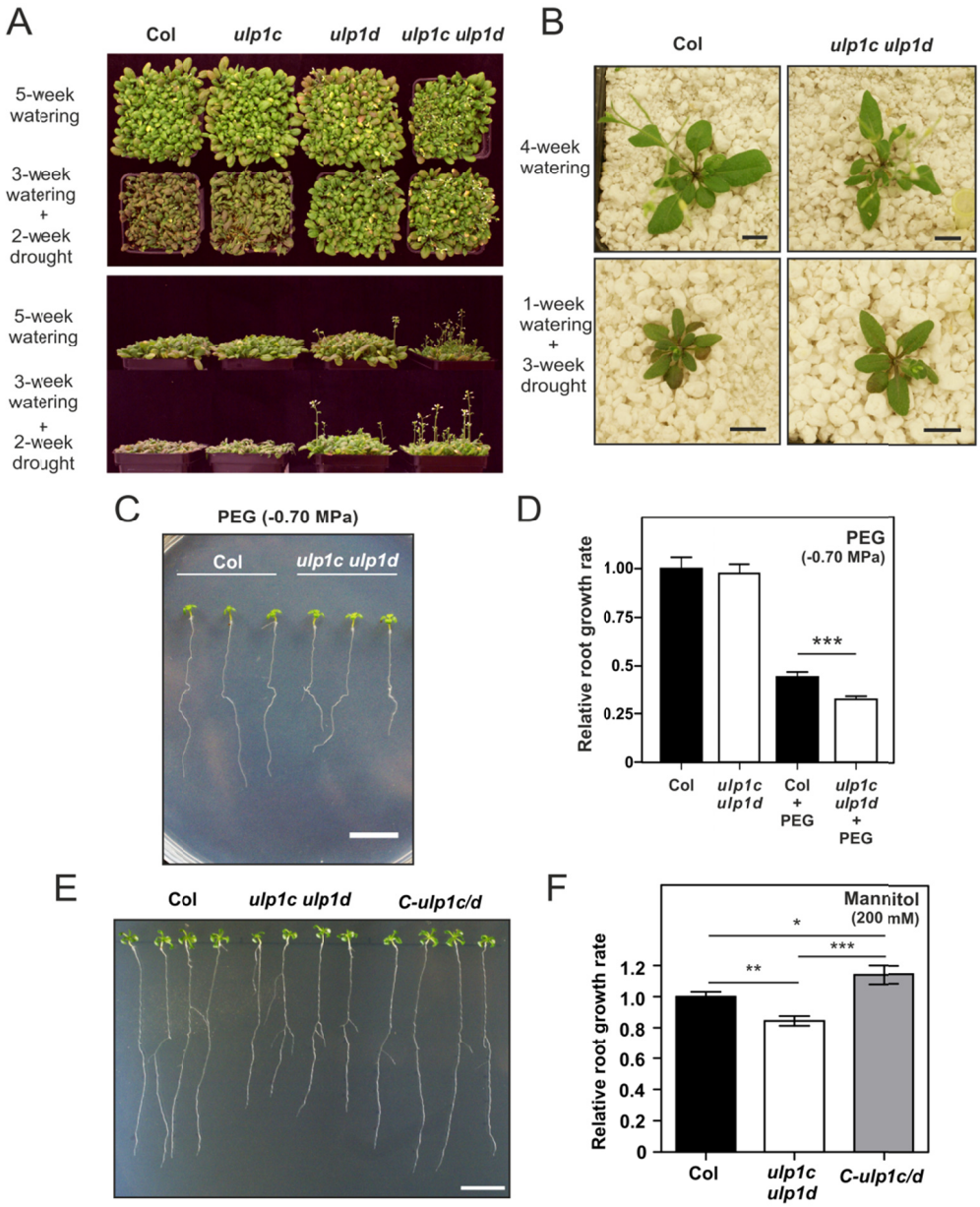

Figure 4.4. Characterization of the *ulp1c/d* mutant in response to drought and osmotic stresses. **A**, Seeds from Col, *ulp1c*, *ulp1d* and *ulp1c ulp1d* genotypes were sown into soil and watered normally for three weeks. Plants were then subjected to drought for two weeks. **B**, Col and *ulp1c/d* seedlings were exposed to gradual dehydration stress in perlite for three weeks. **C**, 7-day-old Col and *ulp1c/d* seedlings were subjected to osmotic stress (-0.70 MPa) in PEG-infused MS plates. **D**, Measurement of relative root growth during PEG-induced osmotic stress; error bars represent SEM ($n \geq 24$). **E**, Root morphology of 7-day-old seedlings transferred to media supplemented with 200 mM mannitol and grown for 10 days. **F**, Relative root growth of 7-day-old seedlings subjected to 200 mM mannitol-induced osmotic stress; error bars represent SEM ($n \geq 10$). Scale bars indicate 1 cm. Asterisks represent statistically significant differences between genotypes (unpaired t test; *, $P<0.05$; **, $P<0.01$; ***, $P<0.001$).

Studies on plant adaptation to low water potencial (ψ_w) stress often use osmotic assays to lower ψ_w in the growth media in a precise fashion (Verslues et al., 2006). Thus, we observed root growth in PEG-infused agar plates with no addition of sugar, providing a ψ_w of -0.70 MPa (similar to

that imposed by 100 mM NaCl). A parallel assay was performed with MS medium containing 200 mM mannitol, a low molecular weight solute used to confer low ψ_w. Six-day-old Col and *ulp1c/d* seedlings grown in MS agar plates were transferred to osmoticum-containing plates and root growth was monitored for seven days. As shown in Figure 4.4C-F, wild-type seedlings showed increased root growth compared to *ulp1c/d*. Complementation efficiently recovered *ulp1c/d* in vitro sensitivity to low ψ_w.

The *ulp1c/d* mutant shows altered stomatal response and density

Stomata are key regulators of the plant water status, they respond to ABA and play a crucial role in avoiding low ψ_w stress and dehydration (Schroeder et al., 2001). Stomatal opening was investigated in the *ulp1c/d* double mutant, after application of exogenous ABA (Fig. 4.5A,B). Under light and stomata-opening solution, aperture was ~10% higher in *ulp1c/d* than in wild-type plants. Addition of ABA proportionally closed the stomata in both genotypes, maintaining the higher aperture in *ulp1c/d* (Fig. 4.5A,B). This was not consistent with our previous results indicating an increased tolerance of *ulp1c/d* to prolonged drought, therefore, stomata size and density were determined. While size was similar between wild-type and *ulp1c/d*, the *ulp1c/d* double mutant displayed less stomata per unit area than the wild-type (Fig. 4.5C,D). Because the rate of water loss is mainly determined by stomatal conductance (Schroeder et al., 2001), we analyzed the influence of the observed stomatal phenotypes in the *ulp1c/d* response to rapid dehydration. The aerial part of each plant was detached from roots and exposed to dehydration while the decline in fresh weight was monitored for six hours. Surprisingly, the rate of water loss was identical between Col and *ulp1c/d* (Fig. 4.5E), suggesting that no net change in water loss is registered via a combination of increased stomatal aperture and reduced stomata density.

Since ABA levels are also fundamental for seed dormancy and maintenance (Finkelstein et al., 2008) and the *ulp1c/d* mutant displayed a delay in germination, we analyzed its phenotype in the presence of ABA (Fig. 4.5F,G). This hormone induced a 6-day delay in germination for both genotypes, and the 1-day-late germination phenotype of *ulp1c/d*, previously observed in ABA-free medium, was maintained in this assay. Similarly, in vitro-grown seedlings did not display differences in root growth inhibition between mutant and wild-type when ABA was incorporated into the medium (data not shown). Overall results indicate that differential *ulp1c/d* phenotypes (delayed seed germination and increased stomatal aperture) are observed independently of the application of exogenous ABA.

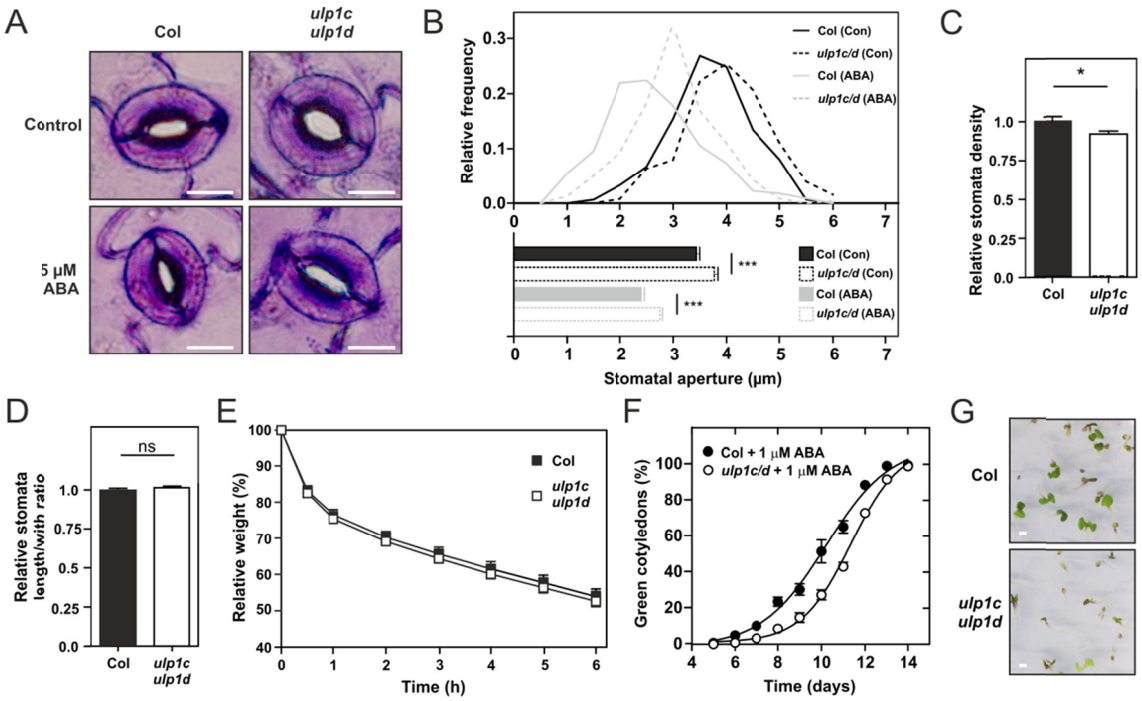

Figure 4.5. Stomata characterization and rapid dehydration analysis of the *ulp1c/d* mutant. **A**, Representative images of stomatal aperture in the presence or absence of 5 µM ABA. Scale bars indicate 5 µm. **B**, Upper panel, relative frequency distribution of stomatal aperture in response to ABA; lower panel, medium values of stomatal aperture in response to ABA; error bars represent SEM (n ≥ 130). **C**, Relative stomata density, in relation to wild-type; error bars represent SEM (n ≥ 85). **D**, Relative stomata length/width ratio, in relation to wild-type; error bars represent SEM (n ≥ 140). **E**, Water loss quantification in percentage of fresh weight lost after exposure to dehydration in 4-week-old Col and *ulp1c ulp1d* plants (n = 6). **F**, Seed germination rate (formation of green cotyledons; n = 6) in the presence of 1 µM ABA. **G**, Seedling morphology 10 days after germination in the presence of 1 µM ABA; scale bar indicates 1 mm. Asterisks represent statistically significant differences between genotypes (unpaired t test; ns, non-significant; *, P<0.05; **, P<0.01; ***, P<0.001).

The *ulp1c/d* mutant displays altered SUMO-conjugate levels

In plants, an increase in SUMO conjugates appears to be an early and common event following numerous abiotic stress challenges including rapid dehydration (Catala et al., 2007; Castro et al., 2012). Thus, we investigated the role of ULP1c and ULP1d in the SUMO conjugation profile after exposure to water stress. Ten-day-old seedlings were subjected to four hours of rapid dehydration and an immunoblot of total protein was performed using an antibody raised against the main SUMO peptides SUM1 and -2 from Arabidopsis (Conti et al., 2008). As shown in Figure 4.6, wild-type plants displayed a low level of high molecular weight SUM1/2 conjugates (HMWC) and heat shock (HS) treatment induced the massive accumulation of HMWC as previously reported (Kurepa et al., 2003; Saracco et al., 2007; Miller et al., 2010). Interestingly, *ulp1c/d* plants

accumulated HMWC in control conditions, indicating an important role for these proteins in the homeostasis of sumoylated proteins. While exposure to dehydration induced the accumulation of HMWC in the wild-type, this accumulation was not altered in *ulp1c/d*. Interestingly, HMWC in the E3 ligase mutant *siz1* were considerably lower, yet increased following stress (though not reaching wild-type levels), indicating that in addition to SIZ1, other E3 ligases contribute to the formation of HMWC after dehydration.

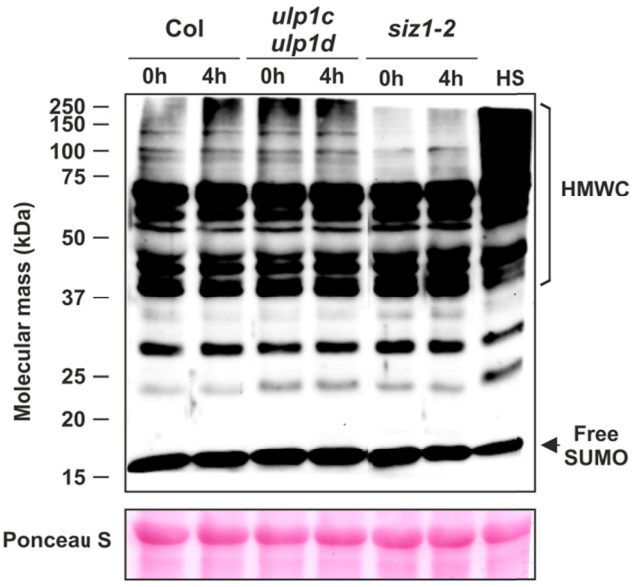

Figure 4.6. Western blot analysis of high molecular weight SUM1-conjugates (HMWC) following rapid dehydration. Ten-day-old plants were subjected to rapid dehydration for 4 h. As a positive control, similar plants were subjected to a 37°C heat shock for 1 h (HS). Protein extracts (50 µg per lane) were analyzed by protein gel blots using anti-AtSUMO1 polyclonal antibodies. As a loading control, Ponceau S staining of the large subunit of Rubisco (55 kDa) is displayed.

The triple mutant *siz1 ulp1c ulp1d* displays an accumulative phenotype

The E3 ligase SIZ1 has been considered an essential element in the SUMO pathway and has been implicated in the regulation of nuclear processes, namely transcriptional programs, important for development and the response to stress (Castro et al., 2012). To investigate the epistatic relationship between *SIZ1*, *ULP1c*, and *ULP1d*, the triple *siz1 ulp1c ulp1d* mutant was generated. As shown in Figure 4.7A and 4.7B, the triple mutant showed enhanced developmental defects in comparison to *siz1*. Similarly the triple mutant displayed stronger delay in seed germination than *siz1-2* or the double *ulp1c/d* mutant (Fig. 4.7C). The additive phenotypes of loss-of-function mutants suggest that ULP1c/d act independently of SIZ1 in the control of key developmental traits. This is supported by the lack of overlap in DEGs between the *siz1* mutant (Catala et al., 2007) and the *ulp1c/d* double mutant (Fig. 4.7D). Concerning the osmotic response, *siz1-2* was resistant whereas *ulp1c/d* was sensitive to the presence of mannitol in the medium,

meanwhile the triple mutant displayed a *siz1*-like phenotype, being more resistant to mannitol-induced osmotic stress (Fig. 4.7E).

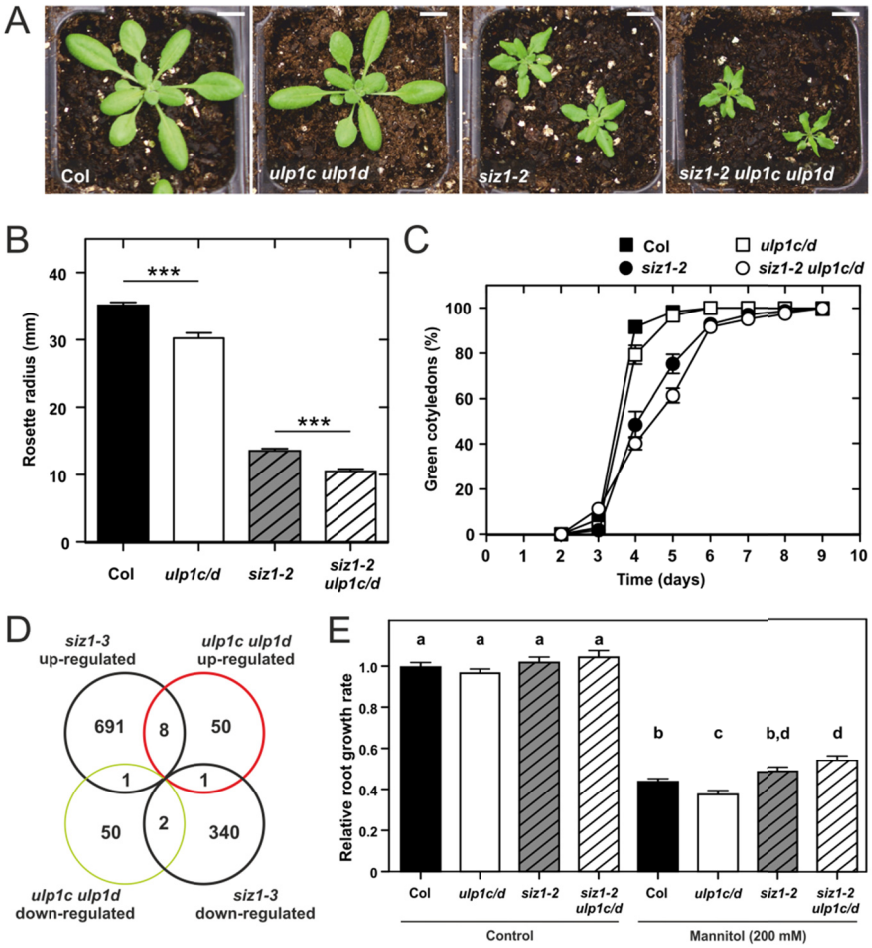

Figure 4.7. Characterization of the triple mutant *siz1 ulp1c ulp1d*. **A**, Morphology of soil-grown 4-week-old plants; scale bar indicates 1 cm. **B**, Maximum radius of the rosette of 4-week-old plants (n ≥ 6). **C**, Seed germination rate inferred by the formation of green cotyledons (n = 6). **D**, Comparison of differentially expressed genes between *ulp1c ulp1d* and previously published *siz1-3* microarray data (Catala et al., 2007). **E**, Relative root growth of 7-day-old seedlings subjected to mannitol-induced osmotic stress; error bars represent SEM (n ≥ 15). Asterisks represent statistically significant differences between genotypes (unpaired t test; *, P<0.05; **, P<0.01; ***, P<0.001; a-d represent statistically different populations).

4.3. DISCUSSION

Functional approaches in *Arabidopsis thaliana* have definitely established an important role for sumoylation in plant development and abiotic stress responses. In the past, lethality of SUM1/2, E1 and E2 knockouts and the redundancy of SUMO proteases meant that the majority of SUMO-related phenotypes were assigned in E3 ligases, particularly SIZ1 (Catala et al., 2007; Saracco et al., 2007; Huang et al., 2009; Ishida et al., 2009; Miura et al., 2010). However, SUMO

proteases are bound to play a fundamental role in the homeostasis of a target's conjugated/deconjugated form and be a source of specificity within the pathway. Studies implicating ESD4 in development and nuclear trafficking (Murtas et al., 2003; Xu et al., 2007), and ULP1c/d in the control of salt stress tolerance (Conti et al., 2008), now help us grasp the importance of plant SUMO proteases. In the present study we were able to extend our knowledge on the role ULP1c/d play in both development and drought stress tolerance.

ULP1c/d control growth and seed germination

Our data support a role for ULP1c/d in development. We observed that *ULP1c* and *ULP1d* expression was prevalent in initial developmental stages, particularly in the vasculature of several tissues (Fig. 4.1), and results were consistent with existing systematic microarray transcript profiling of Arabidopsis development (Appendix IV - Fig. S4.1). GO terms also implicated ULP1c/d in the positive regulation of organ morphogenesis (Fig. 4.3A), and most significantly, we show that various genes related to shoot development are down-regulated in *ulp1c/d* (Table 4.1). These include *AS1/MYB91*, which is associated with leaf development (Byrne et al., 2002), and *TCP3/ TCP4*, two genes essential for the correct morphogenesis of several shoot organs (Koyama et al., 2007). The negative flowering time regulator *FLC* was also down-regulated in *ulp1c/d*. Previous reports showed that *FLC* is transcriptionally repressed by FLOWERING LOCUS D (FLD), and FLD is rendered inactive by SIZ1-dependent SUMO conjugation (Jin et al., 2008). Besides *ulp1c/d*, *FLC* was equally down-regulated in *siz1* and *esd4* (Reeves et al., 2002; Catala et al., 2007), and all three SUMO pathway mutants display early-flowering. Thus, present results reinforce a role for sumoylation in the control of flowering time.

Generally, *ULP1d* was significantly more expressed in seedlings and displayed growth defects that imply a predominant role over *ULP1c* (Fig. 4.1 and 4.2). Compromised growth was subsequently observed in *ulp1c/d* adult plants, suggesting that later development defects are a consequence of earlier events. Phylogeny, synteny and co-expression analysis (Appendix IV – Fig. S4.2) confirmed our experimental data and the previous literature (Chosed et al., 2006; Colby et al., 2006; Conti et al., 2008; Lois, 2010) for the existence of redundancy in the *ULP1c/d* gene pair. Curiously, an inversion in expression levels seemed to occur in specific tissues of later developmental stages, namely flower organs and siliques (Fig. 4.1), giving indication of subfunctionalization within the gene pair. This is consistent with the fact that ULP1d localizes in the nucleoplasm whereas ULP1c is mainly confined to speckle-like bodies (Conti et al., 2008).

It is believed that modulation of SUMO-target function lies in the balance that SUMO E3 ligases and SUMO proteases maintain between a target's conjugated/deconjugated forms (Kurepa et al., 2003; Golebiowski et al., 2009). Developmental defects observed in the *ulp1c/d* double mutant were similar (yet substantially attenuated) to those described in the loss-of-function mutants for the major E3 ligase SIZ1 (Catala et al., 2007), hinting to their involvement in common mechanisms. However our genetic and molecular data suggests that, to some extent, separate mechanisms may be involved in SIZ1 and ULP1c/d control of development, since the triple mutant *siz1 ulp1c/d* presented accumulative phenotypes concerning shoot size and seed germination (Fig. 4.7A-C), and differentially expressed genes in *siz1* and *up1c/d* did not overlap significantly (Fig. 4.7D).

ULP1c/d affect SUMO conjugation and play a role in drought tolerance

We have shown that *ulp1c/d* accumulates higher SUM1/2 conjugate levels than wild-type plants under non-stressed conditions (Fig. 4.6). Even though in vitro studies have attributed both endo- and isopeptidase activities to ULP1c/d (Chosed et al., 2006; Colby et al., 2006), results support previous indications (Conti et al., 2008) that ULP1c/d act predominantly as isopeptidases, with the mutant displaying a lower rate of SUMO deconjugation. Alas, free (unconjugated) SUM1/2 levels, corresponding to the ~16 kDa band, allowed no distinction between processed and unprocessed SUMO forms. Meanwhile, we could observe that SUM1/2 conjugate levels increased following rapid dehydration (Fig. 4.6). SUMO conjugate accumulation during stress imposition is ubiquitous in eukaryotes (Kurepa et al., 2003; Zhou et al., 2004; Golebiowski et al., 2009), and has been consistently observed in plants stressed by rapid dehydration, heat, cold and salt, among other challenges (reviewed by Castro et al., 2012). Conjugation is linked to a decrease in the free SUMO pool, and matches the duration and intensity of the stress (Kurepa et al., 2003; Miller and Vierstra, 2011). However, free SUM1/2 levels did not change considerably with the exception of the HS treatment, indicating that dehydration induces only a moderate change in the sumoylation profile.

Since SUMO conjugate levels were constitutively increased in *ulp1c/d* double mutants, stress imposition did not render significant differences in SUMO conjugate levels in comparison to non-stressed mutants (Fig. 4.6). One can hypothesize that, under standard growth, the *ulp1c/d* SUMO conjugate profile mimics that of drought-stressed plants, triggering a sumoylation-dependent stress-like response. In support, we showed that *ulp1c/d* deregulated genes under normal growth

conditions displayed a drought stress transcriptional signature (Fig. 4.3; Table 4.1), and used qPCR to prove the up-regulation in *ulp1c/d* of several drought-inducible genes such as the drought marker gene *RD20* (Aubert et al., 2010), *HVA22E* (Chen et al., 2002), *GOLS1* that has an important role in the synthesis of raffinose during drought stress (Taji et al., 2002), and CIPK11, an ABA-induced protein kinase associated with stomatal movement (Fuglsang et al., 2007). Moreover, we demonstrated that all transcriptional regulators likely to drive up-regulation in *ulp1c/d* could be associated to the drought-stress response (Table 4.2).

Subsequent analysis showed that adult *ulp1c/d* soil-grown plants were resistant to prolonged drought (Fig. 4.4A,B). Analysis also revealed slightly increased stomatal aperture in *ulp1c/d*, yet no differences in the rate of water loss were detected in *ulp1c/d* during rapid dehydration assays (Fig. 4.5), indicating that stomata-dependent water loss is unlikely to influence the long-term drought response in *ulp1c/d*. In support, we showed that *ulp1c/d* mutants displayed less stomata per unit area than wild-type plants (Fig. 4.5C). It is possible that sumoylation operates at various levels in the control of stomatal density, as known SUMO targets include ICE1, a TF that controls the basal pathway of stomatal lineage (Miura et al., 2007; Kanaoka et al., 2008), and GTL1, which negatively regulates water use efficiency by modulating stomatal density (Miller et al., 2010; Yoo et al., 2010). Even though stomatal closure is an important component of short-term drought avoidance, in the long term, factors such as increased root/shoot ratio, tissue water storage capacity, cuticle thickness, water permeability and cell wall hardening become important (Verslues et al., 2006). Cell wall loosening and tightening traditionally involves xyloglucan endotransglucosylase/hydrolases (XTH), and expansins (EXP; Moore et al., 2008), and both types of enzymes were identified as *ulp1c/d* DEGs (Table 4.1), which could account for both development and drought-related phenotypes in this mutant. In fact, deregulation of XTHs was already associated with reduced leaf cell expansion in the *siz1* mutant (Miura et al., 2010).

Sumoylation has been implicated in the response to long-term drought via the E3 ligases SIZ1 and MMS21; however, studies on SIZ1 have been inconclusive since *siz1* mutants have shown both sensitivity and tolerance to different drought treatments (Catala et al., 2007; Miura et al., 2012; Zhang et al., 2012). Current phenotypical and transcriptional data suggest that ULP1c/d globally act as negative regulators of long-term drought responses. In this context, ULP1c/d-dependent transcriptional regulators (Table 4.2) constitute prime candidates for the identification of novel SUMO targets that will help clarify the molecular mechanisms associated to the ULP1c/d mode-of-action.

ULP1c/d influence responses to low water potential

Overall results support opposing functions for ULP1c/d and SIZ1 in the control of physiological traits that can be associated to water shortage. We demonstrate that ULP1c/d positively regulates in vitro root growth in response to low water potential, as *ulp1c/d* seedlings were more sensitive to incorporation of both PEG and mannitol in the medium (Fig. 4.4C-F). Consistently, loss of ULP1c/d function was previously shown to result in hypersensitivity to salt (Conti et al., 2008). Meanwhile, the *siz1* mutant displayed resistance to low ψ_w and the *siz1 ulp1c/d* triple mutant displayed a *siz1*-like response in the presence of mannitol (Fig. 4.7). Also, stomata displayed higher aperture in *ulp1c/d* (Fig. 4.5A,B), while *siz1* mutants were recently shown to have reduced stomatal aperture (Li et al., 2012; Miura et al., 2012). In this context, a likely model is that ULP1c/d operate strongly as isopeptidases, acting downstream of SIZ1 to promote SUMO-target deconjugation that opposes the E3 ligase activity of SIZ1.

Stomata respond very quickly to ABA and represent a simplified system to screen for possible defects in ABA signaling pathways (Schroeder et al., 2001). Interestingly, the *siz1* stomatal closure phenotype seems to involve SA-dependent reactive oxygen species (ROS) production, rather than ABA-dependent ROS production (Miura et al., 2012). In the present case, the increased stomatal aperture phenotype of *ulp1c/d* was observed independently of exogenous application of ABA (Fig. 4.5A,B). Similarly, exogenous ABA did not promote either hyper- or insensitivity in *ulp1c/d* seed germination time and in vitro root growth (Fig. 4.5F,G; data not shown). A great amount of evidence suggests that both ABA-dependent and -independent mechanisms are involved in the SUMO-abiotic stress association (reviewed by Castro et al., 2012). Even though overall results place *ulp1c/d* phenotypes as independent of exogenous ABA, alterations in endogenous ABA levels or ABA-dependent signaling (as suggested by the *ulp1c/d* transcriptional signature) are not to be excluded.

Present results of *ulp1c/d* in vitro sensitivity to low water potential and adult stage drought tolerance suggest dual roles for ULP1c and ULP1d in drought tolerance and avoidance responses. However, it is known that in vitro osmoticum treatments present a set of potential problems that are enhanced when these treatments are compared with soil drying experiments (Verslues et al., 2006). Also, responses to low ψ_w are controlled by intricate regulatory networks that integrate external stimuli (e.g. loss of turgor and reduced water content) and internal stimuli (e.g. developmental status, hormones, ROS; Verslues and Zhu, 2005). Exemplifying this complexity, in

Arabidopsis, ZAT10 loss- and gain-of-function lines both display tolerance to in vitro salt and osmotic stresses, and the *ABA overly sensitive 3* (*abo3*) mutant displays hypersensitivity to ABA in seed germination and root elongation assays but not in ABA-induced stomatal closure, resulting in reduced drought tolerance (Mittler et al., 2006; Ren et al., 2010). Such an underlying complexity to the role of ULP1c/d in drought tolerance should be the focus of future studies.

Final considerations

Given the predicted existence of hundreds of SUMO targets, it is paradoxical to realize that, unlike the ubiquitination pathway, only a reduced number of components of the SUMO conjugation pathway exist in plant genomes. The relative abundance of ULPs makes them natural candidates for specificity within the pathway (Chosed et al., 2006; Colby et al., 2006; Lois, 2010), also because new classes of SUMO de-conjugating enzymes have recently emerged in non-plant models (Hickey et al., 2012). Characterization of plant ULPs at the molecular level poses several challenges since ULPs (1) must discriminate between SUMO isoforms, (2) are likely to contribute differently to total isopeptidase and endopeptidase activities, (3) present different expression patterns, and (4) display different subcellular/subnuclear localizations (Murtas et al., 2003; Chosed et al., 2006; Colby et al., 2006; Conti et al., 2008; Lois, 2010; Hermkes et al., 2011). In addition, biological redundancy between SUMO proteases above the canonical redundant pairs is not to be excluded. This complexity certainly urges further research on SUMO protease function. We were able to report that Arabidopsis SUMO proteases ULP1c and ULP1d form an unequally redundant gene pair that is broadly expressed and controls developmental traits such as plant growth and seed germination. Microarray analysis in the *ulp1c/d* mutant showed a transcriptional signature typical of drought stress responses, prompting us to assign a functional role for ULP1c/d in drought tolerance, stomatal aperture and the response to low water potential. Baring in mind the dynamics of SUMO conjugation/deconjugation cycles, we used genetic evidence to address the interplay between ULP1c/d and the major E3 ligase SIZ1.

4.4. MATERIALS AND METHODS

Plant material and growth conditions

T-DNA insertion mutants were used to evaluate the effect of *Arabidopsis thaliana ULP1c* (At1g10570) and *ULP1d* (At1g60220) loss-of-function. Ecotype Columbia-0 (Col) was used as the wild-type control. Mutants were identified using SIGnAL (signal.salk.edu); all consisted of SALK lines: SALK_050441 (*ulp1c-2*), SALK_151423 (*ulp1c-3*), SALK_029340 (*ulp1d-2*) and SALK_065397 (*siz1-2*; Miura et al., 2005). Genotypes were ordered through the NASC European Arabidopsis Stock Centre (arabidopsis.info) or the Arabidopsis Biological Resource Stock Center (www.biosci.ohio-state). Homozygous insertion mutants were genotyped based on SIGnAL T-DNA Primer Design (signal.salk.edu/tdnaprimers.2.html), using the primers in Table S4.1 (Appendix IV).

Synchronized seeds were stratified for 3 days at 4°C in the dark. Surface sterilization was performed in a horizontal laminar flow chamber by sequential immersion in 70% (v/v) ethanol for 5 min and 20% (v/v) commercial bleach for 10 min before washing five times with sterile ultra-pure water. Seeds were resuspended in sterile 0.25% (w/v) agarose, sown onto 1.2% agar-solidified MS medium (Murashige and Skoog, 1962) containing 1.5% sucrose, 0.5 g L^{-1} MES, pH 5.7, and grown vertically in culture rooms with a 16 h light/8 h dark cycle under cool white light (80 µE m^{-2} s^{-1} light intensity) at 23°C. For standard growth, 7-day-old in vitro-grown seedlings were transferred to a soil to vermiculite (4:1) mixture, and maintained under identical growth conditions, with regular watering. Developmental characterization of the mutants was based on the developmental map of Boyes and co-workers (2001). For germination assays, seeds were sterilized as detailed, sown onto 0.8% agar MS medium and grown horizontally under identical conditions. Each replica plate contained >30 seeds per genotype.

Drought stress and ABA-related experiments

To assay soil-based long-term drought stress, ~100 seeds per pot were sown directly onto soil and stratified in the dark at 4°C for three days. Pots were watered every two days with 20 mL of ultra-pure H_2O for three weeks. Watering was then discontinued for two weeks, except for control plants. For perlite-based long-term drought stress, 10-day-old in vitro-grown seedlings were transferred to perlite and watered every two days with 20 mL of 0.5x MS for one week. Watering was then interrupted (except for control plants), and plants were observed for three weeks. For rapid dehydration, the rosette of 3-week-old soil-grown plants was detached from roots and air-dried

at room temperature. Fresh weight was measured with an analytical balance at different time points.

To measure root growth, seedlings were grown in vitro for seven days, and subsequently transferred to 0.5x MS 1.2% agar plates. Plates were supplemented with either 10 μM ABA, 200 mM mannitol or PEG-infusion; in the latter, control plants were transferred to mock-infused 0.5x MS agar plates. PEG-infused MS agar plates were prepared as follows: under sterility conditions, 20 mL of fused agarised 0.5x MS media were poured into petri plates, left to cool and then covered with 30 mL of PEG or mock overlay solution; plates were covered and the media was allowed to sit for 12-15 h. PEG overlay solution (-0.7 MPa strength) consisted of 0.5x MS basal salt mixture, 1.2 g L^{-1} MES and 400 g L^{-1} PEG 8000. Excess overlay solution was poured just before seedling transfer and immediately sealed with parafilm to avoid water loss. Vertical root growth was measured every two days for up to 10 days.

Analysis and ABA inhibition of stomatal opening was performed on isolated epidermal strips from rosette leaves of 3- to 4-week-old plants, as previously described (Lozano-Duran et al., 2011). Briefly, leaves were detached from the rosette and submerged in a stomata-opening solution (50 mM KCl; 10 μM $CaCl_2$; 0.01% Tween 20; 10 mM MES-KOH pH 6.15) under cool white light (80 μE m^{-2} s^{-1}) for three hours. Subsequently, 5 μM ABA or mock solution was added to the buffer and the samples were incubated for one hour under identical light conditions. Epidermal peels were obtained with the help of double-sided adhesive tape and subsequently stained with a 0.2% (w/v) toluidine blue solution and observed under the microscope (Leica DM 5000). Stomata size, aperture and density were measured using ImageJ (rsb.info.nih.gov/ij/). ABA germination assays were performed as detailed, in an MS medium supplemented with 1 μM ABA.

Plasmid construction and plant transformation

Plasmids were constructed using standard DNA cloning techniques, and confirmed by DNA sequencing. For *promoter::GUS* constructs, ULP1c and ULP1d promoter regions were amplified by PCR from Arabidopsis genomic DNA (Edwards et al., 1991). Incorporated restriction sites (*Eco*RI and *Nco*I) were used to clone fragments into the pCAMBIA 1303 vector (www.cambia.org/daisy/cambia/585). For complementation purposes, the *ULP1d* open reading frame was amplified from cDNA by PCR with incorporated restriction sites (*Eco*RI and *Cla*I). The amplification product was sub-cloned into the pGEM-T Easy vector (Promega) and subsequently cloned into the pHANNIBAL vector (Wesley et al., 2001) to create a *pro35S::ULP1d-NOS*

terminator fusion. The construct was excised using *Not*I and finally cloned into the plant expression vector pGREEN II 0229 (www.pgreen.ac.uk/). *Agrobacterium tumefaciens* strain EHA105 was used for plant transformation. *Arabidopsis thaliana* (Col ecotype) plants were transformed by the floral dip method (Clough and Bent, 1998). A resistance marker (Kanamycin) strategy was employed to select for homozygous transformants.

Histochemical GUS staining

GUS histochemical staining of transgenic Arabidopsis (Col) plants containing *proULP1c::GUS* and *proULP1d::GUS* constructs was performed as previously described (Posé et al., 2009). Briefly, plants were vaccum infiltrated with a GUS staining solution, containing 100 mM sodium-phosphate buffer (pH 7.0), 20% (v/v) methanol, 0.5 mM potassium ferrocyanide, 0.5 mM potassium ferricyanide and 0.3% (v/v) Triton X-100. Blue-coloration of whole plants in different developmental stages was recorded with a bright field microscope (Leica DM 5000) or a magnifying glass *(Wild Heerbrugg)* coupled to a CCD color camera *(Leica DFC 320)*. GUS stained tissues and plants shown in this paper represent the typical results of at least three independent lines for each construct.

Microarray analysis and quantitative RT-PCR

Genome-wide transcription studies were performed using the ATH1 Affymetrix microarray chip with three independent pools per genotype, each pool representing RNA from nine different 5-week-old plants. Plants were grown in culture chambers with a 16 h dark/8 h light cycle under cool white light (80 µE m^{-2} s^{-1} light intensity) at 23°C. Three rosette leaves were sampled from each plant. RNA was extracted using a standard TRIzol protocol (Invitrogen), including treatment with *Recombinant DNase I* (Takara Biotechnology), followed by *RNeasy Plant Mini kit* (QIAGEN) column cleaning. Microarray execution and differential expression analysis were conducted at Unité de Recherche en Génomique Végétale (Université d'Evry Val d'Essonne, France), and data was deposited in ArrayExpress (www.ebi.ac.uk/arrayexpress/). GO term functional categorization was performed in VirtualPlant 1.2 (virtualplant.bio.nyu.edu/cgi-bin/vpweb/), using the BioMaps function with a 0.05 *p*-value cutoff (Katari et al., 2010). Redundancy exclusion and scatterplot analysis were performed using REVIGO (revigo.irb.hr/), with a 0.9 C-value. Venn diagrams were obtained using Venn Diagram Generator (www.pangloss.com/seidel/Protocols/venn.cgi).

For quantitative Real-Time PCR (qPCR) analysis, RNA from plant tissue was extracted using an *RNeasy Plant Mini kit* (QIAGEN), and RNA quantity and quality were assessed using both a Nanodrop ND-1000 spectrophotometer and standard agarose-gel electrophoretic analysis. The RNA samples were treated with *Recombinant DNase I* (Takara Biotechnology) and, cDNA was subsequently generated using a *SuperScript II Reverse Transcriptase kit* (Invitrogen). *SsoFast EvaGreen Supermix* (BioRad) was used in the qPCR reaction mixture as per the manufacturer's indications. The reaction was performed in a *Rotor Gene Q system* (QIAGEN) or a *MyiQ Single-Color Real-Time PCR Detection system* (Bio-Rad).

Primers for qPCR (Appendix IV - Table S4.2) were designed using NCBI Primer-BLAST (www.ncbi.nlm.nih.gov/tools/primer-blast/; Ye et al., 2012), to ensure specific amplification within the Arabidopsis transcriptome, 100-250 bp PCR amplification product sized, 50-60% GC content and ~60°C T_m. When possible, one of the primers was designed to span an exon junction. *ACT2* (At3g18780) was used as a reference gene (Lozano-Duran et al., 2011).

Protein extraction and Immunoblotting

Plant tissue was grinded in a microtube in liquid nitrogen with the help of polypropylene pestles. Protein extracts were obtained by adding extraction buffer [50 mM Tris; 150 mM NaCl; 0.2% (v/v) Triton X-100] supplemented with *Complete Protease Inhibitor Cocktail* (Roche) as per the manufacturer's instructions. Following incubation for 1 h at 4°C with agitation, microtubes were centrifuged two times for 30 min at 16000 *g*. The supernatant was subsequently recovered and stored at -80°C. Protein was spectrophotometrically quantified using *Bradford reagent* (Sigma; Bradford, 1976). Equal amounts of protein were resolved by standard SDS-PAGE in a 10% (w/v) acrylamide resolving gel, using a *Mini-PROTEAN Cell* (Bio-Rad) apparatus. For immunoblotting, proteins were transferred to a PVDF-membrane using a *Mini Trans-Blot Cell* (Bio-Rad). The membrane was blocked for 1 h at 23°C in blocking solution (5% dry milk powder in PBST). The primary antibody Anti-AtSUMO1 (ABCAM) was added in a 1:2000 dilution and incubated for 3 h. The membrane was washed three times with 10 mL of PBST for 10 min, and incubated with the secondary antibody (anti-rabbit, *Santa Cruz*; 1:5000 in blocking solution) for 1 h. The membrane was washed as previously detailed and developed by a chemiluminescence reaction using the *Immune-Star WesternC Kit* (Bio-Rad) and a *ChemiDoc XRS system* (Bio-Rad) for image acquisition. PVDF membranes were incubated for 15 min with Ponceau S solution [0.1% (w/v) Ponceau S; 5% (v/v) acetic acid] to stain total protein levels.

4.5. REFERENCES

Aroca R, Porcel R, Ruiz-Lozano JM (2012) Regulation of root water uptake under abiotic stress conditions. J Exp Bot **63:** 43-57

Aubert Y, Vile D, Pervent M, Aldon D, Ranty B, Simonneau T, Vavasseur A, Galaud JP (2010) RD20, a stress-inducible caleosin, participates in stomatal control, transpiration and drought tolerance in Arabidopsis thaliana. Plant Cell Physiol **51:** 1975-1987

Boyes DC, Zayed AM, Ascenzi R, McCaskill AJ, Hoffman NE, Davis KR, Görlach J (2001) Growth stage-based phenotypic analysis of Arabidopsis: a model for high throughput functional genomics in plants. Plant Cell **13:** 1499-1510

Bradford MM (1976) A rapid and sensitive method for the quantitation of microgram quantities of protein utilizing the principle of protein-dye binding. Anal Biochem **72:** 248-254

Budhiraja R, Hermkes R, Muller S, Schmidt J, Colby T, Panigrahi K, Coupland G, Bachmair A (2009) Substrates related to chromatin and to RNA-dependent processes are modified by Arabidopsis SUMO isoforms that differ in a conserved residue with influence on desumoylation. Plant Physiol **149:** 1529-1540

Byrne ME, Simorowski J, Martienssen RA (2002) *ASYMMETRIC LEAVES1* reveals knox gene redundancy in Arabidopsis. Development **129:** 1957-1965

Castano-Miquel L, Segui J, Lois LM (2011) Distinctive properties of Arabidopsis SUMO paralogues support the in vivo predominant role of AtSUMO1/2 isoforms. Biochem J **436:** 581-590

Castro PH, Tavares RM, Bejarano ER, Azevedo H (2012) SUMO, a heavyweight player in plant abiotic stress responses. Cell Mol Life Sci **69:** 3269-3283

Catala R, Ouyang J, Abreu IA, Hu Y, Seo H, Zhang X, Chua NH (2007) The Arabidopsis E3 SUMO ligase SIZ1 regulates plant growth and drought responses. Plant Cell **19:** 2952-2966

Chen CN, Chu CC, Zentella R, Pan SM, Ho TH (2002) *AtHVA22* gene family in Arabidopsis: phylogenetic relationship, ABA and stress regulation, and tissue-specific expression. Plant Mol Biol **49:** 633-644

Chosed R, Mukherjee S, Lois LM, Orth K (2006) Evolution of a signalling system that incorporates both redundancy and diversity: Arabidopsis SUMOylation. Biochem J **398:** 521-529

Clough SJ, Bent AF (1998) Floral dip: a simplified method for Agrobacterium-mediated transformation of *Arabidopsis thaliana*. Plant J **16:** 735-743

Colby T, Matthai A, Boeckelmann A, Stuible HP (2006) SUMO-conjugating and SUMO-deconjugating enzymes from Arabidopsis. Plant Physiol **142:** 318-332

Conti L, Price G, O'Donnell E, Schwessinger B, Dominy P, Sadanandom A (2008) Small ubiquitin-like modifier proteases OVERLY TOLERANT TO SALT1 and -2 regulate salt stress responses in Arabidopsis. Plant Cell **20:** 2894-2908

Cutler SR, Rodriguez PL, Finkelstein RR, Abrams SR (2010) Abscisic acid: emergence of a core signaling network. Annu Rev Plant Biol **61:** 651-679

Edwards K, Johnstone C, Thompson C (1991) A simple and rapid method for the preparation of plant genomic DNA for PCR analysis. Nucleic Acids Res **19:** 1349

Finkelstein R, Reeves W, Ariizumi T, Steber C (2008) Molecular aspects of seed dormancy. Annu Rev Plant Biol **59:** 387-415

Fuglsang AT, Guo Y, Cuin TA, Qiu Q, Song C, Kristiansen KA, Bych K, Schulz A, Shabala S, Schumaker KS, Palmgren MG, Zhu JK (2007) Arabidopsis protein kinase PKS5 inhibits the plasma membrane H^+-ATPase by preventing interaction with 14-3-3 protein. Plant Cell **19:** 1617-1634

Fujita Y, Yoshida T, Yamaguchi-Shinozaki K (2013) Pivotal role of the AREB/ABF-SnRK2 pathway in ABRE-mediated transcription in response to osmotic stress in plants. Physiol Plant **147:** 15-27

Garcia-Dominguez M, Reyes JC (2009) SUMO association with repressor complexes, emerging routes for transcriptional control. Biochim Biophys Acta **1789:** 451-459

Gareau JR, Lima CD (2010) The SUMO pathway: emerging mechanisms that shape specificity, conjugation and recognition. Nat Rev Mol Cell Biol **11:** 861-871

Geoffroy MC, Hay RT (2009) An additional role for SUMO in ubiquitin-mediated proteolysis. Nat Rev Mol Cell Biol **10:** 564-568

Golebiowski F, Matic I, Tatham MH, Cole C, Yin Y, Nakamura A, Cox J, Barton GJ, Mann M, Hay RT (2009) System-wide changes to SUMO modifications in response to heat shock. Sci Signal **2:** ra24

Hay RT (2005) SUMO: a history of modification. Mol Cell **18:** 1-12

Hermkes R, Fu YF, Nurrenberg K, Budhiraja R, Schmelzer E, Elrouby N, Dohmen RJ, Bachmair A, Coupland G (2011) Distinct roles for Arabidopsis SUMO protease ESD4 and its closest homolog ELS1. Planta **233:** 63-73

Hickey CM, Wilson NR, Hochstrasser M (2012) Function and regulation of SUMO proteases. Nat Rev Mol Cell Biol **13:** 755-766

Himmelbach A, Hoffmann T, Leube M, Hohener B, Grill E (2002) Homeodomain protein ATHB6 is a target of the protein phosphatase ABI1 and regulates hormone responses in Arabidopsis. EMBO J **21:** 3029-3038

Huang L, Yang S, Zhang S, Liu M, Lai J, Qi Y, Shi S, Wang J, Wang Y, Xie Q, Yang C (2009) The Arabidopsis SUMO E3 ligase AtMMS21, a homologue of NSE2/MMS21, regulates cell proliferation in the root. Plant J **60:** 666-678

Ishida T, Fujiwara S, Miura K, Stacey N, Yoshimura M, Schneider K, Adachi S, Minamisawa K, Umeda M, Sugimoto K (2009) SUMO E3 ligase HIGH PLOIDY2 regulates endocycle onset and meristem maintenance in Arabidopsis. Plant Cell **21:** 2284-2297

Jin JB, Jin YH, Lee J, Miura K, Yoo CY, Kim WY, Van Oosten M, Hyun Y, Somers DE, Lee I, Yun DJ, Bressan RA, Hasegawa PM (2008) The SUMO E3 ligase, AtSIZ1, regulates flowering by controlling a salicylic acid-mediated floral promotion pathway and through affects on *FLC* chromatin structure. Plant J **53:** 530-540

Kanaoka MM, Pillitteri LJ, Fujii H, Yoshida Y, Bogenschutz NL, Takabayashi J, Zhu JK, Torii KU (2008) SCREAM/ICE1 and SCREAM2 specify three cell-state transitional steps leading to Arabidopsis stomatal differentiation. Plant Cell **20:** 1775-1785

Katari MS, Nowicki SD, Aceituno FF, Nero D, Kelfer J, Thompson LP, Cabello JM, Davidson RS, Goldberg AP, Shasha DE, Coruzzi GM, Gutierrez RA (2010) VirtualPlant: a software platform to support systems biology research. Plant Physiol **152:** 500-515

Kilian J, Peschke F, Berendzen KW, Harter K, Wanke D (2012) Prerequisites, performance and profits of transcriptional profiling the abiotic stress response. Biochim Biophys Acta **1819:** 166-175

Koyama T, Furutani M, Tasaka M, Ohme-Takagi M (2007) TCP transcription factors control the morphology of shoot lateral organs via negative regulation of the expression of boundary-specific genes in Arabidopsis. Plant Cell **19:** 473-484

Kurepa J, Walker JM, Smalle J, Gosink MM, Davis SJ, Durham TL, Sung DY, Vierstra RD (2003) The small ubiquitin-like modifier (SUMO) protein modification system in Arabidopsis. Accumulation of SUMO1 and -2 conjugates is increased by stress. J Biol Chem **278:** 6862-6872

Lallemand-Breitenbach V, Jeanne M, Benhenda S, Nasr R, Lei M, Peres L, Zhou J, Zhu J, Raught B, de The H (2008) Arsenic degrades PML or PML-RARalpha through a SUMO-triggered RNF4/ubiquitin-mediated pathway. Nat Cell Biol **10:** 547-555

Li S, Pandey S, Gookin TE, Zhao Z, Wilson L, Assmann SM (2012) Gene-sharing networks reveal organizing principles of transcriptomes in Arabidopsis and other multicellular organisms. Plant Cell **24:** 1362-1378

Lois LM (2010) Diversity of the SUMOylation machinery in plants. Biochem Soc Trans **38:** 60-64

Lozano-Duran R, Rosas-Diaz T, Gusmaroli G, Luna AP, Taconnat L, Deng XW, Bejarano ER (2011) Geminiviruses subvert ubiquitination by altering CSN-mediated derubylation of SCF E3 ligase complexes and inhibit jasmonate signaling in *Arabidopsis thaliana*. Plant Cell **23:** 1014-1032

Lyzenga WJ, Stone SL (2012) Abiotic stress tolerance mediated by protein ubiquitination. J Exp Bot **63:** 599-616

Maruyama K, Sakuma Y, Kasuga M, Ito Y, Seki M, Goda H, Shimada Y, Yoshida S, Shinozaki K, Yamaguchi-Shinozaki K (2004) Identification of cold-inducible downstream genes of the Arabidopsis DREB1A/CBF3 transcriptional factor using two microarray systems. Plant J **38:** 982-993

Miller MJ, Barrett-Wilt GA, Hua Z, Vierstra RD (2010) Proteomic analyses identify a diverse array of nuclear processes affected by small ubiquitin-like modifier conjugation in Arabidopsis. Proc Natl Acad Sci U S A **107:** 16512-16517

Miller MJ, Vierstra RD (2011) Mass spectrometric identification of SUMO substrates provides insights into heat stress-induced SUMOylation in plants. Plant Signal Behav **6:** 130-133

Mittler R, Kim Y, Song L, Coutu J, Coutu A, Ciftci-Yilmaz S, Lee H, Stevenson B, Zhu JK (2006) Gain- and loss-of-function mutations in Zat10 enhance the tolerance of plants to abiotic stress. FEBS Lett **580:** 6537-6542

Miura K, Hasegawa PM (2010) Sumoylation and other ubiquitin-like post-translational modifications in plants. Trends Cell Biol **20:** 223-232

Miura K, Jin JB, Lee J, Yoo CY, Stirm V, Miura T, Ashworth EN, Bressan RA, Yun DJ, Hasegawa PM (2007) SIZ1-mediated sumoylation of ICE1 controls *CBF3/DREB1A* expression and freezing tolerance in Arabidopsis. Plant Cell **19:** 1403-1414

Miura K, Lee J, Gong Q, Ma S, Jin JB, Yoo CY, Miura T, Sato A, Bohnert HJ, Hasegawa PM (2011) SIZ1 regulation of phosphate starvation-induced root architecture remodeling involves the control of auxin accumulation. Plant Physiol **155:** 1000-1012

Miura K, Lee J, Jin JB, Yoo CY, Miura T, Hasegawa PM (2009) Sumoylation of ABI5 by the Arabidopsis SUMO E3 ligase SIZ1 negatively regulates abscisic acid signaling. Proc Natl Acad Sci U S A **106:** 5418-5423

Miura K, Lee J, Miura T, Hasegawa PM (2010) SIZ1 controls cell growth and plant development in Arabidopsis through salicylic acid. Plant Cell Physiol **51:** 103-113

Miura K, Okamoto H, Okuma E, Shiba H, Kamada H, Hasegawa PM, Murata Y (2012) *SIZ1* deficiency causes reduced stomatal aperture and enhanced drought tolerance via controlling salicylic acid-induced accumulation of reactive oxygen species in Arabidopsis. Plant J **73:** 91–104

Miura K, Rus A, Sharkhuu A, Yokoi S, Karthikeyan AS, Raghothama KG, Baek D, Koo YD, Jin JB, Bressan RA, Yun DJ, Hasegawa PM (2005) The Arabidopsis SUMO E3 ligase SIZ1 controls phosphate deficiency responses. Proc Natl Acad Sci U S A **102:** 7760-7765

Moore JP, Vicre-Gibouin M, Farrant JM, Driouich A (2008) Adaptations of higher plant cell walls to water loss: drought vs desiccation. Physiol Plant **134:** 237-245

Murashige T, Skoog F (1962) A revised medium for rapid growth and bio assays with tobacco tissue cultures. Physiol Plant **15:** 473-475

Murtas G, Reeves PH, Fu YF, Bancroft I, Dean C, Coupland G (2003) A nuclear protease required for flowering-time regulation in Arabidopsis reduces the abundance of SMALL UBIQUITIN-RELATED MODIFIER conjugates. Plant Cell **15:** 2308-2319

Nemhauser JL, Hong F, Chory J (2006) Different plant hormones regulate similar processes through largely nonoverlapping transcriptional responses. Cell **126:** 467-475

O'Connor TR, Dyreson C, Wyrick JJ (2005) Athena: a resource for rapid visualization and systematic analysis of Arabidopsis promoter sequences. Bioinformatics **21:** 4411-4413

Park HC, Choi W, Park HJ, Cheong MS, Koo YD, Shin G, Chung WS, Kim WY, Kim MG, Bressan RA, Bohnert HJ, Lee SY, Yun DJ (2011) Identification and molecular properties of SUMO-binding proteins in Arabidopsis. Mol Cells **32:** 143-151

Posé D, Castanedo I, Borsani O, Nieto B, Rosado A, Taconnat L, Ferrer A, Dolan L, Valpuesta V, Botella MA (2009) Identification of the Arabidopsis *dry2/sqe1-5* mutant reveals a central role for sterols in drought tolerance and regulation of reactive oxygen species. Plant J **59:** 63-76

Raghavendra AS, Gonugunta VK, Christmann A, Grill E (2010) ABA perception and signalling. Trends Plant Sci **15:** 395-401

Reeves PH, Murtas G, Dash S, Coupland G (2002) *early in short days 4*, a mutation in Arabidopsis that causes early flowering and reduces the mRNA abundance of the floral repressor *FLC*. Development **129:** 5349-5361

Ren X, Chen Z, Liu Y, Zhang H, Zhang M, Liu Q, Hong X, Zhu JK, Gong Z (2010) ABO3, a WRKY transcription factor, mediates plant responses to abscisic acid and drought tolerance in Arabidopsis. Plant J **63:** 417–429

Saracco SA, Miller MJ, Kurepa J, Vierstra RD (2007) Genetic analysis of SUMOylation in Arabidopsis: conjugation of SUMO1 and SUMO2 to nuclear proteins is essential. Plant Physiol **145:** 119-134

Schroeder JI, Kwak JM, Allen GJ (2001) Guard cell abscisic acid signalling and engineering drought hardiness in plants. Nature **410:** 327-330

Setter TL (2012) Analysis of constituents for phenotyping drought tolerance in crop improvement. Front Physiol **3:** 180

Shen Q, Ho TH (1995) Functional dissection of an abscisic acid (ABA)-inducible gene reveals two independent ABA-responsive complexes each containing a G-box and a novel cis-acting element. Plant Cell **7:** 295-307

Sreenivasulu N, Harshavardhan VT, Govind G, Seiler C, Kohli A (2012) Contrapuntal role of ABA: Does it mediate stress tolerance or plant growth retardation under long-term drought stress? Gene **506:** 265-273

Supek F, Bosnjak M, Skunca N, Smuc T (2011) REVIGO summarizes and visualizes long lists of gene ontology terms. PLoS One **6:** e21800

Taji T, Ohsumi C, Iuchi S, Seki M, Kasuga M, Kobayashi M, Yamaguchi-Shinozaki K, Shinozaki K (2002) Important roles of drought- and cold-inducible genes for galactinol synthase in stress tolerance in *Arabidopsis thaliana*. Plant J **29:** 417-426

Toledo-Ortiz G, Huq E, Quail PH (2003) The Arabidopsis basic/helix-loop-helix transcription factor family. Plant Cell **15:** 1749-1770

van den Burg HA, Kini RK, Schuurink RC, Takken FL (2010) Arabidopsis small ubiquitin-like modifier paralogs have distinct functions in development and defense. Plant Cell **22:** 1998-2016

van den Burg HA, Takken FL (2009) Does chromatin remodeling mark systemic acquired resistance? Trends Plant Sci **14:** 286-294

Verslues PE, Agarwal M, Katiyar-Agarwal S, Zhu J, Zhu JK (2006) Methods and concepts in quantifying resistance to drought, salt and freezing, abiotic stresses that affect plant water status. Plant J **45:** 523-539

Verslues PE, Zhu JK (2005) Before and beyond ABA: upstream sensing and internal signals that determine ABA accumulation and response under abiotic stress. Biochem Soc Trans **33:** 375-379

Wesley SV, Helliwell CA, Smith NA, Wang MB, Rouse DT, Liu Q, Gooding PS, Singh SP, Abbott D, Stoutjesdijk PA, Robinson SP, Gleave AP, Green AG, Waterhouse PM (2001) Construct design for efficient, effective and high-throughput gene silencing in plants. Plant J **27:** 581-590

Wilkinson KA, Henley JM (2010) Mechanisms, regulation and consequences of protein SUMOylation. Biochem J **428:** 133-145

Xu XM, Rose A, Muthuswamy S, Jeong SY, Venkatakrishnan S, Zhao Q, Meier I (2007) NUCLEAR PORE ANCHOR, the Arabidopsis homolog of Tpr/Mlp1/Mlp2/megator, is involved in mRNA export and SUMO homeostasis and affects diverse aspects of plant development. Plant Cell **19:** 1537-1548

Ye J, Coulouris G, Zaretskaya I, Cutcutache I, Rozen S, Madden TL (2012) Primer-BLAST: A tool to design target-specific primers for polymerase chain reaction. BMC Bioinformatics **13:** 134

Yoo CY, Pence HE, Jin JB, Miura K, Gosney MJ, Hasegawa PM, Mickelbart MV (2010) The Arabidopsis GTL1 transcription factor regulates water use efficiency and drought tolerance by modulating stomatal density via transrepression of SDD1. Plant Cell **22:** 4128-4141

Zhang S, Qi Y, Liu M, Yang C (2012) SUMO E3 ligase AtMMS21 regulates drought tolerance in *Arabidopsis thaliana*. J Integr Plant Biol **55:** 83-95

Zhou W, Ryan JJ, Zhou H (2004) Global analyses of sumoylated proteins in *Saccharomyces cerevisiae*. Induction of protein sumoylation by cellular stresses. J Biol Chem **279:** 32262-32268

Chapter 5

The ULP1c/ULP1d SUMO protease pair negatively regulates *Arabidopsis thaliana* defence against *Pseudomonas syringae* pv. *tomato* DC3000

This chapter had the collaboration of Alberto Macho and José Rufián on the infections assays. Alberto Macho performed the RNA extractions for the microarray.

CONTENTS

5.1. INTRODUCTION

Plants are constantly subjected to a variety of external challenges that compromise growth and therefore limit crop yield. To counteract stress-imposing agents in a fast and reversible way, plants have recruited post-translational modification (PTM) mechanisms to modulate protein activity. One such PTM involves ubiquitin and small peptides resembling ubiquitin, appropriately designated Ubiquitin-like modifiers (UBLs), which include Autophagy (ATG), Related to Ubiquitin (RUB) and Small Ubiquitin-like Modifier (SUMO; Miura and Hasegawa, 2010). Sumoylation is the mechanism by which SUMO is conjugated to a target's lysine residue, often in the core consensus ΨKxE (Ψ, large hydrophobic residue; K, lysine; x, any amino acid; E, glutamic acid). This pathway implies a cooperation of four enzymatic steps: SUMO protease-dependent maturation, E1-activation, E2-conjugation, the latter normally aided by an E3-dependent ligation (Gareau and Lima, 2010).

The model plant *Arabidopsis thaliana* expresses four main SUMO isoforms, SUM1, -2, -3 and -5 (Saracco et al., 2007; Budhiraja et al., 2009). The redundant SUM1 and -2 peptides (SUM1/2) are essential for plant development: the double knockout mutant is impaired in embryogenesis and *sum1 amiR-SUM2* (*SUM2* knockdown in *sum1* background) has pleiotropic effects on plant development (Saracco et al., 2007; van den Burg et al., 2010). In contrast, the *SUM3* knockout mutant only shows late flowering (van den Burg et al., 2010). While SUM1/2 are capable of forming SUMO chains, SUM3 is not (Colby et al., 2006; Saracco et al., 2007; van den Burg et al., 2010). SUMO chains are an important structural feature, since SUMO can also interact non-covalently with proteins containing SUMO-interacting motifs (SIMs). For instance, SUMO chains were found to be recognized by SUMO-Targeted Ubiquitin Ligases (STUbLs), targeting sumoylated proteins for degradation via the Ubiquitin Proteasome System (Geoffroy and Hay, 2009). In contrast, SUMO may compete for the same lysine as ubiquitin, resulting in an antagonism between these two PTMs for the same lysine (Hay, 2005). SUMO may also affect the target's activity by controlling its conformation, or creating/blocking interacting interfaces (Wilkinson and Henley, 2010).

In eukaryotes, sumoylation is essential for cell viability, and has been associated with stress response mechanisms (Castro et al., 2012). In plants, SUMO-conjugate levels increase in response to oxidative stress, heat, ethanol, drought and salt (Castro et al., 2012). Recent systematic approaches to map the Arabidopsis sumoylome indicate that SUMO targets cover a wide range of cellular processes and molecular mechanisms, with emphasis on nuclear processes

like gene expression regulation (Elrouby and Coupland, 2010; Miller et al., 2010; Castro et al., 2012; Miller et al., 2013). Interestingly, many of the sumoylated transcription regulators are involved in biotic stress responses (van den Burg and Takken, 2010), and it is not surprising that many pathogens are capable of controlling essential cellular functions or shutting down defences by exploiting the host's sumoylation machinery (Wimmer et al., 2012).

Plants have several levels of defence against pathogen invasion (Spoel and Dong, 2012). As a first layer of protection, plants have reinforced cell walls that function as constitutive barriers (Nuhse, 2012). Furthermore, plants have pattern-recognition receptors capable of detecting pathogen-associated molecular patterns (PAMPs), such as Flagellin-Sensitive 2 (FLS2) and EF-Tu Receptor (EFR), triggering a set of defence responses named PAMP-triggered immunity (PTI; Monaghan and Zipfel, 2012). Bacteria have developed sophisticated ways of neutralizing PTI and overruling the host cell by injecting effectors through the type III secretion system (T3SS; Cunnac et al., 2009). These effectors can deregulate and perturb crucial cellular processes. Meanwhile, plants evolved ways of recognizing these effectors by resistance proteins (R-proteins) that directly interact with pathogen effectors or, in most cases, guard effector-targeted proteins, thus activating a second level of resistance designated as effector-triggered immunity (ETI; Jones and Dangl, 2006; Block and Alfano, 2011). In the site of infection, the plant cell triggers a hypersensitive response (HR) that keeps pathogens, especially biotrophs, from feeding from the cell. In addition, a mobile signal spreads throughout the plant, immunizing the tissues against secondary infections, a process designed as systemic acquired resistance (SAR; Fu and Dong, 2013). Part of these responses and signaling mechanisms rely on hormone regulation. The two major defence hormones are salicylic acid (SA) and jasmonic acid (JA), but many others contribute for the tight regulation of plant immunity (Pieterse et al., 2012). Auxins, for instance, attenuate defence responses in plants by antagonizing SA signaling, while cooperating with JA signaling (Kazan and Manners, 2009).

In plants, few studies have addressed the association between sumoylation and pathogen challenge. Sumoylation was shown to be a negative regulator of basal immunity against the hemibiotrophic pathogen *Pseudomonas syringae* pv. *tomato* (*Pst*) DC3000 (Lee et al., 2007; van den Burg et al., 2010). In Arabidopsis, SUM1/2 and the major E3 ligase SIZ1 were shown to negatively regulate the biosynthesis of the important biotic stress hormone salicylic acid and consequently the expression of *Pathogen-Related* (*PR*) genes (Lee et al., 2007; van den Burg et al., 2010). SUM3 seems to be part of a later response to *Pst* DC3000, promoting defence downstream

of SA (van den Burg et al., 2010). Meanwhile, some pathogens seem to have developed mechanisms that target sumoylation components and deregulate their activity. These include bacterial effectors like XopD and AvrXv4 that have de-sumoylation activity, or viral particles that inhibit SUMO modification by controlling the SUMO E2 conjugating enzyme (SCE; Castillo et al., 2004; Roden et al., 2004; Chosed et al., 2006; Kim et al., 2008; Sanchez-Duran et al., 2011; Kim et al., 2013). Although targeting of SUMO protease activity seems to be a common strategy employed by phytopathogen effectors (Hotson and Mudgett, 2004), endogenous SUMO proteases have never been characterized concerning their role in the host response to infectious agents.

In contrast to the relatively small number of sumoylation components, plants display a fairly large number of SUMO proteases called Ubiquitin-Like Proteases (ULPs). The Arabidopsis genome encodes at least seven ULPs (ESD4, ULP1a-d and ULP2a-b; Chosed et al., 2006; Colby et al., 2006; Lois, 2010; Novatchkova et al., 2012). ESD4, ULP1a/ELS1, ULP1c/OTS2 and ULP1d/OTS1 were shown to have SUMO deconjugating activity both in vitro and in vivo (Chosed et al., 2006; Colby et al., 2006; Conti et al., 2008; Hermkes et al., 2011), but their biological relevance is still poorly understood. ESD4 and ULP1a are phylogenetically close but functionally different, although both are involved in flowering time and plant development (Murtas et al., 2003; Hermkes et al., 2011). ULP1c and ULP1d, in addition to redundantly controlling plant development, have also been associated with abiotic stress responses by positively regulating salt and drought tolerance (Chapter 4; Conti et al., 2008).

In the present work we explored the role of the redundant pair ULP1c/ULP1d in the response to pathogen attack, using as infectious agent the bacteria *Pst* DC3000. Results showed that the ULP1c/d double mutant (*ulp1c/d*) was less susceptible to *Pst* DC3000 comparatively to the wild-type, while no obvious phenotype was observed for ULP1c/d overexpression lines. The infection process triggered plant immune responses that contributed for the down-regulation of *ULP1c* and *ULP1d* transcript levels. Concomitantly, an increment was observed in both the overall SUMO-conjugate level and in specific SUMO targets. Many SUMO-conjugated targets are associated to the regulation of transcription, and in this study we analyzed the transcriptome of *ulp1c/d* after *Pst* DC3000 challenging. Many deregulated genes were involved in pathogen response as well hormonal signaling, including auxin-responsive genes. In addition, *ulp1c/d* displayed sensitivity to exogenous supplementation of auxins. Results implicate ULP1c/d in the modulation of gene transcripts associated with the plant defence response.

5.2. RESULTS

The double mutant *ulp1c/d* is less susceptible to *Pst* DC3000 infection

Little is known about SUMO protease function in plants. Some virus and bacterial pathogen effector proteins have been shown to deregulate SUMO homeostasis by acting as SUMO proteases (Roden et al., 2004; Kim et al., 2008; Wimmer et al., 2012; Kim et al., 2013). Therefore it is likely that SUMO proteases are also involved in the plant response to bacterial pathogens. We have been addressing the role of ULP1c and ULP1d SUMO proteases, and therefore used a T-DNA insertion double mutant for SUMO proteases *ULP1c* (At1g10570; *ulp1c-1*) and *ULP1d* (At1g60220; *ulp1d-1*), hereafter designated *ulp1c/d* (Chapter 4), to study the potential involvement of these ULPs in plant defence. *Pst* DC3000 was inoculated by infiltration of a bacterial suspension [$5x10^4$ colony forming units (CFU) mL^{-1}] and after three days bacterial growth was evaluated through CFU quantification. Considering that ULP1c and ULP1d were previously found to function redundantly (Chapter 4; Conti et al., 2008), only the double mutant was used in the assays. Results showed that the double mutant was significantly less susceptible to *Pst* DC3000 (Fig. 5.1A) than wild-type (Col) plants, while there were no differences in bacteria multiplication in the single mutants (data not shown). As a positive control, the transgenic line *NahG*, that expresses a bacterial SA hydroxylase and is therefore SA-depleted, showed more susceptibility to *Pst* DC3000.

Our previous results revealed that *ULP1c* and *ULP1d* had higher expression levels in younger tissues (Chapter 4). Taking this in consideration together with the fact that bacterial entry through stomata is a crucial step for bacterial infection, we also performed a *Pst* DC3000 inoculation assay by spraying 2-week-old seedlings. Given that SIZ1 was implicated in the *Pst* DC3000 response (Lee et al., 2007), the *siz1* mutant was used as a positive control for resistance. Results confirmed that the *ulp1c/d* is consistently less susceptible to *Pst* DC3000 infection (Fig. 5.1B). To determine if SIZ1 and ULP1c/d are operating in different pathways we generated a triple mutant *siz1 ulp1c/d* and checked responses to *Pst* DC3000 following spraying. The triple mutant, was also less susceptible to *Pst* DC3000 than the wild-type, and it additionally displayed yellowish leaves comparatively to *ulp1c/d* and *siz1* (Fig. 5.1B), which might suggest an increased hypersensitive response in the triple mutant.

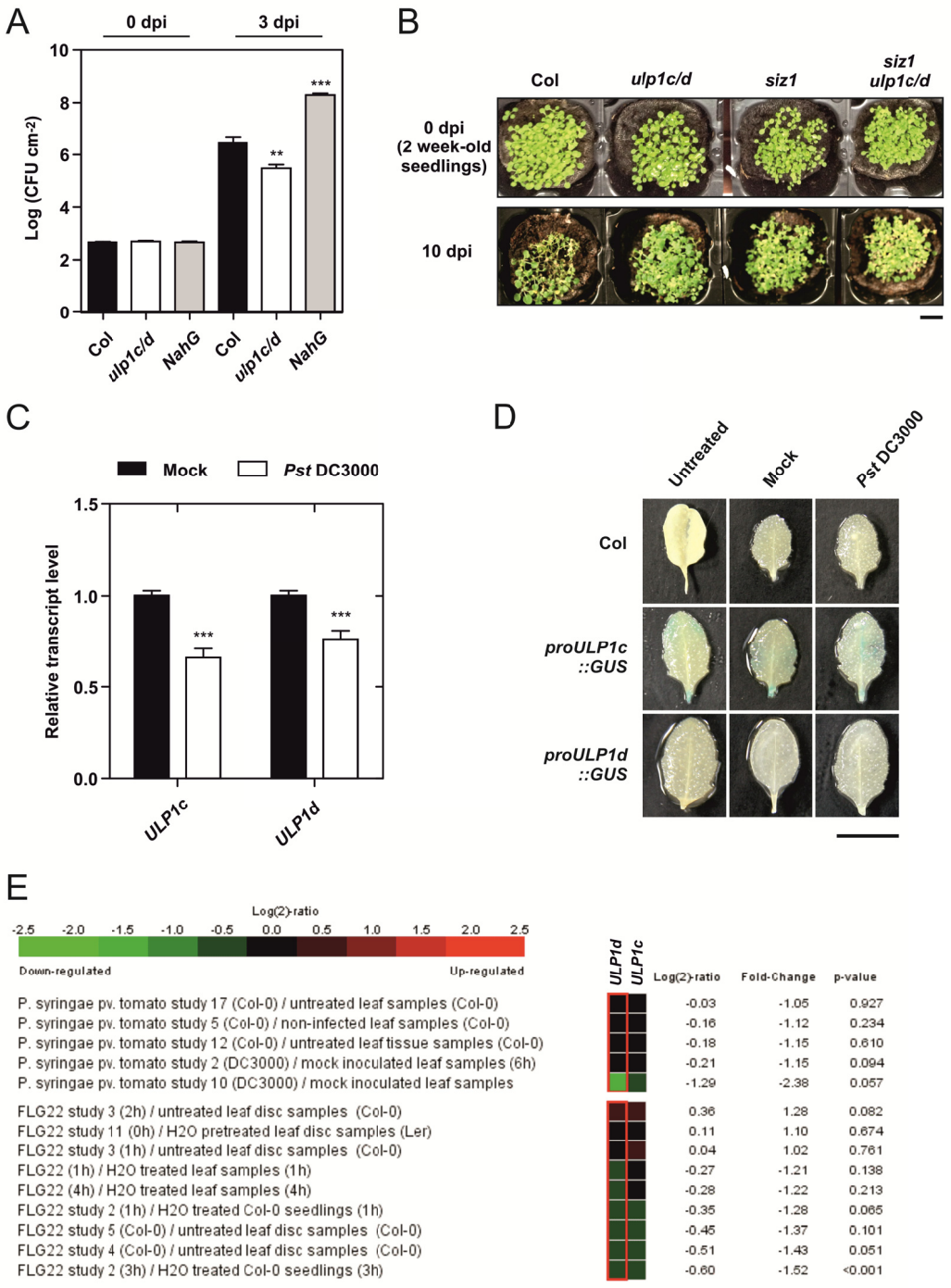

Figure 5.1. SUMO proteases ULP1c and ULP1d are involved in the response to *Pseudomonas syringae* pathovar *tomato* (*Pst*) DC3000 infection. **A**, Bacterial growth was determined in 5-week-old plants infiltrated with *Pst* DC3000. Leaves were harvested within 0 and 3 days post-inoculation (dpi). The *ulp1c ulp1d* (*ulp1c/d*) double mutant showed less bacterial growth (determined as colony forming units, CFU) than the wild-type (Col). The transgenic line *NahG*, that expresses a bacterial SA hydroxylase, was used as susceptibility control. Error bars represent standard error of the means (SEM), n = 5. Asterisks represent statistically significant differences comparatively to wild-type (unpaired t test; **, P<0.01; ***, P<0.001). **B**, Two-week-old seedlings were sprayed with *Pst* DC3000 ($5x10^7$ CFU mL^{-1}) and infection symptoms were observed within 10 dpi in *ulp1c/d*, *siz1* and *siz1 ulp1c/d* mutant backgrounds. The image depicts representative plant symptoms in an experiment with 5 replicates showing similar results; scale bar indicates 1 cm. **C**, Analysis by quantitative Real-Time PCR (qPCR) of *ULP1c* and *ULP1d* transcript level change in Col leaves, 6 hours after *Pst* DC3000 infiltration. *ACT2* (At3g18780) mRNA was used as a reference gene. Error bars represent SEM,

n = 3. Asterisks represent statistically significant differences relatively to mock treatment (unpaired t test; ***, P < 0.001). **D**, Expression pattern of *proULP1c*::*GUS* and *proULP1d*::*GUS*, 6 h after *Pst* DC3000 infiltration, by histochemical β-glucoronidase (GUS) staining. Control and mock treatments are plants untreated or infiltrated with 10 mM $MgCl_2$, respectively. **E**, In silico analysis of *ULP1c* and *ULP1d* expression when challenged with *Pst* DC3000 or the bacterial flagellin peptide flg22, carried out using Genevestigator (Hruz et al., 2008).

We subsequently checked the expression of *ULP1c* and *ULP1d* six hours after infiltration using *proULP1c::GUS* and *proULP1d::GUS* lines and quantitative Real-Time PCR (qPCR). Analysis by qPCR showed that *Pst* DC3000 infection resulted in a reduction of both *ULP1c* and *ULP1d* expression levels by 34% and 24%, respectively (Fig. 5.1C). Meanwhile *promoter::GUS* lines did not resolve changes in expression for both lines, likely due to the low basal expression both genes displayed in control conditions in this tissue (Fig. 5.1D). Results were in accordance with public microarray data of several *P. syringae* infection studies that consistently demonstrated a down-regulation of *ULP1c/d* (Fig. 5.1E). Likewise, in silico analysis showed that flg22 treatment, that is recognized by FLS2 to trigger PTI (Zipfel et al., 2004), reduces *ULP1c* and *ULP1d* expression (Fig. 5.1E).

SUMO-conjugate levels are affected by *Pst* DC3000

We subsequently addressed whether *Pst* DC3000 infection was capable of altering the plant SUMO-conjugate profile. Therefore, we infiltrated 5-week-old Arabidopsis leaves with *Pst* DC3000 ($5x10^4$ CFU mL^{-1}) and harvested samples 6 hours after inoculation. We included untreated plants and mock-treatment (infiltration with 10 mM $MgCl_2$) in the assay. A western blot with anti-NbSUMO1 antibodies allowed the monitoring of the overall changes in AtSUM1/2-specific high molecular weight SUMO-conjugates (HMWC) in wild-type and *ulp1c/d* (Fig. 5.2). In wild-type plants, HMWC were intensified in infected plants, and particularly a specific SUMO-conjugate band with approximately 70 kDa was resolved. This strongly suggests that *Pst* DC3000 infection is not only capable of changing the overall SUMO-conjugate pattern but also of modulating specific sumoylation targets. Interestingly, the increase in HMWC was not observed in *ulp1c/d*, suggesting that it is ULP1c/d-dependent. However, the infection-specific band was present even if it was less intense, suggesting that ULP1c/d controls the overall HMWC status following infection, rather than specific SUMO targets.

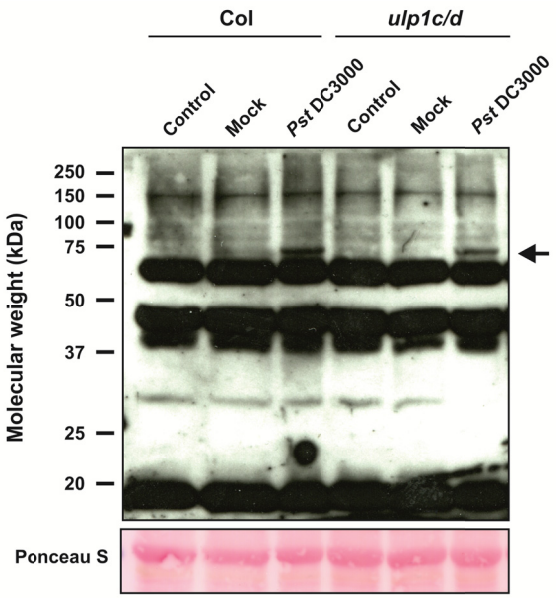

Figure 5.2. SUMO-conjugate profile 6 hours after *Pst* DC3000 inoculation. Leaves of 5-week-old plants were infiltrated with *Pst* DC3000 and with 10 mM $MgCl_2$ (mock treatment). Control refers to plants without any treatment. Each lane contains 40 µg of total protein, and SUMO levels were analyzed by western blot using anti-NbSUMO polyclonal antibody. The arrow indicates a SUMO-conjugate that specifically appears in infected plants. Ponceau S staining of the large subunit of Rubisco (55 kDa) was used as loading control.

ULP1c and ULP1d overexpression lines diminish SUMO-conjugates levels but do not display an obvious *Pst* DC3000 response phenotype

For a gain-of-function approach, we produced one *ULP1c* and two *ULP1d* overexpression (OE) lines in wild-type (Col) background (Fig. 5.3A). Phenotypically, overexpression of *ULP1c* (*ULP1c-OE1*) resulted in altered morphology with the presence of larger leaves. Overexpression of *ULP1d* (*ULP1d-OE1*), did not result in significant differences in leaf morphology (Fig. 5.3A). Using qPCR, we confirmed expression levels to be ~28 fold-change for *ULP1c* in *ULP1c-OE1* and ~35 and ~7 fold-change for *ULP1d* in *ULP1d-OE1* and *ULP1d-OE2*, respectively (Fig. 5.3B). In parallel, we analyzed the sumoylation pattern of OE lines. As depicted in Figure 5.3C, overexpression resulted in a reduction in high molecular weight SUMO-conjugates, indicative of an increased SUMO-deconjugating activity in OE lines. *ULP1c-OE1* displayed lower levels of SUMO-conjugates comparatively to *ULP1d* over-expression lines. Finally, we infiltrated OE lines with *Pst* DC3000, but no significant differences were observed in bacterial growth (Fig. 5.3D).

Microarray analysis of the *ulp1c/d* double mutant in response to *Pst* DC3000

Sumoylation is a PTM that acts rapidly in response to stress challenges, often modulating the activity of transcriptional regulators therefore conditioning the transcriptome (Castro et al., 2012). To study the molecular basis of ULP1c/ULP1d involvement in the response to *Pst* DC3000, we carried out gene expression profiling with the Affymetrix ATH1 microarray chip. The experiment was carried out in 5-week-old plants, and the design involved two genotypes (wild-type and

ulp1c/d) in three experimental conditions: untreated plants, mock plants infiltrated with 10mM $MgCl_2$, and plants infiltrated with *Pst* DC3000 at $5x10^4$ CFU mL^{-1} (Fig. 5.4A). Plants were harvested 6 hours after inoculation.

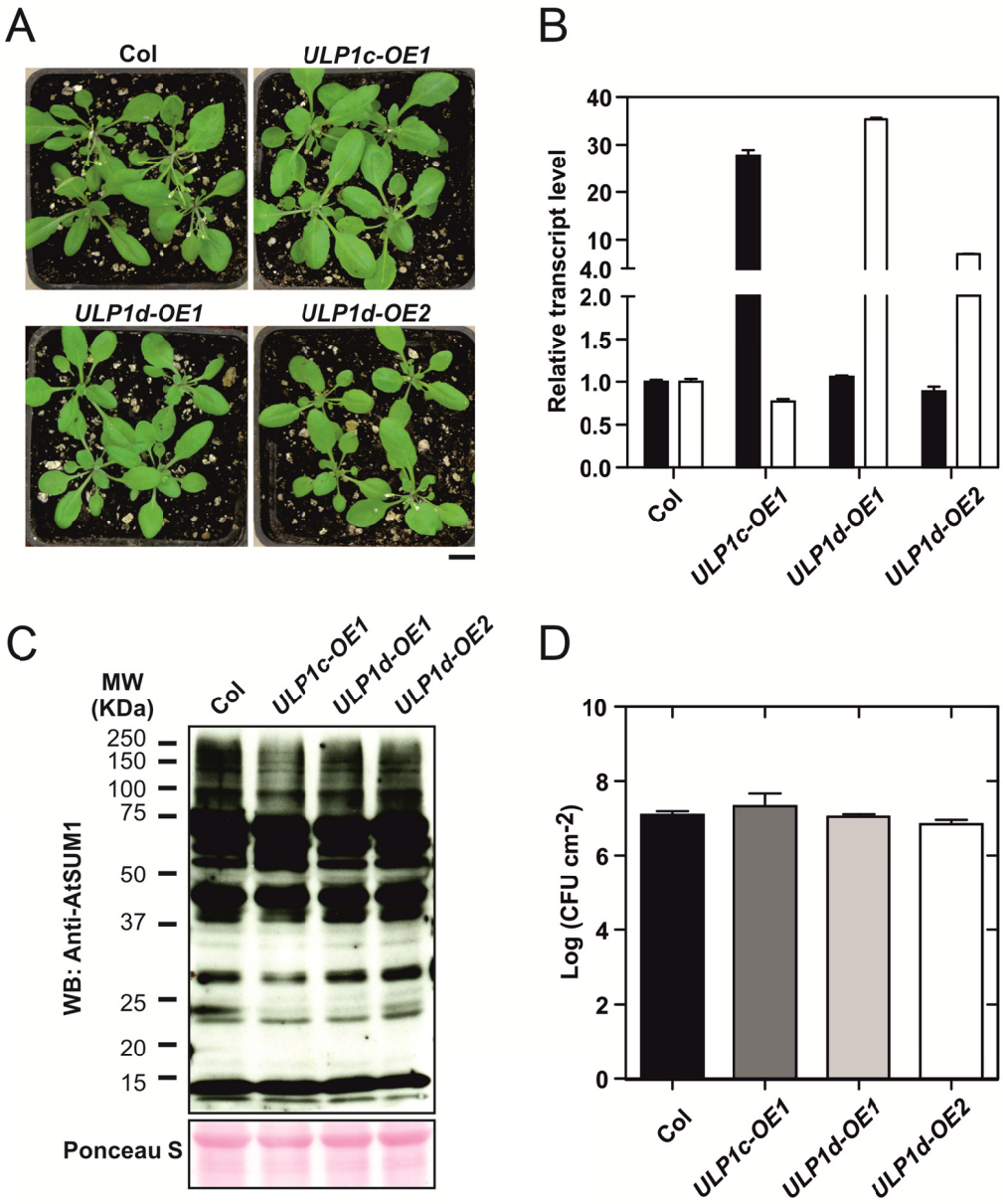

Figure 5.3. Characterization of *ULP1c* and *ULP1d* overexpression (OE) lines *ULP1c-OE1*, *ULP1d-OE1*, and *ULP1d-OE2*. **A**, Morphology of 1-month-old soil-grown plants; scale bar indicates 1 cm. **B**, Estimation of *ULP1c* (black bars) and *ULP1d* (white bars) expression levels in OE lines by qPCR. **C**, Western blot of total protein extracts (50 µg per lane) from 10-day-old seedlings using anti-AtSUM1; Ponceau S staining of the large subunit of Rubisco (55 kDa) was used as a loading control. **D**, Five-week-old plants were infiltrated with *Pst* DC3000 and bacterial growth was determined at 3 dpi. Error bars represent SEM, n = 3 (B) and n = 5 (D).

Principal component analysis (PCA) was used to translate the behavior of the experimental comparisons into a high-dimensional projection (Fig. 5.4B), with adjoining points signifying a similar expression profile throughout the whole set of genes covered by the microarray. We were able to observe that three principal components explained ~90% of the variance (Fig. 5.4B *inset*). Component 1 resolved infiltrated from non-infiltrated plants, while mock and *Pst* DC3000 plants were resolved in component 2. Finally, genotypes (Col vs *ulp1c/d*) were clearly resolved by component 3 (Fig. 5.4B). For each condition, the three hybridizations/replicas were consistently grouped, validating the quality of the experiment.

To determine differentially expressed genes (DEGs) we employed variance modeling by common variance of all genes, as described by Gagnot et al. (2008). Consequently, genes that were too variable between replicates, even if in just one experimental condition, were excluded from the analysis. We established as differentially expressed genes those with a Bonferroni *p*-value lower than 0.05. DEGs of *ulp1c/d* for each situation (control, mock and *Pst* DC3000) were established by comparison with the expression values of the corresponding wild-type (Fig. 5.4A). The *ulp1c/d* DEGs in control conditions were previously analyzed in Chapter 4, and therefore we will now focus in *ulp1c/d* DEGs that are specific of the response to *Pst* DC3000. To identify this subset of genes, we subtracted *ulp1c/d* DEGs in the control and mock treatments to *ulp1c/d* DEGs in *Pst* DC3000 treatment, as can be visualized by its Venn diagram representation (Fig. 5.4C). Analysis resulted in 52 down- and 166 up-regulated genes specifically deregulated in *ulp1c/d* in response to *Pst* DC3000 (Appendix V - Table S5.1). These were the focus of all subsequent studies. To validate the microarray, expression of several genes of interest was determined by qPCR (Fig. 5.4D). Analysis showed a consistent differential expression tendency between the microarray and qPCR data. Genes involved in biotic stress responses (*FLS2* and *TIR-NBS-LRR ULP1c/d-regulated 1* gene, *TUR1*), and the cell wall remodeling gene *XTH22* are all up-regulated in response to *Pst* DC3000 in the *ulp1c/d* background, suggesting that ULP1c/d contributes to the repression of these genes during infection. In addition, these genes are down-regulated when comparing *Pst* DC3000 elicitation with the mock treatment in the *ulp1c/d* background (Fig. 5.4E). Meanwhile, the auxin efflux transmembrane transporter *PIN7* is repressed in *ulp1c/d* in both treatments, possibly modulating auxin distribution in the plant.

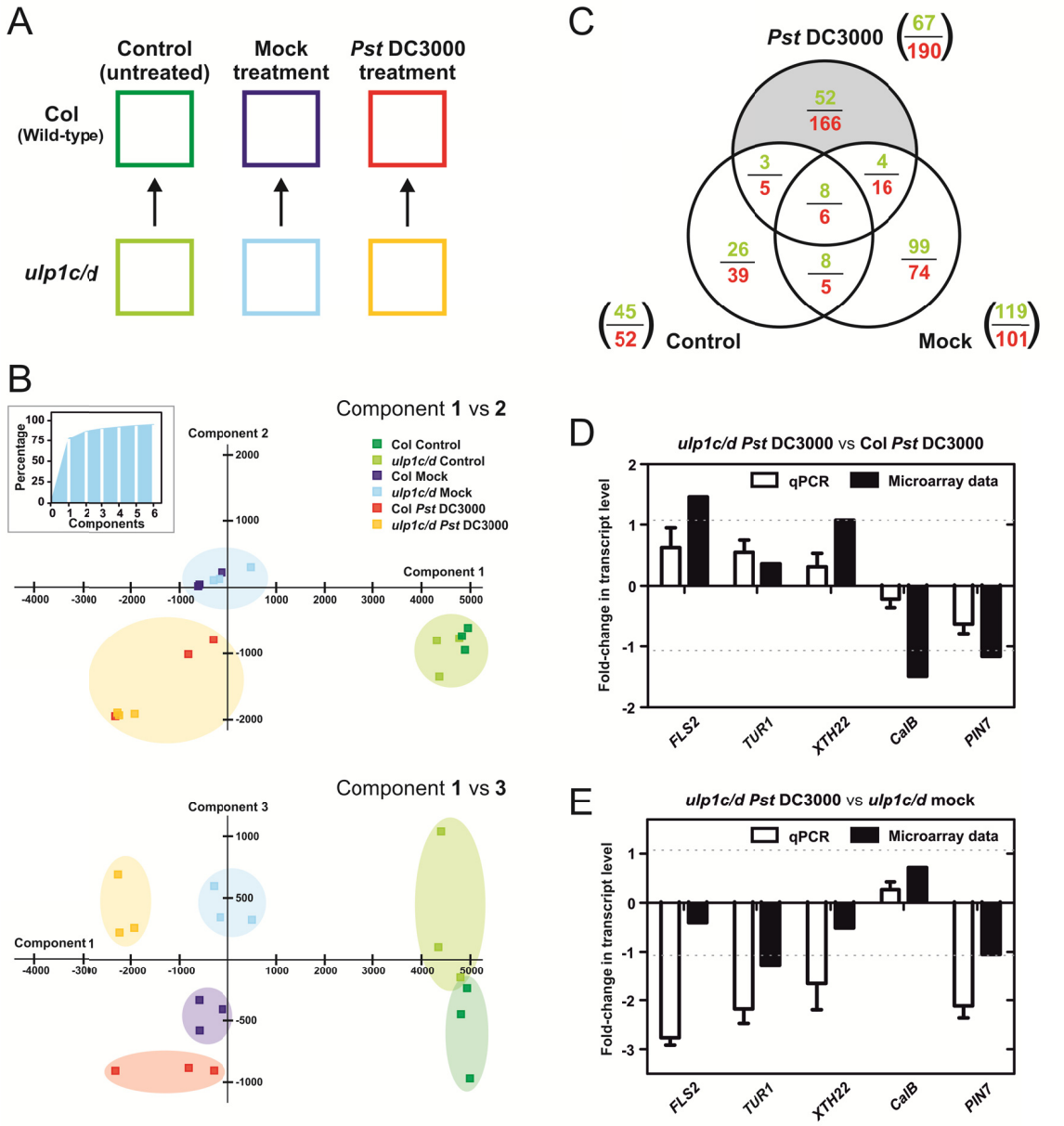

Figure 5.4. Microarray analysis of differentially expressed genes in the *ulp1c/d* double mutant relative to the wild-type (Col), in control (untreated plants), mock treated (10 mM $MgCl_2$) and *Pst* DC3000-elicitated samples. **A**, Experimental design summarizing how expression levels of differentially expressed genes (DEGs) in the *ulp1c/d* background for each condition were relativized to the wild-type. **B**, Principal component analysis (PCA) of each microarray chip (three for each condition) was conducted using the software Multi Experiment Viewer (www.tm4.org/mev/). Only genes differentially expressed in at least one comparison were considered. Graphic inset represents the accumulative percentage for the six main components of the variance analysis. **C**, Venn diagram representing the number of genes down- (green) or up-regulated (red) in *ulp1c/d* in each condition. Highlighted in grey are the genes deregulated specifically after *Pst* DC3000 elicitation in *ulp1c/d*. **D,** qPCR of representative DEGs in *Pst* DC3000-elicited *ulp1c/d* in comparison to *Pst* DC3000-elicited Col. Expression was determined for *FLS2* (At5g46330), the herein designated *TIR-NBS-LRR ULP1c/d-regulated 1* gene (*TUR1*, At5g11250), *XTH22* (At5g57560), *CalB* (At2g45670) and *PIN7* (At1g23080), using as reference gene *ACT2* (At3g18780). **E**, qPCR analysis of *FLS2*, *TUR1*, *XTH22*, *CalB* and *PIN7* in the *Pst* DC3000-elicited treatment in comparison to the mock treatment. In qPCR (D and E), error bars represent SEM; n = 3 independent biological replicates; grey lines represent the threshold for fold-change that was used to set differential expression in the microarray experiment.

Full annotation of DEGs showed that genes fall mostly onto unknown/uncharacterized processes, which suggests a strong involvement of these proteases in unresolved mechanisms of the response to pathogen attack (Appendix V - Table S5.2). Still, differentially expressed genes with relevant function in known biological processes are summarized in Table 5.1. Results show an over-representation of genes involved in auxin signaling, especially by the down-regulation of several auxin-responsive genes. Differentially expressed genes were subjected to functional annotation according to their gene ontology (GO; Appendix V - Table S5.2). Analysis of the *GO Biological Processes* category showed that down-regulated genes were mainly involved in electron transport or energy pathways and developmental processes, while up-regulated genes were involved in stress responses, transport and, once more, in developmental processes. In addition, up-regulated genes were enriched in protein metabolism-related genes (Appendix V - Table S5.3), many involving ubiquitination, which might suggest a strong correlation of ULP1c/d function to ubiquitin-mediated protein degradation. Additionally, the SUMO isoform *SUM4,* which was previously singled out as a pseudogene (Saracco et al., 2007), appeared as being down-regulated (Appendix V - Table S5.3). Analysis of the *GO Molecular Function* categorization suggests an over-representation of nucleotide-binding and transcription factor (TF) activities (Appendix V - Table S5.2 and S5.4). Also, *GO Cellular Component* analysis suggests the involvement of these proteases in the regulation of chloroplast-targeted genes, which are mostly down-regulated in the mutant (Appendix V - Table S5.2). To complement the previous analysis, the MapMan software was used to map expression levels of deregulated genes onto metabolic pathways and processes, including plant defence. Analysis of the MapMan *Metabolism overview pathway*, (Fig. 5.5A), which provides a birds-eye view of the metabolism, indicated an over-representation of genes involved in secondary metabolism and the cell wall, particularly from the *xyloglucan endotransglucosylase/hydrolase* (*XTH*) family (Table 5.1). *XTH* genes have been previously associated with sumoylation, with *XTH8* and *XTH31* being down-regulated in *siz1* due to SA-accumulation (Miura et al., 2010). Since they are enriched in *ulp1c/d* DEGs, we analyzed all annotated *XTHs* present in the ATH1 microarray chip, comparing our experimental data against publically available microarray data of hormone supplementation responses (Fig. 5.5B). Hierarchical clustering evidenced how *XTH30* and *-33* are constitutively up-regulated in the mutant. Most significantly, six *XTHs* were up-regulated after *Pst* DC3000 infection, three of which (*XTH11*, *-19* and *-22*) were singled out as differentially expressed in our microarray (Fig. 5.5B). Analysis also revealed that these *XTHs* display a similar induction pattern when exposed to brassinolide (BL) and the auxin indole acetic acid (IAA).

Table 5.1. Genes differentially expressed in *ulp1c/d* upon *Pst* DC3000 elicitation that possess a representative functional annotation.

AGI ID	Gene name	Log2	*p*-value	Description
Hormone metabolism – auxin				
At1g29430		-1,35	4,81E-5	Auxin-responsive protein
At4g38850	*SAUR15*	-1,29	2,28E-4	Small auxin up-regulated
At1g29450		-1,17	5,13E-3	Auxin-responsive protein
At1g23080	*PIN7*	-1,17	5,32E-3	Auxin efflux transmembrane transporter
At1g29510	*SAUR68*	-1,11	1,88E-2	Small auxin up-regulated
At2g45210		1,11	2,07E-2	Auxin-responsive protein
At4g29080	*IAA27, PAP2*	1,19	3,33E-3	Transcription factor involved in auxin signaling
At1g59500	*GH3.4*	1,19	2,95E-3	Indole-3-acetic acid amido synthetase
Hormone metabolism – ethylene				
At4g37770	*ACS8*	1,77	9,90E-11	1-aminocyclopropane-1-carboxylate synthase; auxin inducible
Hormone metabolism – jasmonate				
At1g76690	*OPR2*	1,17	4,61E-3	12-oxophytodienoate reductase
Signaling				
At3g18890	*TIC62*	-1,52	3,76E-7	Coenzyme binding
At2g47590	*PHR2*	-1,10	2,60E-2	DNA photolyase, blue-light receptor
At4g01090		1,14	9,46E-3	Extra-large G-protein-related
At5g67440	*NPY3, MEL2*	1,15	6,97E-3	Signal transducer, involved in auxin-mediated
At3g04110	*GLR1.1*	1,17	4,48E-3	Glutamate receptor, cation channel
At5g49480	*CP1*	1,18	4,17E-3	Calcium ion binding
At1g62480		1,20	2,31E-3	Vacuolar calcium-binding protein-related
At4g26470		1,42	6,22E-6	Calcium-binding EF hand family protein
At5g46330	*FLS2*	1,45	2,63E-6	Transmembrane receptor protein serine/threonine kinase
At3g50770	*CML41*	1,88	0,00E+0	Putative calmodulin-related protein
Response to biotic stress				
At4g04220	*RLP46*	1,07	4,26E-2	Kinase/ protein binding
At4g37460	*SRFR1*	1,14	9,36E-3	Protein complex scaffold
At1g75030	*TLP-3*	1,24	9,41E-4	PR5-like protein, thaumatin-like
At1g19320		1,47	1,84E-6	Pathogenesis-related thaumatin family protein
At5g64905	*PROPEP3*	1,52	3,37E-7	Elicitor peptide 3 precursor
At4g09420		1,62	1,62E-8	Putative disease resistance protein (TIR-NBS class)
At1g22900		1,82	1,98E-11	Disease resistance response protein
At2g43590		2,24	0,00E+0	Putative chitinase
Cell Wall				
At5g57560	*XTH22, TCH4*	1,07	4,54E-2	Xyloglucan endotransglucosylase / hydrolase
At4g09030	*AGP10*	1,17	4,78E-3	Arabinogalactan protein
At3g45970	*EXPL1, EXLA1*	1,31	1,55E-4	Expansin-like
At4g30290	*XTH19*	1,43	4,91E-6	Xyloglucan endotransglucosylase / hydrolase
At2g22470	*AGP2*	1,49	8,31E-7	Arabinogalactan protein
At4g30280	*XTH18*	1,56	1,09E-7	Xyloglucan endotransglucosylase / hydrolase
At5g51680		1,63	1,17E-8	Hydroxyproline-rich glycoprotein family protein
At3g48580	*XTH11*	2,00	0,00E+0	Xyloglucan endotransglucosylase / hydrolase

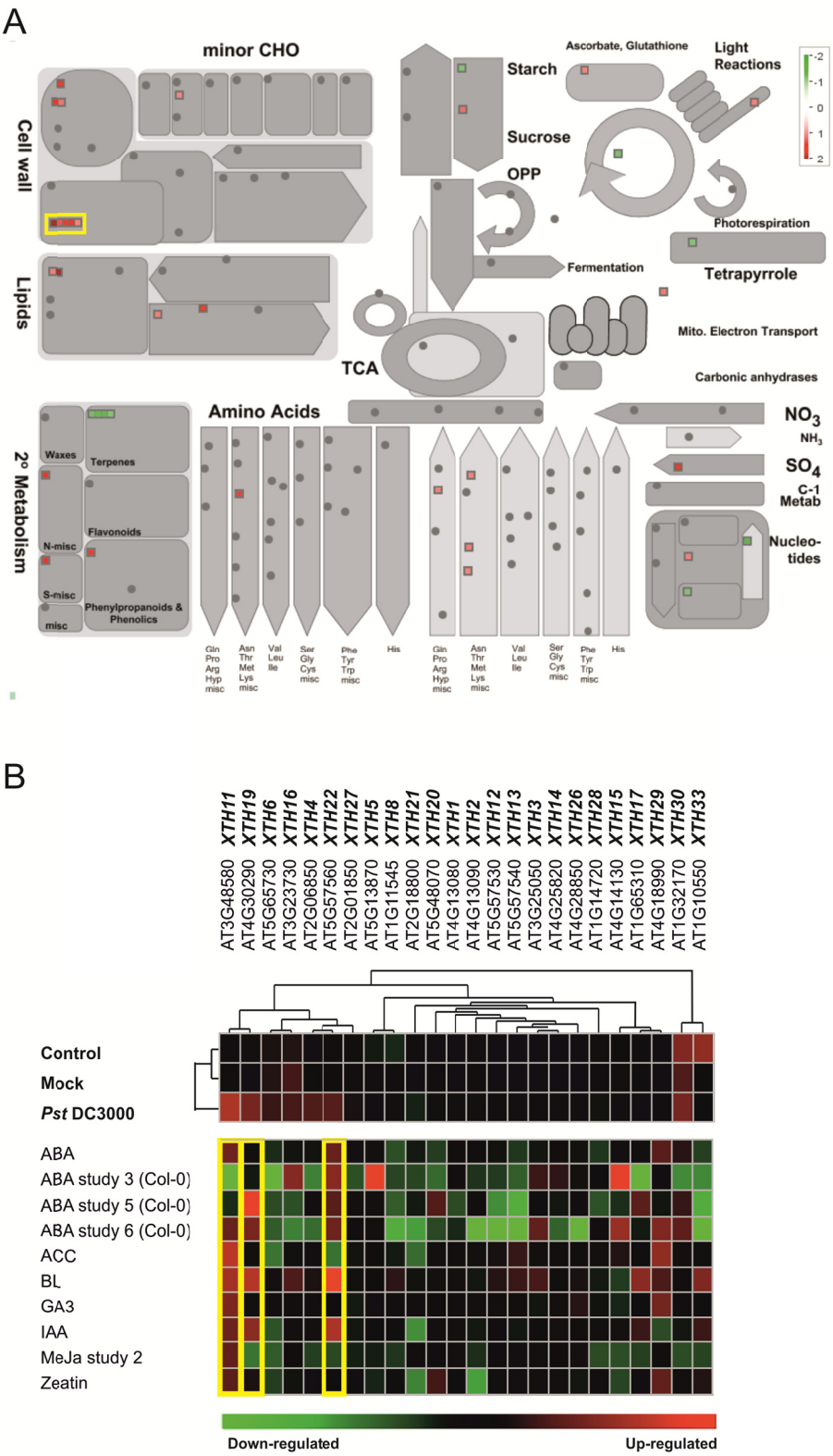

Figure 5.5. Analysis of differentially expressed genes in *ulp1c/d* in *Pst* DC3000-eliciited plants. **A**, MapMan Metabolism Overview of *ulp1c/d* after infection. Scale represents Log2 ratio. The yellow box highlights cell wall-associated genes of the *Xyloglucan endotransglucosylase/hydrolase* (*XTH*) family. **B**, *XTH* expression profile in the current microarray (*upper panel*), compared to the expression pattern following hormone supplementation (*lower panel*), retrieved from public microarray data deposited in Genevestigator (Hruz et al., 2008). The yellow boxes highlight the highest deregulated *XTHs* in *ulp1c/d* after infection. Hierarchical clustering of *XTH* expression in the current microarray was carried out in Multi Experiment Viewer (www.tm4.org/mev/).

Sumoylation is generally assumed to play a repressive effect on transcription, by modulating the activity of transcriptional regulators or intervening in chromatin remodeling components (Garcia-Dominguez and Reyes, 2009; van den Burg and Takken, 2009). We therefore highlighted transcriptional regulators that undergo differential expression in *ulp1c/d* following elicitation by *Pst* DC3000 (Appendix V - Table S5.4). We could observe that most of these transcriptional regulators were up-regulated in the mutant after infection, which suggests that ULP1c/d is involved in the repression of transcriptional regulators upon pathogen attack.

Analysis of promoter regions for *cis*-element enrichment

To search for potential transcription factors involved in gene expression regulation by ULP1c/d during infection, we analysed the promoter regions of *ulp1c/d* DEGs in response to *Pst* DC3000. For that purpose we used the bioinformatics tool Athena (O'Connor et al., 2005) that scans the promoter region of a subset of Arabidopsis genes and displays existing *cis*-element enrichments. Results indicated that only one *cis*-element is enriched in down-regulated genes, the Ibox motif (Table 5.2), involved in light-regulated genes (Borello et al., 1993). In contrast, several *cis*-elements were found in the up-regulated subset of genes. Of particular interest was the W-box element present in many promoters of up-regulated genes that is known as the binding motif of WRKY TFs. Miller et al. (2010) reported that at least 5 WRKYs are modified by SUM1 (Appendix V - Table S5.5). We also observed several motifs associated with drought and ABA-signaling are enriched in up-regulated DEGs (Table 5.2), pointing strongly to ABA-signaling acting upstream in the regulation of the response to *Pst* DC3000 mediated by ULP1c/ULP1d.

The *ulp1c/d* mutant displays altered auxin responses

Auxins are traditionally associated to the regulation of plant growth, but they were recently found to attenuate defence responses in plants (reviewed by Bari and Jones, 2009; Kazan and Manners, 2009). In our microarray analysis, the *ulp1c/d* mutant clearly showed deregulation of members of traditional auxin responsive gene classes, such as *Small Auxin Up-Regulated* genes (*SAURs*) and Aux/IAA transcription factors. Deregulation was also observed for *PIN7*, an auxin efflux transporter, and *GH3.4* an enzyme involved in auxin conjugation to amino acids (Table 5.1). Taking this into consideration, the fact that the mutant displays constitutive developmental defects (Chapter 4), and that sumoylation was previously associated to auxin patterning (Miura et al., 2011) we wanted to analyze whether the *ulp1c/d* mutant displayed deregulated auxin responses.

Table 5.2. *Cis*-elements over-represented in the promoter region of genes differentially expressed in *ulp1c/d* upon *Pst* DC3000 infection. The subsets of down- and up-regulated genes were submitted to Athena scanning analysis (O'Connor et al., 2005) for binding site enrichment.

***Cis*-element name** (conserved sequence*)	**No. of genes**	**Frequency prediction in the genome**	**Frequency observed**	***p*-value**	**Corresponding TFs**
Down-regulated					
Ibox promoter motif (GATAAG)	29	40%	56%	< 10e-3	
Up-regulated					
TATA-box motif (TATAAA)	144	82%	90%	< 10e-5	
W-box promoter motif (TTGACY)	118	67%	73%	< 10e-4	WRKY
ATMYC2 BS in RD22 (CACATG)	73	35%	45%	< 10e-4	MYC, MYB
MYCATERD1 (CATGTG)	73	35%	45%	< 10e-4	MYC, MYB
DRE core motif (RCCGAC)	51	23%	31%	< 10e-4	
GARET (TAACAAR)	99	55%	61%	< 10e-3	
ABRE-like binding site motif (BACGTGKM)	46	20%	28%	< 10e-3	
DREB1A/CBF3 (RCCGACNT)	22	7%	13%	< 10e-3	DREB1A/CBF3

* *R (A/G), M (A/C), Y (C/T), K (G/T), B (C/G/T), N (A/C/G/T)*

In the presence of exogenous auxin supplementation, in vitro-grown *ulp1c/d* displayed a hypersensitivity phenotype (Fig. 5.6A-D). In *ulp1c/d,* auxin supplementation produced an inhibition of primary root growth and induced secondary root formation (Fig. 5.6A-D). To identify whether endogenous auxin levels were constitutively affected in the mutant, we crossed *ulp1c/d* with *proDR5::GUS* transgenic plants that carry an auxin-inducible promoter driving the expression of the *GUS* reporter gene. No obvious differences were observed between *proDR5::GUS* in wild-type and in the *ulp1c/d* background, in 10-day-old seedlings or adult plants (Fig. 5.6E). Since inoculation with *Pst* DC300 may cause alterations in auxin levels in the *ulp1c/d* mutant, we infiltrated *Pst* DC3000 in *proDR5::GUS* in both wild-type and the *ulp1c/d* background. Once again, no noticeable differences were observed (Fig. 5.6F).

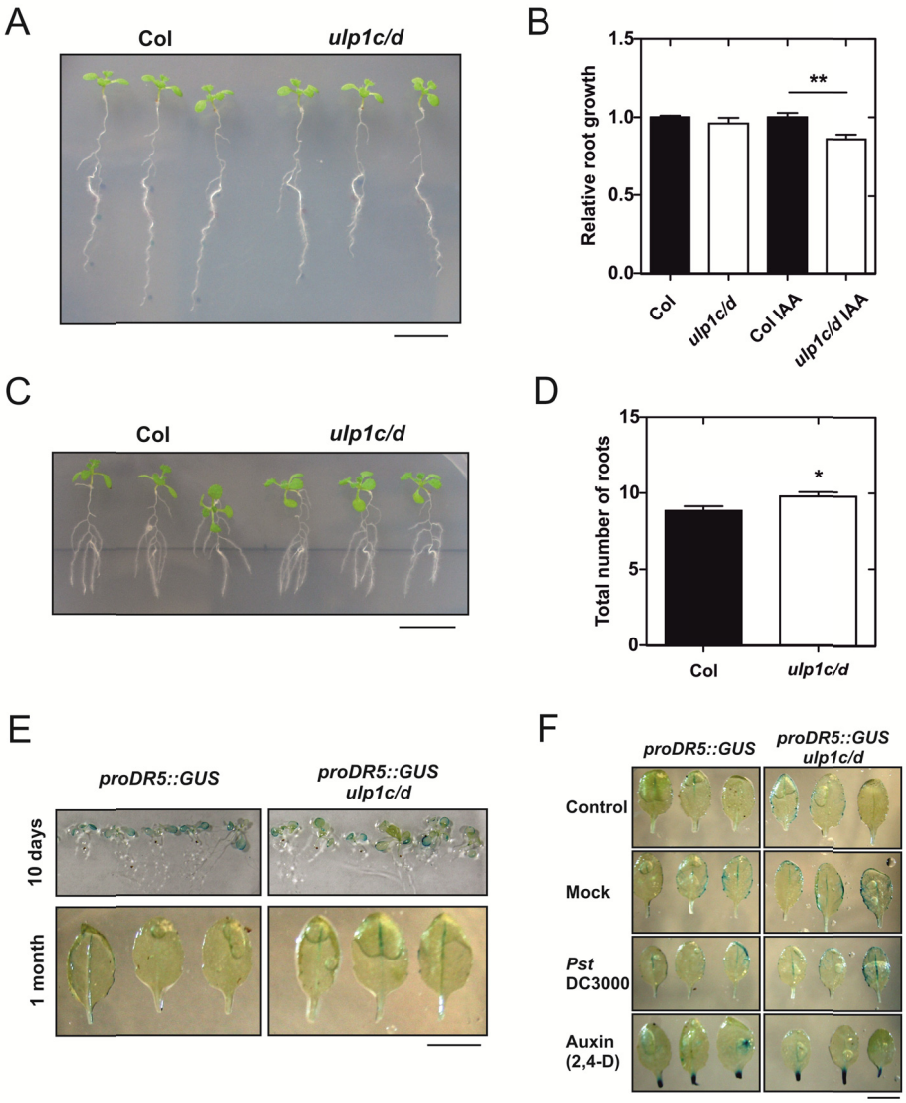

Figure 5.6. ULP1c and ULP1d modulate auxin-responses. **A,B**, Morphology (A) and quantification (B) of root primary growth, of wild-type and the *ulp1c/d* in media supplemented with 10 nM indole acetic acid (IAA). **C,D**, Morphology (C) and quantification (D) of root lateral growth, of wild-type and the *ulp1c/d* in media supplemented with 100 nM of indole acetic acid (IAA). Expression profile of *proDR5*::*GUS* in wild-type and *ulp1c/d* background by histochemical β-glucoronidase (GUS) staining under normal growth conditions (**E**) and after *Pst* DC3000 elicitation (**F**). The auxin 2,4-D treatment was used as positive control for GUS induction. Bars indicate 1 cm (A, C, E and F). Error bars represent SEM, n = 15 plants from 5 separate plates (B) and n = 18 plants from 6 separate plates (D). Asterisks represent statistically significant differences between genotypes (unpaired t test; *, $P < 0.05$; **, $P < 0.01$).

5.3. DISCUSSION

ULP1c/d are negative regulators of *Pst* DC3000 resistance

Sumoylation is an essential mechanism for both plant development and the response to rapidly imposing stress challenges (Castro et al., 2012). Therefore it is not surprising that

pathogens have developed strategies to overcome plant defences by deregulating sumoylation. More specifically, it was shown that phytopathogenic bacteria employ a type-III secretion system to inject effectors with SUMO protease activity (e.g. AvrXv4 and XopD) into the plant cell as part of their infection strategy (Hotson and Mudgett, 2004; Roden et al., 2004; Kim et al., 2008; Wimmer et al., 2012; Kim et al., 2013). It is therefore reasonable to assume that endogenous SUMO proteases may be implicated in the biotic stress response. To address this question, we studied the SUMO protease pair ULP1c and ULP1d, analyzing loss-of-function mutants in the course of challenging with the hemibiotrophic bacteria *Pst* DC3000. We were able to show that the *ulp1c/d* mutant was less susceptible to *Pst* DC3000 by two different infection methodologies (Fig. 5.1A-B). Meanwhile, overexpression lines were not significantly different from wild-type plants, even though *ULP1c-OE1* showed a tendency for susceptibility to *Pst* DC3000 that requires further validation (Fig. 5.3D). Results support the notion that SUMO protease activity leads to susceptibility to infection, since (1) bacteria display SUMO proteases as effectors, and (2) loss of ULP1c/d SUMO protease activity lead to resistance to infection by *Pst* DC3000.

It has been shown that SIZ1 is a negative regulator of SA synthesis, which controls local and systemic-acquired resistance and the expression of *PR* genes (Lee et al., 2007). The *siz1* mutant has increased resistance to the hemibiotroph *Pst* DC3000 but not to *Botrytis cinerea*, a necrotrophic pathogen (Lee et al., 2007). Similarly, a combined knockout *SUM1* and knockdown *SUM2* mutant exhibits SA accumulation, high expression of *PR1*, and increased resistance to *Pst* DC3000 (van den Burg et al., 2010). In an apparent contradiction, when mature SUM1, -2 and -3 are overexpressed, plants are also SA-accumulators and display increased resistance to *Pst* DC3000. It was suggested that high levels of unconjugated SUMOs may exert an inhibitory effect on key SUMO machinery components (van den Burg et al., 2010). Specifically, nonfunctional SUMO variants like SUM1(ΔGG) and SUM2(ΔGG) that are conjugation-deficient, have been proposed to inhibit SIZ1 function in vivo, by binding to the SIZ1 SIM motif. Therefore, overexpression of these variants impacts on SIZ1 function as a repressor of SA-mediated defence (van den Burg et al., 2010). This shows that the effect of SUMO levels on plant physiology is complex, particularly concerning *Pst* DC3000 resistance. Having both endo- and isopeptidase activities (Chosed et al., 2006; Colby et al., 2006), ULP1c/d may increase the pool of free processed SUMO available for conjugation, or modulate the deconjugation of SUMO from targets (Fig. 5.7). SUMO-conjugate profiling 6 hours after *Pst* DC3000 infiltration showed that infection triggers the accumulation of high molecular weight SUMO conjugates, while *ulp1c/d* does not

accumulate SUMO-conjugates to the extent of the wild-type. This suggests that during infection ULP1c/d function mostly as processors of SUM1/2 into maturated forms (Fig. 5.2). One can hypothesize that, similar to SUM1(ΔGG), unmatured SUMO peptides may act as nonfunctional SUMO variants that inhibit SIZ1 repression of SA defence when they accumulate in the *ulp1c/d* background, ultimately leading to increased resistance in the mutant.

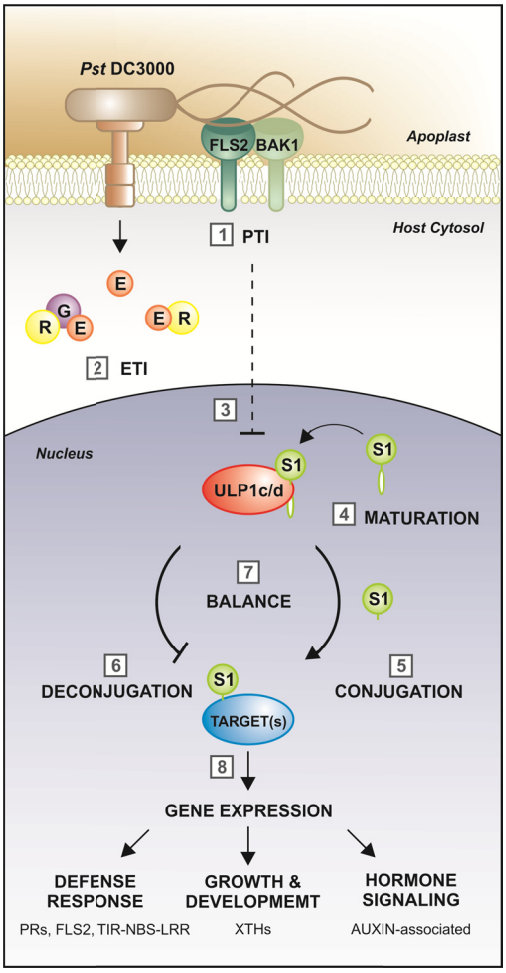

Figure 5.7. ULP1c/d role in response to Pst DC3000 infection. **(1)** At the plasma membrane bacterial flagellin is recognized by the pattern-recognition receptor FLS2 associated with BAK1, activating PAMP-triggered immunity (PTI). **(2)** At the same time the bacteria injects effectors (E) through the type III secretion system (T3SS). Effectors are recognized directly by R-proteins (R), or indirectly through a guarded effector target (G), activating effector-triggered immunity (ETI). **(3)** Defence responses, especially PTI, down-regulates *ULP1c* and *ULP1d* transcript levels. **(4)** ULP1c/d have endopeptidase activity, contributing for SUMO maturation that feeds free processed SUMOs to conjugation. **(5)** SUMO is attached to target(s) via the SUMO E1-E2-E3 cascade. **(6)** In contrast, ULP1c/d also have isopeptidase activity, removing SUMO from the target. **(7)** ULP1c/d are important for the homeostasis of the SUMO cycle, and the balance between both ULP1 activities may dictate the homeostasis of a target's SUMO-conjugated/deconjugated forms. **(8)** Ultimately, target sumoylation will exert an effect on its activity that, in turn, reprograms the plant transcriptome in response to infection. This process includes up-regulation of several *Pathogen-Related* genes (*PRs*), the receptor *FLS2* (which may contribute for *ULP1c/d* down-regulation), and R-proteins of the *TIR-NBS-LRR* class. Plant growth and development is compromised, possibly involving deregulation of several XTHs. Hormonal responses are also compromised, particularly in the case of genes involved in auxin response and signaling.

While overexpressing SUM1 and SUM2 promotes SA-accumulation, SUM3 seems to act downstream of SA synthesis, inducing *PR1* expression and infection resistance (van den Burg et al., 2010). Nevertheless, it is likely that ULP1c/d only regulates the SUM1/2 free and conjugated pools, because no endo- or isopeptidase towards SUM3 was previously observed in vitro (Chosed et al., 2006; Colby et al., 2006).

Developmentally, the triple mutant *siz1 ulp1c/d* is more severely affected than *siz1*, which may suggest independent pathways (Chapter 4). Next we wanted to find if *ULP1c/d* and *SIZ1* were

genetically epistatic in innate immunity to *Pst* DC3000. The triple mutant, as the *siz1* and *ulp1c/d*, was less susceptible to *Pst* DC3000 infection but in addition displayed chlorosis symptoms suggesting that SIZ1 and ULP1c/d may be involved in different defence pathways (Fig. 5.1B).

ULP1c/d triggers transcriptional reprogramming in response to *Pst* DC3000

Targets for sumoylation are commonly transcription regulators, such as transcription factors, chromatin-modifying components and co-repressor complexes (Castro et al., 2012; Mazur and van den Burg, 2012), and their regulation could be crucial to trigger and modulate plant defence responses. Taking this in consideration, we performed a microarray analysis of *ulp1c/d* inoculated with *Pst* DC3000 and analyzed the transcriptional signature during infection (Fig. 5.4).

The number of up-regulated genes in *ulp1c/d* was three times higher than down-regulated genes, and included several transcription factors (Appendix V - Table S5.2 and S5.4). Based on these observations, it would seem that ULP1c and ULP1d are mostly implicated in the down-regulation of the transcriptional machinery during *Pst* DC3000 infection. Up-regulated genes include several biotic stress-related genes, with special focus for the transmembranne receptor FLS2 that recognizes bacterial flg22 (Zipfel et al., 2004; Chinchilla et al., 2006), the mediator of effector-triggered immunity *Suppressor of RPS4-RLD 1* (*SRFR1*; Li et al., 2010), and two pathogen-related genes (At1g75030 and At1g19320; Table 5.1). This up-regulation, particularly of *FLS2,* suggests an increased capacity of *ulp1c/d* to recognize the pathogen and trigger PTI, which is consistent with the observed resistance of *ulp1c/d* to *Pst* DC3000. Meanwhile, SRFR1 contributes negatively for ETI (Li et al., 2010), suggesting opposing effects of ULP1c/d on PTI and ETI. Many *XTHs* are also up-regulated in *ulp1c/d*, either constitutively or especially after pathogen challenging (Fig. 5.5B). XTHs have been implicated in cell wall remodeling and xylem development (reviewed by Cosgrove, 2005). Since there are several cell wall-associated strategies for avoiding pathogen infection (Huckelhoven, 2007; Nuhse, 2012), it is expectable that XTHs play a role in pathogen response, particularly in the basal resistance characteristic of PTI. As shown by GO analysis (Appendix V - Table S5.2), many genes down-regulated in our *ulp1c/d* infected mutant are predicted to be chloroplastic and are enriched in the Ibox motif that is present in light-regulated genes. Previous studies have shown that *P. syringae* effector HopI1 affects chloroplast structure and function, inhibits SA accumulation and ultimately results in the suppression of plant defence (Jelenska et al., 2007; Jelenska et al., 2010). It is possible that the ULP1c/ULP1d pair may also be involved in chloroplast-signaling.

ULP1c/d are implicated in the auxin response

The most representative group of genes deregulated in *ulp1c/d* relates to auxin metabolism (Table 5.1). Contrarily to what might be expected, no genes are significantly deregulated in SA metabolism/signaling, as was shown to occur with other SUMO mechanisms, particularly SIZ1 and SUMO peptides (Lee et al., 2007; Jin et al., 2008; van den Burg et al., 2010). Auxins are well-known regulators of plant growth, but their role in plant defence is gaining significance. Auxin is involved in the attenuation of defence responses in plants, concomitantly, the blocking of auxin responses increases resistance to pathogens (reviewed by Kazan and Manners, 2009). A critical aspect is the regulation by TIR1 of the Aux/IAA family of transcriptional regulators, which is mediated by ubiquitin-mediated protein degradation. Infection with *Pst* DC3000 was shown to induce IAA levels in Arabidopsis and the bacterial type III effector AvrRpt2 (a cysteine protease) modulates host auxin physiology to promote pathogen virulence in Arabidopsis (Chen et al., 2007). Microarray analysis has revealed that *Pst* DC3000 induces auxin biosynthetic genes and represses genes belonging to the Aux/IAA family and auxin transporters, suggesting that it activates auxin production, alters auxin movement and de-represses auxin signaling. During development, auxins traditionally induce transcription of three groups of genes: *Aux/IAA*, *GH3* and *SAUR* family members (Woodward and Bartel, 2005). In our experiment, the *ulp1c/d* mutant displayed down-regulation of auxin responsive genes, *SAUR*, and an *Aux/IAA* (*IAA27*), and displayed up-regulation of *GH3.4* gene. GH3 are involved in the conjugation of auxins to amino acids, particularly IAA-Asp which promotes disease (Staswick et al., 2005; Gonzalez-Lamothe et al., 2012), but in the specific case of *GH3.4* (which is up-regulated in our experiment), the mutant *gh4.3* is more susceptible to infection (Gonzalez-Lamothe et al., 2012). The auxin transporter *PIN7* is also down-regulated in *ulp1c/d* during infection. Results come together to suggest an ULP1c/d-dependent regulation of the auxin response during infection. This means that the double mutant should be more resistant to *Pst* DC3000 by being incapable of inducing the auxin response which is known to be antagonistic to defence (reviewed by Kazan and Manners, 2009). In the event that *Pst* DC3000 effector proteins mimic the action of ULPs, this could explain how *Pst* DC3000 induce auxin responses to its benefit. Even though GUS expression controlled by the auxin inducible *DR5* promoter did not seem affected in *ulp1c/d* background during development or after infection, *ulp1c/d* seems to display a higher sensitivity to exogenous auxin supplementation (Fig. 5.6A-D), which is consistent with an impairment in the auxin response.

Identification of ULP1c/d potential targets

Differentially expressed genes can be used to identify transcriptional regulators whose function is being post-transcriptionally modulated by SUMO. Since co-expressed genes tend to be controlled by the same transcriptional regulators, and therefore share common *cis*-elements in their promoters, an analysis of *cis*-element enrichment can help identify potential SUMO targets. In many up-regulated genes we observed the presence of W-box motifs, the binding site for WRKY transcription factors (Table 5.2). Indeed, five WRKY transcription factors (WRKY3, 4, 6, 33, and 70) are some of the targets found to be sumoylated by SUM1 in Arabidopsis (Miller et al., 2010). All of them were previously associated to SA and defence mechanisms (Appendix V - Table S5.5). WRKYs are also capable of regulating the expression of ABA-signaling genes (Antoni et al., 2011), explaining the incidence of many drought and ABA related *cis*-elements in *ulp1c/d* DEGs. A specific SUMO-conjugate band appeared following *Pst* DC3000 challenging, with size fitting the WRKY sumoylated state, therefore WRKY sumoylation should be evaluated in future analysis. In addition, the identification of this band would be of particular interest and, we should not exclude the hypothesis of this protein being a bacterial protein.

Many other TFs should be considered as potential targets. Van den Burg and Takken (2010) suggested that Ethylene Response Factors (ERF) and transcription repressors such as HDA1 and TPR1 that contribute to chromatin remodeling may be important to modulate biotic stress responses. The R-protein RPM1 is also part of the identified SUM1-modified targets (Grant et al., 1995; Miller et al., 2010), raising the question whether sumoylation levels are being guarded by this protein.

Future perspectives

Identification of specific ULP1c/d targets will be crucial to understand the mechanism behind infection tolerance in the mutant. High-throughput strategies to search for altered SUMO-conjugate levels, such as that described by Miller et al. (2013), would help us find good candidates. Considering that other ULP SUMO proteases contribute for the SUMO cycle and may act redundantly in both the endo- and isopeptidase functions of ULPs, it is important to expand this study by creating several combinations of ULP mutants and subsequently characterizing the infection response. In addition, ULP1c/d endopeptidase activity may contribute negatively to the infection response by feeding the SUMO-conjugation pathway with processed SUMOs. One strategy

to consider would be to monitor the pathogen response while expressing processed SUMO under *proULP1c/d* control. SIZ1 is a negative regulator of innate immunity by limiting SA biosynthesis. Recently, Mutka et al. (2013) proposed that auxin levels enhance the susceptibility to *Pst* DC3000 in an SA-independent mechanism. Since ULP1c/d seems to modulate auxin-responsive genes expression and control plant development, at least partially, in a SIZ1-independent manner, future research should focus on how these two hormones condition plant development and the response to pathogen challenging via ULP1c and ULP1d.

5.4. MATERIALS & METHODS

Plant material and growth conditions

The *Arabidopsis thaliana* T-DNA insertion mutant *ulp1c/d* in the ecotype Columbia-0 (Col) background and transgenic lines *proULP1c::GUS* and *proULP1d::GUS* were previously characterized in Chapter 4. The *ulp1c/d* mutant was crossed with *siz1*-2 (SALK_065397; Miura et al., 2005) and *proDR5::GUS*, kindly provided by Miguel Botella (University of Malaga, Spain), to obtain the respective triple mutants. Homozygous insertion mutants were genotyped based on SIGnAL T-DNA Primer Design (signal.salk.edu/tdnaprimers.2.html), using the primers in Table S5.6 (Appendix V). Homozygous lines for *proDR5::GUS ulp1c/d* were determined by GUS staining using several F3 seedlings. The transgenic line *NahG*, that expresses a bacterial SA hydroxylase, was used as a control for susceptibility.

Synchronized seeds were stratified for 3 days at 4°C in the dark. Seeds were surface sterilized as described in Chapter 4. Seeds were sown onto 1.2% agar-solidified MS medium (Murashige and Skoog, 1962) containing 1.5% sucrose, 0.5 g L^{-1} MES, pH 5.7, and grown vertically in culture rooms with a 16 h light/8 h dark cycle under cool white light (80 µE m^{-2} s^{-1} light intensity) at 23°C. To measure root growth and secondary root formation, seedlings were grown in vitro for six days, and subsequently transferred to 0.5x MS 1.2% agar plates with or without the indicated indole acetic acid (IAA) supplementation. Vertical root growth was measured every two days for up to eight days.

For standard growth, 7-day-old in vitro-grown seedlings were transferred to a soil to vermiculite (4:1) mixture, and maintained under identical growth conditions, with regular watering. For the infection assay, seeds were poured in soil and stratified for 3 days. Seedlings with 2.5

weeks were transferred to sets of individual pots and grown in short days (8h light /16h dark) at 21-22°C.

Bacterial inoculations

Two different inoculation methods, infiltration and spraying, were used to assess reactivity of plants to *Pst* DC3000 infection. Plants were grown in short days (8 h light/16 h dark) cycle conditions in a controlled-environment growth chamber. For the bacteria infiltration assay, 5-week-old plant leaves were infiltrated, using a blunt syringe, with a *Pst* DC3000 cell suspension ($5x10^4$ CFU mL^{-1}) in 10 mM $MgCl_2$. The mock treatment was carried out with 10 mM $MgCl_2$ infiltration, and control plants were untreated. The treatments were done in the morning and samples were taken 6 hours post infiltration for GUS staining, qPCR, microarray, and western blot analysis. To evaluate bacterial growth at 3 days post-infection, three leaf discs with 10 mm diameters each were homogenized with a pestle in 1 mL of 10 mM $MgCl_2$. The bacterial solution was plated in serial dilutions onto LB medium supplemented with 2 mg mL^{-1} cycloheximide. CFU were counted to determine bacterial growth. For spraying inoculation, 2-week-old seedlings growing in *Jiffy-7* pots (Jiffy Products) were sprayed with a bacteria suspension $5x10^7$ CFU mL^{-1} in 10 mM $MgCl_2$ containing 0.02% Silwet as a surfactant (Macho et al., 2010). Plant infection symptoms were evaluated at various time points.

Plasmid construction and plant transformation

Plasmids were constructed using standard DNA cloning techniques, and confirmed by DNA sequencing. To produce ULP1c and ULP1d overexpression lines, the *ULP1c* and *ULP1d* open reading frames were amplified from cDNA by PCR with incorporated restriction sites (*Eco*RI and *Cla*I). The amplification product was sub-cloned into the pGEM-T Easy vector (Promega) and subsequently cloned into the pHANNIBAL vector (Wesley et al., 2001) to create *pro35S::ULP1c-NOS* and *pro35S::ULP1d-NOS* terminator fusions. The constructs were excised using *Not*I and cloned into the plant expression vector pGREEN II 0229 (www.pgreen.ac.uk/). *Agrobacterium tumefaciens* strain EHA105 was used for plant transformation by the floral dip method (Clough and Bent, 1998), and homozygous transformants were selected by resistance to Kanamycin.

GUS staining

GUS histochemical staining was perfomed as described by Posé et al. (2009). The assay included transgenic plants *proULP1c::GUS* and *proULP1d::GUS* (Chapter 4) and *proDR5::GUS* (Miguel Botella, University of Malaga, Spain) both in wild-type and *ulp1c/d* background. After infiltration treatments (untretaed, mock, *Pst* DC3000, or auxin), plant leaves were vaccum infiltrated with a GUS staining solution, containing 100 mM sodium-phosphate buffer (pH 7.0), 20% (v/v) methanol, 0.5 mM potassium ferrocyanide, 0.5 mM potassium ferricyanide and 0.3% (v/v) Triton X-100. Leaves were incubated at 37°C overnight in the dark. In the following day, pigmentation was washed using ethanol, and blue tainted leaves were photographed. As a positive control for GUS induction in *proDR5::GUS* plants, leaves were infiltrated with 100 nM auxin 2,4-D in 10 mM $MgCl_2$.

RNA isolation and quantitative Real-Time PCR

Genome-wide transcription studies were performed using the ATH1 Affymetrix microarray chip, at an external service provider (Unité de Recherche en Génomique Végétale, Université d'Evry Val d'Essonne, France). Significance of differential expression was validated by a Bonferroni test with a *p*-value threshold of <0.05. RNA extraction and cDNA synthesis were performed as described in Chapter 4. The qPCR analyses are also described in Chapter 4 and the primers used are listed in Table S5.7 (Appendix V). *ACT2* (At3g18780) was used as a reference gene (Lozano-Duran et al., 2011). Three replicas were used per condition.

Plant total protein extraction and western blotting

Protein extraction, quantification, and immunoblotting were previously described in Chapter 4. The primary antibody anti-AtSUMO1 (ABCAM) or anti-NbSUMO were added in a 1:2000 and 1:500 dilution, respectively, and incubated for 3 h. The membrane was washed three times with 10 mL of PBST for 10 min, and incubated with the secondary antibody (anti-rabbit IgG-HRP, *Sigma*; 1:10,000 in blocking solution) for 1 h.

5.5. REFERENCES

Antoni R, Rodriguez L, Gonzalez-Guzman M, Pizzio GA, Rodriguez PL (2011) News on ABA transport, protein degradation, and ABFs/WRKYs in ABA signaling. Curr Opin Plant Biol **14:** 547-553

Bari R, Jones JD (2009) Role of plant hormones in plant defence responses. Plant Mol Biol **69:** 473-488

Block A, Alfano JR (2011) Plant targets for *Pseudomonas syringae* type III effectors: virulence targets or guarded decoys? Curr Opin Microbiol **14:** 39-46

Borello U, Ceccarelli E, Giuliano G (1993) Constitutive, light-responsive and circadian clock-responsive factors compete for the different I box elements in plant light-regulated promoters. Plant J **4:** 611-619

Budhiraja R, Hermkes R, Muller S, Schmidt J, Colby T, Panigrahi K, Coupland G, Bachmair A (2009) Substrates related to chromatin and to RNA-dependent processes are modified by Arabidopsis SUMO isoforms that differ in a conserved residue with influence on desumoylation. Plant Physiol **149:** 1529-1540

Castillo AG, Kong LJ, Hanley-Bowdoin L, Bejarano ER (2004) Interaction between a geminivirus replication protein and the plant sumoylation system. J Virol **78:** 2758-2769

Castro PH, Tavares RM, Bejarano ER, Azevedo H (2012) SUMO, a heavyweight player in plant abiotic stress responses. Cell Mol Life Sci **69:** 3269-3283

Chen Z, Agnew JL, Cohen JD, He P, Shan L, Sheen J, Kunkel BN (2007) *Pseudomonas syringae* type III effector AvrRpt2 alters *Arabidopsis thaliana* auxin physiology. Proc Natl Acad Sci U S A **104:** 20131-20136

Chinchilla D, Bauer Z, Regenass M, Boller T, Felix G (2006) The Arabidopsis receptor kinase FLS2 binds flg22 and determines the specificity of flagellin perception. Plant Cell **18:** 465-476

Chosed R, Mukherjee S, Lois LM, Orth K (2006) Evolution of a signalling system that incorporates both redundancy and diversity: Arabidopsis SUMOylation. Biochem J **398:** 521-529

Clough SJ, Bent AF (1998) Floral dip: a simplified method for Agrobacterium-mediated transformation of *Arabidopsis thaliana*. Plant J **16:** 735-743

Colby T, Matthai A, Boeckelmann A, Stuible HP (2006) SUMO-conjugating and SUMO-deconjugating enzymes from Arabidopsis. Plant Physiol **142:** 318-332

Conti L, Price G, O'Donnell E, Schwessinger B, Dominy P, Sadanandom A (2008) Small ubiquitin-like modifier proteases OVERLY TOLERANT TO SALT1 and -2 regulate salt stress responses in Arabidopsis. Plant Cell **20:** 2894-2908

Cosgrove DJ (2005) Growth of the plant cell wall. Nat Rev Mol Cell Biol **6:** 850-861

Cunnac S, Lindeberg M, Collmer A (2009) *Pseudomonas syringae* type III secretion system effectors: repertoires in search of functions. Curr Opin Microbiol **12:** 53-60

Elrouby N, Coupland G (2010) Proteome-wide screens for small ubiquitin-like modifier (SUMO) substrates identify Arabidopsis proteins implicated in diverse biological processes. Proc Natl Acad Sci U S A **107:** 17415-17420

Fu ZQ, Dong X (2013) Systemic acquired resistance: turning local infection into global defense. Annu Rev Plant Biol **64:** 839-863

Gagnot S, Tamby JP, Martin-Magniette ML, Bitton F, Taconnat L, Balzergue S, Aubourg S, Renou JP, Lecharny A, Brunaud V (2008) CATdb: a public access to Arabidopsis transcriptome data from the URGV-CATMA platform. Nucleic Acids Res **36:** D986-990

Garcia-Dominguez M, Reyes JC (2009) SUMO association with repressor complexes, emerging routes for transcriptional control. Biochim Biophys Acta **1789:** 451-459

Gareau JR, Lima CD (2010) The SUMO pathway: emerging mechanisms that shape specificity, conjugation and recognition. Nat Rev Mol Cell Biol **11:** 861-871

Geoffroy MC, Hay RT (2009) An additional role for SUMO in ubiquitin-mediated proteolysis. Nat Rev Mol Cell Biol **10:** 564-568

Gonzalez-Lamothe R, El Oirdi M, Brisson N, Bouarab K (2012) The conjugated auxin indole-3-acetic acid-aspartic acid promotes plant disease development. Plant Cell **24:** 762-777

Grant MR, Godiard L, Straube E, Ashfield T, Lewald J, Sattler A, Innes RW, Dangl JL (1995) Structure of the Arabidopsis RPM1 gene enabling dual specificity disease resistance. Science **269:** 843-846

Hay RT (2005) SUMO: a history of modification. Mol Cell **18:** 1-12

Hermkes R, Fu YF, Nurrenberg K, Budhiraja R, Schmelzer E, Elrouby N, Dohmen RJ, Bachmair A, Coupland G (2011) Distinct roles for Arabidopsis SUMO protease ESD4 and its closest homolog ELS1. Planta **233:** 63-73

Hotson A, Mudgett MB (2004) Cysteine proteases in phytopathogenic bacteria: identification of plant targets and activation of innate immunity. Curr Opin Plant Biol **7:** 384-390

Hruz T, Laule O, Szabo G, Wessendorp F, Bleuler S, Oertle L, Widmayer P, Gruissem W, Zimmermann P (2008) Genevestigator v3: a reference expression database for the meta-analysis of transcriptomes. Adv Bioinformatics **2008:** 420747

Huckelhoven R (2007) Cell wall-associated mechanisms of disease resistance and susceptibility. Annu Rev Phytopathol **45:** 101-127

Jelenska J, van Hal JA, Greenberg JT (2010) *Pseudomonas syringae* hijacks plant stress chaperone machinery for virulence. Proc Natl Acad Sci U S A **107:** 13177-13182

Jelenska J, Yao N, Vinatzer BA, Wright CM, Brodsky JL, Greenberg JT (2007) A J domain virulence effector of *Pseudomonas syringae* remodels host chloroplasts and suppresses defenses. Curr Biol **17:** 499-508

Jin JB, Jin YH, Lee J, Miura K, Yoo CY, Kim WY, Van Oosten M, Hyun Y, Somers DE, Lee I, Yun DJ, Bressan RA, Hasegawa PM (2008) The SUMO E3 ligase, AtSIZ1, regulates flowering by controlling a salicylic acid-mediated floral promotion pathway and through affects on *FLC* chromatin structure. Plant J **53:** 530-540

Jones JD, Dangl JL (2006) The plant immune system. Nature **444:** 323-329

Kazan K, Manners JM (2009) Linking development to defense: auxin in plant-pathogen interactions. Trends Plant Sci **14:** 373-382

Kim JG, Stork W, Mudgett MB (2013) *Xanthomonas* type III effector XopD desumoylates tomato transcription factor SlERF4 to suppress ethylene responses and promote pathogen growth. Cell Host Microbe **13:** 143-154

Kim JG, Taylor KW, Hotson A, Keegan M, Schmelz EA, Mudgett MB (2008) XopD SUMO protease affects host transcription, promotes pathogen growth, and delays symptom development in *Xanthomonas*-infected tomato leaves. Plant Cell **20:** 1915-1929

Lee J, Nam J, Park HC, Na G, Miura K, Jin JB, Yoo CY, Baek D, Kim DH, Jeong JC, Kim D, Lee SY, Salt DE, Mengiste T, Gong Q, Ma S, Bohnert HJ, Kwak SS, Bressan RA, Hasegawa PM, Yun DJ (2007) Salicylic acid-mediated innate immunity in Arabidopsis is regulated by SIZ1 SUMO E3 ligase. Plant J **49:** 79-90

Li Y, Li S, Bi D, Cheng YT, Li X, Zhang Y (2010) SRFR1 negatively regulates plant NB-LRR resistance protein accumulation to prevent autoimmunity. PLoS Pathog **6:** e1001111

Lois LM (2010) Diversity of the SUMOylation machinery in plants. Biochem Soc Trans **38:** 60-64

Lozano-Duran R, Rosas-Diaz T, Gusmaroli G, Luna AP, Taconnat L, Deng XW, Bejarano ER (2011) Geminiviruses subvert ubiquitination by altering CSN-mediated derubylation of SCF E3 ligase complexes and inhibit jasmonate signaling in *Arabidopsis thaliana*. Plant Cell **23:** 1014-1032

Macho AP, Guevara CM, Tornero P, Ruiz-Albert J, Beuzon CR (2010) The *Pseudomonas syringae* effector protein HopZ1a suppresses effector-triggered immunity. New Phytol **187:** 1018-1033

Mazur MJ, van den Burg HA (2012) Global SUMO proteome responses guide gene regulation, mRNA biogenesis, and plant stress responses. Front Plant Sci **3:** 215

Miller MJ, Barrett-Wilt GA, Hua Z, Vierstra RD (2010) Proteomic analyses identify a diverse array of nuclear processes affected by small ubiquitin-like modifier conjugation in Arabidopsis. Proc Natl Acad Sci U S A **107:** 16512-16517

Miller MJ, Scalf M, Rytz TC, Hubler SL, Smith LM, Vierstra RD (2013) Quantitative proteomics reveals factors regulating RNA biology as dynamic targets of stress-induced SUMOylation in Arabidopsis. Mol Cell Proteomics **12:** 449-463

Miura K, Hasegawa PM (2010) Sumoylation and other ubiquitin-like post-translational modifications in plants. Trends Cell Biol **20:** 223-232

Miura K, Lee J, Gong Q, Ma S, Jin JB, Yoo CY, Miura T, Sato A, Bohnert HJ, Hasegawa PM (2011) SIZ1 regulation of phosphate starvation-induced root architecture remodeling involves the control of auxin accumulation. Plant Physiol **155:** 1000-1012

Miura K, Lee J, Miura T, Hasegawa PM (2010) SIZ1 controls cell growth and plant development in Arabidopsis through salicylic acid. Plant Cell Physiol **51:** 103-113

Miura K, Rus A, Sharkhuu A, Yokoi S, Karthikeyan AS, Raghothama KG, Baek D, Koo YD, Jin JB, Bressan RA, Yun DJ, Hasegawa PM (2005) The Arabidopsis SUMO E3 ligase SIZ1 controls phosphate deficiency responses. Proc Natl Acad Sci U S A **102:** 7760-7765

Monaghan J, Zipfel C (2012) Plant pattern recognition receptor complexes at the plasma membrane. Curr Opin Plant Biol **15:** 349-357

Murashige T, Skoog F (1962) A revised medium for rapid growth and bio assays with tobacco tissue cultures. Physiol Plant **15:** 473-475

Murtas G, Reeves PH, Fu YF, Bancroft I, Dean C, Coupland G (2003) A nuclear protease required for flowering-time regulation in Arabidopsis reduces the abundance of SMALL UBIQUITIN-RELATED MODIFIER conjugates. Plant Cell **15:** 2308-2319

Mutka AM, Fawley S, Tsao T, Kunkel BN (2013) Auxin promotes susceptibility to Pseudomonas syringae via a mechanism independent of suppression of salicylic acid-mediated defenses. Plant J **74:** 746-754

Novatchkova M, Tomanov K, Hofmann K, Stuible HP, Bachmair A (2012) Update on sumoylation: defining core components of the plant SUMO conjugation system by phylogenetic comparison. New Phytol **195:** 23-31

Nuhse TS (2012) Cell wall integrity signaling and innate immunity in plants. Front Plant Sci **3:** 280

O'Connor TR, Dyreson C, Wyrick JJ (2005) Athena: a resource for rapid visualization and systematic analysis of Arabidopsis promoter sequences. Bioinformatics **21:** 4411-4413

Pieterse CM, Van der Does D, Zamioudis C, Leon-Reyes A, Van Wees SC (2012) Hormonal modulation of plant immunity. Annu Rev Cell Dev Biol **28:** 489-521

Posé D, Castanedo I, Borsani O, Nieto B, Rosado A, Taconnat L, Ferrer A, Dolan L, Valpuesta V, Botella MA (2009) Identification of the Arabidopsis *dry2/sqe1-5* mutant reveals a central role for sterols in drought tolerance and regulation of reactive oxygen species. Plant J **59:** 63-76

Roden J, Eardley L, Hotson A, Cao Y, Mudgett MB (2004) Characterization of the *Xanthomonas* AvrXv4 effector, a SUMO protease translocated into plant cells. Mol Plant Microbe Interact **17:** 633-643

Sanchez-Duran MA, Dallas MB, Ascencio-Ibanez JT, Reyes MI, Arroyo-Mateos M, Ruiz-Albert J, Hanley-Bowdoin L, Bejarano ER (2011) Interaction between geminivirus replication protein and the SUMO-conjugating enzyme is required for viral infection. J Virol **85:** 9789-9800

Saracco SA, Miller MJ, Kurepa J, Vierstra RD (2007) Genetic analysis of SUMOylation in Arabidopsis: conjugation of SUMO1 and SUMO2 to nuclear proteins is essential. Plant Physiol **145:** 119-134

Spoel SH, Dong X (2012) How do plants achieve immunity? Defence without specialized immune cells. Nat Rev Immunol **12:** 89-100

Staswick PE, Serban B, Rowe M, Tiryaki I, Maldonado MT, Maldonado MC, Suza W (2005) Characterization of an Arabidopsis enzyme family that conjugates amino acids to indole-3-acetic acid. Plant Cell **17:** 616-627

van den Burg HA, Kini RK, Schuurink RC, Takken FL (2010) Arabidopsis small ubiquitin-like modifier paralogs have distinct functions in development and defense. Plant Cell **22:** 1998-2016

van den Burg HA, Takken FL (2009) Does chromatin remodeling mark systemic acquired resistance? Trends Plant Sci **14:** 286-294

van den Burg HA, Takken FL (2010) SUMO-, MAPK-, and resistance protein-signaling converge at transcription complexes that regulate plant innate immunity. Plant Signal Behav **5:** 1597-1601

Wesley SV, Helliwell CA, Smith NA, Wang MB, Rouse DT, Liu Q, Gooding PS, Singh SP, Abbott D, Stoutjesdijk PA, Robinson SP, Gleave AP, Green AG, Waterhouse PM (2001) Construct design for efficient, effective and high-throughput gene silencing in plants. Plant J **27:** 581-590

Wilkinson KA, Henley JM (2010) Mechanisms, regulation and consequences of protein SUMOylation. Biochem J **428:** 133-145

Wimmer P, Schreiner S, Dobner T (2012) Human pathogens and the host cell SUMOylation system. J Virol **86:** 642-654

Woodward AW, Bartel B (2005) Auxin: regulation, action, and interaction. Ann Bot **95:** 707-735

Zipfel C, Robatzek S, Navarro L, Oakeley EJ, Jones JD, Felix G, Boller T (2004) Bacterial disease resistance in Arabidopsis through flagellin perception. Nature **428:** 764-767

Chapter 6

Arabidopsis thaliana ULP2a and ULP2b are SUMO proteases involved in plant development

CONTENTS

6.1. INTRODUCTION

Post-translational modifications (PTMs) are able to rapidly and reversibly reprogram protein activity and are involved in development and the response to environmental challenges. Among the many types of PTMs, one of the most documented mechanisms is the attachment to target proteins of small peptides structurally similar to ubiquitin (Ubiquitin-Like peptides, UBLs; Miura and Hasegawa, 2010; Vierstra, 2012). Small Ubiquitin-like Modifier (SUMO) is an UBL family member that is mainly involved in nuclear-associated functions such as the regulation of transcription, chromatin-remodeling, mRNA biogenesis, nuclear-cytoplasm trafficking and DNA repair (Gareau and Lima, 2010; Mazur and van den Burg, 2012). Briefly, sumoylation, or SUMO attachment, is possible by an enzymatic cascade that sequentially involves peptide maturation by specific SUMO endopeptidases, SUMO E1 activation, E2 conjugation and E3 ligation, which drive the transfer of the modifying peptide to a specific lysine residue, normally within the consensus ψKXE (ϕ , large hydrophobic residue; K, lysine; X, any amino acid; E, glutamic acid; Gareau and Lima, 2010). The attachment can be reverted by specific SUMO isopeptidases, counteracting sumoylation and contributing also for the recycling of the SUMO peptide (Hickey et al., 2012).

SUMO conjugation can exert different effects on a target protein: (1) changes in conformation, (2) aid in protein-protein interactions (PPIs) via SUMO interacting motifs (SIMs), and (3) blocking of PPIs by for instance by competing with other PTMs (Wilkinson and Henley, 2010). The biological consequences of protein sumoylation are manifold, depending on the modified target protein and various other factors, not the least of which resides on SUMO itself. Target proteins can suffer modification by one SUMO peptide (mono-sumoylation), yet can also form polymeric chains (poly-sumoylation) or even have multiple sumoylated sites (multi-sumoylation; Hickey et al., 2012). Moreover, many organisms possess several SUMO isoforms, creating the possibility for mixed chains. Recent publications revealed that SUMO chains can serve as anchors for SUMO-targeted ubiquitin E3 ligases (STUbLs), therefore acting as facilitators of ubiquitination, consequently contributing to protein degradation (Geoffroy and Hay, 2009). This contrasts with another role traditionally associated to SUMO: the competition with ubiquitin for the same lysine residues (Hay, 2005).

Specificity of sumoylation might be determined by the large number of SUMO proteases, rather than being determined by the conjugation machinery, which is traditionally encoded by a limited number of genes. SUMO-specific proteases generically belong to the C48 family of Cys proteases (van der Hoorn, 2008), annotated as Ubiquitin-Like protein-specific Proteases or

Sentrin/SUMO-specific Proteases (ULPs/SENPs). These have been described as modulators of sumoylation through their action on SUMO moieties, namely by (1) processing pre-SUMO (maturation), (2) removing SUMO from modified target proteins (SUMO deconjugation) or (3) editing SUMO chains. ULP/SENP cysteine proteases are a heterogeneous family, which contributes to the specificity and complexity of the SUMO machinery (Hickey et al., 2012).

In plants, sumoylation seems to be essential for embryonic development, organ growth, flowering transition and hormone regulation (Saracco et al., 2007; Jin et al., 2008; Miura et al., 2009; Miura et al., 2010; van den Burg et al., 2010). In addition, SUMO plays a role in stress-associated responses to stimuli such as extreme temperatures, drought, salinity and nutrient assimilation (Castro et al., 2012). During such stresses, the profile of SUMO-modified proteins changes dramatically, greatly increasing SUMO-conjugate levels and decreasing the pool of free SUMO (Miller et al., 2013). After stress imposition, SUMO-conjugates slowly diminish by the action of ULPs. Unfortunately, little is known about the role of ULPs in plant physiology. The *Arabidopsis thaliana* genome includes eight predicted ULPs, and four of them have been shown to function as SUMO proteases in vitro (Chosed et al., 2006; Colby et al., 2006; Novatchkova et al., 2012). Each of these ULPs is likely to individually contribute to specific functions within the plant, judging from the functional characterization available to date. For instance, ESD4 loss-of-function results in a pleiotropic phenotype (severe dwarfism), while the closely related ULP1a/ELS1 does not have such a severe phenotype (Murtas et al., 2003; Hermkes et al., 2011). Additionally, ULP1c and ULP1d act redundantly in flowering transition and plant growth, as well as in salt and drought stress responses (Chapter 4; Conti et al., 2008). ULP2s constitute a main branch of SUMO proteases that has not been, to the best of our knowledge, functionally characterized in plants.

In the present study we have addressed the role of ULP2a and ULP2b SUMO proteases in Arabidopsis. We first performed a structural and phylogenetic characterization of plant ULPs, pointing to ULP2a and ULP2b being reminiscent of ULP2-type proteases. To determine ULP2a and ULP2b function, we characterized the developmental and environmental stress responses of Arabidopsis T-DNA insertion mutants, which showed diverse developmental defects and constitutively displayed increased SUMO-conjugate levels. Moreover, microarray analysis evidenced a specific transcriptional signature that suggests the involvement of ULP2s in secondary metabolism, cell wall remodelling and nitrate assimilation. The *ulp2a/b* mutant also displayed an antagonistic morphological phenotype in respect to the well characterized SUMO E3 ligase mutant

siz1. Most significantly, the triple mutant *ulp2a/b siz1* was phenotypically *siz1*-like, which places ULP2a/b as epistatic and downstream of SIZ1.

6.2. RESULTS

Phylogenetic reconstruction and topological analysis of ULP2s

Predictions on Arabidopsis ULP SUMO protease family members have been inconsistent as to the relationship between the main existing phylogenetic subgroups, either placing ULP1c/ULP1d closer to ESD4/ULP1a/ULP1b or ULP2s (Miura et al., 2007a; Lois, 2010; Novatchkova et al., 2012). To resolve this issue, we extended the existing characterization to include phylogenetically representative plant and non-plant genomes. Plant ULP ortholog search was carried out using Plaza (Van Bel et al., 2012), and was based on homology search with the seven consistently annotated Arabidopsis ULPs (ULP1a-d, ESD4, ULP2a-b) and the putative family member At3g48480. Phylogenetic reconstruction of the ULP family clearly outlined the existence of two major branches, and within these, plant ULPs could be categorized into four phylogenetic subgroups (Fig. 6.1A). Each major branch encompassed the predicted yeast and human ULP1 and ULP2 isoforms and can be considered ULP1- and ULP2-like, respectively. ULP1-like proteins contained only one plant ULP subgroup that included Arabidopsis ESD4, ULP1a and ULP1b. ULP2-like proteins contained the remaining three plant ULP subgroups, including that of annotated plant ULP2s. Interestingly, it also included the ULP1c/ULP1d subgroup, traditionally annotated as ULP1-like. The fourth distinct subgroup was phylogenetically closer to the ULP1c/d subgroup, and contained the orthologs of the putative Arabidopsis ULP At3g48480 that was hereafter designated ULP1e (Fig. 6.1A).

To the best of our knowledge no studies have characterized the ULP2s subgroup of ULPs in plants. Arabidopsis ULP2a and ULP2b display 30.5% identity, as well as a highly conserved region that possesses 46% identity and matches the catalytic domain (Fig. 6.1B,C; Appendix VI - Fig. S6.1). For both proteins, topological analysis revealed the catalytic domain to be located in the center of the protein, while ULP1-like proteins were located in the C-terminal end (Fig. 6.1B). Analysis also demonstrated that ULP1e was restricted to the catalytic domain and lacked both the N- and C-terminal ends of ULP2s (Fig. 6.1B).

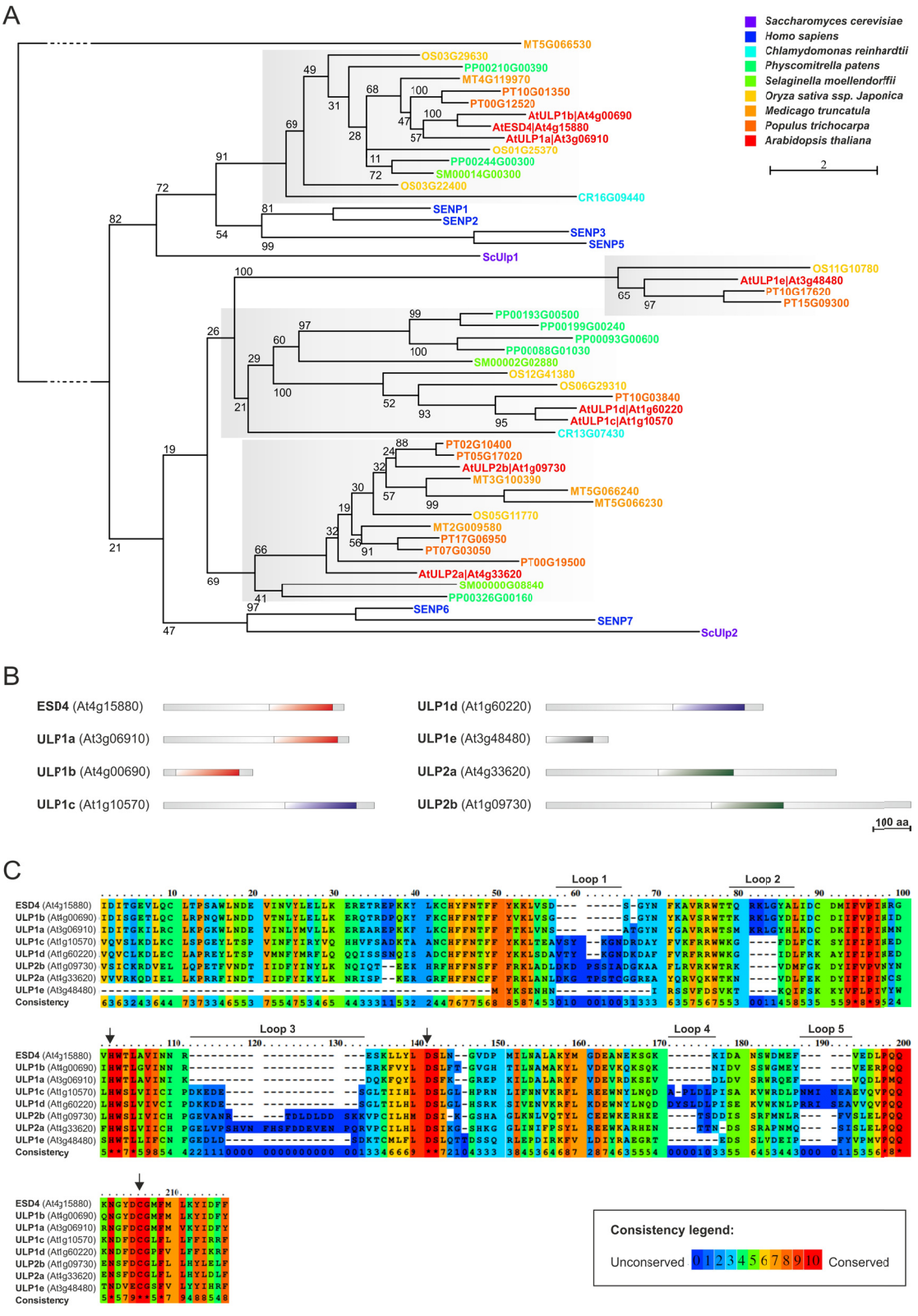

Figure 6.1. Phylogenetic and topological analysis of the plant Ubiquitin-Like Protease (ULP) family. **A**, Phylogenetic reconstruction of ULPs present in representative plant genomes (*Arabidopsis thaliana*, *Chlamydomonas reinhardtii*, *Physcomitrella patens*, *Selaginella moellendorffii*, *Oryza sativa* ssp. Japonica, *Medicago truncatula* and *Populus trichocarpa*), as well as human SENPs and yeast (*Saccharomyces cerevisiae*) ULPs. Phylogenetic analysis was performed using Maximum-likelihood with bootstrap analysis (100 trees). **B**, Schematic representation of Arabidopsis ULP protein topology with the catalytic domain highlighted in colored boxes. **C**, Protein sequence alignment of the catalytic domain in Arabidopsis ULPs. Arrows indicate the three conserved catalytic residues. Consistency between sequences indicates the levels of conservation of each residue.

Remarkably, the catalytic triad (His-Asp-Cys), essential for protease activity, was conserved among all Arabidopsis ULP members (Fig. 6.1C). Within the catalytic domain, it was possible to discriminate five main extensions (loops 1 to 5; Fig. 6.1C). Loops 1/3/4/5 are common to ULP1c/d and ULP2a/b and absent in ULP1a/ULP1b/ESD4, while loop 2 is specific to the latter. Loop 1 and in particular loop 2, are larger in ULP2a/b, whereas loops 3 and 4 are larger in ULP1c/d (Fig. 6.1C).

ULP2a and ULP2b mutants are developmentally compromised

Sumoylation has been shown to modulate many aspects of plant development, as well as key mechanisms in various stress responses. Many of the findings regarding the role of SUMO in plants have been based on reverse genetics approaches (Lois, 2010). To explore the role of the Arabidopsis SUMO proteases ULP2a (At4g33620) and ULP2b (At1g09730), we used a similar reverse genetics approach based on T-DNA insertion lines from SALK: SALK_090744 (*ulp2a-1*) and SALK_040576 (*ulp2b-1*; Fig. 6.2A; Alonso et al., 2003).

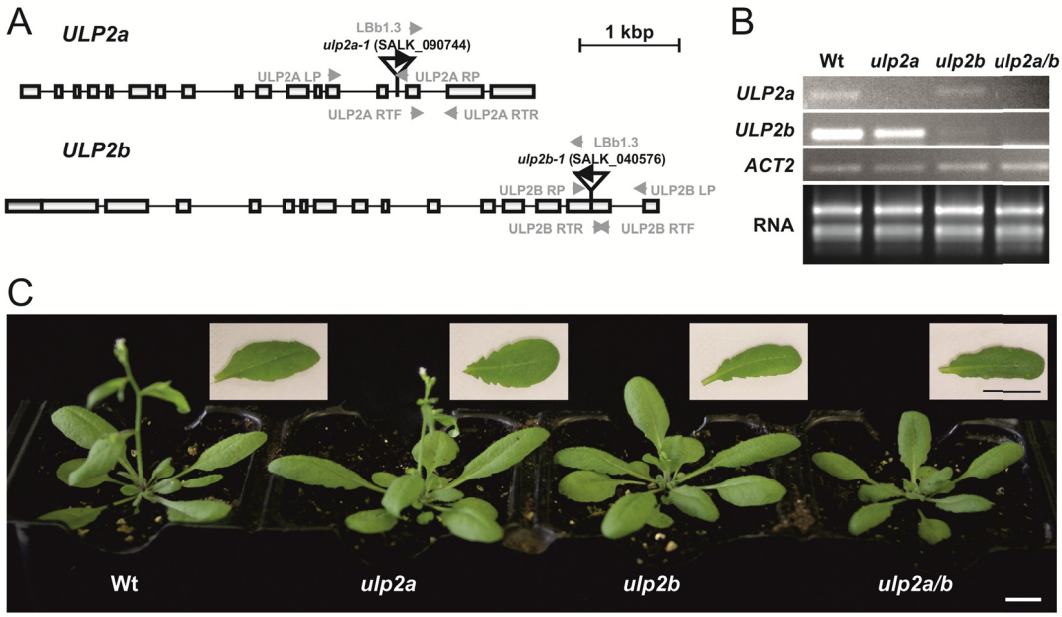

Figure 6.2. Characterization of *Arabidopsis thaliana* T-DNA insertion mutants for *ULP2a* and *ULP2b*. **A**, Schematic representation of *ULP2a* and *ULP2b* displaying exons (grey boxes), introns (thin lines), and UTRs (black boxes). The site and orientation of T-DNA insertions (triangles with SALK line code) and location of primers used for genotyping (LBb1.3, RP and LP) and RT-PCR (RTF and RTR) are represented; scale bar indicates 1 kbp. **B**, Semi-quantitative RT-PCR for wild-type (Wt), *ulp2a-1* (*ulp2a*), *ulp2b-1* (*ulp2b*) and *ulp2a-1 ulp2b-1* (*ulp2a/b*). Fragments were amplified using primers RTF and RTR. *ACT2* was used as a loading control, and the total extracted RNA that was used as template for reverse transcription served as a quality control. **C**, Morphology of 1-month-old plants from Wt and mutant lines grown under long days. Insets show a representative leaf of each genotype. Scale bars indicate 1 cm.

Homozygous lines were selected using diagnostic PCR (data not shown). Considering that ULP2a and ULP2b are phylogenetically close (Fig. 6.1A) and functional redundancy has been displayed by other gene family members (Chapter 4), we generated a double mutant *ulp2a-1 ulp2b-1* (hereafter designated *ulp2a/b*). Expression of *ULP2a* and *ULP2b* was assessed by semi-quantitative RT-PCR in single and double mutant backgrounds (Fig. 6.2B), confirming that in both cases T-DNA insertion abolishes gene expression. Results also suggest that in wild-type Arabidopsis plants, *ULP2b* is considerably more expressed than *ULP2a,* which is corroborated by publically available microarray data (Appendix VI - Fig. S6.2; Genevestigator; Hruz et al., 2008).

Morphological analysis suggested that, in comparison to the wild-type, both the *ulp2b* and *ulp2a/b* mutants displayed altered growth, different leaf morphology and late flowering time (Fig. 6.2C). A systematic characterization of morphological/developmental features was subsequently pursued. The strategy was based on first-phase measurements for soil-based analysis, selecting key stages in Arabidopsis development and measuring morphological features (Fig. 6.3A), according to the standard for *Arabidopsis thaliana* developmental stages previously established by Boyes and co-workers (2001). In the earlier stages of development there were no severe phenotypic differences between genotypes (Fig. 6.3B,C), however we noticed that in vitro, *ulp2a/b* mutant leaves are bigger and darker than wild-type leaves (Appendix VI - Fig. S6.3; data not shown). In soil-grown plants, a differential phenotype started to appear in later stages, with *ulp2a/b* plants showing a clear delay in development that included late flowering and shorter bolt length (Fig. 6.3E,F). Although the *ulp2a/b* rosette displayed a slightly smaller diameter, the most interesting aspect was that the *ulp2a/b* leaves were significantly smaller in width (Fig. 6.2C; 6.3D; Appendix VI - Fig. S6.3). Another striking feature of double mutant plants was the darker tonality of leaves, therefore we measured pigmentation content in leaves of 1-month-old plants (Fig. 6.3G-I). Results indicate that *ulp2a/b* accumulated relatively more chlorophylls, carotenoids, and anthocyanins than the wild-type. Finally, we could observe that *ulp2a/b* seed production and morphology were also severely affected, generating a low number of seeds per silique (Fig. 6.3J), yet seeds were bigger compared to the wild-type (Fig. 6.3K-M).

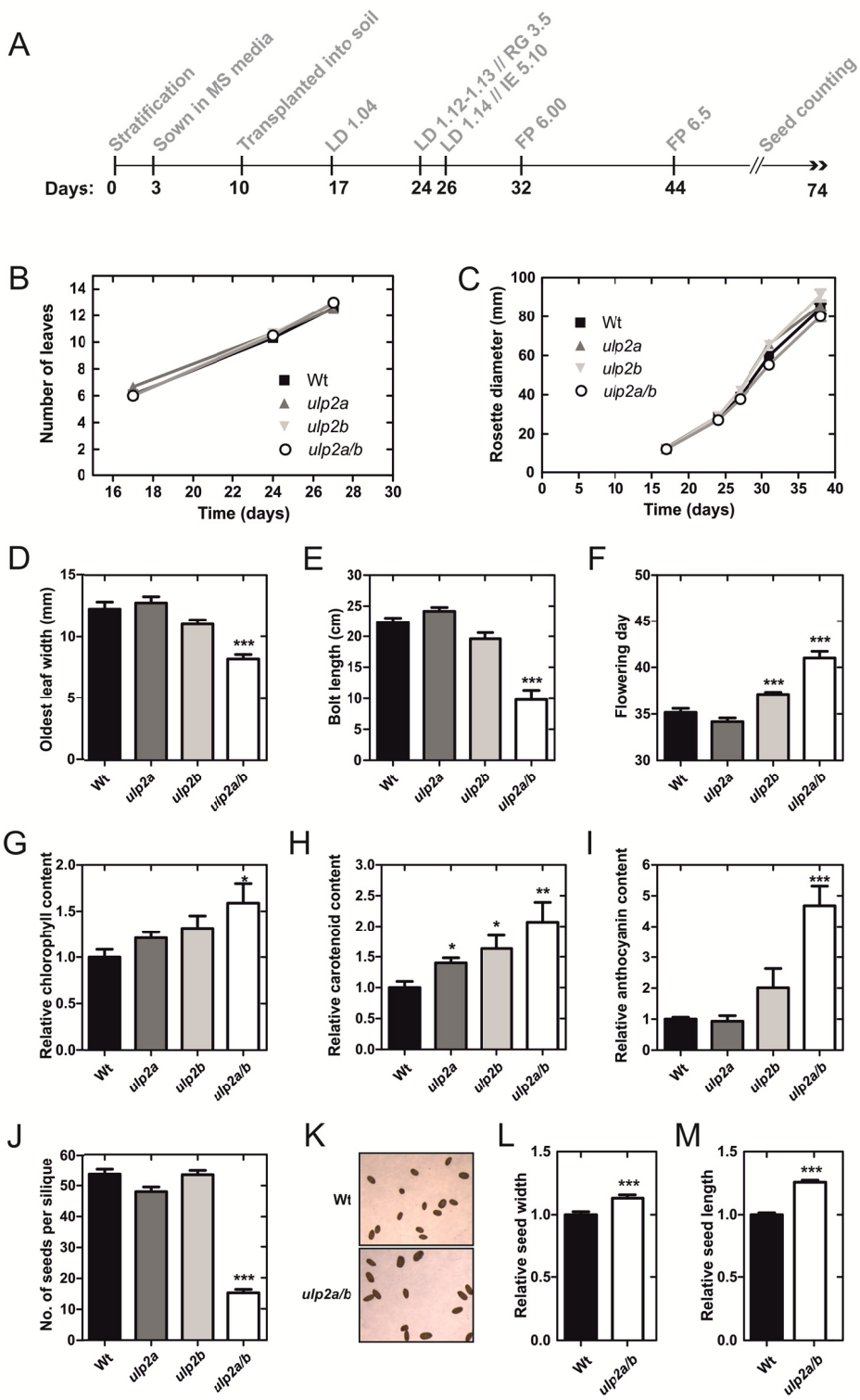

Figure 6.3. Developmental characterization of wild-type (Wt), *ulp2a*, *ulp2b* and *ulp2a/b* mutants. **A**, Chronological scheme of *Arabidopsis thaliana* ecotype Columbia-0 development, with selected stages based on soil-based phenotypic analysis (Boyes et al., 2001); LD – leaf development, RG – rosette growth, IE – inflorescence emergence, FP – flowering production. **B-F**, Morphological measurements of wild-type (Wt), *ulp2a*, *ulp2b* and *ulp2a/b*. **G-I**, Total chlorophyll (G), carotenoid (H) and anthocyanin (I) content in 1-month-old plants. **J**, Number of seeds per silique. **K**, Seed morphology in the Wt and *ulp2/b* mutant. **L,M**, Morphological measurements of Wt and *ulp2a/b* seeds. Error bars represent standard error of the means (SEM), n = 12 (B-F), n = 6 (G,H), n = 5 (I), n = 6 (J), and n > 36 (L-M). Asterisks indicate statistically significant differences with respect to the wild-type (unpaired t test; *, $P < 0.05$; **, $P < 0.01$; ***, $P < 0.001$).

In summary, we observed a series of developmental phenotypes in *ulp2a/b*. Several, less pronounced phenotypes were also observed in *ulp2b* but not in *ulp2a* single mutants. Specifically, the single mutant *ulp2b* revealed a developmental phenotype in flowering time, leave morphology and pigmentation (Fig. 6.2C and 6.3D-I). These results suggest that ULP2a and ULP2b are partial yet unequally redundant, with ULP2b having a predominant role. To genetically confirm present results, second allele mutants were characterized showing similar phenotypes (Appendix VI - Fig. S6.4).

ULP2a and ULP2b have SUMO protease activity

SUMO proteases may display different activities, breaking endopeptidic bounds important for SUMO maturation or having isopeptidic activity for SUMO removal or chain editing (Hickey et al., 2012). Phylogenetic analysis indicated that ULP2a and ULP2b were similar to yeast Ulp2 and human SENP6/7 (Fig. 6.1), and are therefore potential SUMO-chain editing proteins. To ascertain the kind of SUMO protease activity ULP2a and ULP2b have, we checked the sumoylation profile in the *ulp2a/b* mutants. Sumoylation patterns were analyzed by western blot of whole-plant proteins extracts using both anti-AtSUMO1 and anti-AtSUMO3 specific antibodies, thus covering the predominant SUMO peptides (Saracco et al., 2007; van den Burg et al., 2010). Results clearly showed that high molecular weight conjugates for SUM1/2 (the main SUMO peptides in Arabidopsis), constitutively accumulated in the double mutant but also to some extent in the *ulp2b* single mutant, with respect to the wild-type (Fig. 6.4A). Overall conjugation levels of SUM3, a peptide whose expression is lower and restricted to specific tissues (Saracco et al., 2007; van den Burg et al., 2010), seem unaffected in ULP2 mutants. However, specific bands are affected in the double mutant (Fig.6.4B).

SUMO-conjugation increases in response to stress, and this increment can be regulated by an altered balance between conjugation and deconjugation, in which ULPs play an important role (Pinto et al., 2012). Therefore, we checked the level of SUMO conjugates of the Arabidopsis *ulp2a/b* mutant subjected to heat-shock (HS) stress (Fig.6.4C). Although HS stress induced SUM1/2-conjugate accumulation, no major changes were observed in *ulp2a/b* comparatively to the Wt. Analysis of the SUMO-conjugate profile during the HS recovery period is likely to bring additional insight into the potential involvement of ULP2s in the heat stress response. As expected, these SUMO-conjugates failed to accumulate in the *siz1* mutant that was used as a negative control.

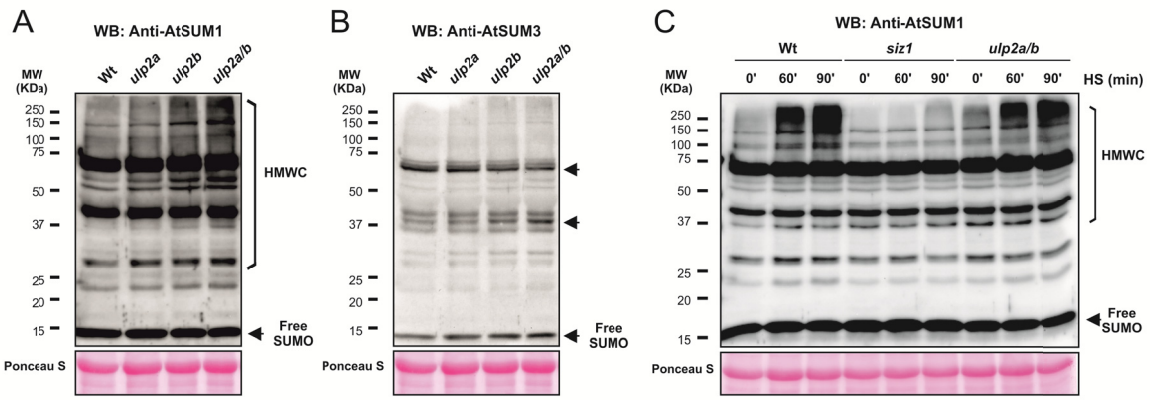

Figure 6.4. Immunoblot analysis of high molecular weight SUM1- and SUM3-conjugates (HMWC) in *ULP2* mutants. **A** and **B**, Analysis of leaf protein extracts from one-month-old plants using anti-AtSUMO1 (A) and anti-AtSUMO3 (B) polyclonal antibodies. **C**, Analysis of in vitro-grown 10-day-old plants subjected to heat-shock (37°C) for 0, 60 and 90 min. Protein extracts (50 µg per lane) were analyzed by immunoblot using anti-AtSUMO1 polyclonal antibodies. The *siz1* mutant was used as a negative control of SUMO-conjugate induction after heat shock. The larger subunit of Rubisco stained with Ponceau S was used as loading control. MW - Molecular weight marker (*Kaleidoscope*, Bio-Rad).

ULP2a and ULP2b subcellular localization

Differential recognition of SUMO substrates by SUMO proteases has been partially attributed to differences in sub-cellular localization (Hickey et al., 2012). Since localization of ULP proteins is crucial for their biological function, we investigated where ULP2a and ULP2b were located within the plant cell. We used the Cell eFP Browser bioinformatic tool (Winter et al., 2007) to predict their potential subcellular location. Both ULP2a and ULP2b are predicted to be nuclear, but this bioinformatic tool does not discriminate specific subnuclear localization (Appendix VI - Fig. S6.5). ULP2 fusions with GFP are currently being generated to estimate in vivo the nuclear and sub-nuclear localizations of ULP2a and ULP2b.

Microarray transcript profiling of *ulp2a/b*

Sumoylation is strongly involved in nuclear-mechanisms, particularly in the control of gene transcription through the regulation of chromatin remodeling complexes, co-repressors and modulators of transcription factor (TF) activity (Mazur and van den Burg, 2012). In light of this, ULP2a and ULP2b would be expected to modulate gene expression by promoting desumoylation and counteracting SUMO-dependent control of transcriptional regulators. To uncover the transcriptional profile controlled by ULP2a/b, we performed a microarray analysis (ATH1 affymetrix chip) of 10-day-old wild-type and *ulp2a/b* plants. Already at this stage, SUMO conjugates are affected and plants display a phenotype (Fig. 6.4, Appendix VI - Fig. S6.3) which may result from differences in transcription in relation to the wild-type. Microarray analysis evidenced 115

down-regulated and 100 up-regulated genes. Gene ontology (GO) and MapMan analysis were used to respectively map differential expression against biological processes and the overall metabolic pathways of Arabidopsis (Fig. 6.5A,B). Results revealed that many DEGs were involved in cell wall and secondary metabolism, including genes involved in the biosynthesis of phenylpropanoids (particularly lignin biosynthesis), glucosinolates and lipids (Fig. 6.5A,B; Table 6.1). The majority of these genes were found to be down-regulated. In contrast, one GO category particularly up-regulated in *ulp2a/b* was the response to hormone stimulus, though no specific hormone could be highlighted (Table 6.1). We compared genes differentially expressed genes in *ulp2a/b* against genes differentially expressed by exogenous hormone supplementation (data not shown; Nemhauser et al., 2006). Results showed that many of the *ulp2a/b* DEGs, when compared with random abundance in the genome, were over-represented within the transcriptional signature that follows application of exogenous abscisic acid (ABA) and methyl jasmonate (MJ).

Table 6.1. Genes constitutively deregulated in *ulp2a/b* comparatively to the wild-type. The categories were chosen taken in consideration the gene ontology (GO) terms enrichment and the list of genes was gathered using Classification SuperViewer (Toufighi et al., 2005) and The Arabidopsis Information Resource (TAIR; Lamesch et al., 2010).

AGI ID	Gene name	Log2 ratio	*p*-value	Description
Hormone metabolism				
Auxin				
At1g77690	*LAX3*	-0,65	2,41E-4	Auxin influx carrier
At5g35735		0,58	9,44E-3	Auxin-responsive
At1g56150		0,59	6,19E-3	SAUR-like auxin-responsive
At4g14560	*AXR5, IAA1*	0,88	2,49E-10	Aux/IAA protein
At5g18060	*SAUR23*	0,96	0,00E+0	SAUR-like auxin-responsive
Brassinosteroid				
At3g30180	*BR6OX2, CYP85A2*	1,30	0,00E+0	Brassinosteroid-6-oxidase
Cytokinin				
At1g22400	*UGT85A1*	0,64	5,00E-4	UDP-Glycosyltransferase
Gibberellin				
At2g14900		0,65	2,58E-4	Gibberellin-regulated
At5g25900	*KO1, CYP701A3, GA3*	0,71	1,45E-5	Kaurene oxidase
Jasmonate				
At1g52070		0,61	2,07E-3	Mannose-binding lectin
At5g42650	*AOS, CYP74A, DDE2*	0,81	2,26E-8	Allene oxide synthase
At1g52100		1,09	0,00E+0	Mannose-binding lectin
Salicylic acid				
At5g38020		0,70	2,23E-5	SAM-Mtases
At5g37990		0,82	1,61E-8	SAM-Mtases

Table 6.1. (Continued)

Secondary metabolism				
Phenylpropanoids (lignin biosynthesis)				
At4g37980	*CAD7,ELI3*	-1,13	0,00E+0	Cinnamyl alcohol dehydrogenase
At5g66690	*UGT72E2*	-0,81	3,20E-8	UDP-Glycosyltransferase
At4g39330	*CAD9*	-0,66	1,29E-4	Cinnamyl alcohol dehydrogenase
At4g36220	*CYP84A1, FAH1, F5H*	-0,56	2,57E-2	Ferulic acid 5-hydroxylase
Lipids				
At1g06080	*ADS1*	-1,51	0,00E+0	Acyl-lipid / acyl-CoA desaturase
At5g14180	*MPL1*	-1,50	0,00E+0	*Myzus persicae*-induced lipase
At5g04530	*KCS19*	-1,02	0,00E+0	3-ketoacyl-CoA synthase
At1g06350		-0,91	4,48E-11	Fatty acid desaturase
At3g08770	*LTP6*	-0,91	4,48E-11	Lipid transfer protein
At4g34250	*KCS16*	-0,62	1,47E-3	3-ketoacyl-CoA synthase
At3g11670	*DGD1*	-0,60	2,80E-3	UDP-glycosyltransferase
At4g38690		-0,56	1,92E-2	PLC-like phosphodiesterase
Glucosinolates				
At3g14210	*ESM1*	-1,72	0,00E+0	Epithiospecifier modifier
At4g13770	*CYP83A1, REF2*	-0,74	2,35E-6	Cytochrome P450
At2g43100	*LEUD1, IPMI2*	-0,68	5,43E-5	Isopropylmalate isomerase
At5g23010	*IMS3, MAM1*	-0,64	5,52E-4	Methylthioalkylmalate synthase
At1g07640	*OBP2*	-0,60	3,01E-3	DOF transcription factor
At3g44320	*NIT3*	0,75	1,26E-6	Nitrilase
At1g54010	*GLL22*	0,90	6,97E-11	GDSL-like lipase / acylhydrolase
Cell Wall				
At5g65730	*XTH6*	-1,61	0,00E+0	XTH
At1g67750		-0,66	1,31E-4	Pectate lyase
At5g47500	*PME5*	-0,63	8,57E-4	Pectin methylesterase
At4g28250	*EXPB3*	-0,59	6,49E-3	Beta-expansin
At3g23730	*XTH16*	-0,59	6,24E-3	XTH
At1g20190	*EXPA11*	0,57	1,08E-2	Alpha-expansin
At1g55850	*CSLE1*	0,57	1,49E-2	Cellulose synthase/ transferase
At3g29810	*COBL2*	0,59	4,76E-3	COBRA-like protein precursor
At2g06850	*XTH4, EXGT-A1, EXT*	0,63	6,61E-4	XTH
At3g28180	*CSLC4*	0,78	1,94E-7	Cellulose synthase/ transferase
At4g30290	*XTH19*	0,88	2,09E-10	XTH
At5g33290	*XGD1*	0,95	0,00E+0	Xylogalacturonan xylosyltransferase
At3g44990	*XTH31, XTR8*	1,29	0,00E+0	XTH
Other				
At2g45660	*SOC1, AGL20*	-0,83	6,01E-9	AGAMOUS-like transcription factor
At1g77760	*NIA1, GNR1, NR1*	-0,83	7,34E-9	Nitrate reductase
At4g21680	*NRT1.8*	0,61	1,81E-3	Nitrate transporter
At5g50200	*NRT3.1, WR3*	0,62	1,11E-3	Nitrate transporter

XTH - Xyloglucan endotransglucosylase / hydrolase; SAM-Mtases - S-adenosyl-L-methionine-dependent methyltransferase

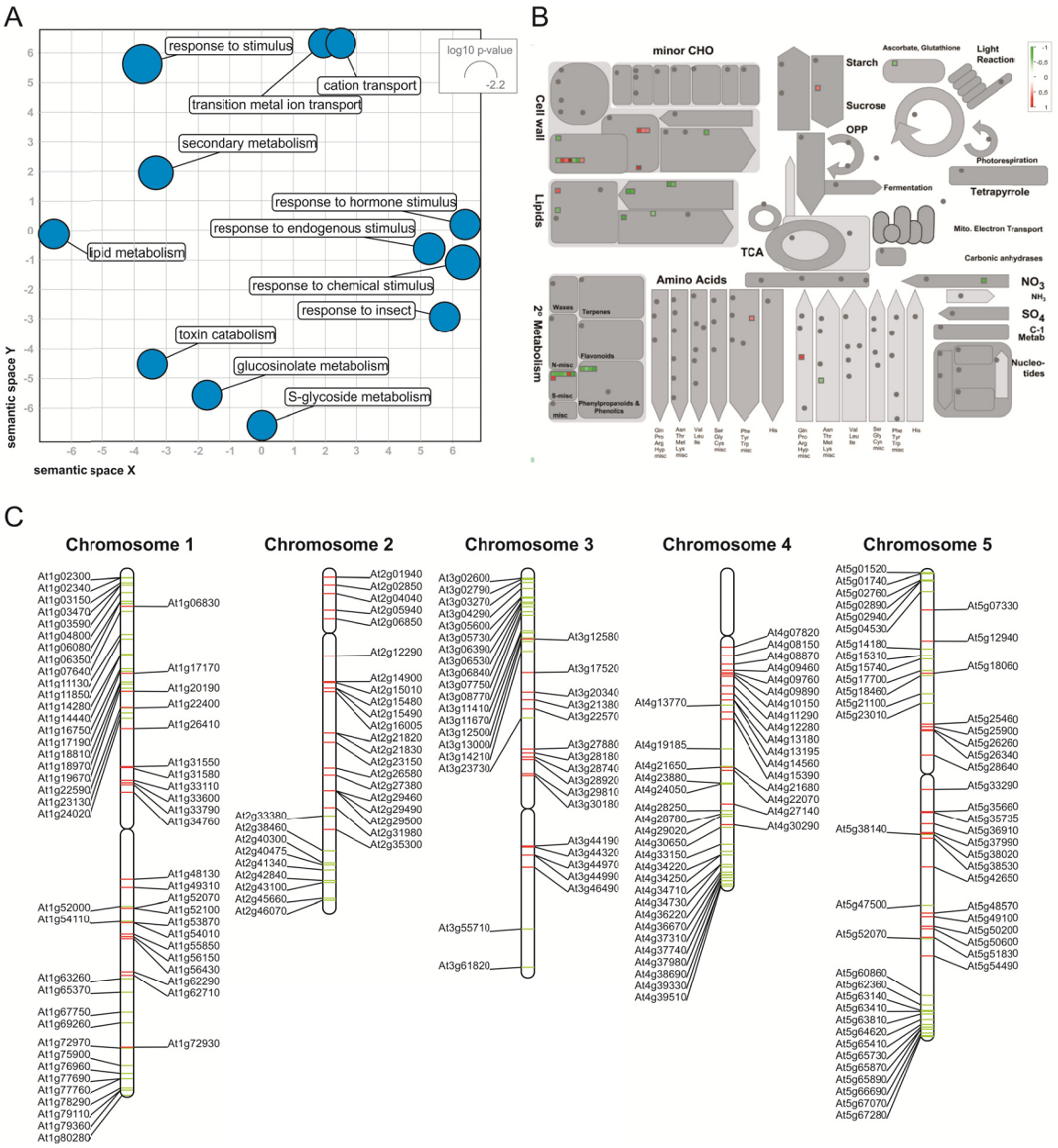

Figure 6.5. Microarray analysis of 10-day-old *ulp2a/b* seedlings. **A**, Scatterplot analysis of enriched gene ontology (GO) terms for *ulp2a/b* differentially expressed genes. The bubble size shows the frequency of the GO term. **B**, MapMan analysis of *ulp2a/b* deregulated genes using the *Metabolism overview pathway* map. **C**, Chromosomic spatial disposition of *ulp2a/b* differentially expressed genes. Color scheme in (B) and (C) represents down-regulated genes (green) and up-regulated genes (red).

Interestingly, some genes previously described as being deregulated in *siz1* mutants are anti-expressed in *ulp2a/b* DEGs. Examples include nitrate reductase *NIA1* (At1g77760), the AGAMOUS-like transcription factor *SOC1* (At2g45660) and the xyloglucan endotransglucosylase/hydrolase *XTH31* (At3g44990; Jin et al., 2008; Miura et al., 2010; Park et al., 2011), that are involved in N-assimilation, flowering time and cell growth, respectively.

In *ulp2a/b*, the observed deregulation in transcript levels for these and other genes was confirmed by quantitative Real-Time PCR (qPCR; Fig. 6.6), thus validating our microarray data.

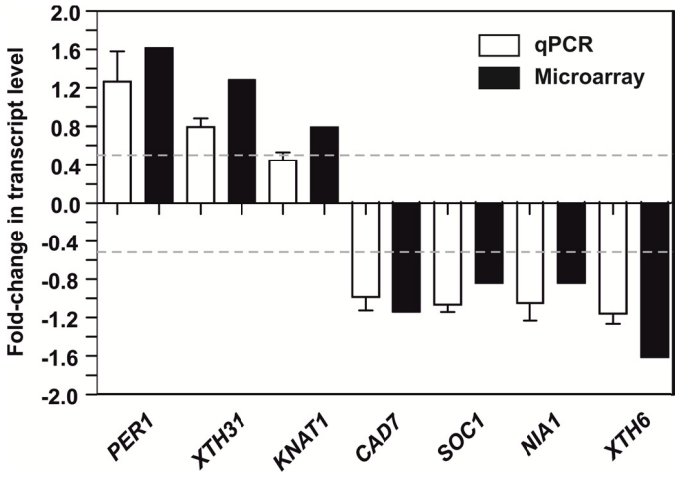

Figure 6.6. Quantitative RT-PCR (qPCR) analysis of differentially expressed genes in 10-day-old *ulp2a/b* seedlings. Fold-change in expression levels in *ulp2a/b* compared to the Wt is depicted for the following genes: *PER1* (At1g48130), *XTH31* (At3g44990), *KNAT1* (At4g08150), *CAD7* (At4g37980), *SOC1* (At2g45660), *NIA1* (At1g77760), *XTH6* (At5g65730). Error bars represent SEM of three independent biological replicates. Grey lines represent the threshold for fold-change that was used to set differential expression in the microarray experiment.

Co-expressed genes tend to be controlled by identical transcriptional regulators, and share common *cis*-elements in their promoters. Considering that sumoylation often targets regulators of transcription, we identified statistically over-represented *cis*-elements in the promoters of *ulp2a/b* DEGs that may act as binding sites for SUMO target candidates. For that purpose we used the bioinformatic tools Athena (O'Connor et al., 2005) and ATCOECIS (Vandepoele et al., 2009), and could observe an enrichment in MYC2-like binding sites (Table 6.2), in both up- and down-regulated genes.

Sumoylation is also known to modulate chromatin structure and function at diverse levels (Cubenas-Potts and Matunis, 2013). We therefore hypothesized that such a regulatory role for ULP2a and ULP2b might reflect on the spatial location of DEGs within the Arabidopsis genome, and subjected *ulp2a/b* DEGs to analysis in the TAIR Chromosome Map Tool. Interestingly, a clear spatial distribution was observed: down-regulated genes were more abundant near the extremities of the chromosomes (telomeric and subtelomeric heterochromatin), while up-regulated genes were closer to the internal region of the chromosome (Fig. 6.5C).

Table 6.2. *Cis*-elements over-represented in the promoter region of differentially expressed genes (DEGs) in *ulp2a/b*. The DEGs were submitted to Athena analysis (O'Connor et al., 2005) scanning for binding sites enrichment.

***Cis*-element name**	***Cis*-element sequence***	**Nr. Of genes**	**Predicted in the genome**	**Found in the genes**	***p*-value**	**Corresponding TFs**
Down-regulated						
AtMYC2 BS in RD22	CACATG	61	35%	53%	< 10e-6	MYC2
MYCATERD1	CATGTG	61	35%	53%	< 10e-6	MYC2
Up-regulated						
AtMYC2 BS in RD22	CACATG	47	35%	47%	< 10e-3	MYC2
MYCATERD1	CATGTG	47	35%	47%	< 10e-3	MYC2
CARGCW8GAT	CWWWWWWWWG	70	59%	70%	< 10e-3	AGL15
TATA-box Motif	TATAAA	91	91%	82%	< 10e-4	

** R (A/G), M (A/C), W (A/T), K (G/T), B (C/G/T), N (A/C/G/T)*

ULP2 mutants do not recover the *siz1* phenotype to wild-type

When we compared *ulp2a/b* to mutants of the Arabidopsis SUMO conjugation pathway, it become clear that *ulp2a/b* displayed antagonistic phenotypes to those of *siz1*. SIZ1 is the major SUMO E3 ligase and has been the subject of most functional studies in the pathway. Contrary to ULP2a/b, loss of SIZ1 function induces diminished SUMO-conjugate accumulation, early flowering, and decreased pigment content (Chapter 2; Catala et al., 2007; Jin et al., 2008), suggesting an epistatic relationship between SIZ1 and ULP2s. To further address this issue, we generated a triple *siz1-2 ulp2a-1 ulp2b-1* (*siz1 ulp2a/b*) mutant, and performed a phenotype characterization. Morphologically, the triple mutant resembled *siz1* and was similarly affected in the accumulation of high molecular weight SUMO conjugates, even after heat shock (HS; Fig. 6.7A-C), suggesting that SIZ1 is acting upstream of ULP2s.

Transcript profiling was extended to the triple mutant *siz1 ulp2a/b*, and was subsequently compared to *siz1-2* and *ulp2a/b* (Fig. 6.7D). We identified DEGs in all three mutant genotypes in comparison to the wild-type, and subsequently cross-referenced the three data subsets (Fig. 6.7D). A total of 26 genes were similarly differentially expressed in all three mutant backgrounds. These

included, for instance, the bHLH transcription factor *FBI1/HFR1/REP1/RSF1* and the putative phytochrome kinase substrate At1g18810, both involved in phytochrome signaling (Fairchild et al., 2000; Schepens et al., 2008). Results showed that a significant percentage of the differential transcriptome was shared between *siz1* and *siz1 ulp2a/b* mutants. When we compared expression values of *siz1 ulp2a/b* directly to *siz1-2*, only 10 genes were down-regulated and 6 genes were up-regulated, indicating that their transcriptome virtually matched (Fig. 6.7E). Trasncriptomic data reinforces the notion that SIZ1 is upstream of and epistatic to ULP2a/b.

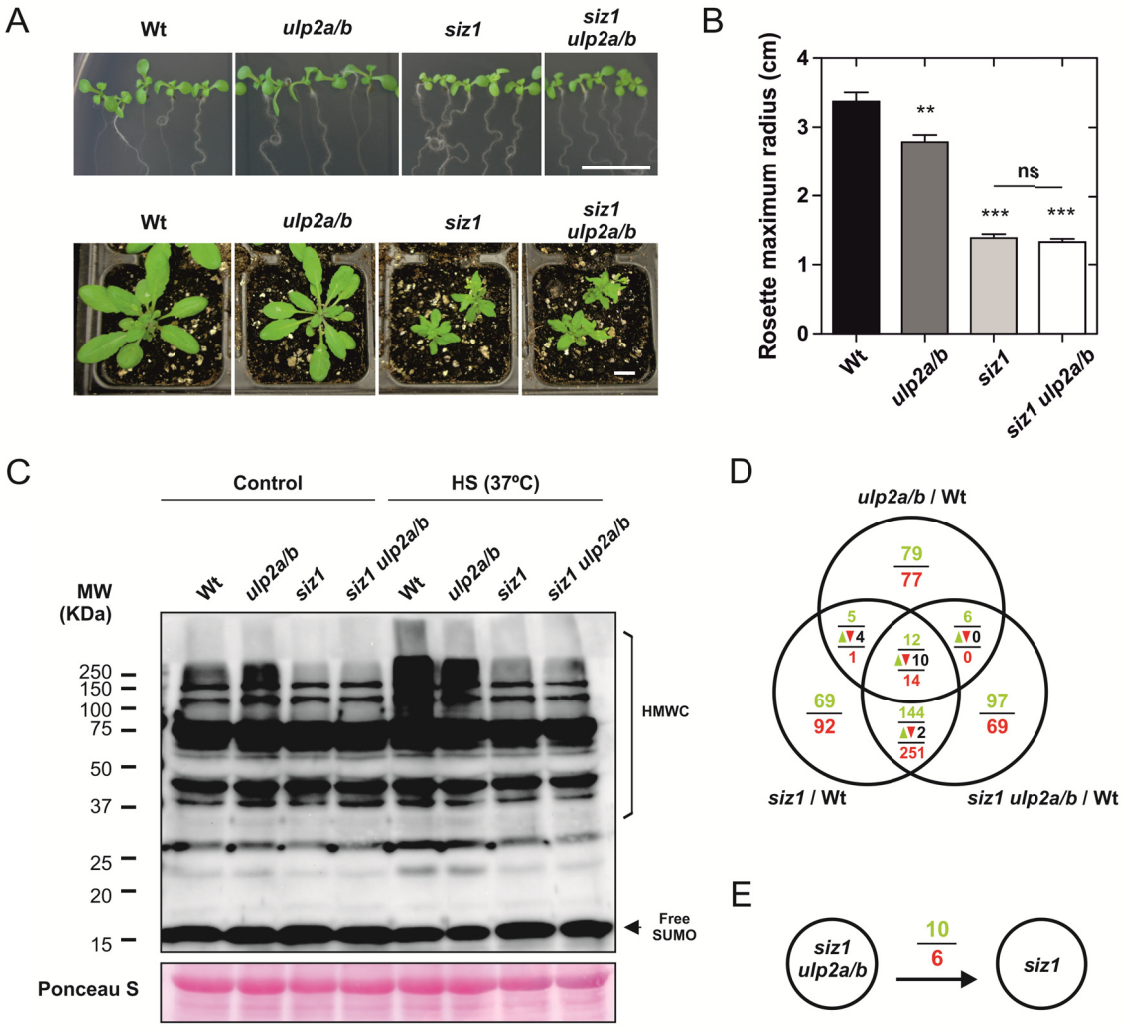

Figure 6.7. Characterization of the *siz1-2 ulp2a-1 ulp2b-1* (*siz1 ulp2a/b*) triple mutant. **A**, Morphology of 10-day-old and 1-month-old plants. **B**, Rosette maximum radius. Error bars represent SEM, n = 7. Symbols represent statistically significant differences of mutants compared to the Wt, and *siz1* compared to *siz1 ulp2a/b* (unpaired t test; ns, non-significant; *, $P < 0.05$; **, $P < 0.01$; ***, $P < 0.001$). **C**, Western blot analysis of high molecular weight SUM1-conjugates (HMWC) in 10-day-old Wt, *ulp2a/b*, *siz1* and *siz1 ulp2a/b*, subjected to heat shock (HS) for 1 h. **D**, Venn diagram representing differentially expressed genes in each mutant genotype compared to the Wt. **E**, Differentially expressed genes in *siz1 ulp2a/b* in relation to the single mutant *siz1*. Color scheme represents down-regulated genes (green), up-regulated genes (red) and anti-expressed genes (black).

6.3. DISCUSSION

Sumoylation is essential for eukaryotic organisms, mainly because it regulates the activity of vital proteins. Therefore, it is crucial that SUMO homeostasis be tightly controlled, and in recent years, some publications have shed light on SUMO protease activity and their essential role in many aspects of cellular homeostasis (reviewed by Hickey et al., 2012). In plant genomes, as in other organisms, SUMO proteases seem to be more abundant than the E1/E2/E3 components of the conjugation machinery, making them prime candidates for the regulation of SUMO conjugate/deconjugate homeostasis. In the present study we were able to initiate the functional characterization of ULP2a and ULP2b, the two putative ULP2s coded in the Arabidopsis genome. Results sustain a redundant role for both proteins in plant growth and development.

ULP2a/b are ULPs with likely isopeptidase activity

Phylogenetic studies have singled out ULP2a and ULP2b as homologs of yeast Ulp2 and mammalian SENP6/7, making them natural candidates for poly-SUMO chain editing proteases in Arabidopsis (Hickey et al., 2012). In the present study we were able to highlight the topological basis behind this assumption, in that plant ULP2a/b share several features with both yeast and mammalian orthologs. The human ULP2-like SENP6 and SENP7 catalytic domains create loops for SUMO recognition (Lima and Reverter, 2008; Alegre and Reverter, 2011). More specifically SENP6/7 loop 1 is essential for activity and SUMO isoform discrimination, but it is not conserved either in yeast or plant ULP2s. The topology of the catalytic domains in Arabidopsis ULPs revealed the existence of five internal loops (Fig. 6.1C), but whether they contribute for SUMO recognition is still to be determined. Another interesting characteristic is that the catalytic domain in Arabidopsis ULP2s is located in the middle of the protein (Fig. 6.1B), a feature shared with yeast Ulp2p. Concerning the function of the N- and C-terminal ends, the model proposed for yeast ULP2 is that the N-terminal domain acts mainly in nuclear targeting (Kroetz et al., 2009), whereas the C-terminal end contains motifs for PTM such as phosphorylation (Baldwin et al., 2009). In agreement, the Arabidopsis ULP2b C-terminal end was previously identified as being a phosphorylation target (PhosPhAt database; Durek et al., 2010).

It is important to refer that other ULP2-like proteases were previously proposed by Kurepa et al. (2003) and Lois (2010). However these putative ULP-like genes are part of transposon elements (Hoen et al., 2006) and were designated *Kaonashi ULP-like* (*KIU*) sequences. Though they potentially have catalytically functional domains, their SUMO protease activities were never

studied. Nevertheless, *KIU* also belong to a phylogenetic distant branch from the remaining ULP family members and are strongly silenced (Hoen et al., 2006), suggesting a minor contribution to SUMO regulation in the event they do function as SUMO proteases. In conclusion, phylogenetic and topology studies place ULP2a and ULP2b as the most likely Arabidopsis ULP2-type SUMO proteases homologues.

SUMO proteases have a dual function as both maturases of the pre-SUMO peptide and as isopetidases removing SUMO conjugates, and it is important to establish the individual contribution of the different ULPs to each role. Loss of ULP2a/b function resulted in the constitutive accumulation of high molecular weight SUMO-conjugates (Fig. 6.4), which is consistent with phylogenetic data that suggests that ULP2s act as major isopeptidases in the sumoylation pathway. Another interesting aspect is that immunoblotting against SUM3 revealed an increment in specific bands/SUMO targets. This result raises the additional question whether these proteases may also act towards SUM3. Previously, only ULP1a showed activity in vitro, though weakly, towards SUM3 (Colby et al., 2006). This SUMO isoform is involved in late responses to pathogen infection and its knockout mutant displays late flowering (van den Burg et al., 2010).

Results have also shown the existence of unequal redundancy between ULP2a and ULP2b: (1) *ULP2b* seems to be much more expressed than *ULP2a* as shown by semi-quantitative RT-PCR and public transcriptomic data (Fig. 6.2B; Appendix VI - Fig. S6.2); (2) compared to *ulp2a*, *ulp2b* mutant plants display more prominent phenotypes in leave morphology, flowering time, pigment accumulation and increased SUMO-conjugates (Fig. 6.3 and 6.4); (3) we have shown that several plant genomes only display one ULP2-like protease, including *Physcomitrella patens*, *Selaginella moellendorffii*, rice and maize (Fig. 6.1A; Appendix VI - Fig. S6.1), suggesting a recent gene duplication event within dicots.

ULP2a/b control plant development downstream of SIZ1

ULP2a/b control a series of development features, making them potentially strategic for the future enhancement of crop yield. The *ulp2a/b* mutant phenotypes include (1) late flowering, indicative of a delay in development, (2) smaller leaves, and (3) severely impaired seed production (Fig. 6.3). However, seeds are also bigger which may be an interesting prospect to increase seed size in crop species (Fig. 6.3K-M). We have shown that ULP2a/b controls several genes involved in secondary metabolism (Fig. 6.5A,B; Table 6.1), which may explain the observed developmental defects. For instance, genes involved in glucosinolates and lignin deposition, such as *Ferulic acid 5-*

hydroxylase (*F5H*), are down-regulated in *ulp2a/b*, suggesting that ULP2a and ULP2b act as positive regulators of lignin deposition. Many components of the cell wall remodeling apparatus are also affected in *ulp2a/b*, particularly members of the xyloglucan endotransglucosylase/hydrolase (XTH) family like *XTH31*, which was previously seen to be down-regulated in *siz1* (Miura et al., 2010), and is over-expressed in *ulp2a/b* (Fig. 6.6). Most significantly, we have provided substantial evidence that many phenotypes displayed by *ulp2a/b* oppose those of *siz1*, including SUMO-conjugate accumulation, late flowering, higher pigment content and reduced ROS accumulation (data not shown). Interestingly, *siz1 ulp2a/b* mutant morphologically resemble the *siz1* single mutant, suggesting that ULP2a/b are epistatic to SIZ1.

Target sumoylation is greatly under the control of SIZ1 (Miura et al., 2005; Catala et al., 2007). Though many SUMO machinery components are sumoylated in normal conditions, SIZ1 is the only heavily sumoylated protein under stress conditions (e.g. HS, ethanol and H_2O_2; Miller et al. 2013). One possibility is that SIZ1 may be one of the major targets of ULP2a/b. In accordance with this hypothesis, yeast Siz1 and Siz2 are high-copy suppressors of *ulp2*Δ phenotypes, suggesting that the requirement for yeast Ulp2 is bypassed by SIZ1 overexpression (Strunnikov et al., 2001; Hannich et al., 2005). Nevertheless, plants might display higher complexity, since in the current data, *ulp2a/b* and *siz1* revealed opposing phenotypes and their transcriptome was not significantly co- or anti-expressed (Fig. 6.7).

Interestingly, in the comparison between *siz1* and *siz1 ulp2a/b*, two genes appeared as anti-expressed that are in fact two different Affymetrix spot IDs for the *SIZ1* gene (247630_at and 247629_at). The opposite signal between these two spots is likely due to the fact that 247629_at is located upstream and 247630_at is downstream of the *siz1-2* T-DNA insertion site. The upstream probes show up-regulation of *SIZ1* in the *siz1-2* mutant while the downstream probes naturally show down-regulation. This suggests that absence of a functional SIZ1 induces *SIZ1* expression in a feedback mechanism. In support, the E2 ligase *SCE1* (At3g57870) seems to be slightly but significantly up-regulated in the *siz1-2* mutant, which suggests that various SUMO conjugation components are targeted for up-regulation in the feedback mechanism.

Another important aspect to consider when addressing the ULP2 role in Arabidopsis is the potential for functional redundancy with other ULPs. In agreement, *esd4* and *ulp1c/d* mutants have been shown to accumulate high molecular weight SUMO-conjugates under non-stress conditions (Chapter 4; Murtas et al., 2003; Xu et al., 2007; Conti et al., 2008), and also ESD4, ULP1a, ULP1c and ULP1d have shown SUMO1/2 isopeptidase activity in vitro (Chosed et al.,

2006; Colby et al., 2006; Conti et al., 2008; Hermkes et al., 2011). On the other hand, the triple mutant *siz1 ulp1c/d* showed accumulative defects, which partially place ULP1c/d and SIZ1 in different pathways (Chapter 4). The *siz1 esd4* mutant, like *siz1 ulp2a/b*, resembles *siz1* (Castro et al. unpublished), but SIZ1 and ESD4 are also likely to function in different pathways since the *siz1* pleiotropic phenotype is greatly reverted in the *NahG* background (expressing a bacterial SA hydroxylase that hydrolyses SA), while *esd4* does not (Hermkes et al., 2011). Discriminating de-sumoylation targets for each ULP will be an important step towards dissecting the circuitry of regulation via SUMO removal, and ultimately identify the origin of specificity within the sumoylation pathway. Such a goal should come from combining ULPs mutant backgrounds with high-throughput sumoylome-identifying strategies such as that described by Miller et al. (2010).

ULP2a/b are nuclear components playing a role in transcription regulation

Both mammalian SENP and yeast ULP vary in their sub-nuclear localization (reviewed by Wilkinson and Henley, 2010), contributing differently to SUMO dynamics within the nucleus. In Arabidopsis, ULPs have been shown to display a variety of subcellular localizations: ESD4 in the nuclear envelope, ULP1c/OTS2 in speckle-like bodies of the nucleoplasm, ULP1d/OTS1 in the nucleoplasm, and ULP1a/ELS1 in the cytoplasm and endomembranes (Murtas et al., 2003; Conti et al., 2008; Hermkes et al., 2011). ULP2a and ULP2b are predicted to locate in the nucleus (Appendix VI - Fig. S6.5), therefore contributing to the regulation of nuclear SUMO-dynamics. Accordingly, plant SUMO-conjugates are mainly nuclear-targeted proteins (Saracco et al., 2007; Elrouby and Coupland, 2010; Miller et al., 2010). Among them are several transcription factors, co-repressor complexes, histones, mRNA biogenesis, and many other components associated to nuclear processes (Mazur and van den Burg, 2012). In addition to previous reports that SIZ1 and ULP1c/d significantly influence the plant transcriptome (Chapter 4 and 5; Catala et al., 2007), ULP2a/b are also involved in transcription regulation, and seem to mainly influence secondary metabolism, N-assimilation and flowering time. Some of the reported DEGs such as *NIA1*, *SOC1* and *XTH31* (Fig. 6.6; Table 6.1) were previously associated to SIZ1-regulation but with opposite behavior. As previously stated, the *siz1 ulp2a/b* mutant phenotypically resembled *siz1*, and accordingly, the transcriptional profile of *siz1 ulp2a/b* superimposed with that of *siz1* but not *ulp2a/b*. Altogether, ULP2a/b function seems to take place downstream of SIZ1. The simplest model is that targets of SIZ1-dependent sumoylation are subjected to ULP2a/b de-sumoylation. Most bona fide candidates include transcription factors such as PHR1, ICE1, ABI5, HSFA2 and

MYB30 (Miura et al., 2005; Miura et al., 2007b; Miura et al., 2009; Cohen-Peer et al., 2010; Zheng et al., 2012). *Cis*-element enrichment analysis also highlighted MYC2 as a potential target for ULP2a/b regulation (Table 6.2), and in fact MYC2 was shown to be sumoylated in vitro (Elrouby and Coupland, 2010). Another potential target is the mediator complex component MED25/PFT1 that interacts with various transcription factors, many of which are also SUMO-modified (e.g. ABI5 and MYC2; Miura et al., 2009; Elrouby and Coupland, 2010; Chen et al., 2012). The Mediator Complex is an essential link between RNA polymerase II and transcription factors, prior to the start of transcription (Borggrefe and Yue, 2011). The Arabidopsis MED25/PFT1 component, in particularly, is a target for sumoylation (Miller et al., 2010; Miller et al., 2013), and could be a link between the sumoylation machinery and transcription regulation through TFs. In support, MED25/PFT1 mutant plants shares many features with *ulp2a/b*, such as late flowering, altered pigment content, and similar microarray signature pattern (Appendix VI - Fig. S6.6; Kidd et al., 2009; Elfving et al., 2011). Additionally, Zhu et al. (2011) demonstrated a new role for the Mediator complex as influencing telomeric silencing. Uncovering a functional link between MED25/PTF1 being a target of ULP2a/b and influencing the distinctive spatial expression pattern of *ulp2a/b* DEGs (Fig. 6.5C) is certainly an interesting prospect.

6.4. MATERIALS AND METHODS

Plant material and growth conditions

T-DNA insertion mutants were used to evaluate loss-of-function in *Arabidopsis thaliana* SUMO proteases ULP2a (At4g33620) and ULP2b (At1g09730). Mutants were ordered through the NASC European Arabidopsis Stock Centre (arabidopsis.info) or the Arabidopsis Biological Resource Stock Center (www.biosci.ohio-state). All mutants were SALK lines in the background ecotype Columbia-0 (Col): SALK_090744 (*ulp2a-1*), SALK_135907.27.50 (*ulp2a-2*), SALK_040576 (*ulp2b-1*), SALK_022079.54.75 (*ulp2b-2*), SALK_080083C (*ulp2b-3*), and also the previously characterized line SALK_065397 (*siz1-2*; Miura et al., 2005). The genotypes were confirmed by diagnostic PCR, following the instructions on SIGnAL T-DNA Primer Design (signal.salk.edu/tdnaprimers.2.html) and using the primers listed in Table S6.1 (Appendix VI).

Synchronized seeds were stratified for 3 days at 4°C in the dark. Surface sterilization was performed in a horizontal laminar flow chamber by sequential immersion in 70% (v/v) ethanol for

5 min and 20% (v/v) commercial bleach for 10 min before washing five times with sterile ultra-pure water. Seeds were resuspended in sterile 0.25% (w/v) agarose, sown onto 1.2% (w/v) agar-solidified MS medium (Murashige and Skoog, 1962) containing 1.5% (w/v) sucrose, 0.5 g L^{-1} MES, pH 5.7, and grown vertically in culture rooms with a 16 h light/8 h dark cycle under cool white light (80 µE m^{-2} s^{-1} light intensity) at 23°C. For standard growth, 7-day-old in vitro-grown seedlings were transferred to a soil to vermiculite (4:1) mixture, and maintained under identical growth conditions, with regular watering. Mutant lines were morphologically characterized according to the developmental map for *Arabidopsis thaliana* described by Boyes et al. (2001).

Pigment extraction and quantification

For estimation of the chlorophyll and carotenoid contents, plant leaves were incubated in 80% (v/v) acetone for 1 h in the dark. The plant material was spinned down and absorbances at 470, 645, and 663 nm were measured in a microplate spectrophotometer (SpectraMax 340PC; Molecular Devices). Pigment contents were determined as follows: total chlorophyll, $C_{Total} = 20.2\ A_{645} + 8.02\ A_{663}$; total carotenoids, $C_{carotenoid} = [1000\ A_{470} - 1.82\ (12.7\ A_{663} - 2.69\ A_{645}) - 85.02\ (22.90\ A_{645} - 4.68\ A_{663})]/198$ (Arnon, 1949; Lichtenthaler and Buschmann, 2001).

Anthocyanin extraction and quantification was adapted from Ticconi et al. (2001). Plant leaves were weighed (fresh weight, FW) and incubated at 100°C for 5 min in extraction buffer composed of 1-propanol, 37% (v/v) HCl and H_2O, in a 18:1:81 ratio. Samples were subsequently incubated overnight at room temperature, in the dark. The plant material was spinned down and absorbance of the supernatant was measured at 535 and 650 nm in a similar microplate spectrophotometer. Total anthocyanins were calculated as $C_{anthocyanins} = A_{535} - A_{650}\ g^{-1}$ FW.

RNA extraction, cDNA synthesis and RT-PCR

For quantitative Real-Time PCR (qPCR) analysis, RNA from plant tissue was extracted using an *RNeasy Plant Mini kit* (QIAGEN). RNA quantity and quality were assessed using both a Nanodrop ND-1000 spectrophotometer and standard agarose-gel electrophoretic analysis, and RNA samples were treated with *Recombinant DNase I* (Takara Biotechnology). Synthesis of cDNA was performed using *SuperScript II Reverse Transcriptase kit* (Invitrogen). *SsoFast EvaGreen Supermix* (BioRad) was used in the qPCR reaction mixture according to the manufacturer's indications. The reaction was performed in a *MyiQ Single-Color Real-Time PCR Detection system* (Bio-Rad). Primers for semiquantitative RT-PCR and qPCR (Appendix VI - Table S6.2) were designed using NCBI

Primer-BLAST (www.ncbi.nlm.nih.gov/tools/primer-blast/; Ye et al., 2012) to ensure specific amplification within the Arabidopsis genome, and obeyed the following guidelines: 100-250 bp PCR amplification product size; 50-60% GC content; ~60°C T_m. Primers were designed to span an exon junction when possible. *ACT2* (At3g18780) was used as a reference gene (Lozano-Duran et al., 2011).

Microarray analysis

Genome-wide transcription studies were performed using the ATH1 microarray chip (Affymetrix) with three independent replicates per genotype, each replicate represented RNA from a pool of four different MS plates containing 10-day-old plants. Plants were grown in a plant growth chamber with 16 h light/8 h dark cycle under cool white light (80 µE m^{-2} s^{-1} light intensity) at 21°C. RNA was extracted as previously detailed, followed by a column cleaning step using an *RNeasy Plant Mini kit* (QIAGEN). Microarray execution and differential expression analysis were conducted at Unité de Recherche en Génomique Végétale (Université d'Evry Val d'Essonne, France). The method to determine DEGs was based on variance modelisation by common variance of all genes (Gagnot et al., 2008).

Plant protein extraction and western blotting

Plant tissue was grinded in a microtube in liquid nitrogen with the help of polypropylene pestles. Protein extracts were obtained by adding extraction buffer [50 mM Tris; 150 mM NaCl; 0.2% (v/v) Triton X-100] supplemented with *Complete Protease Inhibitor Cocktail* (Roche) as per the manufacturer's instructions. Following incubation for 1 h at 4°C with agitation, microtubes were centrifuged two times for 30 min at 16000 *g*. The supernatant was subsequently recovered and stored at -80°C. Protein was spectrophotometrically quantified using *Bradford reagent* (Sigma; Bradford, 1976). Equal amounts of protein were resolved by standard SDS-PAGE in a 10% (w/v) acrylamide resolving gel, using a *Mini-PROTEAN Cell* (BIO-RAD) apparatus. For western blotting, proteins were transferred to a PVDF membrane using a *Mini Trans-Blot Cell* (Bio-Rad). The membrane was blocked for 1 h at 23°C in blocking solution [5% (w/v) dry milk powder in PBST]. The primary antibody anti-AtSUMO1 or anti-AtSUMO3 (ABCAM) were added in a 1:1000 dilution and incubated for 3 h. The membrane was washed three times with 10 mL of PBST for 10 min, and incubated with the secondary antibody (anti-rabbit, *Santa Cruz*; 1:2000 in blocking solution) for 1 h. The membrane was washed as previously detailed and developed by a chemiluminescence

reaction using the *Immune-Star WesternC Kit* (Bio-Rad) and a *ChemiDoc XRS system* (Bio-Rad) for image acquisition. PVDF membranes were incubated for 15 min with Ponceau S solution [0.1% (w/v) Ponceau S; 5% (v/v) acetic acid] to stain total proteins.

Phylogenetic and bioinformatics analysis

Phylogenetic analysis of the Ubiquitin-Like Protease family was carried out using the *SeaView v4.4.0* software (Gouy et al., 2010). Sequences were aligned using the *MUSCLE* algorithm (Edgar, 2004). Evolutionary relationships were inferred using Maximum Likelihood (PhyML) based on the JTT matrix-based model (Jones et al., 1992), with subsequent Bootstrap analysis (100 trees). Protein sequence alignment of the catalytic domain of Arabidopsis ULP2s with homologous proteins from eukaryotic organisms was performed using PRALINE (Simossis and Heringa, 2005).

GO term functional categorization was performed in VirtualPlant 1.2 (virtualplant.bio.nyu.edu/cgi-bin/vpweb/), using the BioMaps function with a 0.05 *p*-value cutoff (Katari et al., 2010). Redundancy exclusion and scatterplot analysis were performed using REVIGO (revigo.irb.hr/), with a 0.7 C-value. The scatterplot represents the cluster representatives in a two dimensional space (x- and y-axis) derived by applying multidimensional scaling to a matrix of the GO terms' semantic similarities (Supek et al., 2011). MapMan was used to plot *ulp2a/b* deregulated genes in the *Metabolism overview pathway* map (mapman.gabipd.org/web/guest/home; Thimm et al., 2004). Spatial plotting of *ulp2a/b* differentially expressed genes in the five *Arabidopsis thaliana* chromosomes was performed using *TAIR Chromosome Map Tool* (www.arabidopsis.org/jsp/ChromosomeMap/tool.jsp). Venn diagrams were obtained using Venn Diagram Generator (www.pangloss.com/seidel/Protocols/venn.cgi).

6.5. REFERENCES

Alegre KO, Reverter D (2011) Swapping small ubiquitin-like modifier (SUMO) isoform specificity of SUMO proteases SENP6 and SENP7. J Biol Chem **286:** 36142-36151

Alonso JM, Stepanova AN, Leisse TJ, Kim CJ, Chen H, Shinn P, Stevenson DK, Zimmerman J, Barajas P, Cheuk R, Gadrinab C, Heller C, Jeske A, Koesema E, Meyers CC, Parker H, Prednis L, Ansari Y, Choy N, Deen H, Geralt M, Hazari N, Hom E, Karnes M, Mulholland C, Ndubaku R, Schmidt I, Guzman P, Aguilar-Henonin L, Schmid M, Weigel D, Carter DE, Marchand T, Risseeuw E, Brogden D, Zeko A, Crosby WL, Berry CC, Ecker JR (2003) Genome-wide insertional mutagenesis of *Arabidopsis thaliana*. Science **301:** 653-657

Arnon DI (1949) Copper enzymes in isolated chloroplasts. Polyphenoloxidase in *Beta Vulgaris*. Plant Physiol **24:** 1-15

Baldwin ML, Julius JA, Tang X, Wang Y, Bachant J (2009) The yeast SUMO isopeptidase Smt4/Ulp2 and the polo kinase Cdc5 act in an opposing fashion to regulate sumoylation in mitosis and cohesion at centromeres. Cell Cycle **8:** 3406-3419

Borggrefe T, Yue X (2011) Interactions between subunits of the Mediator complex with gene-specific transcription factors. Semin Cell Dev Biol **22:** 759-768

Boyes DC, Zayed AM, Ascenzi R, McCaskill AJ, Hoffman NE, Davis KR, Görlach J (2001) Growth stage-based phenotypic analysis of Arabidopsis: a model for high throughput functional genomics in plants. Plant Cell **13:** 1499-1510

Bradford MM (1976) A rapid and sensitive method for the quantitation of microgram quantities of protein utilizing the principle of protein-dye binding. Anal Biochem **72:** 248-254

Castro PH, Tavares RM, Bejarano ER, Azevedo H (2012) SUMO, a heavyweight player in plant abiotic stress responses. Cell Mol Life Sci **69:** 3269-3283

Catala R, Ouyang J, Abreu IA, Hu Y, Seo H, Zhang X, Chua NH (2007) The Arabidopsis E3 SUMO ligase SIZ1 regulates plant growth and drought responses. Plant Cell **19:** 2952-2966

Chen R, Jiang H, Li L, Zhai Q, Qi L, Zhou W, Liu X, Li H, Zheng W, Sun J, Li C (2012) The Arabidopsis mediator subunit MED25 differentially regulates jasmonate and abscisic acid signaling through interacting with the MYC2 and ABI5 transcription factors. Plant Cell **24:** 2898-2916

Chosed R, Mukherjee S, Lois LM, Orth K (2006) Evolution of a signalling system that incorporates both redundancy and diversity: Arabidopsis SUMOylation. Biochem J **398:** 521-529

Cohen-Peer R, Schuster S, Meiri D, Breiman A, Avni A (2010) Sumoylation of Arabidopsis heat shock factor A2 (HsfA2) modifies its activity during acquired thermotholerance. Plant Mol Biol **74:** 33-45

Colby T, Matthai A, Boeckelmann A, Stuible HP (2006) SUMO-conjugating and SUMO-deconjugating enzymes from Arabidopsis. Plant Physiol **142:** 318-332

Conti L, Price G, O'Donnell E, Schwessinger B, Dominy P, Sadanandom A (2008) Small ubiquitin-like modifier proteases OVERLY TOLERANT TO SALT1 and -2 regulate salt stress responses in Arabidopsis. Plant Cell **20:** 2894-2908

Cubenas-Potts C, Matunis MJ (2013) SUMO: A multifaceted modifier of chromatin structure and function. Dev Cell **24:** 1-12

Durek P, Schmidt R, Heazlewood JL, Jones A, MacLean D, Nagel A, Kersten B, Schulze WX (2010) PhosPhAt: the *Arabidopsis thaliana* phosphorylation site database. An update. Nucleic Acids Res **38:** D828-834

Edgar RC (2004) MUSCLE: a multiple sequence alignment method with reduced time and space complexity. BMC Bioinformatics **5:** 113

Elfving N, Davoine C, Benlloch R, Blomberg J, Brannstrom K, Muller D, Nilsson A, Ulfstedt M, Ronne H, Wingsle G, Nilsson O, Bjorklund S (2011) The *Arabidopsis thaliana* Med25 mediator subunit integrates environmental cues to control plant development. Proc Natl Acad Sci U S A **108:** 8245-8250

Elrouby N, Coupland G (2010) Proteome-wide screens for small ubiquitin-like modifier (SUMO) substrates identify Arabidopsis proteins implicated in diverse biological processes. Proc Natl Acad Sci U S A **107:** 17415-17420

Fairchild CD, Schumaker MA, Quail PH (2000) HFR1 encodes an atypical bHLH protein that acts in phytochrome A signal transduction. Genes Dev **14:** 2377-2391

Gagnot S, Tamby JP, Martin-Magniette ML, Bitton F, Taconnat L, Balzergue S, Aubourg S, Renou JP, Lecharny A, Brunaud V (2008) CATdb: a public access to Arabidopsis transcriptome data from the URGV-CATMA platform. Nucleic Acids Res **36:** D986-990

Gareau JR, Lima CD (2010) The SUMO pathway: emerging mechanisms that shape specificity, conjugation and recognition. Nat Rev Mol Cell Biol **11:** 861-871

Geoffroy MC, Hay RT (2009) An additional role for SUMO in ubiquitin-mediated proteolysis. Nat Rev Mol Cell Biol **10:** 564-568

Gouy M, Guindon S, Gascuel O (2010) SeaView version 4: A multiplatform graphical user interface for sequence alignment and phylogenetic tree building. Mol Biol Evol **27:** 221-224

Hannich JT, Lewis A, Kroetz MB, Li SJ, Heide H, Emili A, Hochstrasser M (2005) Defining the SUMO-modified proteome by multiple approaches in *Saccharomyces cerevisiae*. J Biol Chem **280:** 4102-4110

Hay RT (2005) SUMO: a history of modification. Mol Cell **18:** 1-12

Hermkes R, Fu YF, Nurrenberg K, Budhiraja R, Schmelzer E, Elrouby N, Dohmen RJ, Bachmair A, Coupland G (2011) Distinct roles for Arabidopsis SUMO protease ESD4 and its closest homolog ELS1. Planta **233:** 63-73

Hickey CM, Wilson NR, Hochstrasser M (2012) Function and regulation of SUMO proteases. Nat Rev Mol Cell Biol **13:** 755-766

Hoen DR, Park KC, Elrouby N, Yu Z, Mohabir N, Cowan RK, Bureau TE (2006) Transposon-mediated expansion and diversification of a family of *ULP*-like genes. Mol Biol Evol **23:** 1254-1268

Hruz T, Laule O, Szabo G, Wessendorp F, Bleuler S, Oertle L, Widmayer P, Gruissem W, Zimmermann P (2008) Genevestigator v3: a reference expression database for the meta-analysis of transcriptomes. Adv Bioinformatics **2008:** 420747

Jin JB, Jin YH, Lee J, Miura K, Yoo CY, Kim WY, Van Oosten M, Hyun Y, Somers DE, Lee I, Yun DJ, Bressan RA, Hasegawa PM (2008) The SUMO E3 ligase, AtSIZ1, regulates flowering by controlling a salicylic acid-mediated floral promotion pathway and through affects on *FLC* chromatin structure. Plant J **53:** 530-540

Jones DT, Taylor WR, Thornton JM (1992) The rapid generation of mutation data matrices from protein sequences. Comput Appl Biosci **8:** 275-282

Katari MS, Nowicki SD, Aceituno FF, Nero D, Kelfer J, Thompson LP, Cabello JM, Davidson RS, Goldberg AP, Shasha DE, Coruzzi GM, Gutierrez RA (2010) VirtualPlant: a software platform to support systems biology research. Plant Physiol **152:** 500-515

Kidd BN, Edgar CI, Kumar KK, Aitken EA, Schenk PM, Manners JM, Kazan K (2009) The mediator complex subunit PFT1 is a key regulator of jasmonate-dependent defense in Arabidopsis. Plant Cell **21:** 2237-2252

Kroetz MB, Su D, Hochstrasser M (2009) Essential role of nuclear localization for yeast Ulp2 SUMO protease function. Mol Biol Cell **20:** 2196-2206

Kurepa J, Walker JM, Smalle J, Gosink MM, Davis SJ, Durham TL, Sung DY, Vierstra RD (2003) The small ubiquitin-like modifier (SUMO) protein modification system in Arabidopsis. Accumulation of SUMO1 and -2 conjugates is increased by stress. J Biol Chem **278:** 6862-6872

Lamesch P, Dreher K, Swarbreck D, Sasidharan R, Reiser L, Huala E (2010) Using the Arabidopsis information resource (TAIR) to find information about Arabidopsis genes. Curr Protoc Bioinformatics **Chapter 1:** Unit1 11

Lichtenthaler HK, Buschmann C (2001) Chlorophylls and carotenoids: measurement and characterization by UV-VIS spectroscopy. *In* Current Protocols in Food Analytical Chemistry. John Wiley & Sons, Inc.

Lima CD, Reverter D (2008) Structure of the human SENP7 catalytic domain and poly-SUMO deconjugation activities for SENP6 and SENP7. J Biol Chem **283:** 32045-32055

Lois LM (2010) Diversity of the SUMOylation machinery in plants. Biochem Soc Trans **38:** 60-64

Lozano-Duran R, Rosas-Diaz T, Gusmaroli G, Luna AP, Taconnat L, Deng XW, Bejarano ER (2011) Geminiviruses subvert ubiquitination by altering CSN-mediated derubylation of SCF E3 ligase complexes and inhibit jasmonate signaling in *Arabidopsis thaliana*. Plant Cell **23:** 1014-1032

Mazur MJ, van den Burg HA (2012) Global SUMO proteome responses guide gene regulation, mRNA biogenesis, and plant stress responses. Front Plant Sci **3:** 215

Miller MJ, Barrett-Wilt GA, Hua Z, Vierstra RD (2010) Proteomic analyses identify a diverse array of nuclear processes affected by small ubiquitin-like modifier conjugation in Arabidopsis. Proc Natl Acad Sci U S A **107:** 16512-16517

Miller MJ, Scalf M, Rytz TC, Hubler SL, Smith LM, Vierstra RD (2013) Quantitative proteomics reveals factors regulating RNA biology as dynamic targets of stress-induced SUMOylation in Arabidopsis. Mol Cell Proteomics **12:** 449-463

Miura K, Hasegawa PM (2010) Sumoylation and other ubiquitin-like post-translational modifications in plants. Trends Cell Biol **20:** 223-232

Miura K, Jin JB, Hasegawa PM (2007a) Sumoylation, a post-translational regulatory process in plants. Curr Opin Plant Biol **10:** 495-502

Miura K, Jin JB, Lee J, Yoo CY, Stirm V, Miura T, Ashworth EN, Bressan RA, Yun DJ, Hasegawa PM (2007b) SIZ1-mediated sumoylation of ICE1 controls *CBF3/DREB1A* expression and freezing tolerance in Arabidopsis. Plant Cell **19:** 1403-1414

Miura K, Lee J, Jin JB, Yoo CY, Miura T, Hasegawa PM (2009) Sumoylation of ABI5 by the Arabidopsis SUMO E3 ligase SIZ1 negatively regulates abscisic acid signaling. Proc Natl Acad Sci U S A **106:** 5418-5423

Miura K, Lee J, Miura T, Hasegawa PM (2010) SIZ1 controls cell growth and plant development in Arabidopsis through salicylic acid. Plant Cell Physiol **51:** 103-113

Miura K, Rus A, Sharkhuu A, Yokoi S, Karthikeyan AS, Raghothama KG, Baek D, Koo YD, Jin JB, Bressan RA, Yun DJ, Hasegawa PM (2005) The Arabidopsis SUMO E3 ligase SIZ1 controls phosphate deficiency responses. Proc Natl Acad Sci U S A **102:** 7760-7765

Murashige T, Skoog F (1962) A revised medium for rapid growth and bio assays with tobacco tissue cultures. Physiol Plant **15:** 473-475

Murtas G, Reeves PH, Fu YF, Bancroft I, Dean C, Coupland G (2003) A nuclear protease required for flowering-time regulation in Arabidopsis reduces the abundance of SMALL UBIQUITIN-RELATED MODIFIER conjugates. Plant Cell **15:** 2308-2319

Nemhauser JL, Hong F, Chory J (2006) Different plant hormones regulate similar processes through largely nonoverlapping transcriptional responses. Cell **126:** 467-475

Novatchkova M, Tomanov K, Hofmann K, Stuible HP, Bachmair A (2012) Update on sumoylation: defining core components of the plant SUMO conjugation system by phylogenetic comparison. New Phytol **195:** 23-31

O'Connor TR, Dyreson C, Wyrick JJ (2005) Athena: a resource for rapid visualization and systematic analysis of Arabidopsis promoter sequences. Bioinformatics **21:** 4411-4413

Park BS, Song JT, Seo HS (2011) Arabidopsis nitrate reductase activity is stimulated by the E3 SUMO ligase AtSIZ1. Nat Commun **2:** 400

Pinto MP, Carvalho AF, Grou CP, Rodriguez-Borges JE, Sa-Miranda C, Azevedo JE (2012) Heat shock induces a massive but differential inactivation of SUMO-specific proteases. Biochim Biophys Acta **1823:** 1958-1966

Saracco SA, Miller MJ, Kurepa J, Vierstra RD (2007) Genetic analysis of SUMOylation in Arabidopsis: conjugation of SUMO1 and SUMO2 to nuclear proteins is essential. Plant Physiol **145:** 119-134

Schepens I, Boccalandro HE, Kami C, Casal JJ, Fankhauser C (2008) PHYTOCHROME KINASE SUBSTRATE4 modulates phytochrome-mediated control of hypocotyl growth orientation. Plant Physiol **147:** 661-671

Simossis VA, Heringa J (2005) PRALINE: a multiple sequence alignment toolbox that integrates homology-extended and secondary structure information. Nucleic Acids Res **33:** W289-294

Strunnikov AV, Aravind L, Koonin EV (2001) *Saccharomyces cerevisiae* SMT4 encodes an evolutionarily conserved protease with a role in chromosome condensation regulation. Genetics **158:** 95-107

Supek F, Bosnjak M, Skunca N, Smuc T (2011) REVIGO summarizes and visualizes long lists of gene ontology terms. PLoS One **6:** e21800

Thimm O, Blasing O, Gibon Y, Nagel A, Meyer S, Kruger P, Selbig J, Muller LA, Rhee SY, Stitt M (2004) MAPMAN: a user-driven tool to display genomics data sets onto diagrams of metabolic pathways and other biological processes. Plant J **37:** 914-939

Ticconi CA, Delatorre CA, Abel S (2001) Attenuation of phosphate starvation responses by phosphite in Arabidopsis. Plant Physiol **127:** 963-972

Toufighi K, Brady SM, Austin R, Ly E, Provart NJ (2005) The Botany Array Resource: e-Northerns, Expression Angling, and promoter analyses. Plant J **43:** 153-163

Van Bel M, Proost S, Wischnitzki E, Movahedi S, Scheerlinck C, Van de Peer Y, Vandepoele K (2012) Dissecting plant genomes with the PLAZA comparative genomics platform. Plant Physiol **158:** 590-600

van den Burg HA, Kini RK, Schuurink RC, Takken FL (2010) Arabidopsis small ubiquitin-like modifier paralogs have distinct functions in development and defense. Plant Cell **22:** 1998-2016

van der Hoorn RA (2008) Plant proteases: from phenotypes to molecular mechanisms. Annu Rev Plant Biol **59:** 191-223

Vandepoele K, Quimbaya M, Casneuf T, De Veylder L, Van de Peer Y (2009) Unraveling transcriptional control in Arabidopsis using cis-regulatory elements and coexpression networks. Plant Physiol **150:** 535-546

Vierstra RD (2012) The expanding universe of ubiquitin and ubiquitin-like modifiers. Plant Physiol **160:** 2-14

Wilkinson KA, Henley JM (2010) Mechanisms, regulation and consequences of protein SUMOylation. Biochem J **428:** 133-145

Winter D, Vinegar B, Nahal H, Ammar R, Wilson GV, Provart NJ (2007) An "Electronic Fluorescent Pictograph" browser for exploring and analyzing large-scale biological data sets. PLoS One **2:** e718

Xu XM, Rose A, Muthuswamy S, Jeong SY, Venkatakrishnan S, Zhao Q, Meier I (2007) NUCLEAR PORE ANCHOR, the Arabidopsis homolog of Tpr/Mlp1/Mlp2/megator, is involved in mRNA export and SUMO homeostasis and affects diverse aspects of plant development. Plant Cell **19:** 1537-1548

Ye J, Coulouris G, Zaretskaya I, Cutcutache I, Rozen S, Madden TL (2012) Primer-BLAST: A tool to design target-specific primers for polymerase chain reaction. BMC Bioinformatics **13:** 134

Zheng Y, Schumaker KS, Guo Y (2012) Sumoylation of transcription factor MYB30 by the small ubiquitin-like modifier E3 ligase SIZ1 mediates abscisic acid response in *Arabidopsis thaliana*. Proc Natl Acad Sci U S A **109:** 12822-12827

Zhu X, Liu B, Carlsten JO, Beve J, Nystrom T, Myers LC, Gustafsson CM (2011) Mediator influences telomeric silencing and cellular life span. Mol Cell Biol **31:** 2413-2421

Chapter 7

Concluding remarks and future perspectives

CONTENTS

It has become increasingly consensual that SUMO is important for plant development and the response to hostile environmental conditions, however there is an underlying complexity to SUMO function that remains to be resolved. SUMO controls the homeostasis of several hormones, thus impacting on plant growth and development. SUMO is also involved in the transition from normal developmental status to a stress responsive mode. Many transcription regulators are sumoylated in response to specific conditions, and that reflects on the whole-plant transcriptome. The SUMO conjugation and deconjugation cycle has to be tightly regulated, and numerous SUMO proteases are fundamental for this equilibrium. In addition, sumoylation may intercept with other post-translational modifications (PTMs) such as phosphorylation by MAPKs. In the present work, *Arabidopsis thaliana* served as a model to study the role of SUMO in plants, using functional genomics that was based mostly on loss-of-function mutants and reverse genetics. Since SUMO is present in all eukaryotes, it is likely that many regulatory mechanisms described in the present work find parallel in other biological models. The following sections will discuss the main outputs of the current work.

7.1. SUMO PROTEASES ARE A SOURCE OF SPECIFICITY

In contrast to the low number of components involved in each step (E1, E2 and E3) that lead to SUMO conjugation, SUMO proteases are more abundant and diverse. The main family of SUMO proteases is the Ubiquitin-like protease (ULP) family, although new types were recently found in other biological systems and are likely to exist in plants (Hickey et al., 2012). ULPs are a highly likely source of specificity within the SUMO pathway, since they display differential SUMO isoform discrimination, enzymatic activity, subcellular localization and expression pattern (Fig. 7.1).

Our phylogenetic studies (Chapter 6) divided plant ULPs into four subgroups: (1) ESD4/ULP1a/ULP1b, (2) ULP1c/ULP1d, (3) ULP1e, and (4) ULP2a/b. The ULPs amino acid identity is restricted to the catalytic domain, and the proteins' N- and C-terminal ends that flank the catalytic domain may contribute for activity regulation. For instance, ULP2b is predicted to be phosphorylated in the C-terminus. With the exception of *esd4*, *ulp1d* and *ulp2b*, single T-DNA insertion mutants for the remainder of ULPs revealed no obvious developmental phenotypes. Interestingly, within each branch, these three ULPs (*ESD4*, *ULP1d*, and *ULP2b*) are the ones with

highest expression (Fig. 7.1D). Expression levels seem to be particularly important, and partial redundancy is expected within each subgroup. In Chapter 4 we concluded that *ULP1c* and *ULP1d* have a similar expression pattern using *promoter::GUS* lines, while bioinformatic analysis showed them to be highly co-expressed. Still, we were able to establish that *ULP1d* is more expressed and plays a dominant role within the ULP1c/d gene pair. Interestingly, in Chapter 5 we noticed that the *ULP1c* overexpression line showed development phenotypes. Overall results indicate that *ULP1c/d* display unequal redundancy in the control of developmental traits and drought responses.

We also evidenced for the first time that ULP2a and ULP2b display unequal redundancy (Chapter 6), while confirming that *ULP2b* is more expressed than *ULP2a*. Promoter swap and overexpression lines of these proteases in the *ulp2a/b* background will help clarify whether ULP2b is functionally more important because of its increased expression levels, or due to different enzymatic properties compared to ULP2a. A similar strategy can be devised to estimate ULP1c and ULP1d function. As previously established for other ULPs, subcellular localization is an important aspect of their biological function (Fig. 7.1C). ULP2a/b are predicted to be nuclear located (Chapter 6), but future characterization of the subcellular and possibly subnuclear localization of ULP2s will be a key aspect of their functional characterization. Moreover, a complete characterization of ULP2s' in vitro enzymatic activity and isoform discrimination is necessary for their activity classification (Fig. 7.1A,B), especially to establish whether they are SUMO chain editing proteases like ULP2-type in yeast and mammals.

ULPs are a diversified component of the sumoylation pathway, containing many layers of regulation and activities. They are likely to be important for the overall dynamics of sumoylation, and also natural candidates for the control of specific sets of SUMO targets. New high-throughput approaches will be essential to resolve the sumoylome that is modulated by specific sets of ULPs. One possibility is the use of the previously described Arabidopsis line His-H89R-SUMO1 *sum1-1 sum2-1* (Miller et al., 2010), introgressed into ULP mutant backgrounds. This strategy will allow a stringent affinity purification of SUMO-conjugates by sequential Ni-NTA, anti-SUMO1, and Ni-NTA affinity chromatography followed by peptide identification through MS analysis (Miller et al., 2010). Furthermore, combinations of loss-of-function mutants are being produced that will help circumvent the potential functional redundancy between subgroups of ULPs. This strategy will help us address the global contribution of ULPs for plant development and the response to adverse conditions.

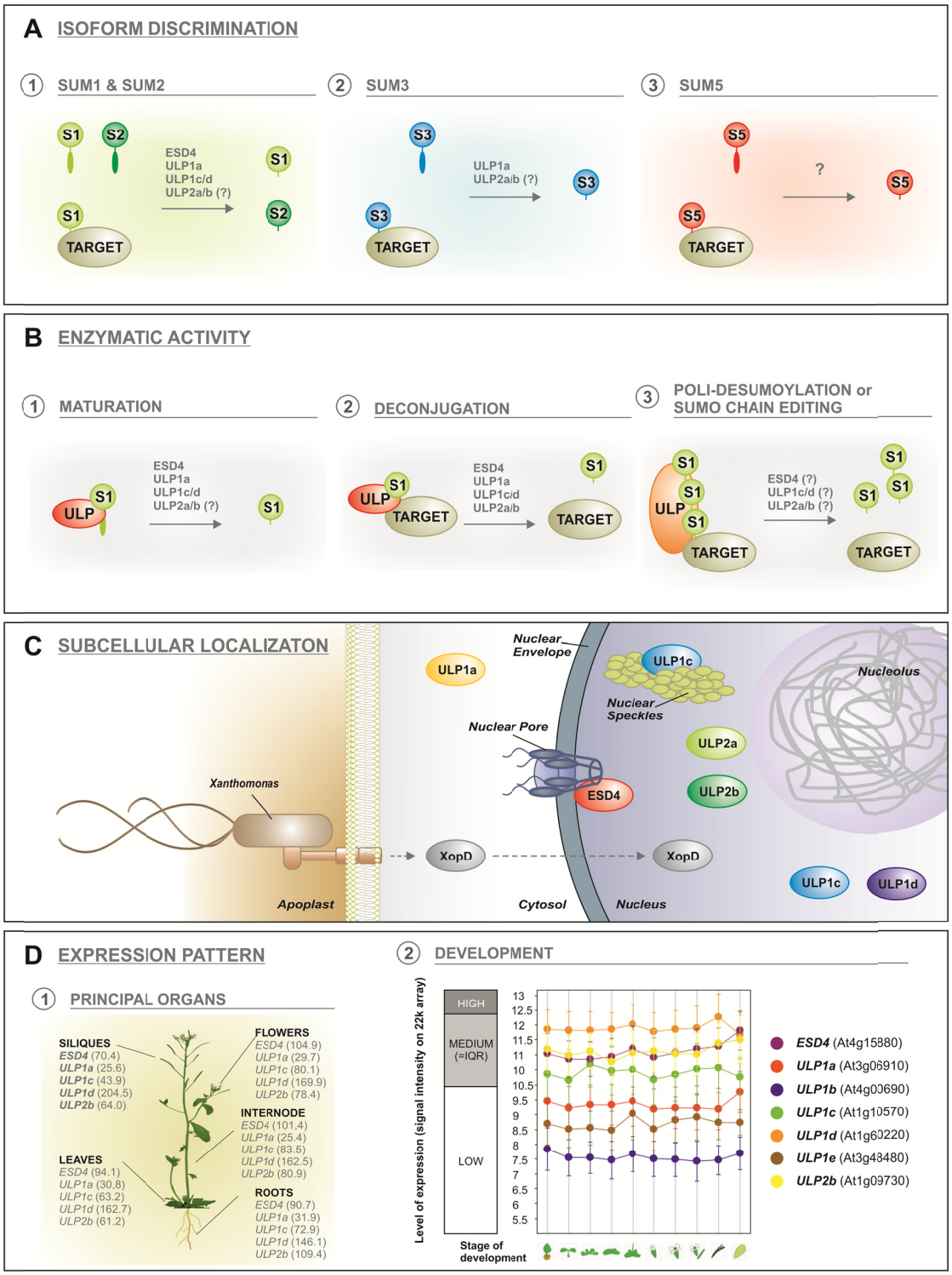

Figure 7.1. Plant Ubiquitin-like proteases (ULPs) are a likely source of specificity within the sumoylation pathway, by displaying a set of differentiating features that include specificity in the recognition of different SUMO peptides (**A**), preferential isopeptidase, endopeptidase or poli-desumoylating activities (**B**), different subcellular and subnuclear locations (**C**), differential whole-plant expression patterns (**D**). In D, the expression values of ULPs for (1) principal organs and (2) developmental stage were determined using *Arabidopsis eFP Browser* (Winter et al., 2007) and *Genevestigator* (Hruz et al., 2008), respectively.

7.2. SUMO COMPONENTS ARE ESSENTIAL FOR PLANT GROWTH AND DEVELOPMENT

SUMO-conjugates differ in plant organ expression pattern (data not shown; Saracco et al., 2007). Arabidopsis SUMO peptides have distinct spatial expression patterns and intensities (Saracco et al., 2007; van den Burg et al., 2010), while *SIZ1*, *ULP1a*, and *ULP1c/d* are expressed throughout plant development (Chapter 4; Catala et al., 2007; Hermkes et al., 2011). This ubiquitous presence of SUMO and sumoylation machinery components in plant organs (Fig. 7.1D) is clearly indicative of a central role in development. Previously, it was reported that disruption of components of the Arabidopsis SUMO conjugation machinery, more specifically SUM1/2 peptides, E1 subunit SAE2 and E2 SCE1, resulted in embryo lethality (Saracco et al., 2007). Loss-of-function mutants for the two characterized Arabidopsis E3 ligases (SIZ1 and HPY2) are not lethal, yet they are severely dwarfed (Chapter 2; Miura et al., 2010; Ishida et al., 2012). The *siz1* dwarfism should be considered a conditional phenotype because exposure to certain environmental conditions significantly reverts the phenotype. One example is the exogenous ammonium supplementation that reverts *siz1* plants to wild-type (Park et al., 2011). In Chapter 3 we found that long-term exposure to a mild increase in temperature (28-30°C) produced a similar effect. This reversion is likely due to salicylic acid (SA), as many other SA-accumulators are reverted by a mild increase in temperature, including *mpk4* and *mkk1/2* (Chapter 3). In addition, *siz1* in the *NahG* background (that enzymatically degrades SA) greatly recovers the wild-type phenotype (Chapter 2) and blocks constitutive defence responses (Lee et al., 2007b).

SIZ1 is involved in the prevention of autoimmunity, controlling SA signaling and reactive oxygen species (ROS) homeostasis. We showed that ROS levels are affected in *siz1*, accumulating hydrogen peroxide, superoxide, and singlet oxygen (Chapter 2). This deregulation in ROS homeostasis is partially due to SA over-accumulation, and SA and ROS are likely to function in an amplification loop (Vlot et al., 2009). One important prospect is to determine whether decreasing endogenous ROS in *siz1* will contribute for phenotype recovery. One strategy would be to knockout the NADPH oxidase *RBOHD*, an important ROS systemic signal generator (Miller et al., 2009) that is up-regulated in *siz1* (Chapter 2). Alternatively, *siz1* may be introgressed into null mutants of major ROS-scavenging enzymes such as CATs and APX1. Although ascorbate peroxidase (APX) activity was not affected in *siz1* seedlings, APX1 may be an important SUMO-target since it is highly sumoylated in response to hydrogen peroxide (Miller et al., 2013). APX1 sumoylation and its effect on protein activity is surely an interesting subject for future research. Additionally, several chromatin remodeling proteins are particularly sumoylated following oxidative stress, and can be

involved in the control of plant development and stress responses trough transcription regulation (Chapter 2; also discussed later).

In the case of SUMO proteases, ULP mutants have a diversity of phenotypes. Indeed, ULP1c/d act redundantly to control plant growth and flowering time (Chapter 4). Albeit *ulp2b* showing some defects, the double mutant *ulp2a/b* has enhanced defects that include altered leaf morphology, higher pigment content, late flowering, lower seed production and bigger seeds (Chapter 6). The *esd4*, *ulp1c/d* and *ulp2a/b* mutants over-accumulate SUMO-conjugates (data not shown; Chapter 4 and 6). In contrast, *ULP1c/d* overexpression lines accumulate less SUMO-conjugates (Chapter 5). In plants, a balance between SUMO conjugation and deconjugation is expected to take place, and ULPs can contribute to both via their endopeptidase and isopeptidase activities, respectively. To genetically test ULP involvement with conjugation components, we produced ULP mutants in the *siz1* background. While no drastic changes were observed for *esd4 siz1* and *ulp2a/b siz1* relatively to *siz1*, *ulp1c/d siz1* showed enhanced growth defects (Table 7.1). The intermediate SUMO-conjugation pattern of *esd4 siz1* and enhanced dwarfism of *ulp1c/d siz1* indicates that some targets are not shared with SIZ1. The *ulp2a/b* double mutant shows an antagonistic phenotype to *siz1*, but the triple *ulp2a/b siz1* mutant's phenotype and SUMO profile is *siz1*-like, placing ULP2a/b epistatically and downstream of SIZ1. Interestingly, some traits are common to several SUMO components, such as the fact that mutants show altered flowering times, and members of the xyloglucan endotransglucosylase/hydrolase (XTH) family are often deregulated, as we demonstrated for *siz1*, *ulp1c/d* and *ulp2a/b* (Chapter 4-6).

Table 7.1. Phenotypes of SUMO protease mutants in the *siz1* background.

Mutant	Phenotype	SUMO profile	References
esd4 siz1	*siz1*-like	Intermediate between *siz1* and *esd4*	Data not shown
ulp1c/d siz1	Enhanced *siz1* dwarfism	n.d.	Chapter 4
ulp2a/b siz1	*siz1*-like but slightly bigger at latter stages	*siz1*-like	Chapter 6

n.d. - not determined

7.3. SUMO CONTROLS PLANT HORMONE HOMEOSTASIS AND HORMONAL RESPONSES

Developmental and environmental responses depend on key hormone circuit signaling, and many development defects in SUMO mutants are a consequence of hormonal deregulation. In Chapter 2 we showed that *siz1* developmental defects are significantly driven by SA accumulation, creating a state of constitutive immune responses that compromise plant growth. Part of the *siz1* dwarf phenotype can be reverted by the transgene *NahG* and the mutant *pad4* (Chapter 2; Lee et al., 2007b; Miura et al., 2010). SIZ1 is upstream of SA, controlling expression of SA-associated genes such as *EDS1*, *PAD4, ESD5* and *NPR1* involved in the signaling pathway of SA, or *Isocorismate Synthase 1* (*ICS1/SID2*), a key enzyme in SA biosynthesis (Wildermuth et al., 2001; Catala et al., 2007; Lee et al., 2007a). Analysis of the Arabidopsis sumoylome described in Chapter 1 allowed us to conclude that many SUMO targets are also associated to ethylene (ET) metabolism and signaling. These include transcription factors such as EIN3, EIL1, and ERFs. EIN3 is a key transcriptional inhibitor of *Isocorismate Synthase 1* (*ICS1/SID2*) expression (Chen et al., 2009), making this transcription factor (TF) a good candidate for constitutive SA-regulation by SUMO, and ethylene signaling as an upstream component to sumoylation. The SIZ1 mutant growing in an ethylene-supplemented medium shows an insensitive phenotype when compared to wild-type plants (Table 7.2). This suggests a positive effect of SIZ1-dependent sumoylation on EIN3. Interestingly ET biosynthesis components also seem to interplay with SUMO at both the transcriptional and PTM levels (data not shown; Miller et al., 2010). The involvement of SUMO in ET signaling via TF regulation is surely an interesting topic for future research.

In addition to these two hormones, jasmonic acid (JA) is normally assumed to be antagonist to SA and agonist to ET (Pieterse et al., 2012). The *siz1* mutant displays a root developmental phenotype characterized by increased root hair formation in the presence of exogenous JA. MYC2, a key TF in the JA pathway, was suggested to be a sumoylation target (being sumoylated in bacteria), and was shown to interact with two SUMO pathway components, SCE and ESD4 (Elrouby and Coupland, 2010). Characterizing MYC2 sumoylation in vivo and establishing its consequences will be important, especially in what concerns root hair development.

Both *siz1* and *ulp1c/d* seem to be involved auxin responses (Chapter 5; Miura et al., 2011). SIZ1 controls auxin patterning during Pi-starvation (Miura et al., 2011), while we have shown that ULP1c/d controls many auxin-regulated genes in response to infection, including *PIN7*, *GH3*, and *SAURs* (Chapter 5). Additionally, the *ulp1c/d* mutant displays root sensitivity to exogenously supplemented auxins (Chapter 5). In the future, ULP1c/d involvement in root growth

and in response to stress that alters specific patterns of auxin signaling can be visualized using the *proDR5::GUS ulp1c/d* line described in Chapter 5.

Table 7.2. Hormone-related phenotypes in mutants of the SUMO pathway studied in the present work.

Hormone	Mutant	Phenotype	References
Ethylene	*siz1*	Root insensitivity to exogenous ACC	Not shown
	ulp1c/d	No phenotype observed	Not shown
Salicylic acid	*siz1*	SA accumulation; dwarf phenotype partially reverted by *NahG* and in a small extent by *sid2*	Chapter 2; not shown
Jasmonic acid	*siz1*	Increased root hair formation	Not shown
	ulp1c/d	No phenotype observed	Not shown
Auxins	*ulp1c/d*	Sensitive to exogenous auxin; auxin-related genes down-regulated during *Pst* DC3000 infection	Chapter 5
Abscisic acid	*siz1*	Hypersensitive to ABA during germination	Not shown
	ulp1c/d	Slight sensitivity during seed germination; no root growth phenotype; ABA-related genes deregulated	Chapter 4
	ulp2a/b	No root growth phenotype	Not shown

Abscisic acid (ABA), a key hormone in abiotic stress responses, was previously associated to sumoylation via the SIZ1-mediated sumoylation of ABI5 (for review see Chapter 1) and more recently of MYB30 (Zheng et al., 2012). ABA genes, such as *ABA1* involved in ABA biosynthesis, are deregulated in the early stages of *siz1* development, even before deregulation of SA-related genes (Chapter 2). This observation suggests that SA and ABA regulation by SUMO are possibly independent. In addition, in Chapter 4 we found that several ABA-regulated genes were deregulated in *ulp1c/d*, but no obvious phenotype for *ulp1c/d* was seen in response to exogenous ABA supplementation.

7.4. SUMO DYNAMICS IS IMPORTANT FOR AN ADEQUATE RESPONSE TO STRESS

Sumoylation is a great example of a PTM that acts rapidly and reversibly in response to stress (reviewed in Chapter 1). For instance, plant exposure to heat shock, even for some minutes, readily leads to accumulation of high molecular weight SUMO-conjugates (Chapter 6; Kurepa et al., 2003). In fact, we have shown that SUMO-conjugate increment is partially dependent of SIZ1 in response to heat shock, drought, and oxidative stresses (Chapter 2, 4 and 6). Oxidative stress is common to various stresses and may be a link between stress perception and sumoylation. In Chapter 2 we show that the *siz1* knockout mutant is a ROS over-accumulator and, at the same time, sensitive to exogenous ROS inducers. SIZ1 may be involved in the sumoylation of SA-regulatory proteins or directly regulate ROS scavenging enzymes (Fig. 7.2), although no altered ROS scavenger activity was detected in *siz1* (Chapter 2). Miller et al. (2013) recently showed that in plants, diverse stresses do not generate an increase in the variety of SUMO-conjugated proteins, rather they increase the abundance of the sumoylated form of pre-existing SUMO targets. However, we concluded that specific sumoylation can occur. For instance, in Chapter 5, specific bands appeared in response to *Pst* DC3000 challenging. The identification of this target would be important to understand the involvement of SUMO in biotic stress. In addition to salt stress, we have found that ULP1c/d may be involved in the drought stress response (Chapter 4). The *ulp1c/d* mutant displayed up-regulation of drought and ABA responsive genes under normal growth conditions, suggesting an involvement of ULP1c/d in low water availability responses. The double mutant *ulp1c/d* is less susceptible to drought in late developmental stages, but seedlings are more sensitive to low water potential media. Moreover, in Chapter 5 we showed that *ulp1c/d* is less susceptible to *Pst* DC3000, possibly interfering with auxin perception. ULP2a and ULP2b proteases lack a functional association to stress, but since they seem to act antagonistically to SIZ1, it is very likely that they are involved in multiple environmental stress responses.

7.5. SUMO CONTROLS THE TRANSCRIPTOME BY MODIFYING TRANSCRIPTION REGULATORS

We have been witness to an increase in strategies towards the identification of the total pool of SUMO-conjugates (Chapter 1), establishing what can be designated as the sumoylome. Recent publications already include the identification of SUMO-conjugates specifically induced by

stress (Miller et al., 2013). One overall observation is that many SUMO targets are transcription factors, components involved in RNA metabolism, or chromatin remodeling proteins (Chapter 1). As expected, mutating SUMO components has consequences on gene expression (Chapter 2 to 6). Since genes that are co-expressed are likely to be regulated by the same set of transcriptional regulators, transcriptome analysis of mutants allows us to establish co-expression networks that can be surveyed for *cis*-element enrichment. Because *cis*-elements are binding sites that are recognized by specific transcriptional regulators, we can cross-reference this information with already known SUMO-conjugates, to identify putative targets for each SUMO component.

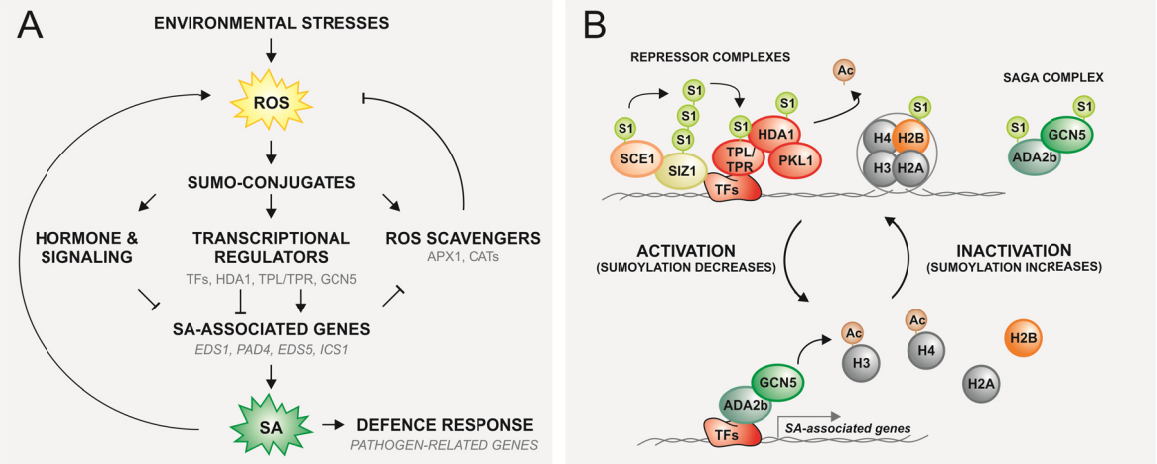

Figure 7.2. Interplay between reactive oxygen species (ROS), salicylic acid (SA) and sumoylation in the control of transcription. **A**, ROS induces SUMO-conjugates that are involved in hormone/signaling, transcription regulation and ROS scavenging. Transcriptional regulators that are sumoylated are involved in both histone acetylation and deacetylation. De-repression of chromatin lead to the expression of SA-associated genes, contributing for SA and ROS accumulation, and ultimately to enhanced defence responses. **B**, Proposed molecular mechanism for the regulation of SA-associated gene expression, by transcriptional regulators that are sumoylated in response to oxidative stress. Red coloring highlights transcriptional repression components and green represents positive regulators, such as members of the SAGA complex involved in histone acetylation. Sumoylation of transcriptional repressors contributes for the assembly of repression complexes, while desumoylated SAGA may alleviate repression by acetylation of histones.

In Chapter 2 we compared the *siz1* microarray analysis with that of Catala et al. (2007). Some aspects differ between the two microarray experiments. Different mutant alleles were used, and our plants were grown in vitro for 10 days, while Catala et al. (2007) used adult plants grown in soil. This could explain why only ~20% of DEGs overlapped between both experiments. However, some conclusions can be assumed, such as the fact that no key SA-associated genes were observed in in vitro-grown seedlings. Therefore, common DEGs to both microarrays are likely to be involved in SIZ1 functions other than those involving SA.

ULP1c/d growing in standard conditions showed many deregulated ABA- and drought-responsive genes, and we observed an over-representation of *cis* elements binding ATHB6. ATHB6 controls ABA responses and was predicted to be SUM1 modified (Miller et al., 2010; Lechner et al., 2011). Also the DREB1A/CBF3-binding site was enriched in *ulp1c/d* DEGs, but as previously described, this TF is regulated transcriptionally by SIZ1 via ICE1 (Miura et al., 2007), making ICE1 the most likely ULP1c/d target. In response to infection, promoters of ULP1c/d DEGs were enriched in W-box elements, the binding site for WRKY TFs. Many WRKYs are sumoylated (Chapter 5), and it is tempting to speculate that the specific band identified in the SUMO pattern following pathogen infection (Fig. 5.3) could be a sumoylated WRKY. One important observation reported in Chapter 3 is that MAPK mutants and the *siz1* transcriptome profiles match. In accordance, many targets are common to both PTM cascades, including WRKY TFs. Future research should focus on WRKY-SUMO interplay and how PTMs dynamically control the activity of this TF class.

ULP2a/b-regulated genes were enriched in the MYC2 binding site (Chapter 6), and MYC2 interacts with SCE1 and ESD4 (Elrouby and Coupland, 2010). The most intriguing aspect of the *ulp2a/b* transcriptional signature is that DEGs display a specific chromosomal distribution (Chapter 6). Down-regulated genes are located near the telomeric zone, while up-regulated genes are at the middle of the chromosomic arms. One plausible hypothesis is that ULP2a/b regulates specific telomere gene expression through the Mediator complex. Zhu et al. (Zhu et al., 2011) showed that the Mediator complex in yeast influences telomeric silencing, and MED25/PTF1 was found in SUM1-modified targets (Miller et al., 2010; Miller et al., 2013). Also the histone H2B was previously associated to the telomere, and is thus a good candidate for SIZ1 sumoylation followed by ULP2a/b de-conjugation. Techniques such as co-immunoprecipitation (CoIP) and ChIP-on-chip analysis would help clarify if ULP2a/b interact with these targets and consequently influence gene expression.

SUMO components are themselves the subject of transcriptional regulation. In Chapter 2 we noticed that 10-day-old *siz1* seedlings showed up-regulation of *SIZ1* and *SCE1* expression. This suggests that the expression of *SIZ1* and *SCE1* is elevated in an attempt to compensate dysfunctional SUMO conjugation. Apart from the sumoylome, SUMO-interacting proteins may be just as important for SUMO functioning. Covalent and non-covalent interactions with SUMO are involved in assembly complexes, and it has been well established that SUMO works as a recruiting protein, for instance of histone deacetylases (Fig. 7.2; Mazur and van den Burg, 2012; Cubenas-Potts and Matunis, 2013). ULP2a/b may act as SUMO chain editing proteases (Chapter 6),

avoiding docking sites for SUMO-interacting proteins. One such example are SUMO-targeted ubiquitin ligases (STUbLs) that target poly-sumoylated proteins for degradation in yeast and human (Geoffroy and Hay, 2009). SIZ1 is heavily sumoylated during stress imposition (Miller et al., 2013) and its activity can be modulated by SUMO and ULP2-type proteases.

In the present work a series of developments were achieved concerning the functional characterization of several SUMO pathway components. Implications to the role of SUMO in development, hormonal regulation, biotic and particularly abiotic stress responses were established, providing an important framework for future studies. The current knowledge ensures us that SUMO and the sumoylation pathway will continue to be a highly relevant topic in plant physiology in forthcoming years.

7.6. REFERENCES

Catala R, Ouyang J, Abreu IA, Hu Y, Seo H, Zhang X, Chua NH (2007) The Arabidopsis E3 SUMO ligase SIZ1 regulates plant growth and drought responses. Plant Cell **19:** 2952-2966

Chen H, Xue L, Chintamanani S, Germain H, Lin H, Cui H, Cai R, Zuo J, Tang X, Li X, Guo H, Zhou JM (2009) ETHYLENE INSENSITIVE3 and ETHYLENE INSENSITIVE3-LIKE1 repress *SALICYLIC ACID INDUCTION DEFICIENT2* expression to negatively regulate plant innate immunity in Arabidopsis. Plant Cell **21:** 2527-2540

Cubenas-Potts C, Matunis MJ (2013) SUMO: A multifaceted modifier of chromatin structure and function. Dev Cell **24:** 1-12

Elrouby N, Coupland G (2010) Proteome-wide screens for small ubiquitin-like modifier (SUMO) substrates identify Arabidopsis proteins implicated in diverse biological processes. Proc Natl Acad Sci U S A **107:** 17415-17420

Geoffroy MC, Hay RT (2009) An additional role for SUMO in ubiquitin-mediated proteolysis. Nat Rev Mol Cell Biol **10:** 564-568

Hermkes R, Fu YF, Nurrenberg K, Budhiraja R, Schmelzer E, Elrouby N, Dohmen RJ, Bachmair A, Coupland G (2011) Distinct roles for Arabidopsis SUMO protease ESD4 and its closest homolog ELS1. Planta **233:** 63-73

Hickey CM, Wilson NR, Hochstrasser M (2012) Function and regulation of SUMO proteases. Nat Rev Mol Cell Biol **13:** 755-766

Hruz T, Laule O, Szabo G, Wessendorp F, Bleuler S, Oertle L, Widmayer P, Gruissem W, Zimmermann P (2008) Genevestigator v3: a reference expression database for the meta-analysis of transcriptomes. Adv Bioinformatics **2008:** 420747

Ishida T, Yoshimura M, Miura K, Sugimoto K (2012) MMS21/HPY2 and SIZ1, two Arabidopsis SUMO E3 ligases, have distinct functions in development. PLoS One **7:** e46897

Kurepa J, Walker JM, Smalle J, Gosink MM, Davis SJ, Durham TL, Sung DY, Vierstra RD (2003) The small ubiquitin-like modifier (SUMO) protein modification system in Arabidopsis. Accumulation of SUMO1 and -2 conjugates is increased by stress. J Biol Chem **278:** 6862-6872

Lechner E, Leonhardt N, Eisler H, Parmentier Y, Alioua M, Jacquet H, Leung J, Genschik P (2011) MATH/BTB CRL3 receptors target the homeodomain-leucine zipper ATHB6 to modulate abscisic acid signaling. Dev Cell **21:** 1116-1128

Lee J, Miura K, Bressan RA, Hasegawa PM, Yun DJ (2007a) Regulation of Plant Innate Immunity by SUMO E3 Ligase. Plant Signal Behav **2:** 253-254

Lee J, Nam J, Park HC, Na G, Miura K, Jin JB, Yoo CY, Baek D, Kim DH, Jeong JC, Kim D, Lee SY, Salt DE, Mengiste T, Gong Q, Ma S, Bohnert HJ, Kwak SS, Bressan RA, Hasegawa PM, Yun DJ (2007b) Salicylic acid-mediated innate immunity in Arabidopsis is regulated by SIZ1 SUMO E3 ligase. Plant J **49:** 79-90

Mazur MJ, van den Burg HA (2012) Global SUMO proteome responses guide gene regulation, mRNA biogenesis, and plant stress responses. Front Plant Sci **3:** 215

Miller G, Schlauch K, Tam R, Cortes D, Torres MA, Shulaev V, Dangl JL, Mittler R (2009) The plant NADPH oxidase RBOHD mediates rapid systemic signaling in response to diverse stimuli. Sci Signal **2:** ra45

Miller MJ, Barrett-Wilt GA, Hua Z, Vierstra RD (2010) Proteomic analyses identify a diverse array of nuclear processes affected by small ubiquitin-like modifier conjugation in Arabidopsis. Proc Natl Acad Sci U S A **107:** 16512-16517

Miller MJ, Scalf M, Rytz TC, Hubler SL, Smith LM, Vierstra RD (2013) Quantitative proteomics reveals factors regulating RNA biology as dynamic targets of stress-induced SUMOylation in Arabidopsis. Mol Cell Proteomics **12:** 449-463

Miura K, Jin JB, Lee J, Yoo CY, Stirm V, Miura T, Ashworth EN, Bressan RA, Yun DJ, Hasegawa PM (2007) SIZ1-mediated sumoylation of ICE1 controls *CBF3/DREB1A* expression and freezing tolerance in Arabidopsis. Plant Cell **19:** 1403-1414

Miura K, Lee J, Gong Q, Ma S, Jin JB, Yoo CY, Miura T, Sato A, Bohnert HJ, Hasegawa PM (2011) SIZ1 regulation of phosphate starvation-induced root architecture remodeling involves the control of auxin accumulation. Plant Physiol **155:** 1000-1012

Miura K, Lee J, Miura T, Hasegawa PM (2010) SIZ1 controls cell growth and plant development in Arabidopsis through salicylic acid. Plant Cell Physiol **51:** 103-113

Park BS, Song JT, Seo HS (2011) Arabidopsis nitrate reductase activity is stimulated by the E3 SUMO ligase AtSIZ1. Nat Commun **2:** 400

Pieterse CM, Van der Does D, Zamioudis C, Leon-Reyes A, Van Wees SC (2012) Hormonal modulation of plant immunity. Annu Rev Cell Dev Biol **28:** 489-521

Saracco SA, Miller MJ, Kurepa J, Vierstra RD (2007) Genetic analysis of SUMOylation in Arabidopsis: conjugation of SUMO1 and SUMO2 to nuclear proteins is essential. Plant Physiol **145:** 119-134

van den Burg HA, Kini RK, Schuurink RC, Takken FL (2010) Arabidopsis small ubiquitin-like modifier paralogs have distinct functions in development and defense. Plant Cell **22:** 1998-2016

Vlot AC, Dempsey DA, Klessig DF (2009) Salicylic Acid, a multifaceted hormone to combat disease. Annu Rev Phytopathol **47:** 177-206

Wildermuth MC, Dewdney J, Wu G, Ausubel FM (2001) Isochorismate synthase is required to synthesize salicylic acid for plant defence. Nature **414:** 562-565

Winter D, Vinegar B, Nahal H, Ammar R, Wilson GV, Provart NJ (2007) An "Electronic Fluorescent Pictograph" browser for exploring and analyzing large-scale biological data sets. PLoS One **2:** e718

Zheng Y, Schumaker KS, Guo Y (2012) Sumoylation of transcription factor MYB30 by the small ubiquitin-like modifier E3 ligase SIZ1 mediates abscisic acid response in *Arabidopsis thaliana*. Proc Natl Acad Sci U S A **109:** 12822-12827

Zhu X, Liu B, Carlsten JO, Beve J, Nystrom T, Myers LC, Gustafsson CM (2011) Mediator influences telomeric silencing and cellular life span. Mol Cell Biol **31:** 2413-2421